

1-1-2013

Studies of the structural boundaries of solid-state photodimerization reactions via isocoumarins and heteromeric assemblies

Mihiri S. Weerasinghe

Eastern Illinois University

This research is a product of the graduate program in [Chemistry](#) at Eastern Illinois University. [Find out more](#) about the program.

Recommended Citation

Weerasinghe, Mihiri S., "Studies of the structural boundaries of solid-state photodimerization reactions via isocoumarins and heteromeric assemblies" (2013). *Masters Theses*. 1116.
<http://thekeep.eiu.edu/theses/1116>

This Thesis is brought to you for free and open access by the Student Theses & Publications at The Keep. It has been accepted for inclusion in Masters Theses by an authorized administrator of The Keep. For more information, please contact tabruns@eiu.edu.

*******US Copyright Notice*******

No further reproduction or distribution of this copy is permitted by electronic transmission or any other means.

The user should review the copyright notice on the following scanned image(s) contained in the original work from which this electronic copy was made.

Section 108: United States Copyright Law

The copyright law of the United States [Title 17, United States Code] governs the making of photocopies or other reproductions of copyrighted materials.

Under certain conditions specified in the law, libraries and archives are authorized to furnish a photocopy or other reproduction. One of these specified conditions is that the reproduction is not to be used for any purpose other than private study, scholarship, or research. If a user makes a request for, or later uses, a photocopy or reproduction for purposes in excess of "fair use," that use may be liable for copyright infringement.

This institution reserves the right to refuse to accept a copying order if, in its judgment, fulfillment of the order would involve violation of copyright law. No further reproduction and distribution of this copy is permitted by transmission or any other means.

THESIS MAINTENANCE AND REPRODUCTION CERTIFICATE

TO: Graduate Degree Candidates (who have written formal theses)

SUBJECT: Permission to Reproduce Theses

An important part of Booth Library at Eastern Illinois University's ongoing mission is to preserve and provide access to works of scholarship. In order to further this goal, Booth Library makes all theses produced at Eastern Illinois University available for personal study, research, and other not-for-profit educational purposes. Under 17 U.S.C. § 108, the library may reproduce and distribute a copy without infringing on copyright; however, professional courtesy dictates that permission be requested from the author before doing so.

By signing this form:

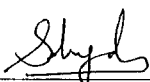
- You confirm your authorship of the thesis.
- You retain the copyright and intellectual property rights associated with the original research, creative activity, and intellectual or artistic content of the thesis.
- You certify your compliance with federal copyright law (Title 17 of the U.S. Code) and your right to authorize reproduction and distribution of all copyrighted material included in your thesis.
- You grant Booth Library the non-exclusive, perpetual right to make copies of your thesis, freely and publicly available without restriction, by means of any current or successive technology, including but not limited to photocopying, microfilm, digitization, or Internet.
- You acknowledge that by depositing your thesis with Booth Library, your work is available for viewing by the public and may be borrowed through the library's circulation and interlibrary department or accessed electronically.
- You waive the confidentiality provisions of the Family Educational Rights and Privacy Act (FERPA) (20 U.S.C. § 1232g; 34 CFR Part 99) with respect to the contents of the thesis, including your name and status as a student at Eastern Illinois University.

Petition to Delay:

I respectfully petition that Booth Library delay maintenance and reproduction of my thesis until the date specified and for the reasons below. I understand that my degree will not be conferred until the thesis is available for maintenance and reproduction.

Date:

Reasons:



Author's Signature

05/22/2013

Date

This form must be submitted in duplicate.

Studies of the Structural Boundaries of
Solid-State Photodimerization Reactions
via Isocoumarins and Heteromeric Assemblies
(TITLE)

BY

Mihiri S. Weerasinghe

THESIS

SUBMITTED IN PARTIAL FULFILLMENT OF THE REQUIREMENTS
FOR THE DEGREE OF

Master of Science in Chemistry

IN THE GRADUATE SCHOOL, EASTERN ILLINOIS UNIVERSITY
CHARLESTON, ILLINOIS

2013
YEAR

I HEREBY RECOMMEND THAT THIS THESIS BE ACCEPTED AS FULFILLING
THIS PART OF THE GRADUATE DEGREE CITED ABOVE

 5/22/13
THESIS COMMITTEE CHAIR DATE

 5/22/13
DEPARTMENT/SCHOOL CHAIR DATE
OR CHAIR'S DESIGNEE

 5/16/2013
THESIS COMMITTEE MEMBER DATE

 5/16/2013
THESIS COMMITTEE MEMBER DATE

 5/16/2013
THESIS COMMITTEE MEMBER DATE

THESIS COMMITTEE MEMBER DATE

ABSTRACT

The study of molecules in crystals has gained considerable attention in the field of structural chemistry. Much interest has focused on the use of molecular crystals for the construction of materials with specific functional properties. Because the design of such materials requires a critical understanding of intermolecular interactions, use of the building-block approach continues to offer an important strategy to multimolecular frameworks. Though the use of template and metal-ligand interactions has provided successful opportunities to organize chemical reactions in solids, these methods require secondary molecules and are limited to achiral starting materials. As such, exploring chiral synthesis with simplified precursors holds much promise to the design of next generation materials. Recent research conducted in Dr. Wheeler's group focused on [2+2] photodimerization reactions of olefins by investigating a family of cinnamylsulfonamides that self-assemble to give photoreactive dimers. Though photodimerization in solids has been extensively studied, photobehavior of cocrystalline systems constructed from two chemically distinct molecules and chiral materials are rare.

This thesis focuses on a cocrystalline approach for the construction of multicomponent assemblies to study solid-state [2+2] photodimerization reactions. Racemic alanine sulfonamidecinnamic acid (a fish hook shaped molecule) successfully cocrystallized with co-formers 4,4'-dipyridyl, 4,4'-dipyridyl-N,N'-dioxide dehydrate, and *trans*-1,2-bis(4-pyridyl)ethylene by use of the complementary features of hydrogen bonds and molecular shape to form supramolecular tetramers. The co-former (*E*)-but-2-enediamide did not result in cocrystal formation. Though cocrystals obtained from co-former *trans*-1,2-bis(4-pyridyl)ethylene effectively organized adjacent olefins for [2+2]

photodimerization reaction via an inter-dimer route, UV illumination did not result in the cyclobutane photoproduct.

In a second study, racemic and chiral syntheses of sulfonamide isocoumarin compounds and their [2+2] photodimerization reactions were examined. Two fish-hook shape molecules were synthesized by use of racemic and homochiral sulfonamide isocoumarin compounds. All synthetic steps were analyzed using NMR techniques, and where possible, X-ray crystallography. Racemic isocoumarin was crystallized by use of hydrogen bonds to form a supramolecular homodimer. These homodimers aligned with favorable olefin···olefin spacing for UV initiated single-crystal-to-single-crystal (SCSC) [2+2] photodimerization reactions to give cyclobutane photoproduct in 100% conversion. While homochiral isocoumarin could not be processed as a SCSC reaction, photoirradiation of a powdered sample gave cyclobutane photoproduct in 64.6% conversion as revealed by NMR studies.

ACKNOWLEDGEMENT

My stay at EIU encountered many friendly people who helped me withstand homesickness and many cultural barriers. First of all I am deeply thankful to Dr. K. A. Wheeler, my research advisor, for his great support and guidance throughout my academic life at EIU. Beside the great knowledge he shared with us, Dr. Wheeler is one of the most organized and caring professor I have experienced. My success at EIU as a graduate student would be less successful without his guidance and encouragement.

I would also like to express my heartfelt thanks to Dr. Barbara Lawrence and to Dr. Daniel Sheeran (Departmental Chair) for their nice and kind personalities which make me feel very comfortable. I owe special thanks to my thesis committee, Drs. Barbara Lawrence, Douglas Klarup, and Mark McGuire for reviewing my work regardless to their busy schedules and extended support to fulfill my degree requirements.

I would like to convey my sincere thanks to the entire EIU chemistry department faculty for their valuable supports and guidance. My thanks also go to the stock room personnel for helping me in various ways.

I would like to thank all my lab mates including Raj, Megan, Teage and Cody for their support and sharing loving memories with me. Finally, I would like to thank my loving husband, my parents and all my other friends for their help and encouragement to accomplish my goals.

TABLE OF CONTENTS

Abstract	i
Acknowledgement	iii
Table of Contents	iv
List of Figures	vi
List of Tables	ix
Introduction	1
1.1 General Overview	1
1.2 Supramolecular Chemistry	3
1.3. Crystal Engineering	6
1.4 Organic Solid-State Reactions	10
1.5 [2+2] Photodimerization	16
1.6 Co-crystallization and [2+2] photodimerization	20
1.7 Synthesis and Photodimerization of Isocoumarin/Coumarin Containing Molecules	22
1.8 Synopsis of Thesis Work	29
1.9 References	35
Experimental	39
2.1 General Considerations	39
2.2 Photochemical Studies	39
2.3 X-ray Crystallography	40
2.4 Preparation of Cocrystalline Materials	41
2.5 Preparation of Isocoumarin Precursors and Compounds	44
2.6 References	51

Results and Discussion	52
3.1 Approaches to the Construction of Photoactive Bimolecular Assemblies	52
3.1.1 Introduction	52
3.1.2 Crystal Structure Assessment of Cocrystal 23·24	54
3.1.3 Crystal Structure Assessment of Cocrystal 23·25	56
3.1.4 Crystal Structure Assessment of Cocrystal 23·26	57
3.1.5 Crystal Structure Assessment of 28	59
3.1.6 Developments Towards Photoactive Bimolecular Assemblies	61
3.2 Synthesis and Photodimerization of 7-(3-hydroxy-2-methyl-3-oxo-propyl) sulfonyl-oxo-isochromene-3-carboxylic acid (30/31)	62
3.2.1 Introduction	62
3.2.2 Synthesis of Methyl 2-(2-methoxy-2-oxo-ethyl)benzoate (35)	64
3.2.3 Synthesis of dimethyl 1-oxoisochromene-3,4-dicarboxylate (36)	65
3.2.4 Synthesis of 1-oxoisochromene-3-carboxylic acid (37)	66
3.2.4.a Crystal Structure Analysis of 37-I and 37-II	66
3.2.5 Synthesis of 7-chlorosulfonyl-1-oxo-isochromene-3-carboxylic acid (38)	70
3.2.6 Synthesis of 7-(3-hydroxy-2-methyl-3-oxo-propyl)sulfonyl-1-oxo-isochromene-3-carboxylic acid (30/31)	71
3.2.6.a Crystal Growth, Selection and Mounting	72
3.2.6.b Crystal Structure Assessment	73
3.2.6.c Photodimerization of Racemic Isocoumarin 30	77
3.2.6.d Photodimerization of Homochiral Isocoumarin 31	79
3.3 Conclusions	83
3.4 References	85
Appendix	86

LIST OF FIGURES

Figure 1. Lock-and-key model showing the formation of a supermolecule constructed from the complementary shapes of substrate and enzyme species.	4
Figure 2. Complementary base pairing in DNA.	5
Figure 3. From molecules to periodical supermolecules.	7
Figure 4. Self-assembly via supramolecular synthons using 3-hydroxybenzoic acid.	8
Figure 5. Crystal structure of the cocrystal of theophylline and salicylic acid showing hydrogen bond patterns.	10
Figure 6. Photochemical reactions in solid-state: A) [2+2] photodimerization and B) photopolymerization.	12
Figure 7. Schematic of the bromination reaction of chalcone (1) in CH ₂ Cl ₂ solution.	14
Figure 8. Schematic of the oxidative coupling of β -naphthol (4) to produce bis- β -naphthol (5) in the solid-state.	14
Figure 9. Solid-state etherification of diphenylmethanol (6).	15
Figure 10. Hydrogen bond formation between diphenylmethanol molecules in solid-state.	15
Figure 11. Chemical structures of α,ω -diphenylpolyenes a-c.	17
Figure 12. Use of templates to direct photodimerization reaction in molecular crystals.	17
Figure 13. Template based [2+2] photodimerization of trans-1,2-bis(4-pyridyl)ethylene.	18
Figure 14. Schematic representation of the SCSC [2+2] photodimerization of 2-benzyl-1-5-benzylidenecyclopentanone: A. Crystal structures B, C, D and E represents the various stages of the photoreaction: B. 0%, C. 56%, D. 81%, and E.100%.	19
Figure 15. The crystal structures of α - <i>trans</i> -cinnamic acid at various stages of tail irradiation: a. 0% unirradiated crystal, b. 40% partially dimerized, c. 100% dimerized truxillic acid.	20
Figure 16. [2+2] photodimerization of a 1:1 cocrystal of 10 and 11 .	21
Figure 17. Structure of (A) 4,4'-bpe, (B) resorcinol and (C) hydrogen bond tetramer.	22

Figure 18. Photodimerization of coumarin in benzene.	26
Figure 19. Photodimerization of 2:3 inclusion complex of β -cyclodextrin and coumarin.	27
Figure 20. Single-crystal photodimerization of coumarin inclusion crystals.	28
Figure 21. X-ray crystal structure of 1:1 inclusion complex of coumarin 14 and (-)- 16 .	28
Figure 22. Orientation of coumarin (left) and the <i>anti-head-head</i> dimer (-)- 18 (right).	29
Figure 23. Photodimerization of coumarins inside inclusion crystals with diacetylenediols.	29
Figure 24. Design strategy (top) and molecular target (bottom) for the exploring heterodimerization between different olefin compounds.	31
Figure 25. Design strategy of hydrogen bond tetramer formation.	32
Figure 26. Molecular components used in the design of reactive cocrystals.	52
Figure 27. Asymmetric unit and labeling scheme (70% probability ellipsoids) for co-crystal 23·24 (disordered atom labels not shown).	55
Figure 28. Crystal packing of 23·24 showing hydrogen bond patterns (H atoms deleted for clarity) (minor disorder component excluded).	55
Figure 29. Crystal structures of 23·25 showing (A) asymmetric unit and labeling schemes (70% probability ellipsoids) (disordered part is not labeled) and (B) disorder components separately.	56
Figure 30. Crystal packing of 23·25 showing hydrogen bond patterns (H atoms deleted for clarity) (minor disorder component excluded).	57
Figure 31. Asymmetric unit and atomic labeling (70% probability ellipsoids) of crystalline 23·26 (disordered portion of structure not labeled).	58
Figure 32. Crystal packing of 23·26 showing (A) hydrogen bond patterns (H atoms deleted for clarity) and (B) heterodimer alignment (minor disorder component excluded).	59
Figure 33. Crystal structure of 28 showing asymmetric unit and labeling scheme (70% probability ellipsoids).	60
Figure 34. Crystal packing of 28 showing (A) the hydrogen bond pattern (H atoms deleted for clarity) and (B) photostable alignment of neighboring olefins.	61

Figure 35. Schematic presentation of photodimerization reaction of compound 37 .	63
Figure 36. Design strategy (top) and molecular targets (bottom) for the construction of photoreactive sulfonamide isocoumarin compounds.	64
Figure 37. The reaction mechanism for the synthesis of 36 .	65
Figure 38. Asymmetric units and labeling schemes (70% probability ellipsoids) of two crystalline phases of 37 .	67
Figure 39. Crystal packing of 37-I showing (A) the dimer formation with hydrogen bonds and (B) photostable alignment of neighboring olefins (H atoms deleted for clarity).	69
Figure 40. Crystal packing of 37-II showing (A) the solvate formation with hydrogen bonds and (B) photostable alignment of neighboring olefins (H atoms deleted for clarity).	69
Figure 41. ¹ H NMR spectrum of sulfonylchloride 38 showing signals and splitting in the aromatic region.	71
Figure 42. Single crystal of 30 mounted on a glass fiber (left) and goniometer head for diffraction studies (right).	72
Figure 43. Asymmetric unit of racemic 30 showing the ‘fish hook’ shape molecular arrangement (top) and homodimer formation by use of hydrogen bonds (bottom, minor disorder component excluded).	74
Figure 44. Asymmetric unit of 30 showing (A) disordered crystal projections separately and (B) combined structure.	75
Figure 45. Crystal packing of 30 showing hydrogen bond patterns (top) (H atoms deleted for clarity) and favorable alignment of neighboring olefins of the homodimer (bottom) (minor disorder component excluded).	76
Figure 46. Crystal structure of photoproduct 33 (racemate) showing the combined disorder model (left) and each disorder component separately (right).	78
Figure 47. Expected photoproduct from UV irradiation of homochiral 31 .	79
Figure 48. ¹ H NMR of homochiral 31 showing the solid-state reactivity at 0, 2, 8.5, and 56.5 hours.	80
Figure 49. Solid-state conversion of 31 to the homochiral photoproduct.	81
Figure 50. ¹ H NMR of UV irradiated solid 31 (56.5 hours) showing both starting material and photoproduct.	82

LIST OF TABLES

Table 1a. Crystal data and structure refinement for cocrystal of 23 and 4,4'-dipyridyl (24).	86
Table 1b. Fractional atomic coordinates and isotropic or equivalent isotropic displacement parameters (\AA^2) for cocrystal of 23 and 4,4'-dipyridyl (24).	87
Table 1c. Atomic displacement parameters (\AA^2) for Cocrystal of 23 and 4,4'-dipyridyl (24).	90
Table 1d. Geometric parameters (\AA , $^\circ$) for Cocrystal of 23 and 4,4'-dipyridyl (24).	91
Table 1e. Hydrogen-bond geometry (\AA , $^\circ$) for Cocrystal of 23 and 4,4'-dipyridyl (24).	97
Table 2a. Crystal data and structure refinement for cocrystal of 23 and of 4,4'-dipyridyl-N,N'-dioxide dihydrate (25).	98
Table 2b. Fractional atomic coordinates and isotropic or equivalent isotropic displacement parameters (\AA^2) for cocrystal of 23 and of 4,4'-dipyridyl-N,N'-dioxide dihydrate (25).	99
Table 2c. Atomic displacement parameters (\AA^2) for cocrystal of 23 and of 4,4'-dipyridyl-N,N'-dioxide dihydrate (25).	100
Table 2d. Geometric parameters (\AA , $^\circ$) for cocrystal of 23 and of 4,4'-dipyridyl-N,N'-dioxide dihydrate (25).	101
Table 2e. Hydrogen-bond geometry (\AA , $^\circ$) for cocrystal of 23 and of 4,4'-dipyridyl-N,N'-dioxide dihydrate (25).	104
Table 3a. Crystal data and structure refinement for cocrystal of 23 and <i>trans</i> -1,2-bis(4-pyridyl)ethylene (26).	105
Table 3b. Fractional atomic coordinates and isotropic or equivalent isotropic displacement parameters (\AA^2) for cocrystal of 23 and <i>trans</i> -1,2-bis(4-pyridyl)ethylene (26).	106
Table 3c. Atomic displacement parameters (\AA^2) for cocrystal of 23 and <i>trans</i> -1,2-bis(4-pyridyl)ethylene (26).	108
Table 3d. Geometric parameters (\AA , $^\circ$) for cocrystal of 23 and <i>trans</i> -1,2-bis(4-pyridyl)ethylene (26).	110
Table 3e. Hydrogen-bond geometry (\AA , $^\circ$) for cocrystal of 23 and <i>trans</i> -1,2-bis(4-pyridyl)ethylene (26).	115

Table 4a. Crystal data and structure refinement for (E)-but-2-enediamide (28).	116
Table 4b. Fractional atomic coordinates and isotropic or equivalent isotropic displacement parameters (\AA^2) for (E)-but-2-enediamide (28).	116
Table 4c. Atomic displacement parameters (\AA^2) for (E)-but-2-enediamide (28).	117
Table 4d. Geometric parameters (\AA , $^\circ$) for (E)-but-2-enediamide (28).	117
Table 4e. Hydrogen-bond geometry (\AA , $^\circ$) for (E)-but-2-enediamide (28).	117
Table 5a. Crystal data and structure refinement for 1-oxoisochromene-3-carboxylic acid (37-I).	118
Table 5b. Fractional atomic coordinates and isotropic or equivalent isotropic displacement parameters (\AA^2) for 1-oxoisochromene-3-carboxylic acid (37-I).	118
Table 5c. Bond lengths [\AA] and angles [$^\circ$] for 1-oxoisochromene-3-carboxylic acid (37-I).	119
Table 5d. Atomic displacement parameters (\AA^2) for 1-oxoisochromene-3-carboxylic acid (37-I).	121
Table 5e. Geometric parameters (\AA , $^\circ$) for 1-oxoisochromene-3-carboxylic acid (37-I).	122
Table 5f. Hydrogen-bond geometry (\AA , $^\circ$) for 1-oxoisochromene-3-carboxylic acid (37-I).	123
Table 6a. Crystal data and structure refinement for 1-oxoisochromene-3-carboxylic acid (37-II).	124
Table 6b. Fractional atomic coordinates and isotropic or equivalent isotropic displacement parameters (\AA^2) for 1-oxoisochromene-3-carboxylic acid (37-II).	125
Table 6c. Atomic displacement parameters (\AA^2) for 1-oxoisochromene-3-carboxylic acid (37-II).	125
Table 6d. Geometric parameters (\AA , $^\circ$) for 1-oxoisochromene-3-carboxylic acid (37-II).	126
Table 6e. Hydrogen-bond geometry (\AA , $^\circ$) for 1-oxoisochromene-3-carboxylic acid (37-II).	127
Table 7a. Crystal data and structure refinement for recemic 7-(3-hydroxy-2-methyl-3-oxo-propyl)sulfonyl-1-oxo-isochromene-3-carboxylic acid (30).	128

Table 7b. Fractional atomic coordinates and isotropic or equivalent isotropic displacement parameters (\AA^2) for recemic 7-(3-hydroxy-2-methyl-3-oxo-propyl)sulfonyl-1-oxo-isochromene-3-carboxylic acid (30).	129
Table 7c. Atomic displacement parameters (\AA^2) recemic 7-(3-hydroxy-2-methyl-3-oxo-propyl)sulfonyl-1-oxo-isochromene-3-carboxylic acid (30).	130
Table 7d. Geometric parameters (\AA , $^\circ$) for recemic 7-(3-hydroxy-2-methyl-3-oxo-propyl)sulfonyl-1-oxo-isochromene-3-carboxylic acid (30).	131
Table 8a. Crystal data and structure refinement for 7-(3-hydroxy-2-methyl-3-oxo-propyl)sulfonyl-1-oxo-isochromene-3-carboxylic acid (31).	135
Table 8b. Fractional atomic coordinates and isotropic or equivalent isotropic displacement parameters (\AA^2) for 7-(3-hydroxy-2-methyl-3-oxo-propyl)sulfonyl-1-oxo-isochromene-3-carboxylic acid (31).	135
Table 8c. Atomic displacement parameters (\AA^2) for 7-(3-hydroxy-2-methyl-3-oxo-propyl)sulfonyl-1-oxo-isochromene-3-carboxylic acid (31).	136
Table 8d. Geometric parameters (\AA , $^\circ$) for 7-(3-hydroxy-2-methyl-3-oxo-propyl)sulfonyl-1-oxo-isochromene-3-carboxylic acid (31).	137

CHAPTER 1: INTRODUCTION

1.1 General Overview

The ability to form covalent bonds is a fundamental tenet to the field of synthetic organic chemistry.¹ Developing countries require a broad range of chemical materials that deliver beneficial functional properties to such critical areas as “pharmaceuticals, synthetic fabrics and pesticides”.² A new generation of advanced materials is needed to meet rising expectations of developing nations by improving the quality of modern life and solving real world problems. As an example, several decades ago farmers controlled pest problems in agricultural areas by traditional pest control methods such as crop rotation, mixed cropping and selective breeding of pest-resistant cultivars. Although this general approach is capable of fulfilling small scale demand, increased pressure related to population growth no longer satisfies the requirements presented by developing countries. The introduction of pesticides to modern cultures has provided opportunities for improved crop production, but access to sustainable crop commodities is not the only resource essential for healthy communities and countries. Disease and other health issues also pose a significant challenge for emerging cultures. In addition to quality medical care, the development of new drugs and the access to such resources is essential. One indication of this growing need is the HIV-AIDS epidemic of the early 1980's. This world health threat required (and still requires) focused attention that ranges from distribution of medical supplies to the development of effective treatment strategies. Whether the need is medical or agricultural based, it is clear that developing countries will continue to require a wide-range of materials that serve specific functions. Because such commodities have far reaching impact on the societal well-being of cultures,

materials development holds much importance for the outcome of how we will navigate future world challenges.

Fulfilling the growing demand of human needs through naturally occurring substances is essentially an impossible task. As early as a few centuries ago synthesizing alternatives for natural products such as rubber and medicines was a key topic among the scientific community. At first, the collective efforts of scientists explored chemical synthesis through a trial and error approach² and, prior to 1820's, scientists believed that chemical synthesis of organic compounds could only be accomplished within living matter. In 1828, The German chemist Friedrich Wohler synthesized urea from ammonium cyanate.³ Urea synthesis was a seminal discovery that provided the first example of constructing an organic compound in a laboratory setting. The development of these experimental results and those that followed in the 19th century gave considerable insight to atoms, molecules, and molecular bonding. In 1916, Gilbert Lewis presented two concepts: i) single bonds are derived from a pair of electrons shared between the valence shells and ii) the rule of eight.⁴ A few years later, Langmuir presented the term covalent bond and renamed the concept of "shared electron pair bond" by accepting Lewis' two concepts.³ Much later, scientist Linus Pauling extended Lewis' concepts by proposing resonance.⁵ Christopher Ingold used the concept of reaction mechanisms to understand the sequence of changes in a chemical reaction.⁵ The synthesis of acetylsalicylic acid (aspirin) by Bayer at the end of the 19th century opened the doors to the pharmaceutical industry.⁶ The development of organic chemistry gave way to produce and modify complex molecules starting from the early 20th century. The understanding and use of covalent bond formation continues to inspire scientists to explore such areas as

the design of new catalysts, molecular machines and new drug formulations.⁷ Although scientists possess a variety of chemical tools to synthesize complex molecules with valuable and specific properties, there remains a need to also understand how large molecules (e.g. DNA) are produced by smaller components and how the specific structural properties foster self assembly. This thesis explores the design, synthesis, and crystal chemistry of unique materials constructed from isocoumarin frameworks that are found in a variety of natural products and are very useful in medicinal applications.^{8,9} Continuing with this theme of solid-state chemistry, this work also investigates the heterodimerization between significantly different olefin compounds by synthesizing pharmaceutical cocrystals and how supramolecular chemistry and crystal engineering can be used to effectively engineer and prepare complex molecules that contain cyclobutane ring systems.

1.2 Supramolecular Chemistry

For the last hundred years, researchers have focused on understanding nature at a molecular level with an early belief that all functions and structures of biological systems involved covalent bonds.¹⁰ Since those early years it has become clear that not all biological functions arise from covalent bonds. Instead, a wide selection of biological materials and their structures and functions result from the individual components held together by non-covalent interactions.^{10, 11} As an example, the formation and dissociation of non-covalent bonds (e.g., hydrogen bonds) are essential to protein synthesis.⁷ Non-covalent interactions play a major role in reorganizing smaller units (molecules) into complex assemblies (supermolecules) with unique properties and functions.¹⁰⁻¹¹ At first,

an understanding of this phenomenon was quite cursory, but in 1894 Emil Fischer described enzyme substrate interactions using a lock-and-key mechanism (Figure 1).¹⁰ This mechanism contains two underlying principles - molecular recognition and supramolecular function. According to this model, the shape and non-covalent contacts between interacting molecules should be complementary to promote the assembly of the two components. This concept is known as molecular recognition.¹⁰ Specific non-covalent interactions help to determine material function and its use to explain such areas as enzyme-substrate interactions has paved the way for the scientific discipline of Supramolecular Chemistry.

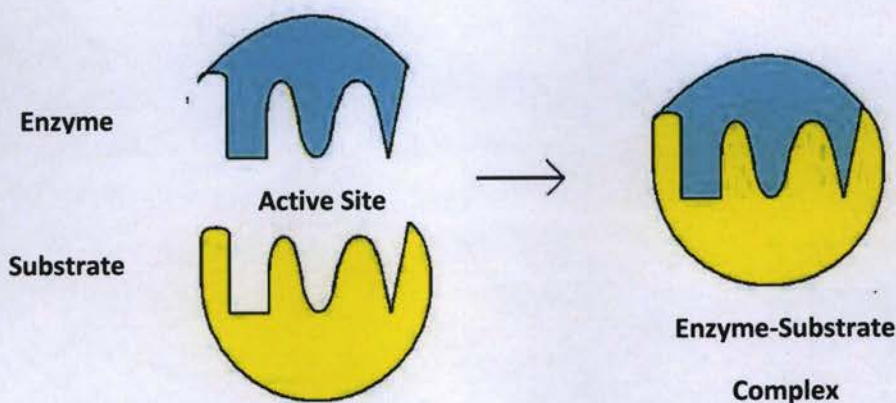


Figure 1. Lock-and-key model showing the formation of a supermolecule constructed from the complementary shapes of substrate and enzyme species.

In 1969, the term Supramolecular Chemistry was coined by Jean-Marie Lehn.¹² He defined Supramolecular Chemistry as “the Chemistry of the intermolecular bond”.¹⁰⁻¹² Lehn stated that a molecule is formed connecting atoms by covalent bonds; however, a supermolecule is formed from connecting molecules by intermolecular interactions.¹³ Supramolecular chemistry focuses on how molecules recognize each other (molecular

recognition); both assemblies and function on a molecular scale play important roles with investigation of supramolecular materials. Since the time of Latimer and Rodebush's description of hydrogen bonds, chemists have explored non-covalent bonds and their impact on understanding biological processes.¹⁴ According to the precepts of supramolecular chemistry, hydrogen bonds have the ability to control and direct the structures of molecular assemblies.¹⁰⁻¹³ Supramolecular structures (supermolecules) are not only formed from the collection of single components, but from the additive effects of intermolecular interactions. Therefore, it is possible and often the case that the properties of the molecular building blocks widely differ from the motif they form. These supramolecular properties are useful in both material science and biology. DNA and its double helix is a good example of a natural self-assembling structure present in biological systems where the two nucleotide strands are held together by non-covalent hydrogen bonds.¹⁵ In DNA strands, guanine (G) selectively interacts with cytosine (C) forming triple hydrogen bonds and adenine interacts with thymine (T) forming a set of hydrogen bonds (Figure 2).¹⁵ An understanding of these interactions has proved useful to uncovering the details of DNA replication. Identifying the fundamental principles behind the construction of biological molecular assemblies has provided key knowledge for the development of new materials with functional properties.

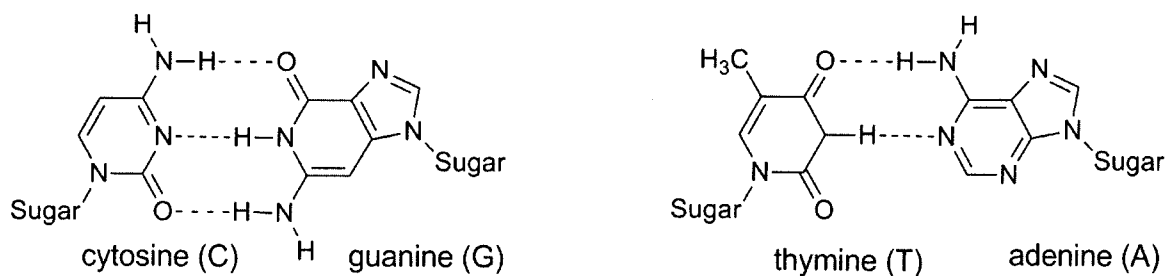


Figure 2. Complementary base pairing in DNA.

1.3. Crystal Engineering

A crystal of an organic compound ultimately becomes the perfect supermolecule constructed from molecules held together by intermolecular interactions.¹⁰⁻¹² Crystal engineering is the “rational design of functional molecular solids”¹⁶ with desired properties. The goal of crystal engineering is to generate reliable connections between molecular and supramolecular structures based on an understanding and exploitation of intermolecular interactions.¹³ The term “crystal engineering” was first coined by R. Pepinsky in 1955 and subsequently applied by Schmidt¹⁷ in the 1960’s to the solid-state photochemical reactivity of trans-cinnamic acids.¹⁸ In 1988, Gautam Desiraju defined crystal engineering as “*the understanding of intermolecular interactions in the context of crystal packing and the utilization of such understanding in the design of new solids with desired physical and chemical properties*”.¹¹ One clear description of crystal engineering is the “bottom up” construction of crystalline assemblies. This paradigm shows the capability of molecules to assemble into desired architectures based on intermolecular interactions between individual building blocks.¹⁹ This bottom-up approach organizes molecular components directed by the periodicity and symmetry operators of the crystalline frameworks (Figure 3).²⁰

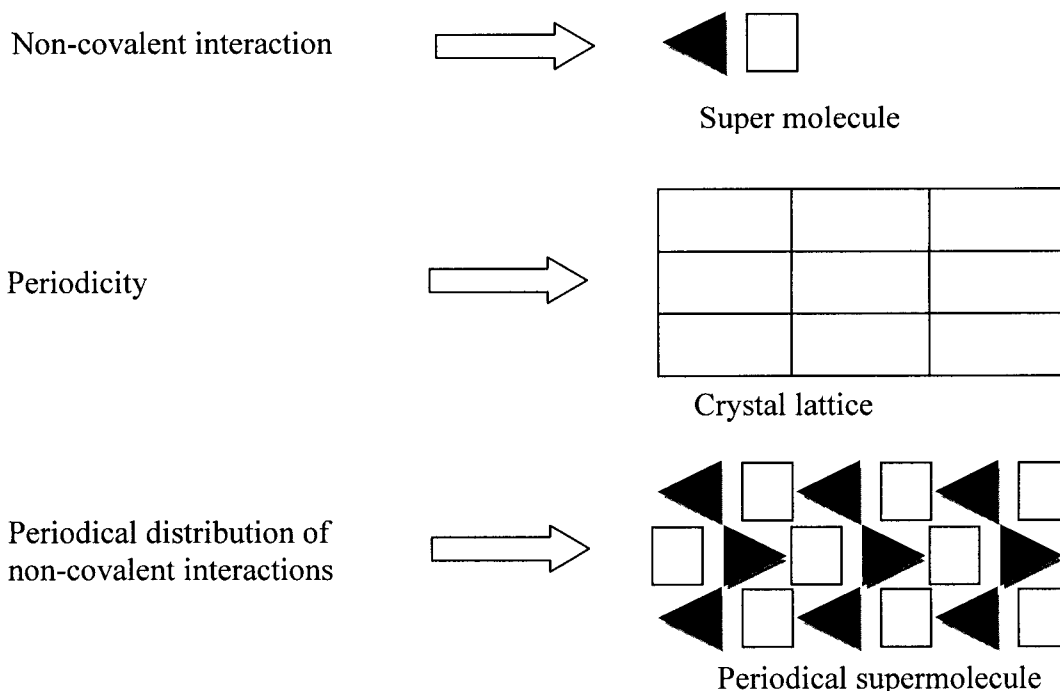


Figure 3. From molecules to periodical supermolecules.

In general, molecules are generated by connecting atoms by use of covalent bonds, and crystals (supermolecules) are generated by linking molecules with intermolecular interactions. Examples of weak non-covalent intermolecular forces that govern the formation of these supermolecules include hydrogen bonding, halogen bonding, π - π stacking, metal-ligand coordination, ionic interaction and host-guest interaction.^{21,22} The concepts from crystal engineering can also be applied to other intermolecular assemblies such as “protein-ligand recognition, design of supramolecular polymers and systems for drug delivery”.¹³ Although the field of crystal engineering has been active for 30 years, its origin started earlier with the development of X-ray crystallography. The development of this area was highlighted in one of Bragg’s²³ early diffraction experiments that compared the crystal structures of naphthalene and anthracene.¹³ Robertson was the first to relate molecular structure of organic compounds

with their crystal structure and studied a variety of crystal structures in the 1940s and 1950s.¹³ In the late 1980's, Ermer²⁴ was able to offer a good contribution to X-ray crystallography by presenting the crystal structure of adamantane-1,3,5,7-tetra-carboxylic acid with a novel analysis of complex packing of this molecule.

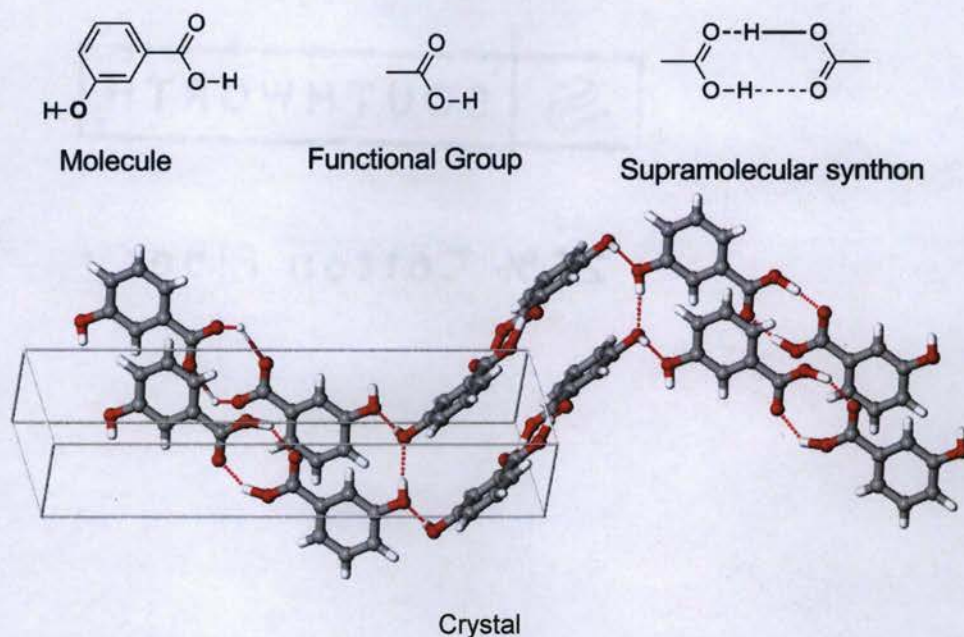


Figure 4. Self-assembly via supramolecular synthons using 3-hydroxybenzoic acid.¹⁷

A crystal can be defined also as a network built by smaller components. Since crystals are constructed by the assembly of molecular functional groups held together by an array of non-covalent interactions, X-ray crystallographic assessment can be used to assess these motifs and the repetitive units recognized. These units have been termed “supramolecular synthons” indicating the importance of these building-blocks to construction of the crystal structure.²⁵ The term “synthon” was introduced by Corey in 1967 as “*structural units within molecules which can be formed and/or assembled by known or conceivable synthetic operations*”.¹¹ At present, crystal engineers are able to

predict the construction of many supramolecular synthons that allow for further design of crystalline motifs based on the interplay of functional groups (Figure 4).²⁶

Early crystal engineering studies of single-component systems paved the way for more complex materials consisting of two or more distinct components. These materials are commonly referred to as cocrystals. Even though the definition of a cocrystal is a still controversial, it can be defined as “a multiple component crystalline solid formed in a stoichiometric ratio between two compounds that are crystalline solids under ambient conditions”.¹⁷ In the pharmaceutical industry, co-crystals are gaining much attention since the co-crystallization process can alter the physicochemical properties of pharmaceutical materials by changing the molecular interactions. Pharmaceutical cocrystals are constructed of an active pharmaceutical ingredient (API) and a molecular cocrystal former (Figure 5).²⁷ Many factors such as dissolution rate, solubility, chemical stability and moisture uptake can affect the therapeutic efficacy of drugs, and in turn the market value of the drug; the use of API cocrystals has been explored as a possible answer to the ongoing challenges with drug development.²⁸ By effective use of crystal engineering strategies, a target property of a compound can be achieved with the aid of a co-crystal former. This is accomplished by combining the two components to give different crystal packing that ultimately changes the physical properties of the original material. Given the proper selection of co-crystal former compounds available, this approach offers an interesting avenue to pharmaceutical materials design with tailor-made additives and properties.

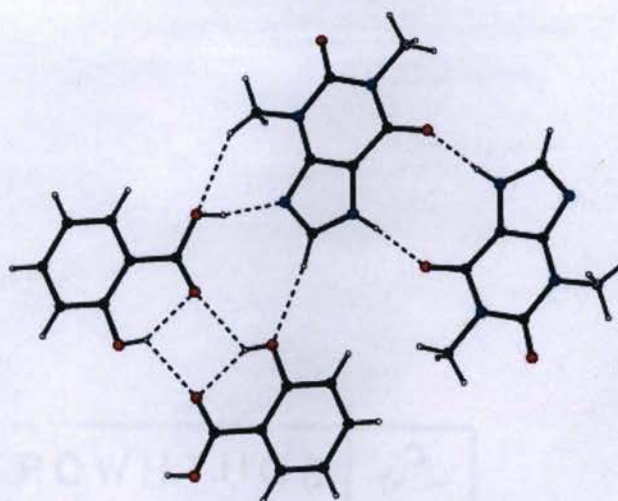


Figure 5. Crystal structure of the co-crystal of theophylline and salicylic acid showing hydrogen bond patterns.²⁷

1.4 Organic Solid-State Reactions

Studies that seek to organize chemical reactions confined in crystalline materials extensively utilize the principles from supramolecular chemistry and crystal engineering. Since solid-state reactions involve chemical transformations that occur in a solvent free environment, controlling the spatial arrangement of reacting species is paramount to the outcome of these processes. Conventional chemical syntheses are typically carried out with the aid of various chemical solvents. With these methods molecular movement is not restricted and often results in a probability distribution of molecular approaches that give way to an assortment of favorable reaction trajectories and ultimately bond formation. Because of this random molecular motion, multiple reaction intermediates are accessed that result in decreased reaction efficiency and selectivity. An unwanted reaction outcome is just one of the drawbacks generally associated with solution chemistry. As

such, solution methods often require significant effort to optimize reaction conditions and purify product mixtures. At present, restricting the motion of reactants via use of the solid-state has received considerable attention due to their inherent value and application to the area of ‘Green Chemistry’. Reactions that occur in the solid-state can be considered environmentally friendly processes since they require no attention with the handling and disposal of solvents.^{29,30} Further, solid-state processes may be considered more cost effective since they often result in single products. A previous report suggests that solid-state processes also provide opportunities to explore new reactions and products that are impossible, or nearly inaccessible, from conventional solution techniques.²⁹ Therefore, the use of transformations in molecular solids is an attractive alternative to traditional synthetic methods for the construction of organic molecules.

In the early stages of solid-state chemistry, the limited understanding of factors that govern crystal packing made it difficult to engineer materials with predetermined reactivity. Although reactivity of crystalline solids is dependent on the structure of the crystal lattice, the use of crystallography techniques to understand reaction patterns occurred well after Bragg’s discovery of X-rays in 1913.^{13,23} Even so, the steady use of X-ray diffraction tools in the 1960’s provided a turning point for the field that continues to play an important role in understanding the structure-reactivity relationships for many solid-state reactions.

As mentioned in the preceding discussion, chemical transformation restricted to a crystalline lattice provides significant advantage to solution chemistry techniques because these processes often proceed with a limited number of reaction outcomes. This advantage arises when reactant species orient in close proximity with suitable geometry.

When limited molecular movement is needed to reach the reaction product, these types of solid-state reactions are commonly known as topochemically¹⁸ controlled reactions. Photochemical reactions are very common in solid-state chemistry and many occur topochemically by preserving the reaction environment during the process.³¹ Reactions such as [2+2] photodimerization and polymerization of diacetylenes (Figure 6) are two examples of UV-induced solid-state reaction that date back more than a century.

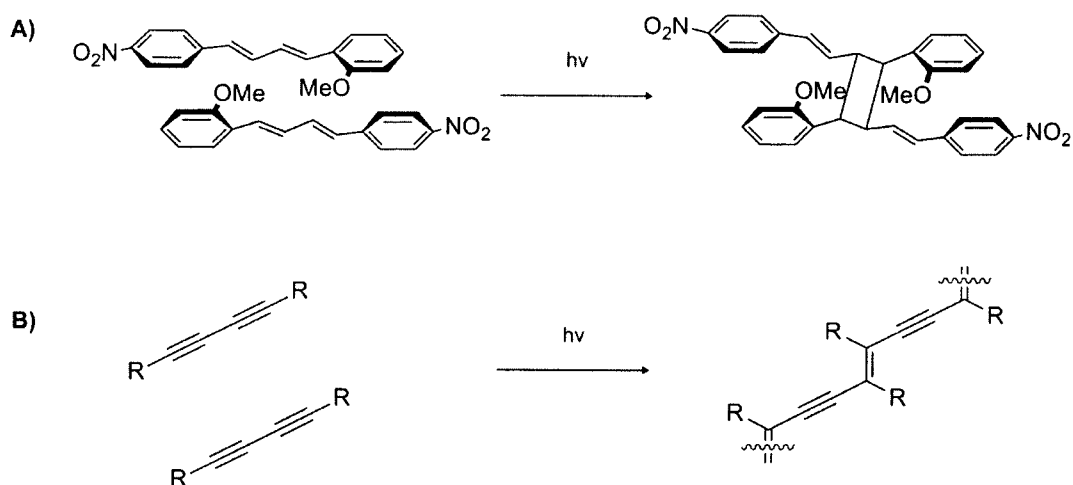
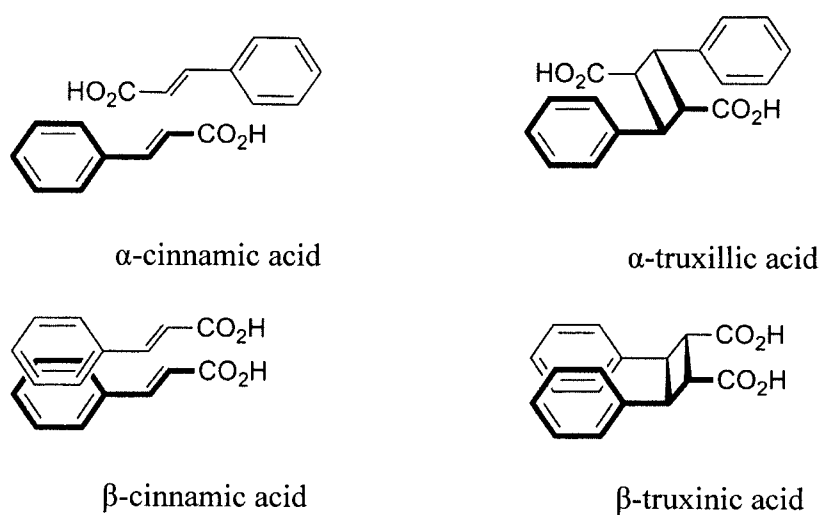


Figure 6. Photochemical reactions in solid-state: A) [2+2] photodimerization and B) photopolymerization.

The fundamental principles behind topochemical reactions were not well understood until Schmidt and coworkers presented their findings in the early 1960s.¹⁸ Results from their pioneering work on organic solid-state chemistry established very important principles still used today. According to their studies, solid-state “reaction occurs with a minimum amount of atomic and molecular movement” suggesting that the reaction process depends on the orientation of the reactive centers and the distance between the reactive centers.¹⁸ Their work showed that carbon-carbon double bonds

(C=C) should be aligned in a parallel fashion and separated by $< 4.2 \text{ \AA}$ to undergo [2+2] photodimerization reactions in the solid-state. Further, their studies also revealed the relationship between reactant orientation and the molecular structure of the product. Their studies explored this connection by performing a series of photodimerization reactions of solid cinnamic acid derivatives and showed UV irradiation of α -trans-cinnamic acid gives α -truxillic acid, while irradiation of β -trans-cinnamic acid produces β -truxinic acid (Scheme 1). Ultimately, their studies provided support that dimerization in the solid-state occurs stereospecifically and consistent with the geometric relation of the olefins (reactive center) in the crystal lattice.

Scheme 1



In the solid-state molecular conformations are effectively maintained that would otherwise be impossible to achieve in solution or the gas phase. The organization of molecules in a crystal can offer an important avenue to stereoselective high-yielding reaction outcomes.³² Solid-state bromination of chalcon (1) is one example that highlights the efficiency of solid-state organic reactions. When reacted with bromine, crystalline

chalcone (**1**) produces only erythro-**2**; however, the analogous CH_2Cl_2 solution reaction results in a mixture of both erythro-**2** (84% ee) and threo-**3** (16% ee) (Figure 7).³³

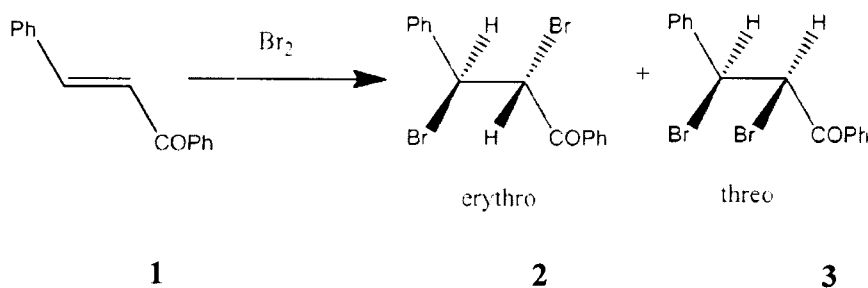


Figure 7. Schematic of the bromination reaction of chalcone (**1**) in CH_2Cl_2 solution.

In another example, Fumio Toda and coworkers observed that oxidative coupling of β -naphthol (**4**) in the presence of $\text{FeCl}_3 \cdot 6\text{H}_2\text{O}$ produced bis- β -naphthol (**5**) in 95% yield at 50 $^\circ\text{C}$ in solid-state (Figure 8). However, the same reactants could only produce bis- β -naphthol (**5**) in 60% yield in 50% aqueous MeOH under reflux condition after a 2h reaction time.³⁴

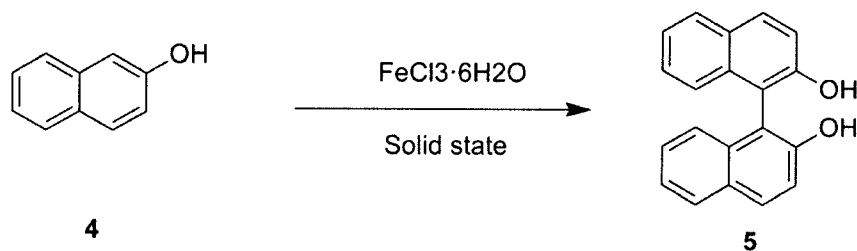


Figure 8. Schematic of the oxidative coupling of β -naphthol (**4**) to produce bis- β -naphthol (**5**) in the solid-state.

Etherification of diphenylmethanol (**6**) with TsOH (1:1) provides a final example of the impact of conducting reactions in molecular crystals. As it has been reported earlier,³⁵ solid diphenylmethanol (**6**) with TsOH (1:1) produce ether **7** in 95% yield in the

solid-state (Figure 9). In contrast, the yields for the same reaction, but in various solvents (solution-state) result in diminished yields. For example, according to Fumio Toda, when benzene was used as a solvent the observed yield for the same etherification reaction was 45% and from a methanol solution the yield was only 34%. The orientation of the biphenylmethanol molecules in the solid is limited due to strong hydrogen bonds (Figure 10) and results in a favorable distance between reactants necessary for etherification.³⁵ Due to solvation, the orientation of biphenylmethanol molecules is not restricted, even with a hydrogen bond donor-acceptor, and thus, favorable reactant orientation is not consistently maintained throughout the reaction process giving less than optimal yields.

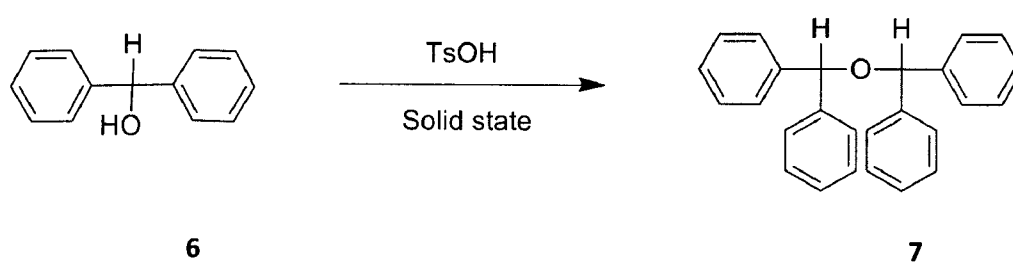


Figure 9. Solid-state etherification of diphenylmethanol (6).

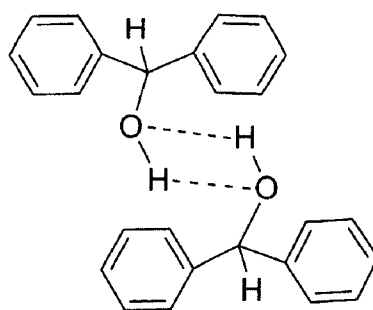


Figure 10. Hydrogen bond formation between diphenylmethanol molecules in solid-state.

1.5 [2+2] Photodimerization

[2+2] photodimerization of olefins is a “photon-induced chemical reaction in which a pair of double bonds forms a cyclobutane ring”.³⁶ In general, the formation of cyclobutane rings in the organic solid-state is largely inaccessible using conventional solution methods. Because the requirement for cyclobutane formation from olefins is the introduction of light, this reaction has much attraction as a ‘Green Chemistry’ process since it lacks solvent requirements. Woodward and Hoffmann provided the theoretical basis for the [2+2] photodimerization reaction, while Schmidt and co-workers offered insight into the geometric criteria for such solid-state processes.^{18,37} [2+2] photodimerizations are a well-known class of photoinduced cycloaddition reactions that have been extensively studied using powders with lesser attention given to single crystal studies. Because it is now commonly understood that solid-state reactions can be triggered by controlling reactant geometries, significant effort has been directed to developing strategies for organizing molecules with suitable alignment of neighboring olefins for [2+2] photodimerization reactions. Intramolecular substitution³⁸ and metal coordination⁷ are two strategies that have been successfully used to organize molecules with suitable crystal packing.

Sonoda and co-workers have used the intramolecular substitution strategy for the study of the solid-state photoreactions of ring-substituted α,ω -diphenylpolyenes (Figure 11). They reported the [2+2] photodimerization and photopolymerization of polyenes occurred in the solid state.³⁸ With the use of intramolecular ring-substitution, molecules effectively maintain the appropriate geometry and crystal packing for reactions to occur while unsubstituted adducts gave photostable arrangements.

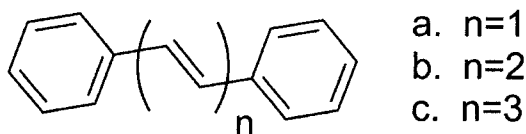


Figure 11. Chemical structures of α,ω -diphenylpolyenes a-c.

Inclusion complexes³⁹ and cocrystallization with hydrogen-bonded templates are two other strategies for generating the pre-alignment of reactants. MacGillivray's group successfully demonstrated the use of linear templates to control the organization and reactivity of solid-state [2+2] photodimerization reactions.¹ With this method, the use of small organic molecules or metal organic complexes behave as templates to direct the formation of supramolecular motifs, that when exposed to UV light, result in covalent bond formation. Effective use of the molecular template approach requires use of recognition sites (functional groups capable of hydrogen bonding) positioned on the reactant to orient molecules for reactions. Small template molecules encoded for predetermined supramolecular assembly offers a facile pathway to reactive crystalline phases that undergo photodimerization reactions in the solid-state (Figure 12).⁷

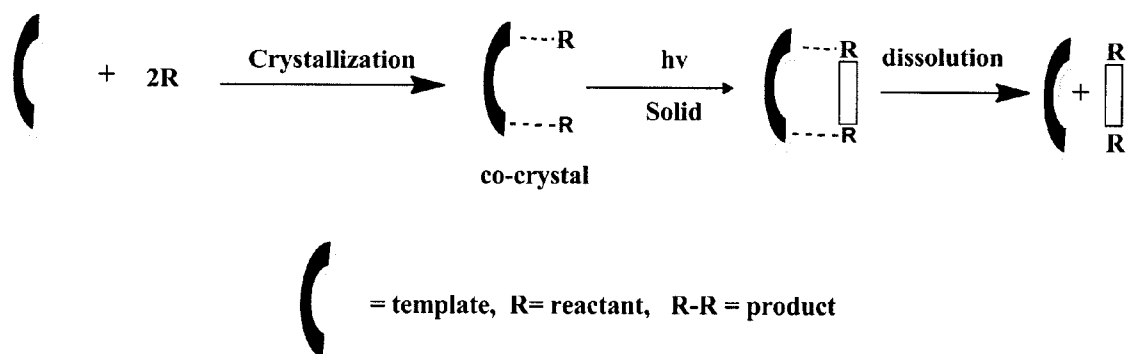


Figure 12. Use of templates to direct photodimerization reaction in molecular crystals.

Recently, MacGillivray and coworkers successfully demonstrated the use of resorcinol as a linear template to steer solid-state [2+2] photodimerizations of trans-1,2-bis(4-pyridyl)ethylene (4,4'-bpe) (Figure 13). 4,4'-bpe is photostable as a pure solid and undergoes photodimerization in solution giving multiple cyclobutane products in low yield. However, use of resorcinol as a linear template with 4,4'-bpe gave the expected photoproduct in 100% yield upon UV irradiation. In this example, resorcinol effectively behaves as the linear template that assembles two reactant molecules with favorable alignment via hydrogen bonds.¹

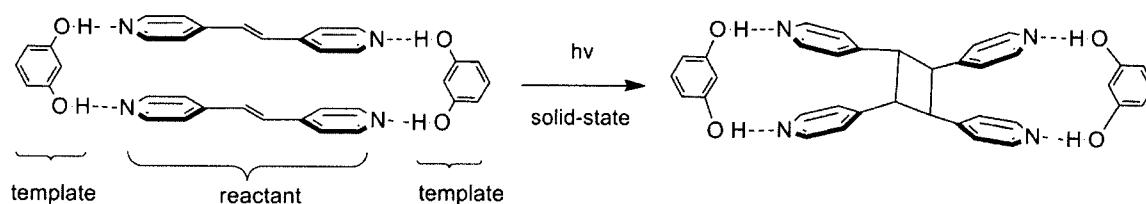


Figure 13. Template based [2+2] photodimerization of trans-1,2-bis(4-pyridyl)ethylene.

The [2+2] photodimerization of olefins can be accomplished using powders; even so, there is growing interest with transformations that begin and end as a single crystal. [2+2] photodimerization reactions that occur in single crystals are commonly referred to as single-crystal-to-single-crystal (SCSC) [2+2] photodimerizations and are well-known in organic solid-state chemistry.³⁶ SCSC reactions can occur even when the product experiences a significant amount of chemical and physical change. As such, structural information regarding the reactant and product from the same crystal offers critical insight to the reaction process. 2-Benzyl-5-benzylidenecyclopentanone (**9**) was the first compound that was reported to undergo single-crystal-to-single-crystal [2+2]

photodimerization and this reaction has proceeded in 100% yield (Figure 14) under the given conditions.^{36,40}

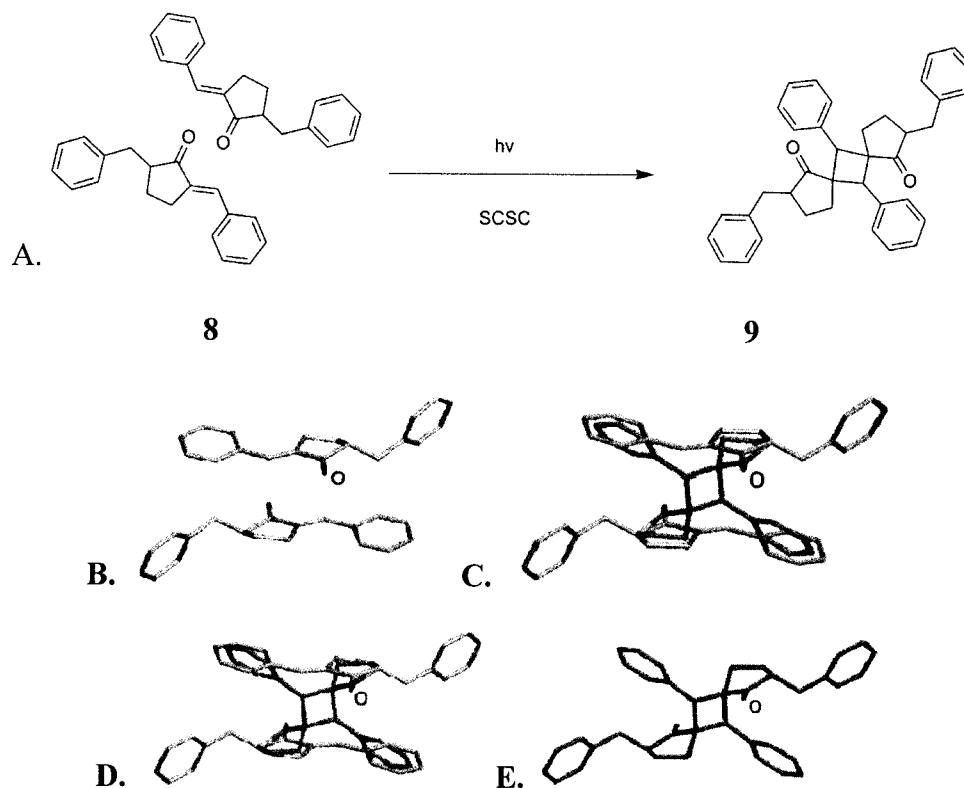


Figure 14. Schematic representation of the SCSC [2+2] photodimerization of 2-benzyl-5-benzylidenecyclopentanone: A. Crystal structures B, C, D and E represents the various stages of the photoreaction: B. 0%, C. 56%, D. 81%, and E. 100%.³⁶

Enkelman and co-workers have also explored the SCSC photodimerization of cinnamic acids and presented the first example for the homogeneous photodimerization of cinnamic acids.⁴¹ When a crystal of cinnamic acid is irradiated with the light in the maximum of its absorption spectrum, the light intensity is higher on the incident surface of the crystal. Because product formation initially occurs at the surface these product molecules absorb the UV radiation, thus producing a heterogeneous crystalline phases

(reactant and product). In contrast, when a photoactive crystal of cinnamic acid is irradiated with light with low absorption, the light intensity is even on both incident surface and throughout inner bulk of the crystal; thus product formation occurs randomly and spatial distribution of the product formation is homogeneous. Enkelman and co-workers showed this phenomenon for the α -*trans*-cinnamic acid and Figure 15 shows the projections of crystal structures at various stages of tail irradiation. Therefore, they explored the first homogeneous single-crystal-to-single-crystal photodimerization of cinnamic acids.

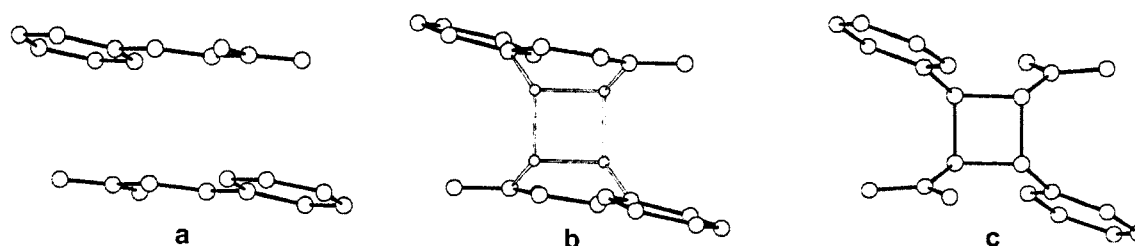


Figure 15. The crystal structures of α -*trans*-cinnamic acid at various stages of tail irradiation: a. unirradiated, b. 40% partially dimerized, c. 100% dimerized truxillic acid.

1.6 Co-crystallization and [2+2] photodimerization

Co-crystallization is a process utilized to design multiple-component assemblies. A target molecule is co-crystallized with a crystallizing agent known as a cocrystal former for the preparation of a cocrystal. In a cocrystal, the intermolecular interactions govern the molecular arrangement of the components in the solid. In 1844, Friedrich Wohler reported the first co-crystalline material constructed from hydroquinone and benzoquinone.⁴² In general, slow evaporation is widely used for the preparation of cocrystals with grinding, kneading, and solvent assisted techniques providing other routes to cocrystal formation.⁴³ One significant utility of this cocrystal approach is that for a

given target molecule, the use of different cocrystal formers often results in a set of materials that differ widely in physical properties.

Solid state chemists have applied supramolecular chemistry to engineer cocrystals with the purpose of studying topochemical reactions of olefins in solids to give cyclobutanes. Utilizing cocrystallization can provide an effective means to align reaction centers with favorable alignment for a [2+2] photodimerization. Sharma and co-workers reported the photodimerization of a two-component system (cocrystal) consisting of 2,5-dimethoxy-substituted (**10**) and 3,5-dinitro-substituted (**11**) (*E*)-cinnamic acids. This work underscored the importance of intramolecular substitution and cocrystallization to key molecular stacking of neighboring olefins necessary for [2+2] photodimerization.⁴⁴ UV illumination studies of this co-crystalline system gave **12** as the photoproduct in 60% yield (Figure 16). Since this dimerization process occurs between two chemically different compounds, this represents one of the rare examples of photochemically initiated heterodimerization using molecular crystals.

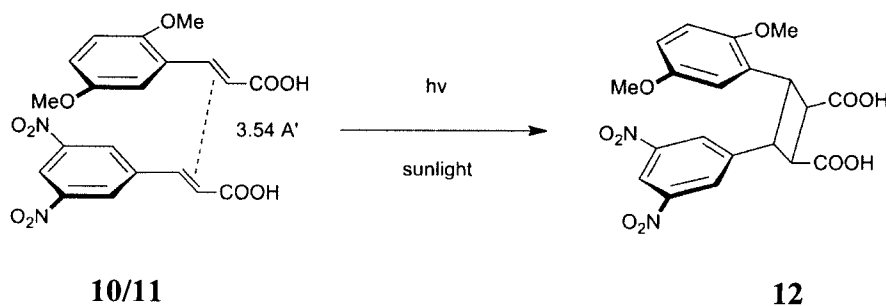


Figure 16. [2+2] photodimerization of a 1:1 cocrystal of **10** and **11**.

MacGillivray successfully demonstrated photodimerization of another class of cocrystals using linear templates. Cocrystallization of 4,4'-bpe with an equimolar amount of resorcinol gave a photoactive hydrogen bond tetramer with an olefin...olefin distance

of 3.65 Å to yield cyclobutane product from UV initiation (Figures 13 and 17).⁴⁵ Since this dimerization forms from the reaction of two 4,4'-bpe molecules, this type of process may be classified as a cocrystal assisted homodimerization.

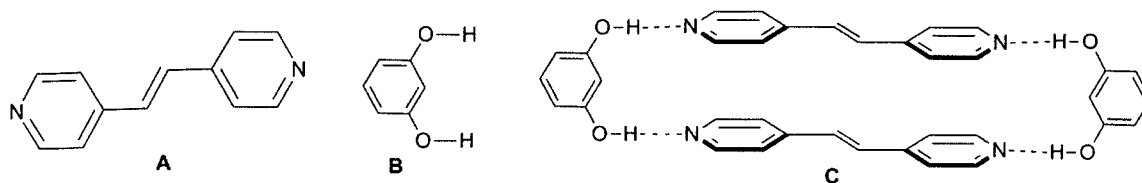
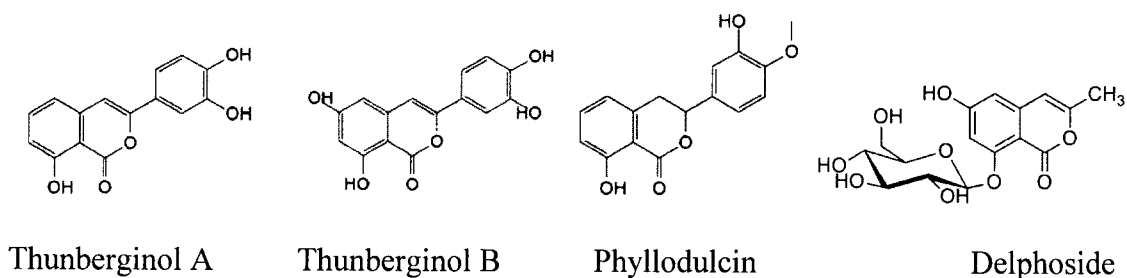


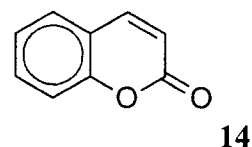
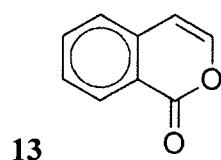
Figure 17. Structure of (A) 4,4'-bpe, (B) resorcinol and (C) hydrogen bond tetramer.

1.7 Synthesis and Photodimerization of Isocoumarin/Coumarin Containing Molecules.

Isocoumarins are naturally occurring lactones that can be isolated from a variety of microorganisms (fungi, molds and bacteria), insects, and plants and show important biological activity such as antifungal, anticoagulant, antimicrobial, antitumor, antiangiogenic, cytotoxicity and anti-inflammatory properties.^{46,8} Thunberginol A and thunberginol B are two examples of common naturally occurring isocoumarins retrieved from plant *Hydrangea macrophylla* and Phyllodulcin is yet another natural isocoumarin isolated from plant *Hydrangea serrata*. Delphoside is a natural isocoumarin that was extracted from the Delphinium plant that serves as a metabolite for the blue-stain fungi.⁴⁷



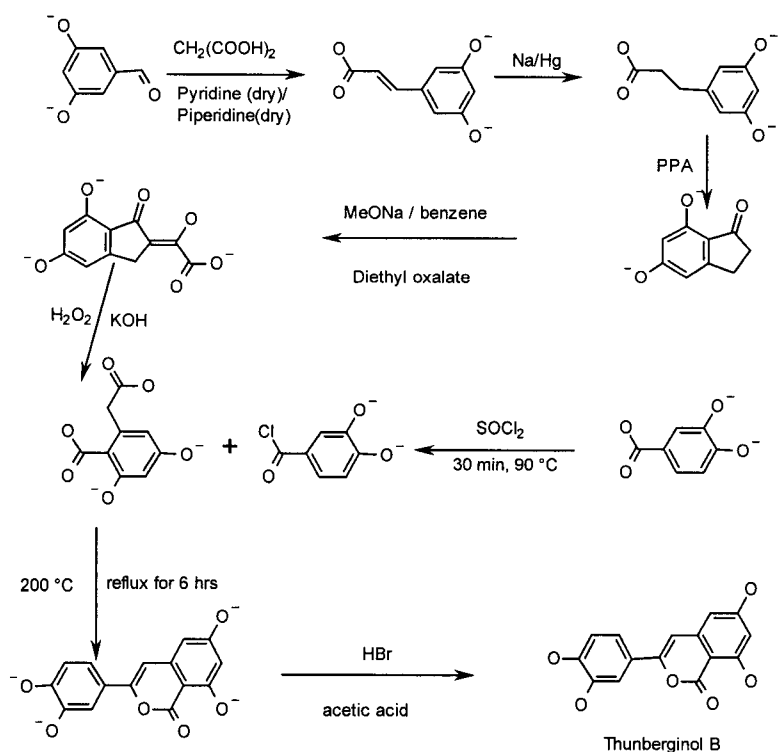
Examples of isocoumarin and coumarin frameworks are shown as **13** and **14**, respectively. Isocoumarins are also useful as key intermediates in the synthesis of important compounds such as isocarbostyrils, isochromenes, isoquinolines or pyridones.⁴⁸ The name isocoumarin is derived from the class of compounds referred to as coumarins due to their isomeric relationship. In an isocoumarin a lactonic pyran ring is fused to a benzene ring. Interestingly, structurally simple isocoumarin **13** has never been found naturally, but a wide variety of related derivatives have. Isocoumarin derivatives form by the substitution on the lactone or aromatic rings or both.



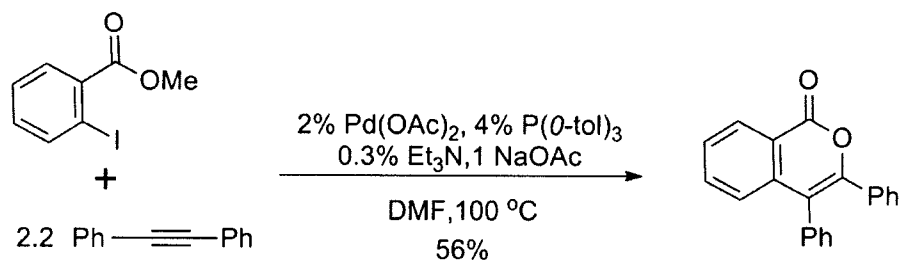
Extensive studies to understand the bioactivity and synthesis of isocoumarins have appeared in the recent literature. The collection of synthetic methods employed to date builds on a blend of classical and innovative methodologies to produce this key framework. As an example, Qadeer and co-workers synthesized natural isocoumarin based thunberginol B using 3,5-dimethoxyhomophthalic acid as a key intermediate (Scheme 2).⁸ The direct condensation of this homophthalic acid followed by demethylation with hydrobromic acid gave thunberginol B. This thunberginol B is more potent as a histamine release inhibitor. Various catalysts such as palladium, rhodium and copper are useful for the synthesis of isocoumarins. One approach for this is using a palladium catalyst for the synthesis of 3,4-disubstituted isocoumarins from internal alkynes with good yields (Scheme 3).⁴⁹ In this method, the synthesis of isocoumarins follows the annulation of internal alkynes by suitable halogen- or triflate substituted esters and the needed starting materials are readily available. Another approach is the

synthesis of isocoumarin derivatives using a copper-catalyst from 2-iodo-N-phenyl benzamides and acyclic diketones as starting materials (Scheme 4).⁵⁰ In this method, the efficient synthesis of isocoumarin derivatives follows the copper-catalyzed tandem sequential cyclization as the key step. 4-Iodoisocoumarin was prepared in an alkyne cyclization reaction using 2-(1-alkynyl)arenecarboxylate esters as the starting material (Scheme 5).⁵¹ Sonogoshira coupling of this starting material that was prepared by the commercially available 2-iodo-4,5-dimethoxybenzoic acid, with an appropriate terminal alkyne gave the intermediate *o*-(1-alkynyl)benzoates that was needed to synthesize 4-iodoisocoumarin. Electrophilic cyclization of *o*-(1-alkynyl)benzoates gave 4-iodoisocoumarin that is a key intermediate for synthesis of various isocoumarins. Therefore for the successful synthesis of isocoumarins, the above methods are very useful.

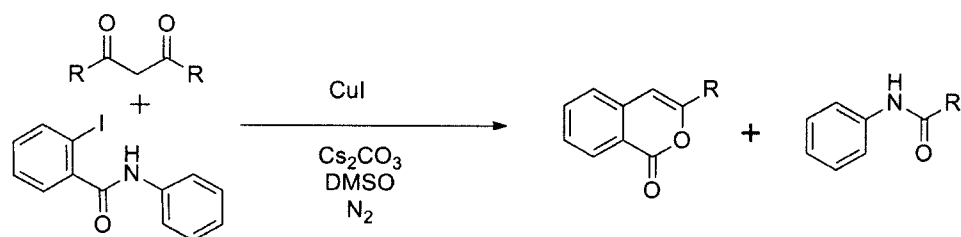
Scheme 2



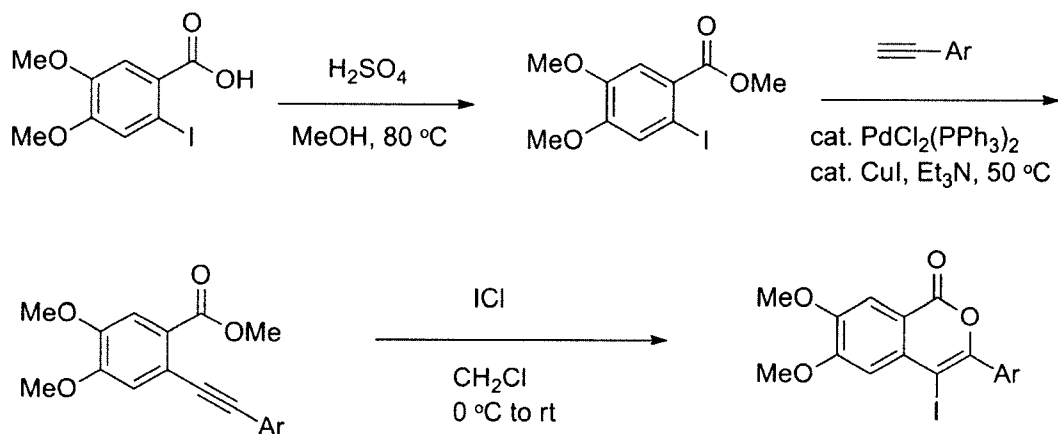
Scheme 3



Scheme 4



Scheme 5



Because of the importance of the isocoumarin/coumarin compounds in terms of a wide range of biological activities, [2+2] photodimerization of these compounds have been extensively studied in both solution and the solid state. Even with this attention,

controlling the stereo- and regioselectivity of coumarin photodimerization from either solution or solid-state processes remains a considerable challenge. For example, Yu and co-workers reported that direct photodimerization of coumarin in benzene solution gave mixtures of four isomeric products (i.e. *syn-head-head*, *anti-head-head*, *syn-head-tail*, and *anti-head-tail*) with a ratio of 2.3:91.2:2.3:4.2 in low conversion (9%) (Figure 18).⁵² Ramamurthy and Venkatesan further studied the solid-state photodimerization of coumarins and showed that use of appropriate substituents can direct reactant molecules into favorable crystal packing for successful photoreactions.⁵³

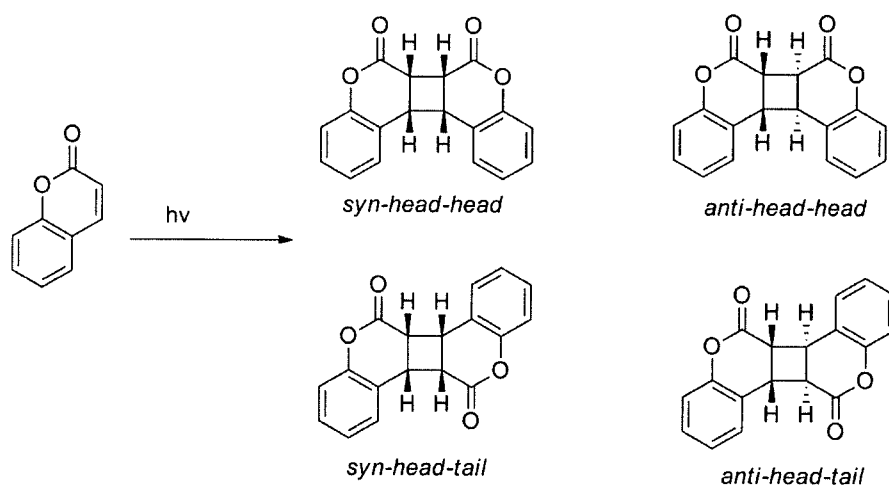


Figure 18. Photodimerization of coumarin in benzene.

Recently, supramolecular hosts such as β -cyclodextrin, cucurbituril, a Pd-nanocage, a bis-urea macrocycle and diacetylenediols have been used successfully to control coumarin photodimerization with inclusion crystals from chiral host compounds providing a unique strategy to enantioselective coumarin photodimerizations. Yu and co-workers studied the enantioselective photodimerization in the context of solid coumarin-cyclodextrin inclusion complexes (Figure 19).^{39,52} This example indicated that

photoirradiation of the inclusion complex gave the dimeric *syn-head-head* product with a 64% yield from the solid-state and 20% yield when irradiated in water.

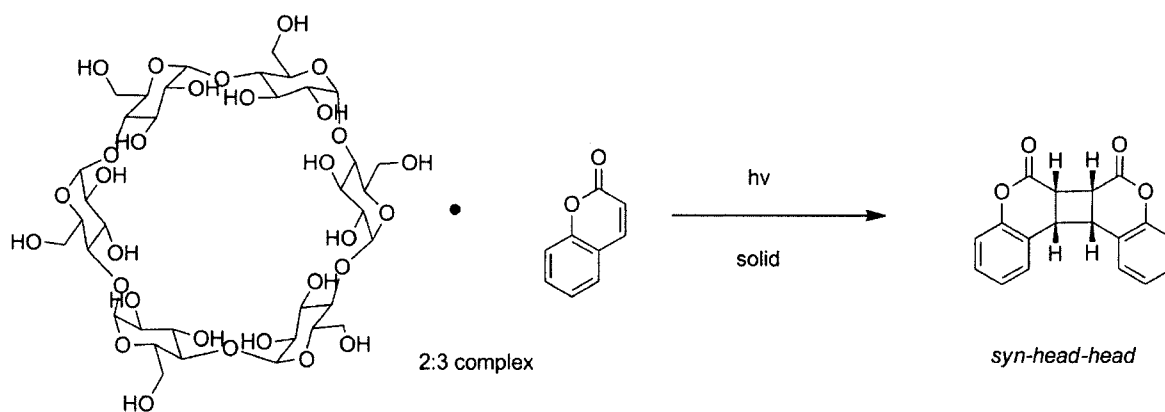


Figure 19. Photodimerization of 2:3 inclusion complex of β -cyclodextrin and coumarin.

Tanaka, Toda and co-workers discovered the successful regio- and stereoselective single-crystal-to-single-crystal photodimerization of coumarin **14** and thiocoumarin **15** using host diols **16** and **17** (Figure 20).⁵⁴ Irradiation of a 1:1 inclusion complex of coumarin **14** and (-)-**16** in the solid-state proceeded via a single crystal transformation to give the 2:1 complex of (-)-**16** and the optically active *anti-head-head* dimer (-)-**18**. Recrystallization of the 2:1 complex from DMF- H_2O gave *anti-head-head* dimer as colorless needles in 99% yield and 100% ee. The X-ray crystallography studies of reaction behavior showed that two molecules of coumarin **14** formed hydrogen bonds to host molecule **16** and resulted in the *anti-head-head* dimer (-)-**18** after photoirradiation. The authors speculate that the favorable geometry between reacting olefins (3.59 and 3.42 Å) provide a key structure-property relationship for this [2+2] photoreaction (Figure 21 and 22). In another example Moorthy and Venkatesan investigated the solid-state photodimerization of coumarin in solid inclusion complexes with two diacetylenediols 1,1,6,6-tetraphenylhexa-2,4-diyne-1,6-diol (**20**) and (S,S)-1,6-bis(o-chlorophenyl)-1,6-

diphenyl-hexa-2,4-diyne-1,6-diol (**21**). They observed that inclusion of coumarin **14** with achiral host **20** gave a photoinert material; however, complexation with chiral host **21** gave a *syn-head-head* dimer in 100% yield (Figure 23).⁵⁵

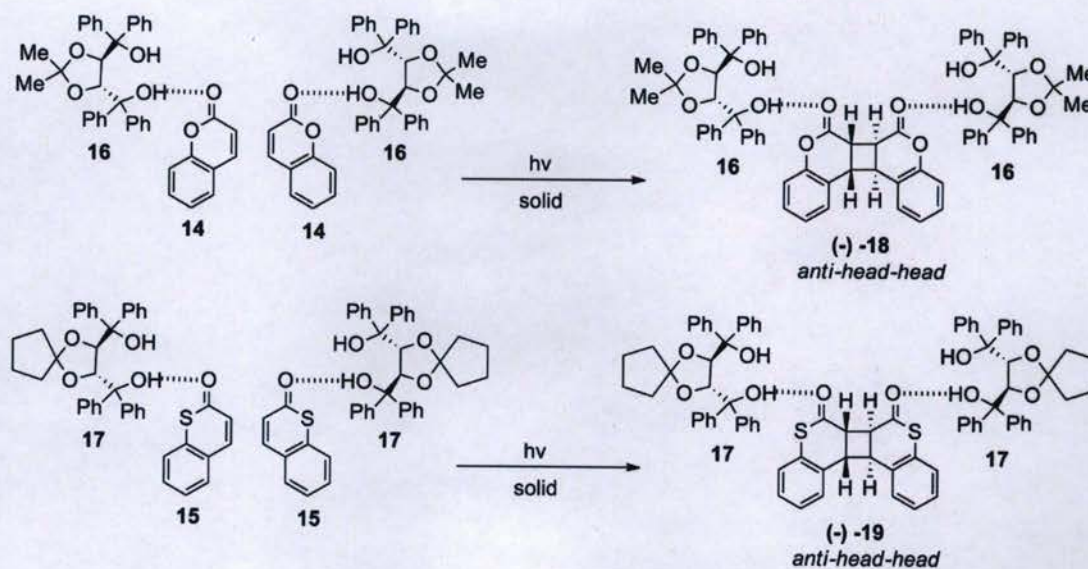


Figure 20. Single-crystal photodimerization of coumarin inclusion crystals.

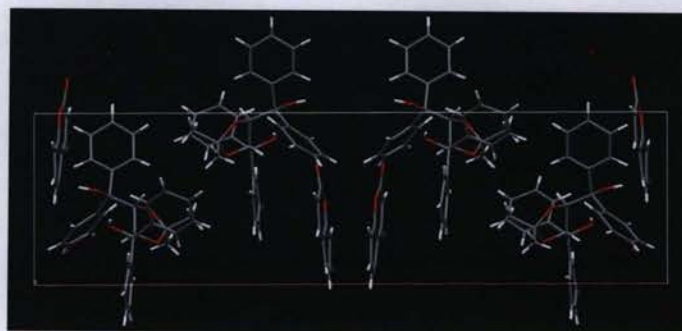


Figure 21. X-ray crystal structure of 1:1 inclusion complex of coumarin **14** and **(-) -16**.

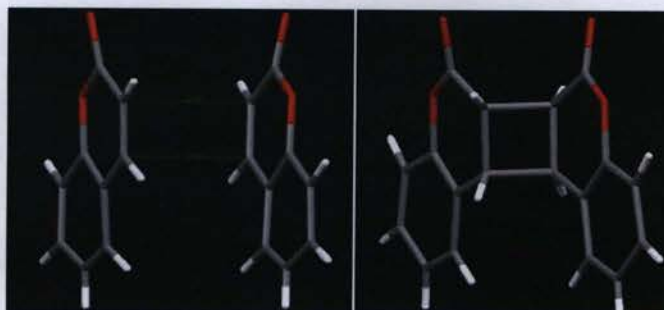


Figure 22. Orientation of coumarin (left) and the *anti-head-head* dimer (-)-**18** (right).

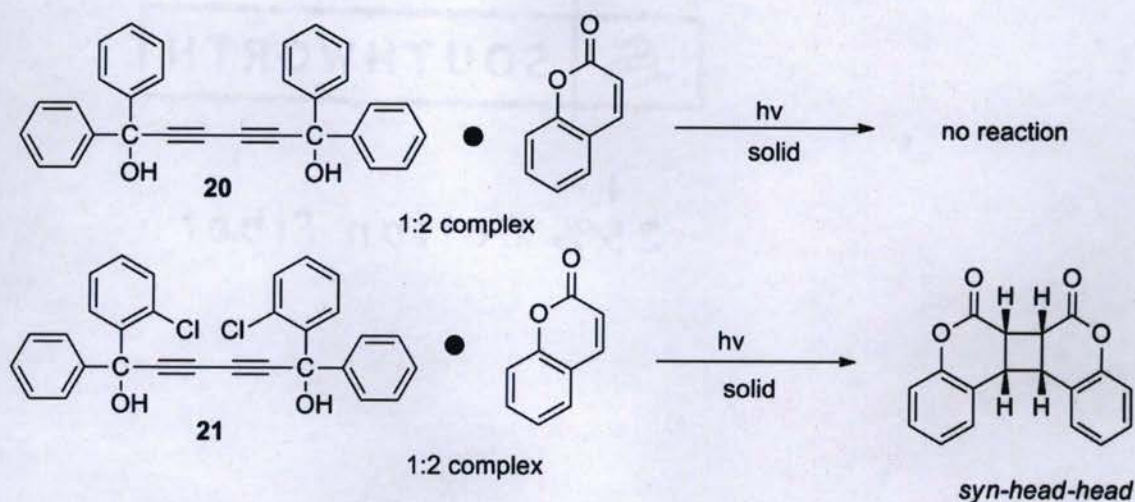


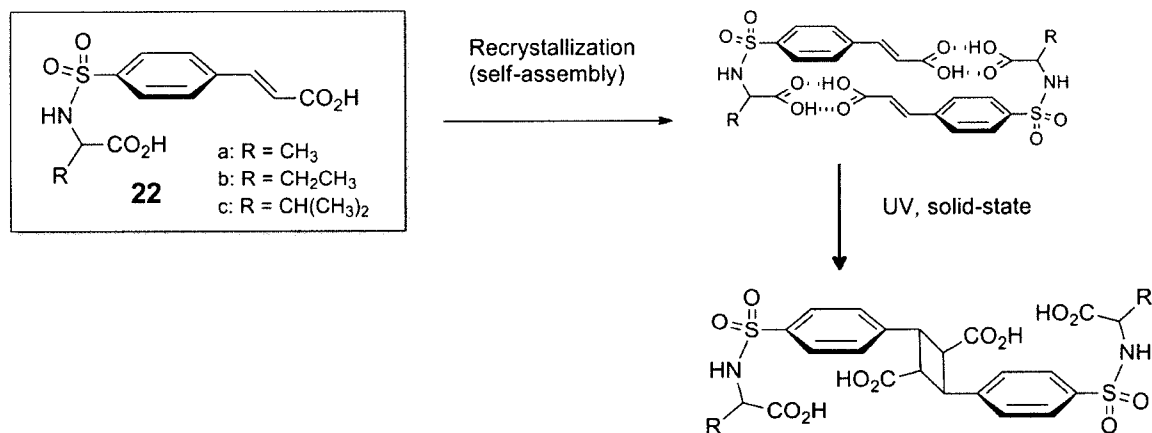
Figure 23. Photodimerization of coumarins inside inclusion crystals with diacetylenediols.

1.8 Synopsis of Thesis Work

This thesis investigates the synthesis and photodimerization of isocoumarin derivatives. Although the approach of MacGillivray is useful to control the organization of molecular crystals for photodimerization reactions, their method is limited to achiral starting materials and requires use of secondary template molecules. Therefore, chiral synthesis that lack templates would offer considerable advantage for access to next generation solid-state reactions. Research conducted in the Wheeler group recently

focused on [2+2] photodimerization reactions of olefins. Over the last few years work here at EIU has involved investigating a family of cinnamylsulfonamides that self-assemble to give photoreactive dimers.⁵⁶ As shown in the Scheme 6, the target sulfonamidecinnamic acids (**22**) can form dimeric molecular assemblies by recrystallization. Exploration of the supramolecular behavior of these systems and their photochemical behavior moved beyond simple racemic forms to include both quasiracemic and homochiral single component building blocks to construct chiral motifs.⁵⁶ Each of these compounds undergoes topochemically controlled single-crystal-to-single-crystal photodimerization reactions in good yield (61-100% conversion) to give homochiral photodimers and enantiocontrolled outcomes in the case of quasiracemates and single component homochiral phases.

Scheme 6



Work presented in this thesis explored two areas that seek to further understand the role of ‘fish hook’ shaped molecules to the construction of photoactive supramolecular assemblies. The first study goes beyond current technology and utilizes a co-crystalline approach to construct molecular assemblies capable of heterodimerization.

The design strategy for these materials includes use of complementary non-bonded contacts, arylsulfonamide frameworks, and two significantly different olefin containing compounds (Figure 24). Pilot studies of the co-crystalline tendencies of sulfonamidedecinnamic acid **23** showed successful inclusion of bipyridines **24** and **25**. Crystallographic investigation of these materials showed the desired tetrameric motifs assembled by use of strong $\text{CO}_2\text{H}\cdots\text{N}$ interactions. Though the bipyridine components are photostable, these initial investigations provided critical structural support for other olefin containing compounds such as **26** and **23·26**. Though compound **26** is photostable, it is possible this material could be converted to a photoreactive phase by cocrystallizing with compound **23** and forming the desired tetrameric assembly (**23·26**). Subsequent crystallographic assessment of this system does indeed show the anticipated supramolecular tetramer; however, UV illumination of **23·26** lacks solid-state reactivity to photoproduct **27** due to unfavorable $\text{C}=\text{C}\cdots\text{C}=\text{C}$ contacts in the crystal structure.

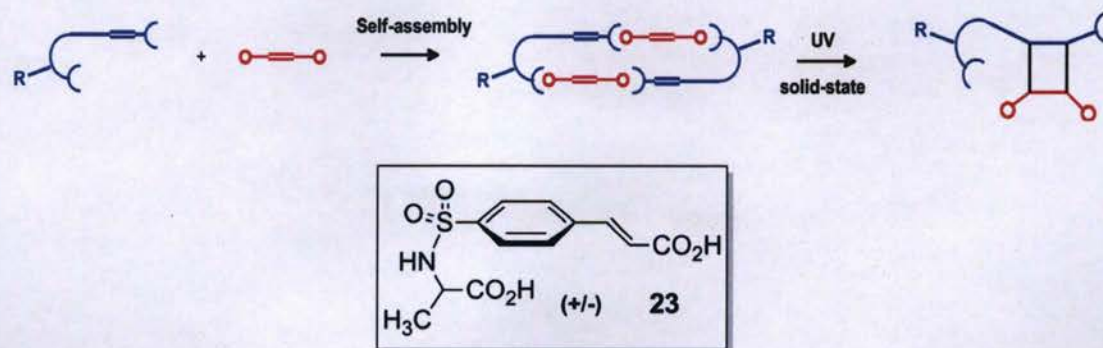
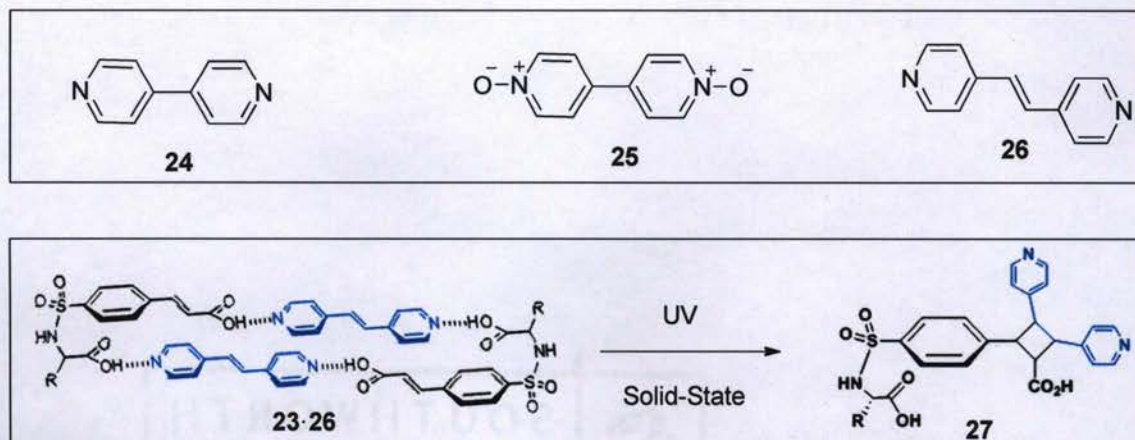


Figure 24. Design strategy (top) and molecular target (bottom) for the exploring heterodimerization between different olefin compounds.



The possibility of including a second molecule in the lattice of **23** that could yield a hydrogen-bonded tetramer and photoactive phase is still interesting (Figure 25). For this reason we also explored the possibility of using dimethyl fumaramate (**28**) as a target component for the construction of a hydrogen-bonded tetramer with **23**. Further studies of the photochemical behavior of **28** to obtain product **29** were also of interest (Scheme 7). Though unsuccessful, this exercise emphasized i) the complexity of assembling two distinct crystal components and ii) the design criteria necessary to construct bimolecular systems with functional properties.

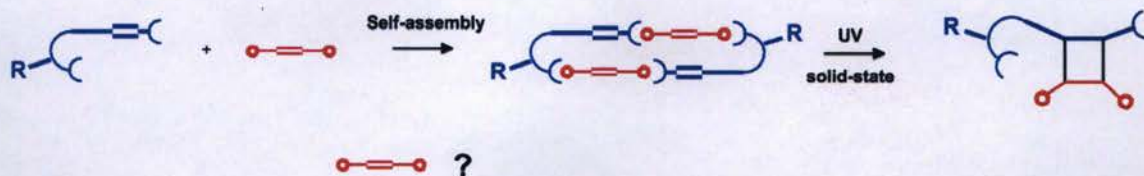
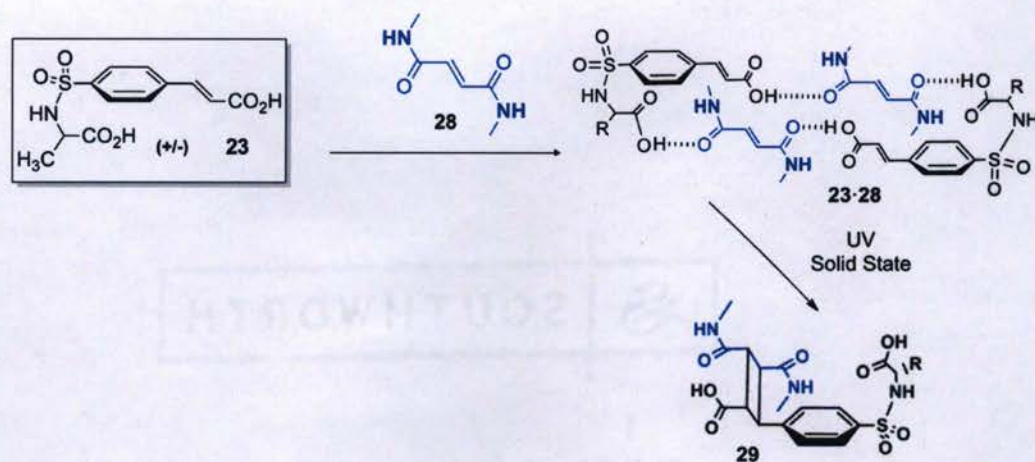


Figure 25. Design strategy of hydrogen bond tetramer formation.

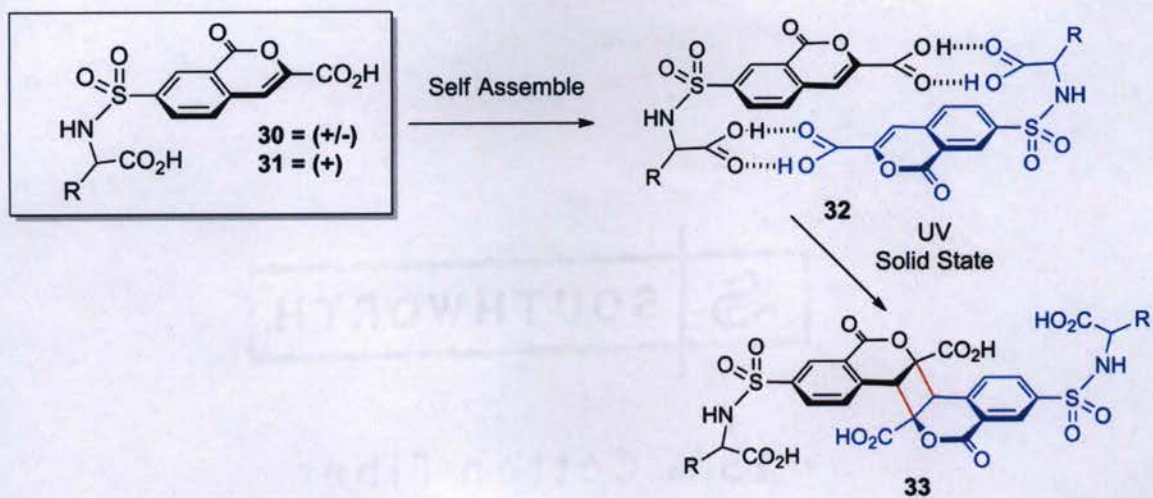
Scheme 7



The family of previously studied sulfonamidecinnamic acids has provided notable opportunities to explore the role of molecular shape and crystalline motifs to the generation of photoactive solid-state materials. Moving beyond these initial investigations to include new molecular architectures offers much value to understand the structure-property relationships for these aryl sulfonamides and also the design of next generation materials.

In a second study, this thesis looked at the synthesis and solid-state [2+2] photodimerization reactions of isocoumarin derivatives with sulfonamide-amino acid moieties. Sulfonamide isocoumarin compounds **30** and **31** are structurally similar to the original cinnamic acid derivative **23**. The synthesis of **30/31** followed a five-step sequence and subsequent studies into the crystal structures and photochemistry of this material provided access to the expected photoproduct **33** (Scheme 8).

Scheme 8



1.9 References

1. Friscic, T.; Drab, D. M.; MacGillivray, L. R. *Org. Lett.* **2004**, *6*, 4647-4650.
2. Petrucci, R. H.; Harwood, W. S.; Herring, F. G.; Madura, J. D. *General Chemistry Principles and Modern Applications*; 9th ed.; Pearson Education, Inc; New Jersey, 2007.
3. Schummer, J. *Stud. Hist. Phil. Sci.* **2003**, *34*, 705-736.
4. Gillespie, R. J.; Robinson, E. A. *J. Comput. Chem.* **2007**, *28*, 87-97.
5. Ingold, C. K. *Chem. Rev.* **1934**, *15*, 225-274.
6. Sneader, W. *British Med. J.* **2000**, *321*, 1591-1594.
7. MacGillivray, L. R.; Papaefstathiou, G. S.; Friscic, T.; Hamilton, T. D.; Bucar, D.; Chu, Q.; Varshney, D. B.; Geogiev, I. G. *Acc. Chem. Res.* **2008**, *41*, 280-291.
8. Qadeer, G.; Rama, N. H.; Shah, S. J. H. *J. Arkivoc.* **2007**, *14*, 12-19.
9. Asgarpanah, J.; Kazemivash, N. *Afr. J. Pharm. Pharmacol.* **2012**, *6*, 2340-2345.
10. Desiraju, G. R. *Nature* **2001**, *412*, 397-400.
11. Desiraju, G. R. *Angew. Chem. Int. Ed. Engl.* **1995**, *34*, 2311-2327.
12. Lehn, J.-M. *Supramolecular Chemistry: Concepts and Perspectives*, VCH; Weinheim, 1995.
13. Desiraju, G. R. *J. Chem. Sci.* **2010**, *122*, 667-675.
14. Desiraju, G. R.; Steiner, T. *The Weak Hydrogen Bond in Structural Chemistry and Biology*, Oxford Univ. Press; Oxford, 1999.
15. Stryer, L. *Biochemistry*; 4th ed.; W.H. Freeman and Company; New York, 1995.
16. Desiraju, G. R. *Angew. Chem. Int. Ed. Engl.* **2007**, *46*, 8342-8356.

17. Shattock, T. R.; Arora, K. K.; Vishweshwar, P.; Zaworotko, M. J. *Cryst. Growth Des.* **2008**, *8*, 4533-4545.
18. Cohen, M.; Schmidt, G. M. J. *J. Chem. Soc.* **1964**, 1996-2000.
19. Braga, D.; D'Addario, D.; Giaffreda, S. L.; Maini, L.; Polito, M.; Grepioni, F. *Top. Curr. Chem.* **2005**, *254*, 71-94.
20. Braga, D.; D'Addario, D.; Maini, L.; Polito, M.; Giaffreda, S.; Rubini, K.; Grepioni, F. *Applications of Crystal Engineering Strategies in Solvent-free Reactions: Toward a Supramolecular Green Chemistry*; Tiekink, E. R. T.; Vittal, J. J. Ed.; John Wiley & Sons, Ltd: Chichester, UK. 2006.
21. Sun, Q.; Wang, Y.; Cheng, A.; Wang, K.; Gao, E. *Cryst. Growth. Des.* **2012**, *12*, 2234-2241.
22. Li, S.; Xiao, T.; Lin, C.; Wang, L. *Chem. Soc. Rev.* **2012**, *41*, 5950-5968.
23. Bragg, W. H. *Proc. Phys. Soc.* **1921**, *34*, 33.
24. Ermer, O. *J. Am. Chem. Soc.* **1988**, *110*, 3141-3154.
25. Anderson, A. M.; Goeta, A. E.; Steed, J. W. *Cryst. Growth. Des.* **2008**, *8*, 2517-2524.
26. Desiraju, G. R. *J. Mol. Struct.* **2003**, *656*, 5-15.
27. http://www4.rgu.ac.uk/pharmacy_life/aboutus/page.cfm?pge=74924, accessed 2012/10/01.
28. Sekhon, B. S. *Ars Pharm*, **2009**, *50*, 99-117.
29. Braga, D.; Grepioni, F. *Angew. Chem. Int. Ed.* **2004**, *43*, 4002-4011.
30. MacGillivray, L. R. *J. Org. Chem.* **2008**, *73*, 3311-3317.
31. Allen, F. H.; Mahon, M. F.; Raithby, P. R.; Shields, G. P.; Sparkes, H. A. *New. J. Chem.* **2005**, *29*, 182-187.

- 32 . Fumo, T. *Organic solid-state reactions*, Kluwer Academic. Publishers: Dordrecht, 2002.
33. Tanaka, K; Shiraishi, R.; Toda, R. *J. Chem. Soc., Perkin Trans.* **1999**, *1*, 3069-3070.
34. Toda, F.; Tanaka, K.; Iwata, S. *J. Org. Chem.* **1989**, *54*, 3007-3009.
35. (a) Toda, F.; Takumi, H.; Akehi, M. *J. Chem. Soc., Chem. Commun.* 1990, 18, 1270-1271. (b) Toda, F.; Okuda, K. *J. Chem. Soc., Chem. Commun.* **1991**, *17*, 1212-1214.
36. Friscic, T.; MacGillivray, L. R. *Z. Kristallogr.* **2005**, *220*, 351–363.
37. Vollmer, J. J.; Servisl, K. L. *J. Chem. Ed.* **1970**, *47*, 491-500.
38. Sonoda, Y. *Molecules.* **2011**, *16*, 119-148.
39. Moorthy, J. N.; Venkatesan, K.; Weiss, R. G. *J. Org. Chem.* **1992**, *57*, 3292-3297.
40. Nakanishl, H.; Jones, W.; Thomas, J. M.; Hursthouse, M. B.; Motevalll, M. *J. Phys. Chem.* **1981**, *85*, 3636-3642.
41. Enkelmann, V.; Wegner, G.; Novak, K.; Wagener, K. B. *J. Am. Chem. Soc.* **1993**, *115*, 10390-10391.
42. Wohler, F. *Annalen.* **1844**, *51*, 153.
43. Berry, D. J.; Seaton, C. C.; Clegg, W.; Harrington, R. W.; Coles, S. J.; Horton, P. N.; Hursthouse, M. B.; Storey, R. S.; Jones, W.; Friscic, T.; Blagden, N. *Cryst. Growth. Des.* **2008**, *8*, 1697-1712.
44. Sharma, K. C. V.; Panneerselvam, K.; Shimoni, L.; Katz, H.; Camell, H. L.; Gesiraju, G. R. *J. Chem. Mater.* **1994**, *6*, 1282-1292.
45. Friscic, T.; Hamilton, T. D.; Papaefstathiou, G. S.; MacGillivray, L. R. *J. Chem. Ed.* **2005**, *82*, 1679-1681.
46. Hagiwara, H.; Fujimoto, N.; Suzuki, T.; Ando, M. *Heterocycles*, **2000**, *53*, 549-552.

47. Aamer, S. *Chinese J. Chem.*, **2005**, *23*, 762-766.
48. Peuchmaur, M.; Lisowski, W.; Gandreuil, C.; Maillard, L.T.; Martinez, J.; Hernandez, J.F. *J. Org. Chem.* **2009**, *74*, 4158-4165.
49. Larock, R. C.; Doty, M. J.; Han, X. *J. Org. Chem.* **1999**, *64*, 8770-8779.
50. Kavala, V.; Wang, C. C.; Barange, D. K.; Kuo, C. W.; Lei, P.; Yao, C. F. *J. Org. Chem.* **2012**, *77*, 5022-5029.
51. Roy, S.; Neuenswander, B.; Hill, D.; Larock, R. C. *J. Comb. Chem.* **2009**, *11*, 1128-1135.
52. Yu, X.; Scheller, D.; Rademacher, O.; Wolff, T. *J. Org. Chem.* **2003**, *68*, 7386-7399.
53. Gnanaguru, K.; Ramasubbu, N.; Venkatesan, K.; Ramamurthy, V. *J. Org. Chem.* **1985**, *50*, 2337-2346.
54. Tanaka, K.; Mochizuki, E.; Yasui, N.; Kai, Y.; Miyahara, I.; Hirotsu, K.; Toda, F. *Tetrahedron* **2000**, *56*, 6853-6865.
55. Moorthy, J. N.; Venkatesan, K. *J. Org. Chem.* **1991**, *56*, 6957-6960.
56. (a) Grove, R. C.; Malehorn, S.H.; Breen, M. E.; Wheeler, K. A. *Chem. Commun.* **2010**, *46*, 7322-7324. (b) Wheeler, K. A.; Wiseman, J. D.; Grove, R. C. *Cryst. Eng. Comm.* **2011**, *13*, 3134-3137.

CHAPTER 2: EXPERIMENTAL

2.1 General Considerations

All chemicals and solvents were purchased from the Aldrich Chemical Company or Acros Chemicals and used without further purification. Melting point measurements were obtained by using a Mel-Temp apparatus. Chromatography purifications were performed using silica gel 60 (Acros Organics, 40-60 μm). Thin-layer chromatography (TLC) was performed on silica-gel plates w/UV254 (200 μm). Chromatograms were visualized by UV-light. ^1H and ^{13}C -NMR spectral data were recorded using a 400 MHz Bruker Avance NMR spectrometer using TopSpin v.2.1. The chemical shift values are expressed as δ values (ppm) and the value of coupling constants (J) in Hertz (Hz). The following abbreviations were used for signal multiplicities: s, singlet; d, doublet; dd, doublet of doublets; t, triplet; q, quartet; m, multiplet. For the recrystallization experiments, slow evaporation and vapor diffusion techniques were performed at room temperature using reagent-grade solvents.

2.2 Photochemical Studies

Photoirradiation studies were conducted as previously described¹ and were carried out at room temperature (296 K) using a focused 200 W Xe(Hg) arc lamp (Newport Corp., 67005, 6292) equipped with a 360 nm optical edge filter (Newport Corp., CGA-360). Photodimerization conversion of **30** was assessed via X-ray diffraction of irradiated single crystals that indicated quantitative conversion to photoproduct. Due to significant crystal fracturing of **31** during the UV illumination process, evaluation of this transformation was not practical and thus further investigation of the photodimerization

was conducted using polycrystalline samples with a 360 nm optical edge filtered radiation. During the illumination period, samples were periodically assessed with ^1H NMR spectroscopy after 2.0, 8.5, and 56.5 hours.

2.3 X-ray Crystallography

Polarized light microscopy was used to assess crystal quality with a single crystal mounted on a glass fiber affixed to a brass pin using cyanoacrylate adhesive. The sample was then attached to a Huber XYZ-goniometer head (Model 1004) for subsequent diffraction studies. X-ray diffraction data for crystals were collected using a Bruker APEX-II equipped with a graphite-monochromator using Cu K α radiation ($\lambda = 1.54178$ Å). All structure solutions and refinements were performed using X-SEED² software equipped with SHELXS.³ Data was reduced using the XSCANS software package.⁴ Empirical absorption corrections were applied using SADABS.⁵ All non-hydrogen atoms were refined anisotropically by full-matrix least-squares. H-atoms were located in difference density maps or they were calculated using C-H distance criteria. H-atoms of OH and NH were refined isotropically with O/N-H distances restrained to 0.84 Å. The remaining H atoms were positioned in idealized geometric positions with $U_{\text{iso}} = 1.2 U_{\text{eq}}$ of the atom to which they were bonded (for $U_{\text{iso}} = 1.5 U_{\text{eq}}$ for methyl groups). The data were reduced ($I \rightarrow |F_o|$) by applying Lorents- Polarization (Lp) corrections. The structure factor had the form $|F_o| = (1/Lp)^{1/2}$ where Lp is defined as follows:

$$Lp = \frac{1 + \cos^2 2\theta}{2 \sin 2\theta}$$

Data were sorted and equivalent reflections averaged using the XPREP program.

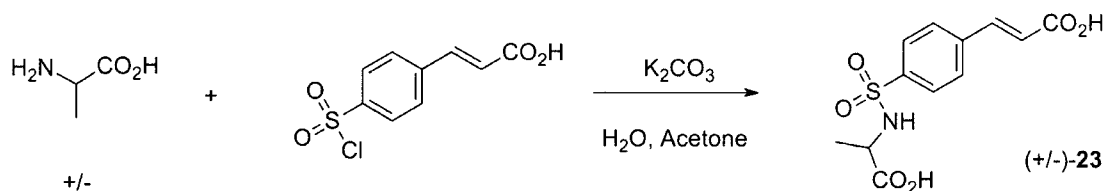
The agreement factor, R_{int} , for the equivalent reflections was calculated using:

$$R_{\text{int}} = \frac{\sum |F_0^2 - F_0^2(\text{mean})|}{\sum F_0^2}$$

The details for all these crystal data collections and structure refinements, atomic coordinates, atomic displacement parameters, geometric parameters, and hydrogen bond geometry of all crystal structures are included in Tables 1 – 8. These tables are presented in the appendix section of this thesis.

2.4 Preparation of Cocrystalline Materials

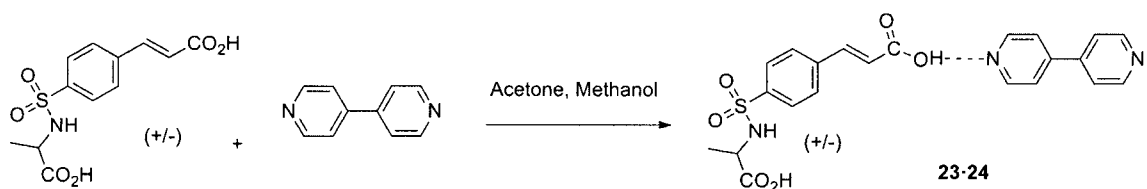
Synthesis of (+/-)-2-[[4-[(E)-3-hydroxy-3-oxo-prop-1-enyl]phenyl]sulfonylamino]-propanoic acid (**23**).



Compound (+/-)-**23** was prepared using a parallel procedure as described previously for sulfonamidecinnamic acids.⁶ To a 250 mL round bottom flask, DL-alanine (0.536 g, 6.022 mmol), 4-chlorosulfonylcinnamic acid (1.510 g, 6.302 mmol), 75 mL of reagent-grade acetone and 25 mL of distilled water were added. This mixture was stirred at 0°C for 10 minutes to give a light-yellow heterogeneous mixture. A solution of K_2CO_3 (2.561 g, 18.522 mmol) dissolved in 20 mL of deionized H_2O was then added to the reaction flask via an addition funnel over a 20 minute period. Upon complete addition of the base, the reaction mixture appeared as a homogeneous light-yellow solution that was allowed to stir at 0°C for an additional six hours. Reaction progress was assessed via TLC (10:30:1; hexane, EtOAc, AcOH) showing the presence of both product ($R_f = 0.53$), DL-

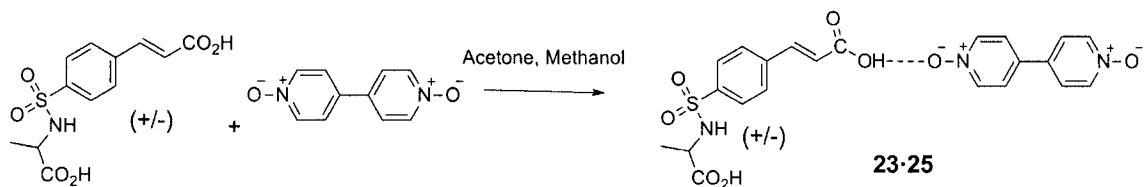
alanine (0.0) and sulfonyl chloride ($R_f = 0.78$). Acetone from the reaction mixture was removed under vacuo (rotovap, 30°C water bath). The resulting light-yellow homogeneous aqueous layer was cooled to 0°C and acidified (pH= 2-3) using 6 M HCl (~50 drops). The acidified aqueous layer was extracted with 3x25 mL EtOAc. The combined organic extracts were dried over anhydrous $MgSO_4$ and reduced under vacuo (rotovap, 30°C water bath) to give (+/-)-**23** as a light-yellow solid (0.823 g, 2.741mmol, 45.52%).

1:1 Co-crystal of 4,4'-dipyridyl (**24**) and (+/-)-**23**



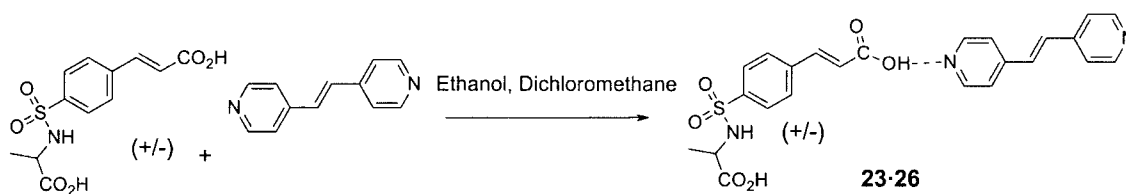
To a 25 mL Erlenmeyer flask was added 4,4'-dipyridyl (0.014 g, 0.091 mmol) and compound (+/-)-**23** (0.030 g, 0.091 mmol). The mixture was dissolved in a solution of acetone (6 mL) and methanol (1 mL), and filtered into a 4 dram vial using a mini column consisting of a Pasteur pipet, glass wool plug, and 3 cm of silica gel to give a clear solution. The resulting clear light-yellow solution was allowed to recrystallize by slow evaporation at room temperature to give light-yellow crystals with needle morphologies.

1:1 Co-crystal of 4,4'-dipyridyl- N,N' -dioxide dihydrate (**25**) and (+/-)-**23**



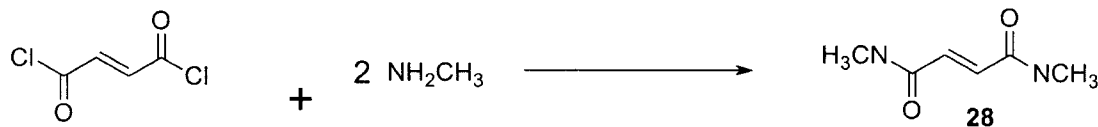
To a 25 mL Erlenmeyer flask was added 4, 4'-dipyridyl-N,N'-dioxide dihydrate (0.050 g, 0.222 mmol) and compound (+/-)-**23** (0.067 g, 0.222 mmol). The mixture was dissolved in a solution of acetone (12 mL) and methanol (8 mL). The resulting light yellow clear solution was added into a 4 dram vial and recrystallized by slow evaporation at room temperature to give light-brown crystals with needle morphologies.

1:1 Co-crystal of *trans*-1,2-bis(4-pyridyl)ethylene (**26**) and (+/-)-**23**



To a 25 mL Erlenmeyer flask, *trans*-1,2-bis(4-pyridyl)ethylene (0.050 g, 0.274 mmol) and compound (+/-)-**23** (0.822 g, 0.274 mmol) were added. The mixture was dissolved in a solvent mixture of ethanol (8 mL) and CH₂Cl₂ (8 mL) and heated to ~60°C for five minutes to get a homogeneous clear solution. The resulting solution was added into a 4 dram vial and recrystallized by slow evaporation at room temperature to give light-yellow crystals with prism morphologies.

Synthesis of (E)-but-2-enediamide (**28**).



In a 50 mL round bottom flask (long neck), fumaryl chloride (1 mL, 9.218 mmol, 1.0 eqv.) was dissolved in 5 mL of anhydrous Et₂O, and CH₃NH₂ (2 M, 23.0451 mmol, 2.5 eqv.) was added on a ice bath. A white solid was formed in a yellow color solution. The mixture was stirred one hour at room temperature and filtered and washed with ethyl

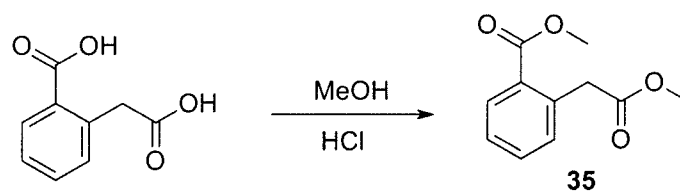
acetate to give (E)-but-2-enediamide (**28**) as an a white solid (1.1907 g, 90.96% yield). ¹H-NMR (400 MHz, CDCl₃): δ 8.34 (m, 2H, NH); 6.77 (s, 2H, C_{sp2}-H); 1.37 (d, *J* = 4.76 Hz, 6H, CH₃).

Crystal growth studies of (E)-but-2-enediamide (**28**).

In a 25 mL Erlenmeyer flask, (E)-but-2-enediamide (0.020 g, 0.141 mmol) was dissolved in methanol (5 mL) to get a homogeneous light-yellow solution. The resulting solution was added into a 4 dram vial and recrystallized by slow evaporation at room temperature to give colorless crystals with rod morphologies.

2.5 Preparation of Isocoumarin Precursors and Compounds

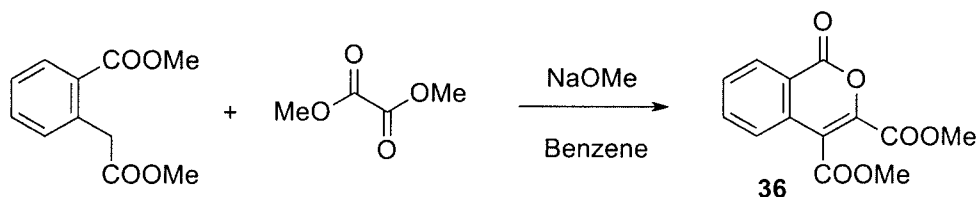
Synthesis of methyl 2-(2-methoxy-2-oxo-ethyl)benzoate (**35**).⁷



To a 500 mL round bottom flask was added homophthalic acid (30.001 g, 166.552 mmol), MeOH (140 mL, 593 mmol) and concentrated HCl (6 mL, 408.723 mmol). The mixture was stirred at reflux for 72 hours. MeOH was removed under *vacuo* (rotvap 30°C water bath). The remaining mixture was placed in a 500 mL separatory funnel with saturated NaHCO₃ (100 mL) and extracted with 2x50 mL CH₂Cl₂. The combined organic layers were washed with deionized water (100 mL), brine (100 mL), dried over anhydrous MgSO₄, and then reduced under *vacuo* (rotovap) to give **35** as a yellow oil (31.724 g, 152.50 mmol, 91.6%). ¹H NMR (400 MHz, acetone-*d*₆): δ 8.02 (dd, *J* = 7.8,

1.4 Hz, 1H, Ar-H); 7.49 (dt, $J = 7.5, 1.4$ Hz, 1H, Ar-H); 7.37 (dt, $J = 7.68, 1.3$ Hz, 1H, Ar-H); 7.26 (d, $J = 7.56$ Hz, 1H, Ar-H); 4.01 (s, 2H, C_{sp3}-H); 3.87 (s, 3H, C_{sp3}-H); 3.70 (s, 3H, C_{sp3}-H). ¹³C NMR (100 MHz, CDCl₃): δ 172.1, 167.6, 136.1, 132.5, 132.4, 131.2, 129.7, 127.6, 52.1, 52.1, 40.6.

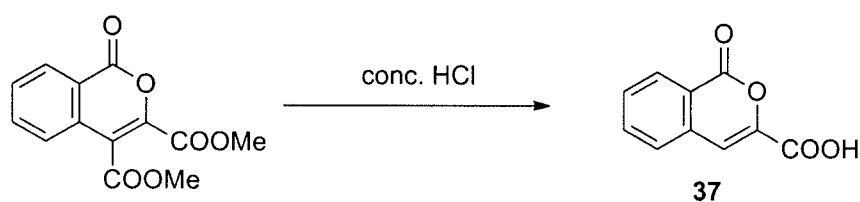
Synthesis of dimethyl 1-oxoisochromene-3,4-dicarboxylate (**36**).⁷



Sodium metal (0.502 g, 21.833 mmol, 1.52 eqv.) was isolated from a mineral oil solution and washed in ~5 mL of hexanes and added to a 250 mL round bottom flask purged with nitrogen gas. The flask was chilled to 0°C by use of an ice bath followed by the addition of dry methanol (7.0 mL)(4Å molecular sieves) to form a clear yellow solution. The hexanes were removed via a mechanical vacuum pump (10⁻³ torr) and the residue suspended in 30 mL of dry benzene (4Å molecular sieves). Two solutions consisting of dimethyl homophthalate (**35**) (2.983 g, 14.342 mmol, 1.0 eqv.) dissolved in benzene (4 mL) and dimethyl oxalate (2.233 g, 18.923 mmol, 1.32 eqv.) dissolved in benzene (4 mL) were mixed together and added over one hour using an addition funnel. The mixture was stirred at room temperature for an additional 18 hours under nitrogen gas to form a bright yellow homogenous solution. 2M HCl (10 mL) was then added and stirred for 5 minutes to give a heterogeneous mixture of a white solid and yellow solution. The organic layer was separated and washed with distilled water (20 mL), dried over anhydrous MgSO₄, and concentrated under *vacuo* to yield a yellow oil. The oil was heated at 100°C for 2 hours and upon cooling to room temperature formed a light-yellow solid. This mixture

was allowed to stand for 16 hours and then refluxed in 10 mL of reagent grade methanol for 30 minutes. After cooling to room temperature, the resulting solid was collected by vacuum filtration and washed with MeOH to give isocoumarin **36** as colorless needles (1.844 g, 7.043 mmol, 50.07%). Mp 128-133°C; ¹H NMR (400 MHz, CDCl₃): δ 8.39 (dd, *J* = 8.0, 0.8 Hz, 1H, Ar-H); 7.85 (dt, *J* = 8.0, 0.8 Hz, 1H, Ar-H); 7.71 (dt, *J* = 8.0, 0.8 Hz, 1H, Ar-H); 7.54 (dd, *J* = 8.0, 0.8 Hz, 1H, Ar-H); 4.00 (s, 3H, CH₃); 3.94 (s, 3H, CH₃). ¹³C NMR (100 MHz, CDCl₃): δ 165.0, 160.1, 159.2, 140.81, 135.5, 132.7, 131.2, 130.3, 125.5, 121.9, 119.0, 53.4 (2C)

Synthesis of 1-oxoisochromene-3-carboxylic acid (**37**).⁷



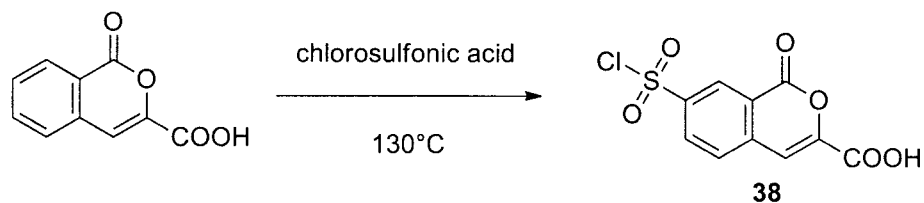
In a 250 mL round bottom flask (long neck), conc. HCl (60 mL, 1.643 mol, 96 eqv.) was heated to 110°C. 3,4-(Dimethoxy-carbonyl) isocoumarin (**36**) (4.483 g, 17.113 mmol, 1.0 eqv.) was added to the flask in portions and the mixture was refluxed. A yellow solution with white solid was formed. The suspension was heated and stirred for an additional 22 hours. The resulting white solid and yellow solution was allowed to cool to ambient temperature and the solid was collected by vacuum filtration. The solid was placed in a 100 mL round-bottom flask and further dried using a mechanical vacuum pump (10⁻³ torr) and heated over a hot water bath at 50-60°C for 1 hour to give isocoumarin **37** as an off white solid (2.843 g, 14.953 mmol, 87.37%). Mp 218-223°C; ¹H NMR (400 MHz, acetone-*d*₆): δ 8.21(dd, *J* = 0.6, 6.8 Hz, 1H, Ar-H); 7.87 (dt, *J* = 1.3, 7.3 Hz, 1H, Ar-H);

7.81 (dd, $J = 1.2, 7.8$ Hz, 1H, Ar-H) 7.71 (dt, $J = 1.2, 7.2$ Hz, 1H, Ar-H); 7.60 (s, 1H, C_{sp2}-H). ¹³C NMR (100 MHz, acetone-*d*₆): δ 161.4, 161.3, 144.5, 136.3, 136.2, 131.8, 130.3, 129.0, 123.7, 113.0.

Crystal growth studies of 1-oxoisochromene-3-carboxylic acid (**37**).

Crystal growth studies were carried out by dissolution of 3-carboxyisocoumarin (**37**) (0.050 g, 0.262 mmol) using tetrahydrofuran, 2-butanone, acetone, and methanol. Slow evaporation of these solutions at room temperature gave plates (2-butanone and acetone), prisms (THF) or needles and lathes (MeOH). X-ray quality crystals were retrieved only from the MeOH and acetone experiments. Crystallographic assessment of these samples revealed two distinct crystalline phases of isocoumarin **37**.

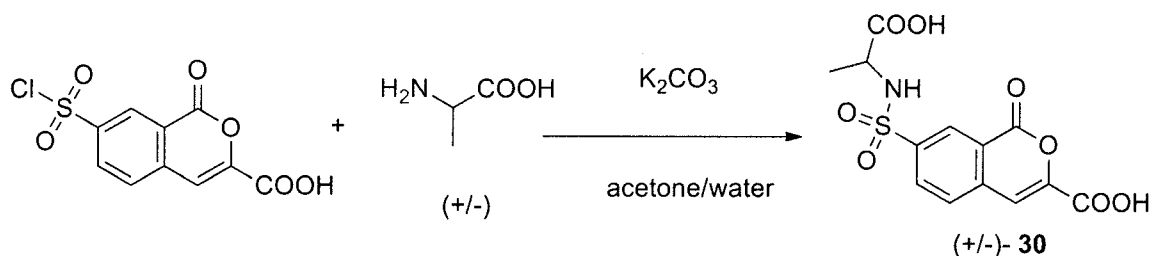
Synthesis of 7-chlorosulfonyl-1-oxo-isochromene-3-carboxylic acid (**38**).⁷



Under a nitrogen atmosphere, chlorosulfonic acid (40 mL, 601.524 mmol, 38.0 eqv.) was cooled to -4°C in an ice-salt bath and 3 carboxyisocoumarin (**37**) (3.003 g, 15.805 mmol, 1.0 eqv.) was added to a 100 mL round bottom flask portionwise for one hour. The yellow homogenous solution was heated at 120-130°C for 7 hours using a sand bath to give a dark-brown solution that was cooled to room temperature and added dropwise onto ice (~ 70.0 g) with stirring. The resulting white solid was washed by ice cold water and vacuum filtered, redissolved in acetone (10 mL), dried with anhydrous MgSO₄, and

reduced under *vacuo* to give isocoumarin **38** as a white solid (0.734 g, 2.543 mmol, 16.08%). ¹H NMR (400 MHz, acetone-*d*₆): δ 8.80 (d, *J* = 2.2 Hz, 1H, Ar-H); 8.59 (dd, *J* = 8.5 Hz, 2.2 Hz, 1H, Ar-H); 8.30 (d, *J* = 8.5 Hz, 1H, Ar-H); 7.85 (s, 1H, C_{sp2}-H). ¹³C NMR (100 MHz, acetone-*d*₆): δ 160.9, 160.0, 147.6, 145.5, 142.4, 133.1, 131.5, 129.2, 124.7, 111.6.

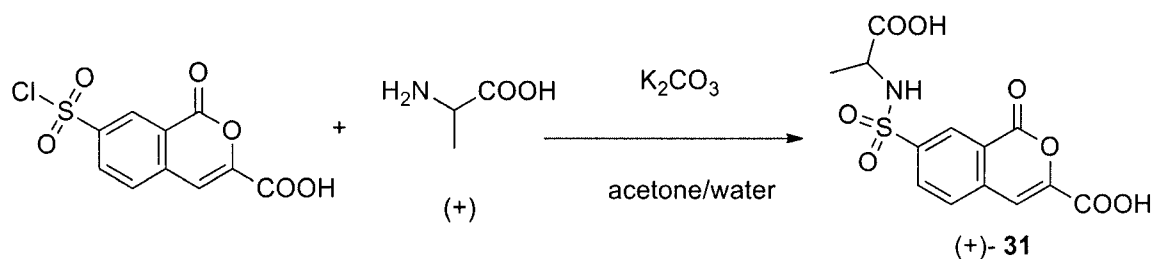
Synthesis of 7-(3-hydroxy-2-methyl-3-oxo-propyl)sulfonyl-1-oxo-isochromene-3-carboxylic acid (30**).**



To a 250 mL round-bottom flask, was added DL-alanine (0.230 g, 2.583 mmol), 3-carboxy-7-chlorosulfonylisocoumarin (0.466 g, 1.623 mmol), acetone (50 mL, reagent grade) and deionized water (40 mL) were added. The mixture was cooled to 0°C and stirring was continued for 10 minutes. To the white heterogeneous solution, K₂CO₃ (1.318 g, 9.554 mmol) dissolved in 75 mL of deionized water, was added via an addition funnel and continued stirring at 0°C for 4 hrs. A yellow solution formed. Acetone from the mixture was removed under *vacuo* (rotovap, 30°C). The resulting aqueous layer was then cooled to 0°C, and acidified to pH =2 (6M HCl, 30 drops). The solution was then extracted with 3x25 mL of EtOAc. The combined EtOAc extracts were washed with 25 mL of deionized water, dried over anhydrous MgSO₄, and reduced under *vacuo* (rotovap, 30°C) to give isocoumarin ((+/-)-**30**) as a white solid (0.114 g, 0.334 mmol, 20.68%). Mp

233-236°C; ^1H NMR (400 MHz, acetone- d_6): δ 8.68 (d, J = 1.9 Hz, 1H, Ar-H); 8.31 (dd, J = 8.2, 1.9 Hz, 1H, Ar-H); 8.06 (d, J = 8.2, 1H, Ar-H); 7.74 (s, 1H, $\text{C}_{\text{sp}^2}\text{-H}$); 7.28 (d, J = 8.7 Hz, 1H, NH); 4.11 (m, 1H, CH); 1.38 (d, J = 7.2 Hz, 3H, CH_3). ^{13}C NMR (100 MHz, acetone- d_6): δ 173.2, 161.1, 160.6, 146.2, 144.4, 139.4, 133.7, 130.0, 129.0, 123.9, 112.0, 52.5, 19.5.

Synthesis of 7-(3-hydroxy-2-methyl-3-oxo-propyl)sulfonyl-1-oxo-isochromene-3-carboxylic acid (31**).**



To a 100 mL round-bottom flask, was added D-alanine (0.066 g, 0.72 mmol), 3-carboxy-7-chlorosulfonylisocoumarin (0.131 g, 0.45 mmol), acetone (15 mL, reagent grade) and deionized water (10 mL) were added. The mixture was cooled to 0°C and stirred for 10 minutes. To the yellow heterogeneous solution, K_2CO_3 (0.358 g, 2.58 mmol) dissolved in 20 mL of deionized water, was added via an addition funnel and stirring was continued at 0°C for 4.5 hrs. A yellow solution was formed. Acetone from the mixture was removed under *vacuo* (rotovap, 30°C). The resulting aqueous layer was then cooled to 0°C, and acidified to pH = 2 (6M HCl, 20 drops). The solution was then extracted with 3x25 mL of EtOAc. The combined EtOAc extracts were washed with 25 mL of deionized water, dried over anhydrous MgSO_4 , and reduced under *vacuo* (rotovap, 30°C) to give isocoumarin ((+)-**31**) as a light-yellow solid (0.080 g, 0.236 mmol, 52.15%). ^1H NMR

(400 MHz, acetone- d_6): δ 8.67 (d, $J = 0.68$ Hz, 1H, Ar-H); 8.31 (dd, $J = 10.04, 0.76$ Hz, 1H, Ar-H); 8.06 (d, $J = 8.2$ Hz, 1H, Ar-H); 7.74 (s, 1H, C_{sp2}-H); 7.27 (d, $J = 8.7$ Hz, 1H, NH); 4.11 (m, 1H, CH); 1.37 (d, $J = 7.2$ Hz, 3H, CH₃).

2.6 References

1. Yan, Z.; Bolokowicz, A. J.; Collett, T. K.; Reeb, S. A.; Wiseman, J. D.; Wheeler, K. A. *Cryst. Eng. Comm.* **2013**, *15*, 27-30.
2. Barbour, L. J. *J. Supramol. Chem.* **2001**, *1*, 189.
3. Sheldrick, G. M. *Acta Crystallogr.* **2008**, *64*, 112.
4. XSCANS. Diffractometer Controller Software. Bruker AXS Inc., Madison, Wisconsin, USA, 2001.
5. G. M. Sheldrick, SADABS. Program for Area Detector Absorption Corrections, University of Gottingen, Gottingen, Germany, 2008.
6. Grove, R.C.; Malehorn, S.H.; Breen, M. E.; Wheeler, K. A. *Chem. Comm.* **2010**, *46*, 7322.
7. Seitz, M.; Pluth, M. D.; Raymond, K. M. *Inorg. Chem.* **2007**, *46*, 351-353.

CHAPTER 3: RESULTS and DISCUSSION

3.1 Approaches to the Construction of Photoactive Bimolecular Assemblies.

3.1.1 Introduction

Results presented in this thesis section highlight strategies towards the formation of bimolecular assemblies for the purpose of solid-state [2+2] photodimerization reactions in molecular crystals. Conceptually, the approach of these studies seeks to cocrystallize fish-hook shaped molecules such as sulfonamidocinnamic acid **23** with secondary olefins to form tetrameric assemblies with neighboring C=C groups in close proximity (Figure 26). As previously described, bimolecular reactions in solids most often result from pairs of chemically identical (or nearly identical) reactants. Transformations between two molecules with distinct chemical properties, functional groups, and frameworks are rare in the literature.¹ This goal of constructing reactive multicomponent systems offers a significant technological challenge due to the structural complexity and interdependence of functional group associations (*e.g.* hydrogen bonds), molecular topologies, and the alignment of reactive centers.

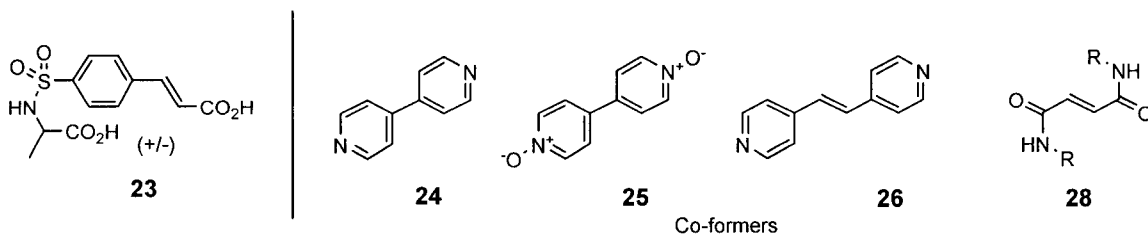
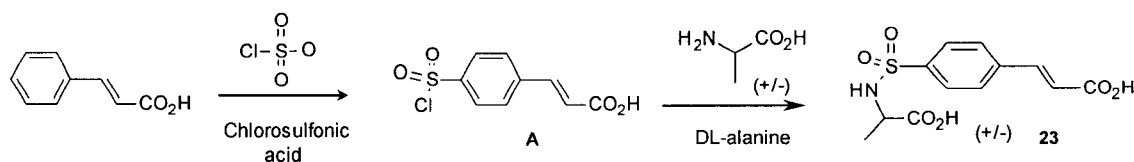


Figure 26. Molecular components used in the design of reactive cocrystals.

Work described in this section focuses on a wide range of experimental techniques such as material design, chemical synthesis, crystal growth and selection, X-ray data collection, crystal structure solution and refinement, crystal packing analysis,

and UV irradiation of samples. As shown in Figure 26, results from these studies centered on cocrystalline systems generated from sulfonamide **23** and a series of co-formers (**24-26**, **28**). Each framework of these co-formers was designed to include a linear template decorated with functional groups capable of forming hydrogen bonds with carboxyl groups. Pyridine, pyridine-N-oxide, and amide moieties each are capable of non-bonded association with CO₂H groups and, thus offer a viable entry to cocrystal formation. Though the first two co-formers **24** and **25** lack reactive groups, their use in pilot studies provided important information to understand the structural tendencies of these systems. The additional two co-formers included in the study, 1,2-di(4-pyridyl)ethylene (**26**) and fumaramide derivatives (**28**), provided appropriate molecular scaffolds for heterodimerization that occurs between two significantly different olefin containing compounds. The selection of sulfonamidocinnamic acid **23** as one of the components was inspired from previous studies conducted in the Wheeler research group.² Additionally, compound **23** is easily accessed by a straightforward two-step procedure involving electrophilic aromatic sulfonation of cinnamic acid to sulfonyl chloride **A** that gives way to sulfonamide **23** upon treatment with DL-alanine.²



The cocrystallization study of sulfonamide **23** with co-formers **24-26** and **28** offers a considerable opportunity to not only investigate the affinity of these systems to form the anticipated tetramers, but also to explore unique bimolecular systems capable of [2+2] photodimerizations. The following sections (3.1.2 – 3.1.6) describe the crystal

chemistry of these bimolecular materials and at least in one case, UV illumination studies and the subsequent results. Though cocrystals of **23·24** and **23·25** both produced crystal structures with tetrameric motifs, it was expected that the lack of necessary reaction centers in components **24** and **25** would effectively prevent solid-state reactivity. Even so, these structures anchor this section of the thesis and provide clear structural data to understand the desired structure-property relationships. In the cases of components **26** and **28** recrystallized with **23**, these materials ultimately lacked the fidelity to form reactive systems. For the **23·26** system, the crystal structure shows promise and indicates successful formation of a bimolecular system, but lacks sufficient olefin close contacts for solid-state reactivity. Fumaramide **28** does not form a cocrystal with **23**, likely due to the combined effect of solubility differences and hydrogen-bond affinities of the components.

3.1.2 Crystal Structure Assessment of Cocrystal **23·24**

Suitable crystals of **23·24** were grown from slow evaporation of an equimolar mixture of **23** and **24** dissolved in an acetone-methanol (6:1) solution. The crystal structure from this sample was determined with pertinent details provided in Table 1. Inspection of Figure 27 reveals this structure contains four molecules in the asymmetric unit – two molecules of 4,4'-dipyridyl (**24**) and two molecules of sulfonamide **23**. These components are organized in space group *P*-1 and assemble across an approximate inversion symmetry linked by strong CO₂H···N interactions to form a supramolecular tetramer. Several components of the cocrystal **23·24** exhibit disorder. Both bipyridine molecules show whole molecule disorder while one of the sulfonamidocinnamic acids

exhibits partial disorder of the sulfonamide-amino acid fragment. As shown in Figure 28, crystal packing of **23·24** reveals these tetrameric assemblies link to adjacent motifs via N-H \cdots O=C and C-H \cdots O=C contacts that propagate along the *a* axis.

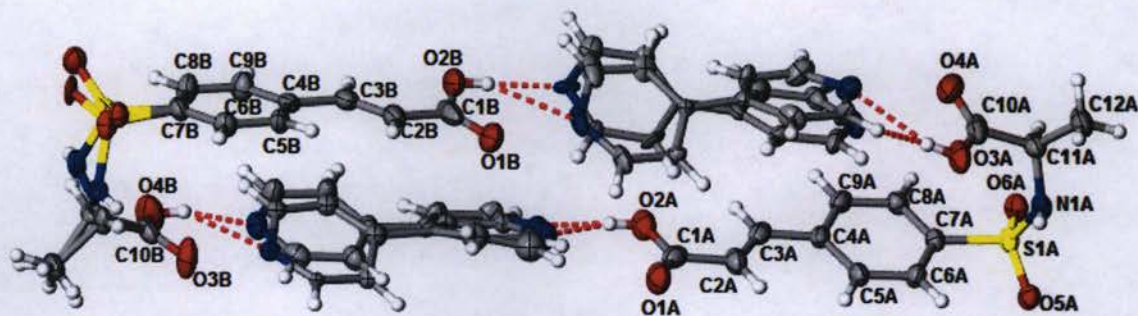


Figure 27. Asymmetric unit and labeling scheme (70% probability ellipsoids) for cocrystal **23·24** (disordered atom labels not shown).

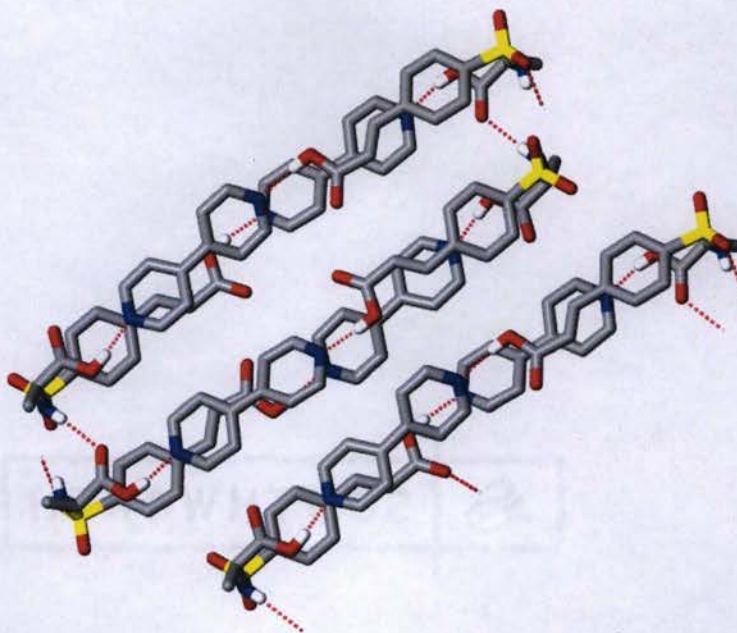


Figure 28. Crystal packing of **23·24** showing hydrogen bond patterns (H atoms deleted for clarity) (minor disorder component excluded).

3.1.3 Crystal Structure Assessment of Cocrystal **23·25**.

Crystals of **23·25** formed from slow evaporation of a 3:2 acetone:methanol solution and the structure was determined using X-ray crystallography (Table 2). Inspection of Figure 29 reveals the structure of **23·25** contains three molecules in the asymmetric unit – a molecule of 4, 4'-dipyridyl-N,N'-dioxide (**25**), a molecule of sulfonamide **23**, and a water molecule. These components link to form a supramolecular trimer assembled by use of $\text{O}_2\text{H}\cdots\text{O}-\text{N}$ and $\text{carboxyl}\cdots\text{H}-\text{C}$ hydrogen bonds (Figure 29). This system also exhibits partial disorder of the cinnamic acid fragment (Figure 29B). As seen in Figure 30, the components of **23·25** lack the anticipated cyclic tetrameric motifs constructed from components **23** and **25**. Instead, this system includes a molecule of water likely introduced during the cocrystalliation study using acetone-methanol as the solvent system. The two-dimensional crystal patterns produced from these components arise from $\text{N}-\text{O}\cdots\text{H}-\text{O}$ and $\text{O}-\text{H}\cdots\text{O}-\text{C}$ contacts in the *ab* plane (Figure 30).

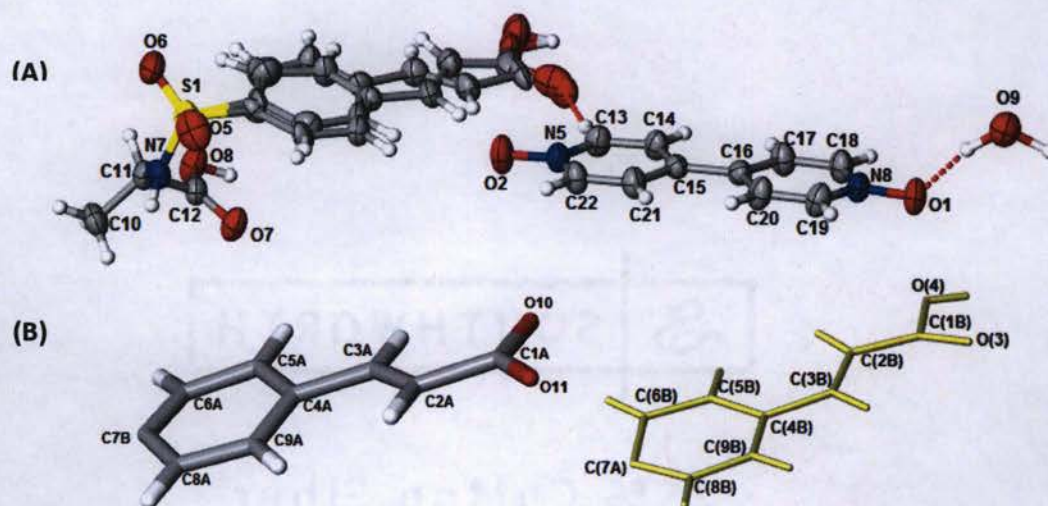


Figure 29. Crystal structures of **23·25** showing (A) asymmetric unit and labeling schemes (70% probability ellipsoids) (disordered part is not labeled) and (B) disorder components.

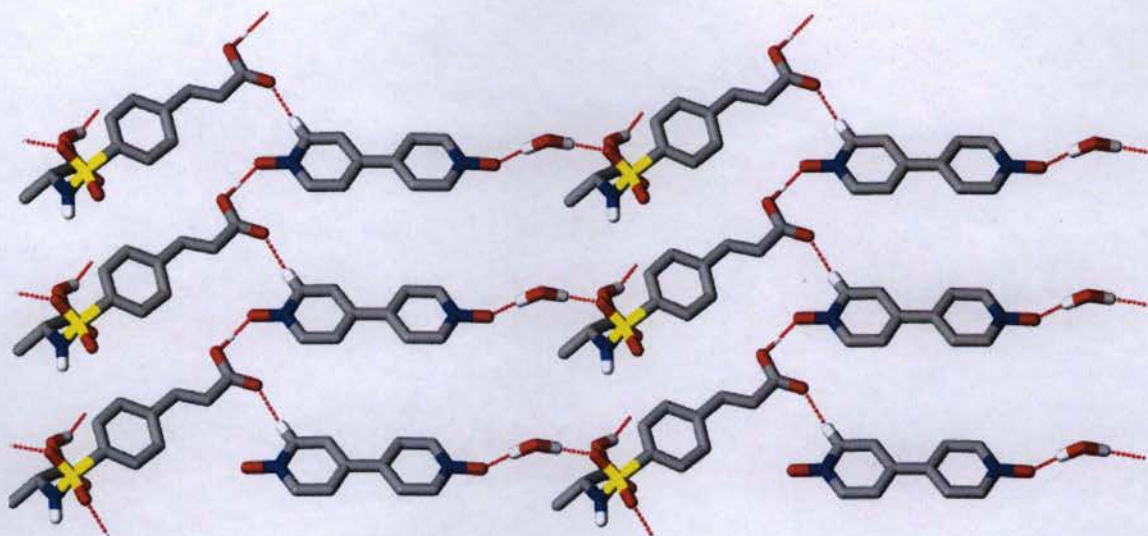


Figure 30. Crystal packing of **23·25** showing hydrogen bond patterns (H atoms deleted for clarity) (minor disorder component excluded).

3.1.4 Crystal Structure Assessment of Cocrystal **23·26**.

The structure of crystalline **23·26** formed from slow evaporation of a solvent system of ethanol and dichloromethane (1:1) solution was determined using X-ray crystallography (Table 3). Inspection of Figure 31 revealed this structure contains 4 molecules in the asymmetric unit - two molecules of sulfonamide **23** and two molecules of *trans*-1,2-bis(4-pyridyl)ethylene (**26**). These components organize across an approximate inversion symmetry and link to form a supramolecular tetramer assembled by use of strong CO₂H...N interactions. Analysis of the crystal structure of **23·26** shows components aligned in the triclinic space group *P*-1 and the unit cell is occupied by 4 molecules. As shown in Figure 31, molecules of **23·26** assemble by O-H...N type hydrogen-bond interactions. The cocrystal **23·26** also shows the part of the structure disorder (non-labeled part of the Figure 31). In this structure, one molecule of *trans*-1,2-bis(4-pyridyl)ethylene and the cinnamic acid part of molecule **23** show disorder.

Inspection of the crystal packing of **23·26** (Figure 32A) revealed adjacent heterodimers linked by use of N-H \cdots O=C contacts to give 2D patterns.

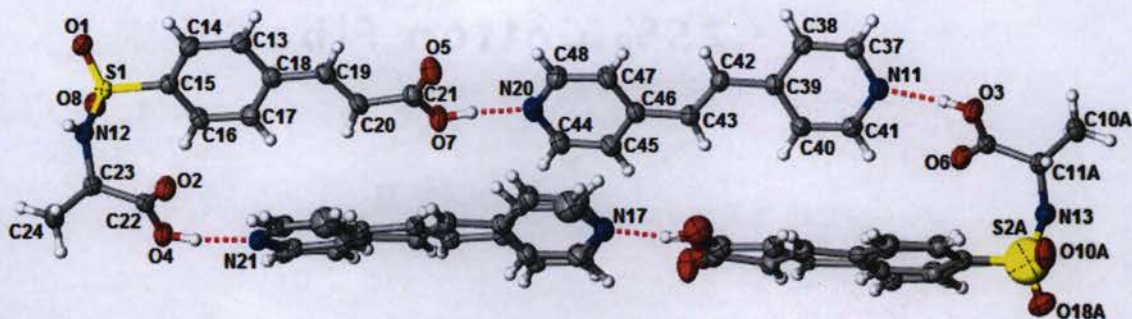


Figure 31. Asymmetric unit and atomic labeling (70% probability ellipsoids) of crystalline **23·26** (disordered portion of structure not labeled).

Crystallographic study of **23·26** revealed hydrogen-bonded tetramers with different intra- and inter-dimer olefin distances (Figure 32). As shown in the Figure 32B, the adjacent olefins contained in the intra-dimer of **23·26** lack favorable spatial alignment. Even so, the same figure shows a pair of olefin positioned between tetrameric motifs that satisfies Schmidt's³ geometry criteria for [2+2] photodimerization reactions. For the intra-dimer contacts of **23·26**, the shortest C=C \cdots C=C distances occur at 4.541 Å while the olefins observed for the inter-dimer pattern are displaced by 3.868 Å. This favorable alignment of inter-dimer C=C groups falls within Schmidt's' distance criteria of 4.2 Å for topochemically controlled photodimerization reactions and suggests further investigations to explore the [2+2] photodimerization behavior of this material. A single crystal of **23·26** was irradiated via the UV tail-irradiation technique using a 200 W Xe(Hg) arc lamp and a 360 nm optical edge filter. After 10.5 hours of UV illumination, the crystal was placed on the diffractometer and X-ray data collected. From structure

solution and refinement of the data, it was observed that the crystal did not significantly change or convert to the expected photoproduct **27**.

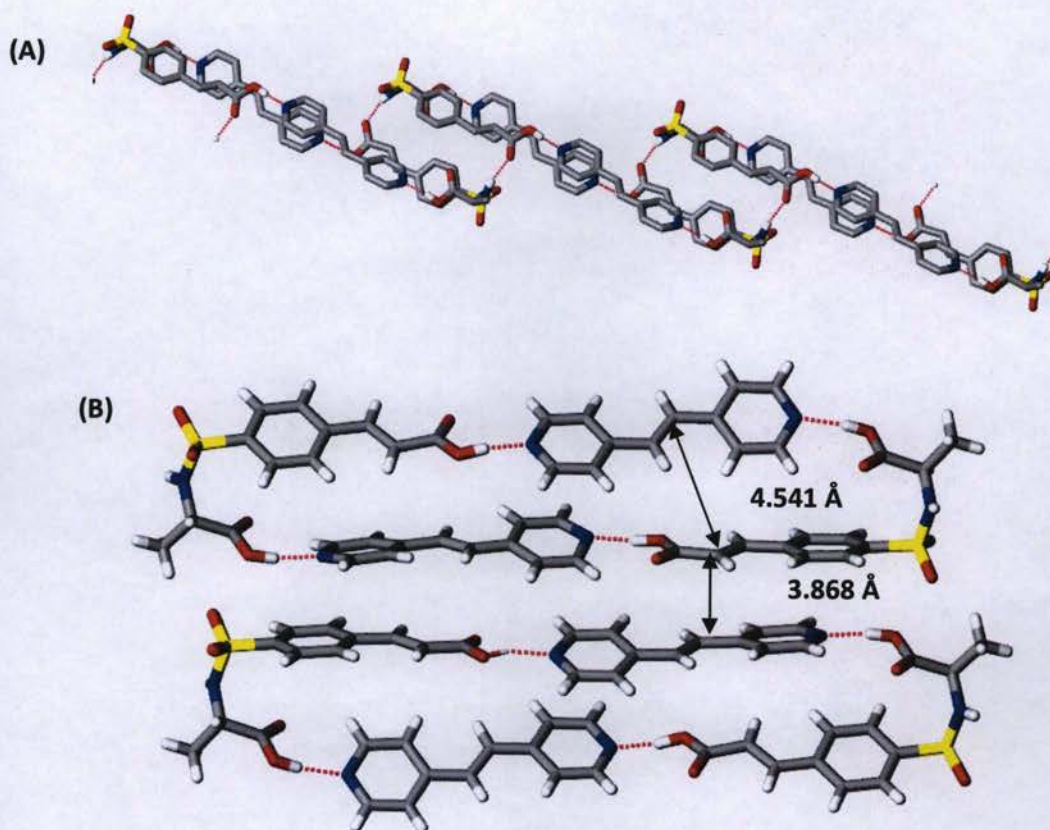


Figure 32. Crystal packing of **23·26** showing (A) hydrogen bond patterns (H atoms deleted for clarity) and (B) heterodimer alignment (minor disorder component excluded).

3.1.5 Crystal Structure Assessment of **28**

This structural investigation also includes fumaramide **28** because i) its crystal structure is unreported in the literature and ii) the framework contains potentially reactive C=C groups. The structure of crystalline **28**, formed from slow evaporation of 5 mL of methanol solution, was determined using X-ray crystallography (Table 4). Inspection of Figure 33 reveals the asymmetric unit of this material contains a half molecule of *N,N*-dimethylfumaramide in monoclinic space group $P2_1/n$. Further assessment also indicates

two asymmetric units covalently connect and are related by inversion symmetry to generate a complete molecule of **28**.

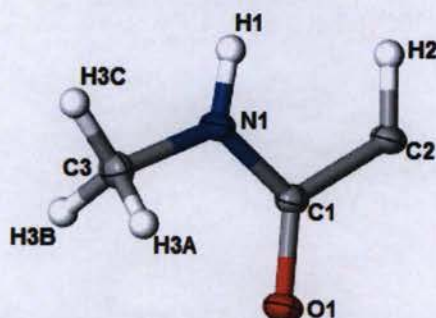


Figure 33. Crystal structure of **28** showing asymmetric unit and labeling scheme (70% probability ellipsoids).

As shown in Figure 34, the crystal structure of **28** also offers an interesting view of the packing preferences of dimethylfumaramide molecules. Each molecule of **28** is linked to adjacent molecules by $\text{N-H}\cdots\text{O}=\text{C}$ hydrogen bonds to form molecular ribbons along the *b* axis (Figure 34A). In crystalline **28**, the observed adjacent motifs are not positioned with favorable spatial alignment (Figure 34B). For **28**, the shortest $\text{C}=\text{C}\cdots\text{C}=\text{C}$ contacts occur at a distance of 4.842 Å. In this case, the olefin \cdots olefin contact lacks proper orientation and an adequate distance to undergo a UV initiated photodimerization reaction.

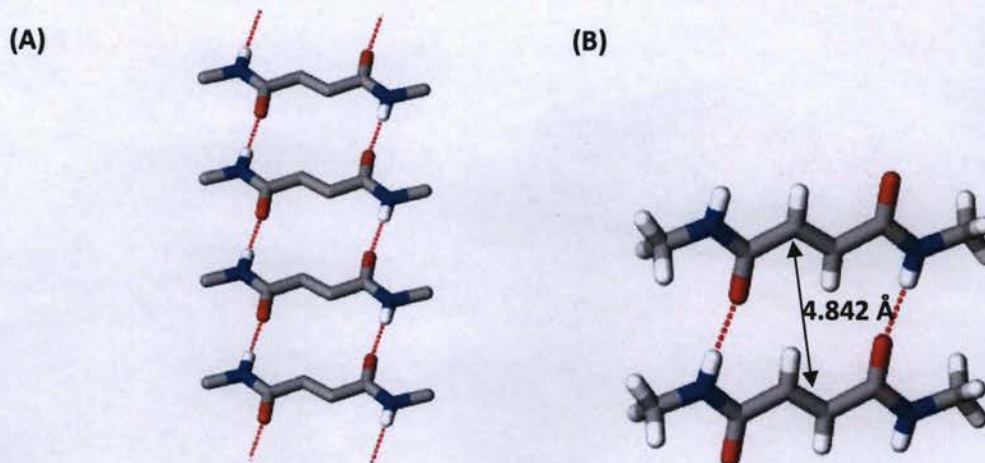


Figure 34. Crystal packing of **28** showing (A) the hydrogen bond pattern (H atoms deleted for clarity) and (B) photostable alignment of neighboring olefins.

3.1.6 Developments Towards Photoactive Bimolecular Assemblies

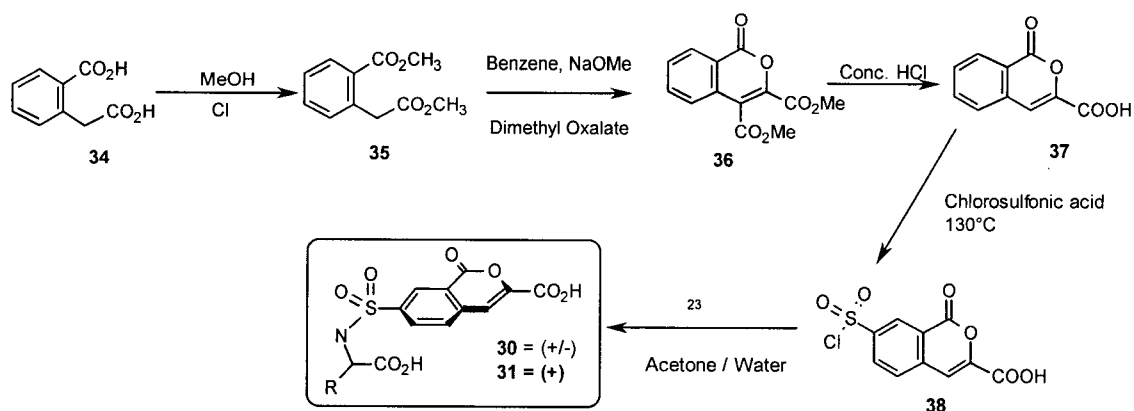
The structural results presented above provide evidence of key structural preferences. Three of the four examined systems (*i.e.* **23·24**, **23·25**, and **23·26**) result in the formation of the expected supramolecular tetramer constructed of alternating components. These motifs stem from the formation of strong $\text{C}=\text{O}\cdots\text{N}$ and $\text{C}=\text{O}\cdots\text{O}^-\text{N}^+$ hydrogen bonds. In the case of component **26** where the added $\text{C}=\text{C}$ group was expected to catalyze reactivity, the central olefin group does not sufficiently overlap with the olefin attached to the adjacent sulfonamide **23** components. The skewed geometries of the shortest $\text{C}=\text{C}\cdots\text{C}=\text{C}$ contact produce distances well beyond the 4.2 Å criteria established for [2+2] photodimerization. Additionally, though the lack of cocrystallization behavior for **23·28** was unexpected, the carboxyl \cdots amide contact is noticeably weaker than those employed with other systems present in this section. Another factor that may contribute

to the lack of cocrystal formation relates to the near insoluble nature of **28** in most common organic solvents.

3.2 Synthesis and Photodimerization of 7-(3-hydroxy-2-methyl-3-oxo-propyl) sulfonyl-oxo-isochromene-3-carboxylic acid (**30/31**)

3.2.1 Introduction

Racemic and homochiral sulfonamide isocoumarin compounds were designed with the aim to synthesize fish hook shape molecules that undergo UV initiated solid-state reactions. Target isocoumarin compounds **30** and **31**, which are structurally similar to the original cinnamic acid derivative **23**, were prepared using a five-step synthetic process. The successful preparation of isocoumarins **30/31** utilized the reaction sequence of **34** to **38** and was based on a previous report by Raymond *et al.*⁴ The synthetic sequences of these materials are quite amenable to parallel processing because of the common intermediate sulfonylchloride **38** and similar reaction conditions necessary for the conversion to **30** and **31**.



Each step of the reaction sequence (**34** - **30/31**) was assessed using NMR spectroscopy and where possible, X-ray crystallography was employed for structure elucidation. Because intermediate **37** contains a cinnamyl fragment, the project also explored the solid-state reactivity of this material that ultimately provided an opportunity to examine the importance of crystal engineering strategies to the assembly of reactive components. If photoreactive, the solid state transformation of intermediate **37** should proceed by one of two chemoselective pathways to give either the head-to-head or head-to-tail dimer products (Figure 35).

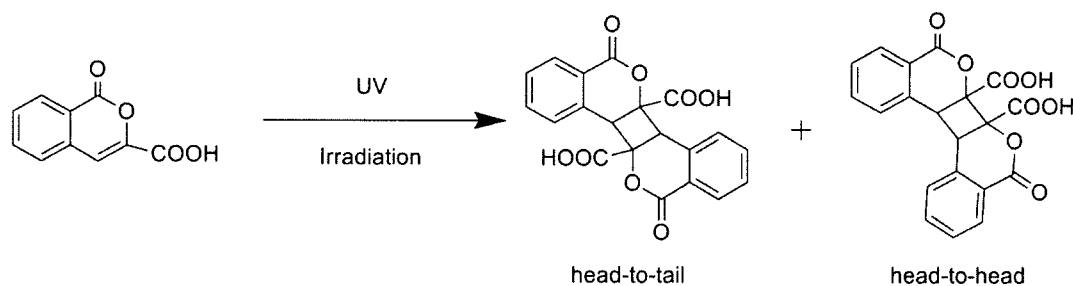


Figure 35. Schematic presentation of photodimerization reaction of compound **37**.

Crystal growth trials with compound **37** were performed using the slow evaporation technique with different solvent systems. Solutions containing acetone (**37-I**) and methanol (**37-II**) were explored and the crystals formed gave two distinct crystalline phases assessed by X-ray crystallography (Tables 5 and 6). The crystal growth studies of **30** and **31** were also performed. As with the study of **23**, the design strategy of this investigation explores the formation of supramolecular dimers with favorable olefin alignment by use of the complementary features of molecular shape and carboxyl O-H \cdots O interactions (Figure 36).

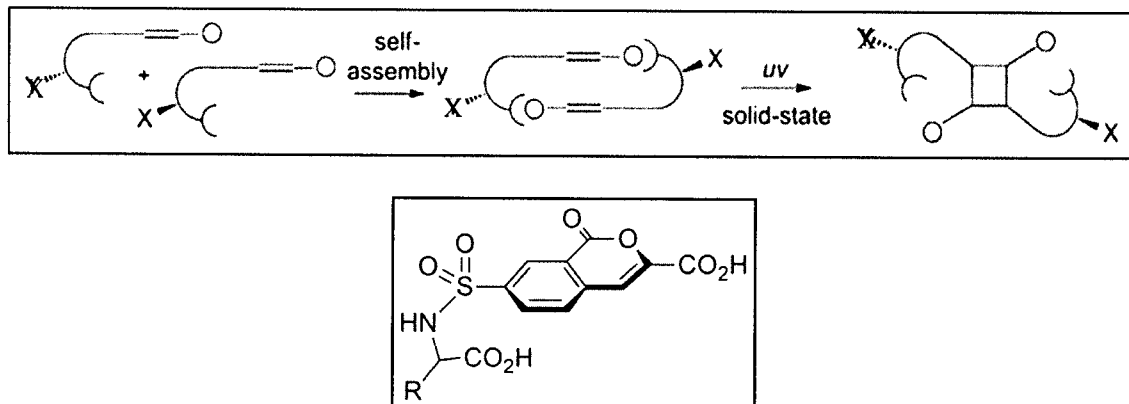


Figure 36: Design strategy (top) and molecular targets (bottom) for the construction of photoreactive sulfonamide isocoumarin compounds.

Crystal structure analysis and UV illumination studies of crystalline **30** and **31** provided interesting opportunities to investigate new photodimerization reactions in molecular crystals. In the case of **30**, the photochemically initiated reaction gave cyclobutane photoproduct **33** (racemic) in 100% conversion. The synthesis and photochemistry of crystalline homochiral **31** was also pursued. Because crystal growth from either slow evaporation or vapor diffusion techniques were unsuccessful, UV illumination studies of **31** were performed on powdered samples. This investigation resulted in conversion of **31** to photoproduct **33** in 65% yield via ^1H NMR assessment.

3.2.2 Synthesis of Methyl 2-(2-methoxy-2-oxo-ethyl)benzoate (**35**).

Homophthalic acid (**34**) was esterified with MeOH using a catalytic amount of concentrated HCl to give methyl 2-(2-methoxy-2-oxo-ethyl) benzoate (**35**). Product formation was supported by the addition of two new NMR signals (^1H , 3.87 and 3.70 ppm, ^{13}C NMR, 52.18 and 52.12 ppm) corresponding to the newly formed methyl esters.

During the course of experiments it was determined that reaction time for the synthesis of **35** proved to be critical with near optimal transformation occurring at 72 hours (92% yield).

3.2.3 Synthesis of dimethyl 1-oxoisochromene-3,4-dicarboxylate (**36**).

The reaction of **35** with dimethyl oxalate in the presence of strong base (NaOMe) gave dimethyl 1-oxoisochromene-3,4-dicarboxylate (**36**) by an intramolecular annulization process. The disappearance of the ^1H NMR singlet corresponding to the methylene group (CH_2 , 4.01 ppm) in **35** and ^{13}C NMR signals >100 ppm indicates product **36** formation. The reaction mechanism of this material follows several steps that begin with deprotonation of **35** by NaOMe (Figure 37). Intermediate A then reacts with dimethyl oxalate in a nucleophilic fashion to form keto ester B. A second deprotonation involving intermediate B followed by intramolecular cyclization gives rise to product **36**. Under ambient conditions, this condensation reaction does not proceed to completion and, thus an additional heating cycle at 100°C for two hours was necessary to give **36** in 50% yield.

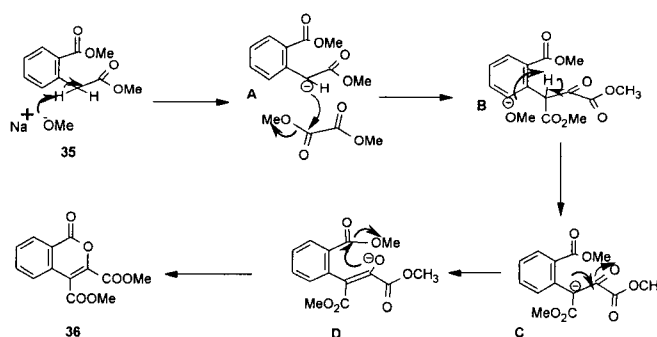
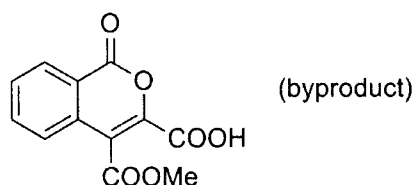


Figure 37: The reaction mechanism for the synthesis of **36**.

3.2.4 Synthesis of 1-oxoisochromene-3-carboxylic acid (**37**)

Hydrolysis and decarboxylation of intermediate **36** by reaction with hot concentrated hydrochloric acid gave 1-oxoisochromene-3-carboxylic acid (**37**) as an off white solid in reasonable yields (> 85% yield). As with the **36**, the reaction time for the production of **37** is critical. As previously reported⁴, it was observed that short reaction times (10-15 hours) result in mono-saponified byproducts; however, reaction times of >22 hours gave **37** as the major product. Product identity was supported by loss of two methyl esters (¹H, 4.03 and 3.97 ppm, ¹³C NMR, 53.37 and 53.37 ppm) and appearance of a C_{sp2}-H group (¹H NMR, 7.67 ppm, ¹³C NMR, 113.03 ppm) in the NMR spectra.



3.2.4.a Crystal Structure Analysis of **37-I** and **37-II**

The structure of crystalline phase **37-I** formed from slow evaporation of an acetone solution was determined using X-ray crystallography (Table 5). Inspection of Figure 38 reveals this structure contains two molecules in the asymmetric unit. These molecules are organized across an approximate inversion symmetry and linked to form a supramolecular dimer by carboxyl...carboxyl hydrogen bonds. In the case of crystalline phase **37-II**, the isocoumarin molecules crystallize with a molecule of solvent (MeOH) incorporated in the lattice (Table 6).

Analysis of the crystal structure of **37-I** reveals components aligned in the monoclinic space group $P2_1/n$, whereas **37-II** organize in the orthorhombic space group

Pbca. In both phases the unit cells are occupied by eight molecules of **37**. As shown in Figure 39A, molecules of **37-I** assemble by O-H...O=C type hydrogen-bond interactions. Inspection of the crystal packing of **37-II** (Figure 40A) revealed isocoumarin molecules linked by adjacent MeOH solvent molecules to form chains those propagate along the *b* axis. These interactions between neighboring components consist of O-H...O=C and O-H...O-H contacts.

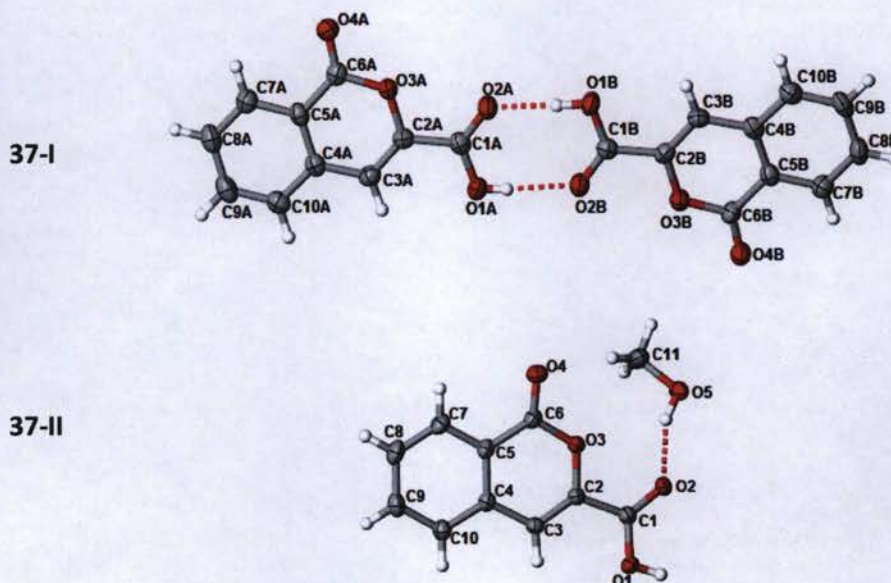


Figure 38. Asymmetric units and labeling schemes (70% probability ellipsoids) of two crystalline phases of **37**.

As shown in the Figures 39B and 40B, the adjacent olefins present in the structures of **37-I** and **37-II** lack favorable spatial alignment that satisfies Schmidt's³ geometry criteria for [2+2] photodimerization reactions. For **37-I**, the shortest C=C...C=C contacts occur at 5.086 Å while the olefins in **37-II** are displaced by 4.466 Å distance. In each case, the olefin...olefin contacts do not orient with the correct geometry or adequate distance to undergo a UV initiated photodimerization reaction. These structures, **37-I** and

structures, **37-I** and **37-II**, offer an interesting view of the practical challenges that exist when designing reactions in molecular crystals. As with Schmidt and Cohen's seminal work on cinnamic acids, it is not sufficient to construct molecules that contain reactive fragments. Equally important is the notion of incorporating key structural features that provide predetermined alignment of components for functional purposes. In the case of isocoumarin **37**, such molecules crystallize to give a variety of serendipitous packing patterns. By adding a chiral auxiliary group (sulfonamide and amino acid) to the isocoumarin framework, the design strategy of the investigation shifts from reactions of happenstance to engineered materials that undergo unique solid-state transformations. This approach is easily appreciated by comparing the molecules and structures of **37** and **30/31**. Though **37** readily forms hydrogen-bonded dimers (Figure 38), the factors that control the association of neighboring molecules are not well defined and thus, the spatial distribution of olefin groups for this system lack any degree of predictability. On the other hand, compounds **30** and **31**, when recrystallized, assemble into foreseeable motifs. This thesis highlights the structures and photochemical behavior of these crystalline materials and explores the chemical features and boundaries responsible for single-crystal-to-single-crystal reactions.

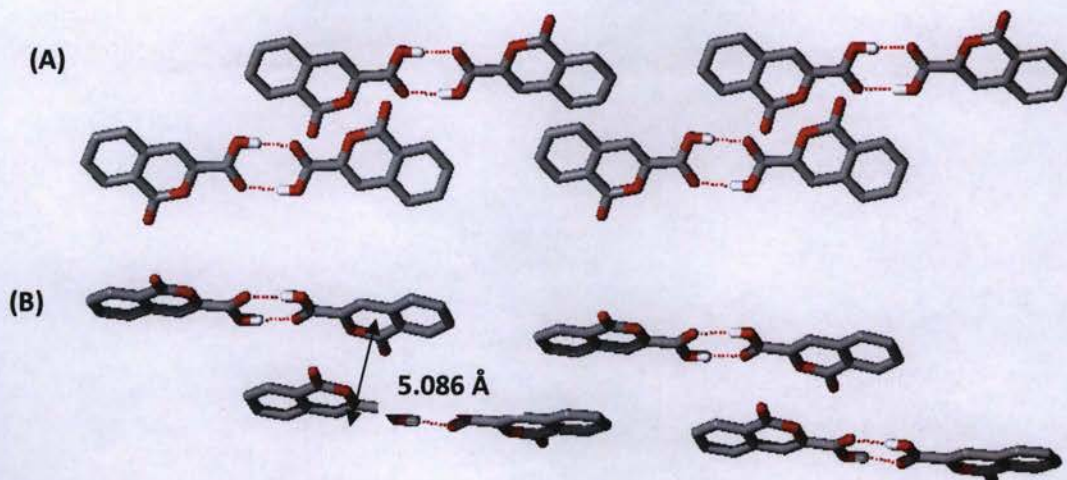


Figure 39. Crystal packing of **37-I** showing (A) the dimer formation with hydrogen bonds and (B) photostable alignment of neighboring olefins (H atoms deleted for clarity).

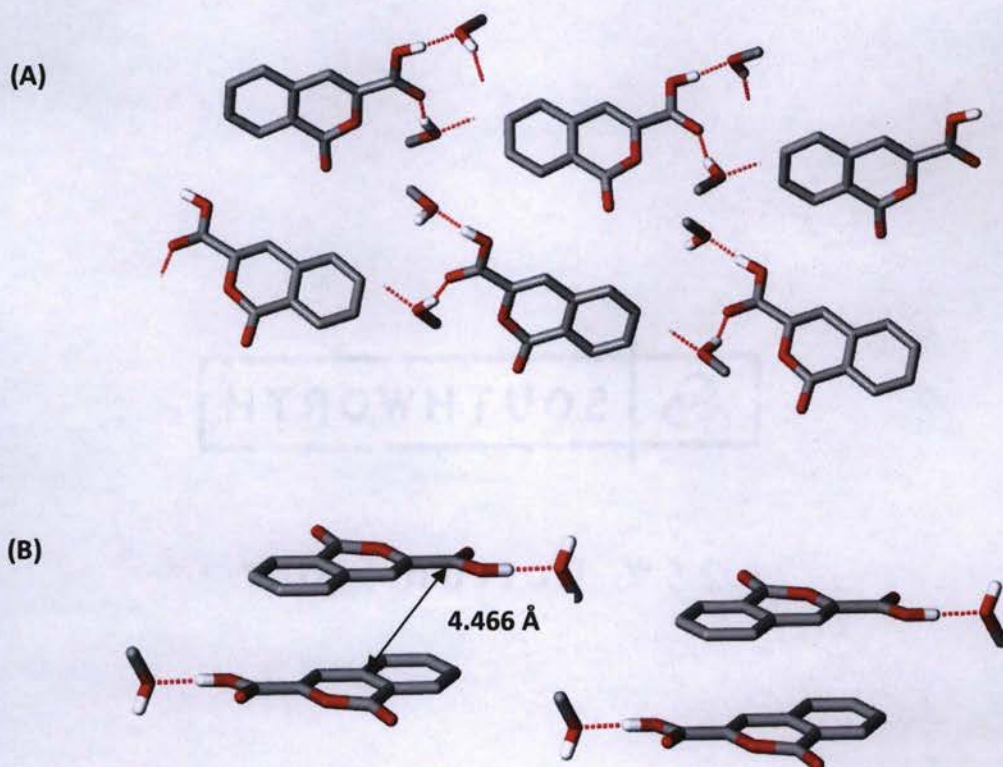


Figure 40. Crystal packing of **37-II** showing (A) the solvate formation with hydrogen bonds and (B) photostable alignment of neighboring olefins (H atoms deleted for clarity).

3.2.5 Synthesis of 7-chlorosulfonyl-1-oxo-isochromene-3-carboxylic acid (**38**).

The fourth step of the synthetic sequence involves treatment of isocoumarin **37** with anhydrous chlorosulfonic acid to yield the desired 7-chlorosulfonyl-1-oxo-isochromene-3-carboxylic acid (**38**) via electrophilic aromatic substitution. As previously mentioned, sulfonyl chloride **38** provides a common intermediate to the synthesis of the sulfonamideisocoumarin **30/31** targets. Compared to cinnamic acid, isocoumarin **37** is less activated towards electrophilic addition and thus requires nonambient reaction conditions. An optimized yield of 34% for **38** was achieved by refluxing the reaction at 130°C for 9 hours under a nitrogen atmosphere followed by removal of starting material and other impurities by flash column chromatography. The regioselectivity of the reaction is controlled by the electronic and steric effects of the attached groups. Since the directing abilities of the carbonyl (deactivator, meta director) and olefin (activator, ortho/para director) substituents are cooperative, the most logical positions for substitution is on the C5 and C7 atoms of the aromatic ring. A comparison of the aromatic ring substitution patterns for the starting material and product from sulfonation of **37** provides key structural differences that can be easily identified using ¹H NMR spectroscopy. As shown in Figure 41, the set of signals (chemical shifts and coupling constants) in the aromatic region clearly shows a pattern indicative of a 1,2,4-trisubstituted benzene that corresponds to compound **38**.

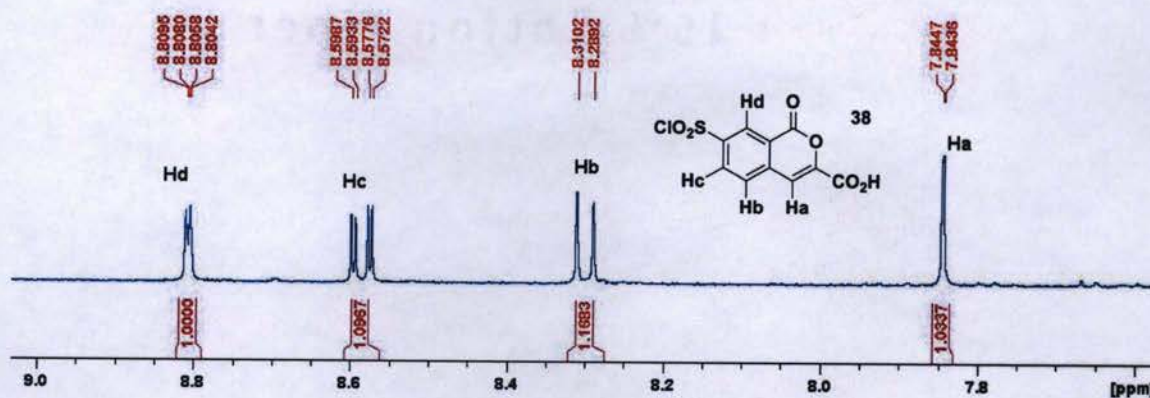


Figure 41. ^1H NMR spectrum of sulfonylchloride **38** showing signals and splitting in the aromatic region.

3.2.6 Synthesis of 7-(3-hydroxy-2-methyl-3-oxo-propyl)sulfonyl-1-oxo-isochromene-3-carboxylic acid (**30/31**).

Treatment of sulfonylchloride isocoumarin **38** with alanine gave sulfonamides **30/31**. Because these target compounds only differ by chirality, they are easily accessed by use of either the racemic or enantiopure forms of alanine. This nucleophilic addition reaction is conducted in one pot under ambient conditions and uses a weak base (K_2CO_3) to generate the nucleophile. In addition, the mild conditions and use of a H_2O /acetone solvent system promotes straightforward work-up of the reactions. Products are obtained as white or off-white solids in 21-51% yields and can be identified by the ^1H NMR signals generated from the NH (7.30ppm, doublet, $J = 8.8$ Hz) and CHCH_3 (4.13 (m) and 1.37 (doublet, 7.2 Hz) ppm) groups of the alanine fragment.

3.2.6.a Crystal Growth, Selection and Mounting

The approach of combining 'fish hook' shaped sulfonamides and isocoumarin frameworks were initially pursued with compound **30**. Because slow evaporation at room temperature of acetone solutions gave either crystals of insufficient size or amorphous solids, crystal growth from vapor diffusion was then investigated. Dissolution of **30** in acetone with dichloromethane as the diffusion solvent produced X-ray quality crystals with plate-like morphologies (Figure 42). Polarized light microscopy was used to assess crystal quality with a single crystal mounted on a glass fiber affixed to a brass pin using cyanoacrylate adhesive. As shown in Figure 42B, this sample was then attached to a goniometer head for subsequent diffraction studies.

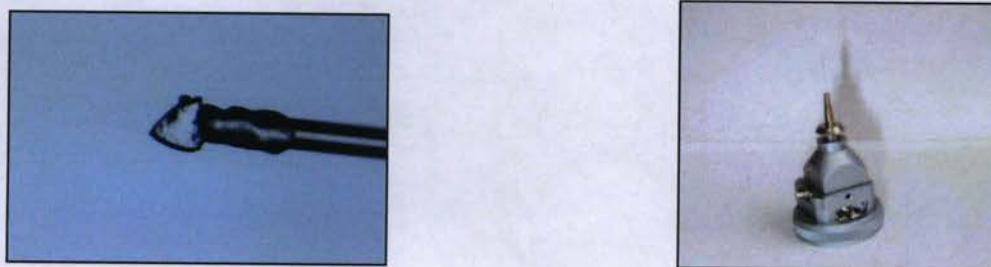


Figure 42. Single crystal of **30** mounted on a glass fiber (left) and goniometer head for diffraction studies (right).

Crystal growth studies were also explored for **31** using an array of solvent systems and crystal growth techniques. Both slow evaporation and vapor diffusion methods were employed using a wide selection of solvents (acetone, acetonitrile, methanol, 2-butanone, and chloroform) to give crystals of insufficient size or amorphous solids. As a result, powdered samples of **31** were used for all photochemical studies.

3.2.6.b Crystal Structure Assessment

As determined by X-ray crystallography, the asymmetric unit consists of one molecule of **30** that adopts the desired ‘fish hook’ conformation with the carboxyl component of the alanine fragment positioned directly beneath the phenyl isocoumarin group (Figure 43, top). The molecule in the asymmetric unit was modeled with two-part disorder and refined to give a 60:40 occupancy ratio. Though the isocoumarin disordered fragments reside in similar positions, the atomic coordinates of the sulfonamide groups are quite distinct by forming a crisscross pattern. In an attempt to explore the permanence of the observed disorder, a total of three datasets collected on two single-crystal X-ray diffractometers [Bruker D8 (EIU) and Bruker D8 (University of California San Diego)] were obtained. In each case, independent solution and refinement of the data gave nearly indistinguishable crystal structures. These crystal components organize in the monoclinic space group $P2_1/n$ with each racemic pair assembled into centrosymmetrically related homodimers by carboxyl...carboxyl interactions (Figure 43, bottom).

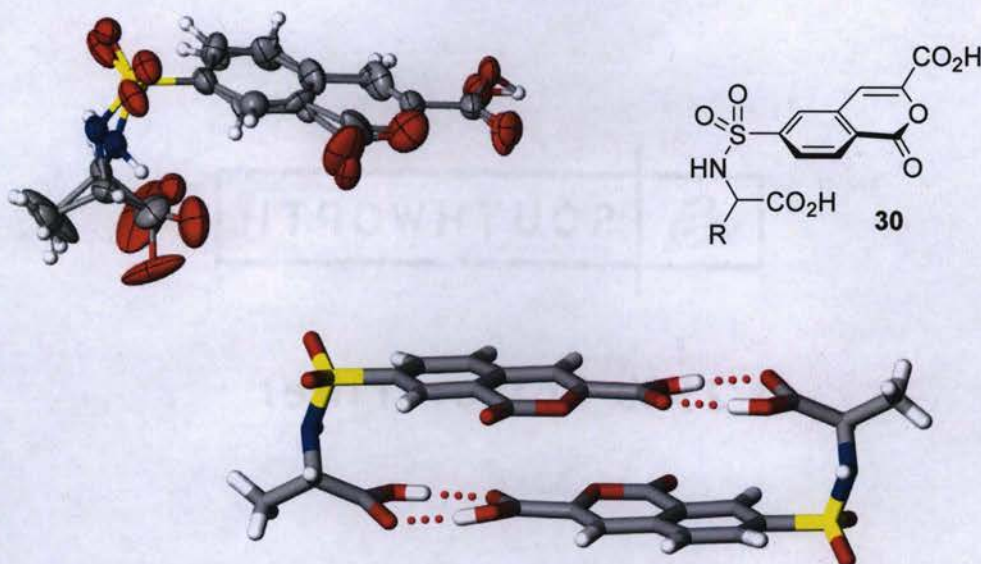


Figure 43. Asymmetric unit of racemic **30** showing the ‘fish hook’ shape molecular arrangement (top) and homodimer formation by use of hydrogen bonds (bottom, minor disorder component excluded).

As stated above, molecules of **30** crystallize with disorder where the asymmetric unit component exhibits more than one crystallographically independent orientation. Unlike the majority of disordered crystal structures reported in the literature, **30** exhibits whole molecule disorder that significantly adds to the complexity of the structure solution and refinement process. Structure refinement with a data:parameter ratio of 10:1 is often expected, but in the case of **30** this ratio is 4.4:1 due to the additional refinement parameters associated with the second disordered component. Though the chemical model is not in question, the accuracy of the atomic positions is less than ideal as reflected by the elongated atomic displacement parameters shown in Figure 43.

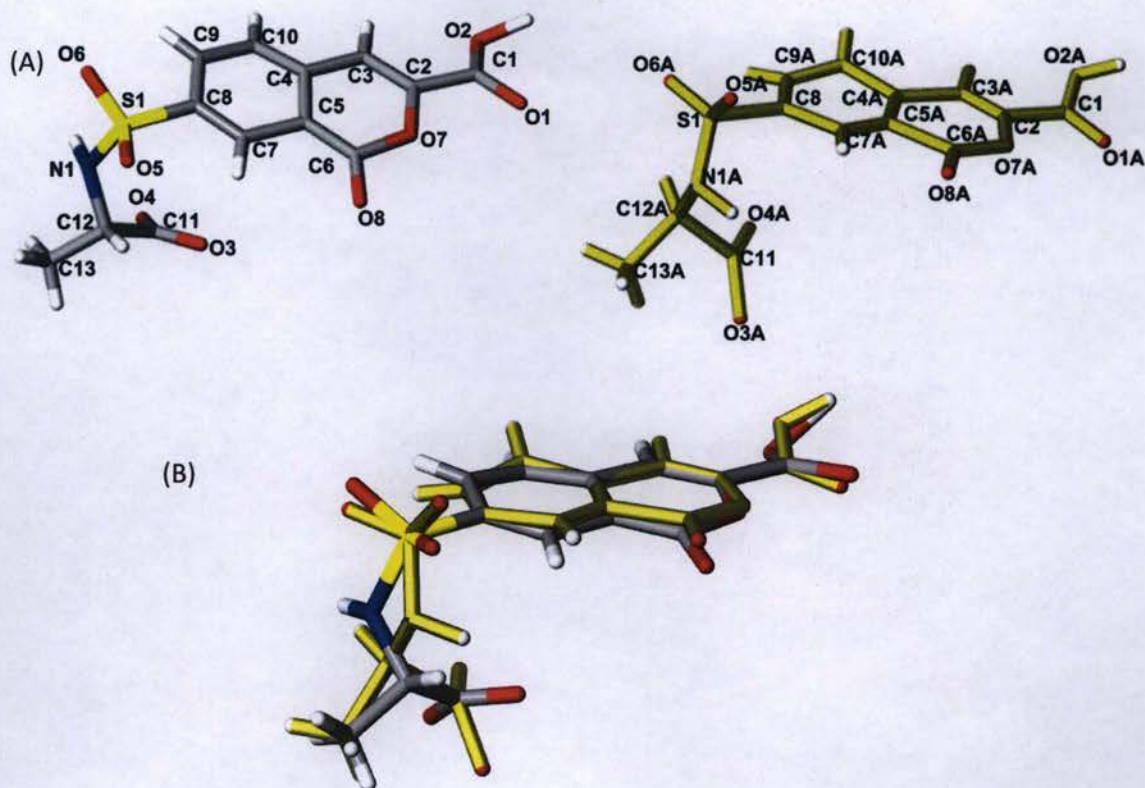


Figure 44. Asymmetric unit of **30** showing (A) disordered crystal projections separately and (B) combined structure.

Interestingly, despite this collection of disordered molecular components, each molecule of **30** assembles with an inversion symmetry neighbor to give distinct supramolecular dimers (Figure 43). The first structural feature that contributes to this motif is molecular shape. Though the sulfonamide alanine fragment contains at least four degrees of rotational freedom, molecules of **30** adopt the anticipated ‘fish hook’ conformation necessary to construct discrete dimer motifs. The second principal feature relates to the molecular recognition of these components. The framework of each molecule contains two well-positioned carboxylic acid groups that have a penchant of forming carboxyl...carboxyl contacts. The complementary shapes and CO₂H groups of

this general class of arylsulfonamides facilitate the recognition of a second molecule to give robust dimeric motifs. The fidelity of this motif is somewhat surprising given each molecule of **30** contains three hydrogen bond donors and six acceptors. Conceptually, such an assortment of acceptor/donor groups could give rise to several different crystal packing features that could disrupt dimer formation. As shown in Figure 45, the NH group is not involved in dimer formation, but rather links adjacent *n*-glide related dimer motifs via N-H \cdots O contacts ($x-1/2, -y-1/2, z-1/2$).

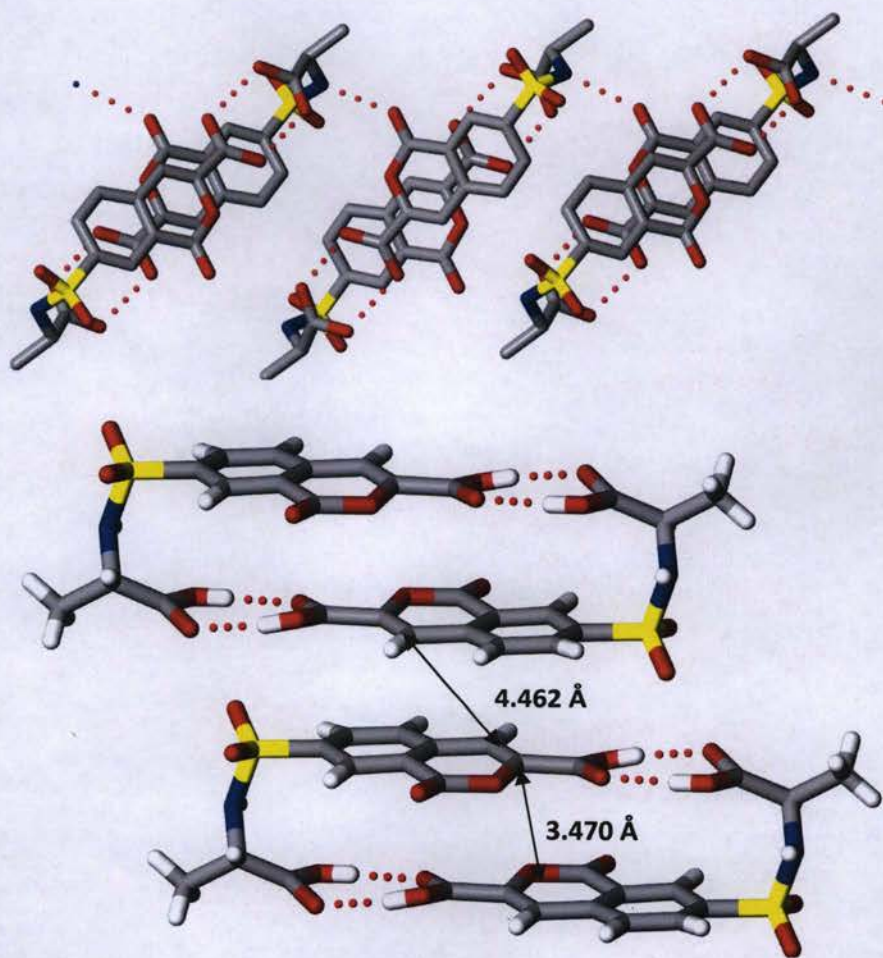


Figure 45. Crystal packing of **30** showing hydrogen bond patterns (top) (H atoms deleted for clarity) and favorable alignment of neighboring olefins of the homodimer (bottom) (minor disorder component excluded).

3.2.6.c Photodimerization of Racemic Isocoumarin **30**

Inspection of the crystal structure of **30** in Figure 45 reveals close olefin...olefin interactions that appear favorable for photodimerization. The close proximity of these olefin groups for the major disorder component is isolated to an intradimer (3.470 Å) pathway with contacts between dimer motifs significantly longer (4.462 Å). Olefin...olefin distances observed for the minor component are similar (intra, 3.480 Å; inter, 4.730 Å). This favorable alignment of C=C groups falls within Schmidt's³ distance criteria of 4.2 Å for topochemically controlled photodimerization reactions and provides support for further investigation to explore the [2+2] photodimerization behavior of this material.

A single crystal of **30** was irradiated via the UV tail-irradiation technique using a 200 W Xe(Hg) arc lamp and a 360 nm optical edge filter.⁵ After 8 hours of UV illumination, the crystal was placed on the diffractometer and X-ray data collected. From structure solution and refinement of the data, it was observed that the crystal had quantitatively converted to photoproduct **33**. As observed in Figure 46, the structure of the irradiated sample still retains a significant portion of disorder behavior from **30**, but the electron density initially associated with the olefin groups shifted to form racemic cyclobutane product **33**. In a similar fashion to starting material **30**, the crystal structure of **33** is characterized by molecules organized in monoclinic space group $P2_1/n$. The structures represented in Figure 46 feature two molecular fragments covalently connected across an inversion center. Similar to isocoumarin **30**, the crystal structure of **33** exhibits two-part disorder with a 60:40 ratio of refined occupancy factors. This transformation occurs via a single-crystal-to-single-crystal transformation and is thus quite rare

compared to other solid-state reactions reported in the literature where product phases are often polycrystalline or amorphous. The ability of **30** to proceed to **33**, while maintaining crystallinity, is likely related to the minimal motion required for this transformation. Close inspection of the reactant and product crystal structures indicates the peripheral sulfonamide groups undergo negligible movement while the internal olefin condenses to a cyclobutane moiety. The preserved crystal integrity is somewhat surprising given the change in geometry and spatial requirements of the olefin carbon atoms of **30** (*i.e.* trigonal planar to tetrahedral). This structural characteristic of the reaction also results in a splayed carboxyl group. Though this feature seems significant, it apparently does not generate considerable strain that could result in crystal fractures or compromise the lattice of the original sample.

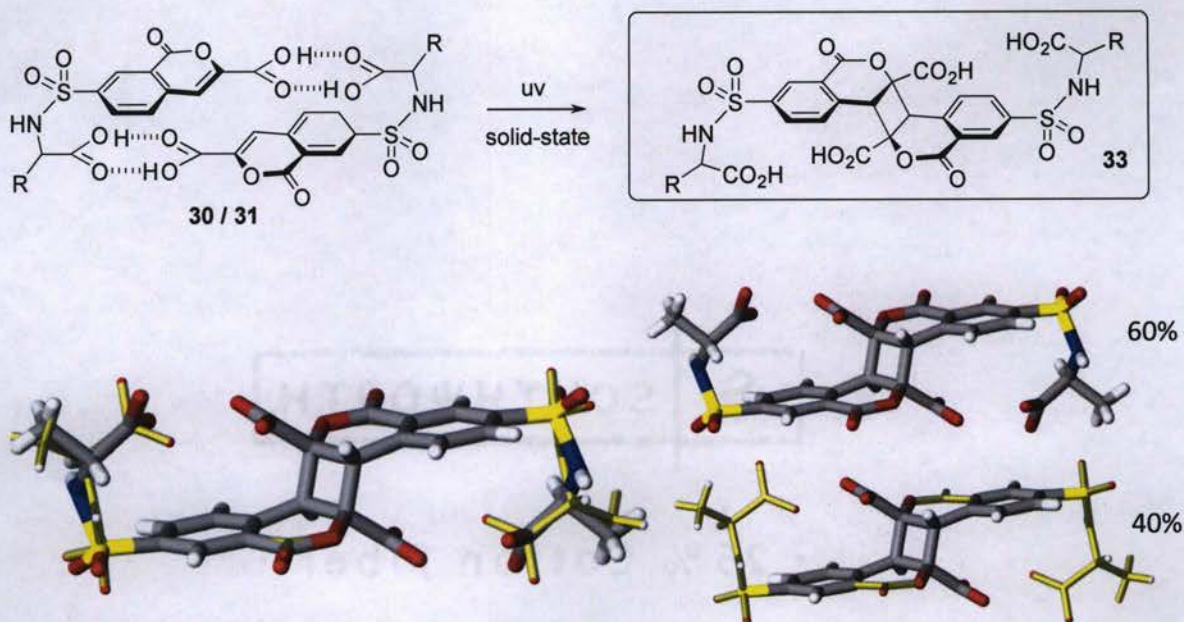


Figure 46. Crystal structure of photoproduct **33** (racemate) showing the combined disorder model (left) and each disorder component separately (right).

3.2.6.d Photodimerization of Homochiral Isocoumarin **31**

Though the crystal structure of homochiral **31** could not be determined, the design strategy employed for this material was derived from the photoactive supramolecular dimer achieved for racemate **30**. In the case of **31**, the anticipated formation of a hydrogen-bonded dimer would require the assembly of two molecules of the same chirality. If this crystal packing motif were realized, the result would provide access to an asymmetric environment for the purpose of enantiospecific solid-state reactions. The expected outcome of the UV irradiation of **31** is shown in Figure 47.

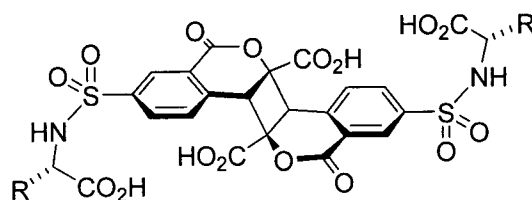


Figure 47. Expected photoproduct from UV irradiation of homochiral **31**.

UV irradiation of powdered **31** made use of the tail-end illumination technique using a 200 W Xe(Hg) arc lamp and a 360 nm optical edge filter.⁵ The powder was exposed for a total of 56.5 hours with samples retrieved periodically and examined via ¹H NMR. This data, shown in Figure 48, provides evidence of the progress of the transformation for **31** in the region of 3 to 9 ppm. cursory inspection of the NMR spectra reveals a complex set of signals related to starting material **31** and a set of signals that develop with increasing irradiation. One notable change is the signal at 4.35 ppm, corresponding to the olefinic =C-H proton H_d of **31**, diminished with time as a signal at 5.14 ppm developed. The chemical shift and peak multiplicity of this new signal is consistent with proton H_f attached to the cyclobutane fragment of the photoproduct.

Integration of these signals also offered a method to determine the conversion of homochiral **31** to photoproduct. Reaction progress has been tabulated with a maximum conversion of 65% after 56.5 hours (Figure 48).

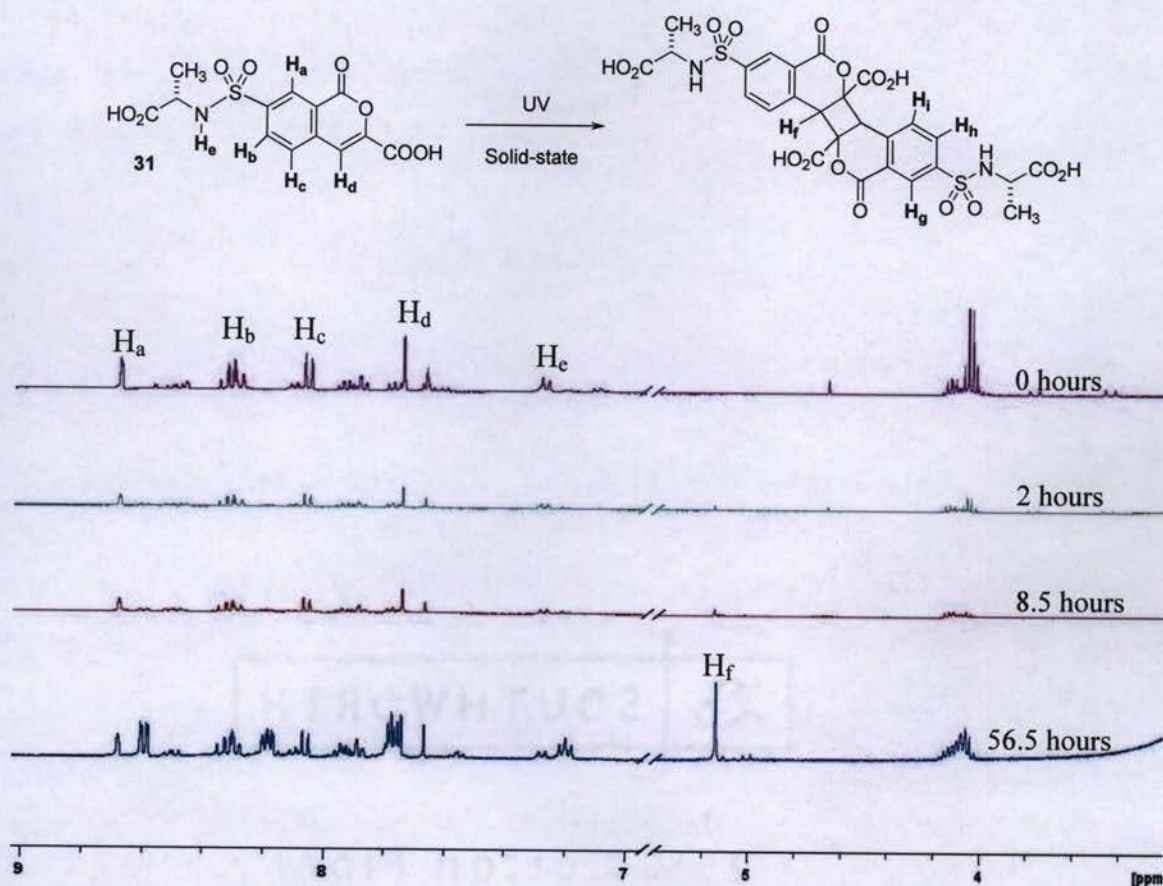


Figure 48. ^1H NMR of homochiral **31** showing the solid-state reactivity at 0, 2, 8.5, and 56.5 hours.

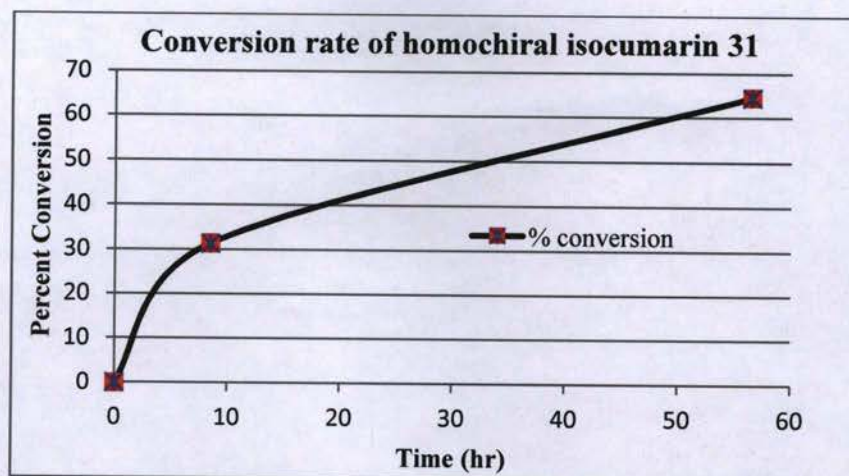


Figure 49. Solid-state conversion of **31** to the homochiral photoproduct.

Figure 50 shows an expanded view of the ^1H NMR of **31** after 56.5 hours of UV illumination. This spectral area draws attention to the aromatic and olefin regions of the NMR data and, though many spurious peaks of unknown origin exist, several well resolved signals related to both starting material and photoproduct are present. Details of these signals follow:

Starting material (**31**)

Ha	8.68 ppm, d, $J = 1.90$ Hz
Hb	8.31 ppm, dd, $J = 1.90, 8.26$ Hz
Hc	8.06 ppm, d, $J = 8.26$ Hz

Photoproduct from UV irradiation of solid **31**

Hg/Hg'	8.60 ppm, d, $J = 1.90$ Hz and 8.58 ppm, d, $J = 1.90$ Hz
Hh/Hh'	8.19 ppm, dd, $J = 1.90, 8.24$ Hz and 8.17 ppm, dd, $J = 1.90, 8.24$ Hz
Hi/Hi'	7.77 ppm, d, $J = 8.24$ Hz and 7.77 ppm, d, $J = 8.24$ Hz

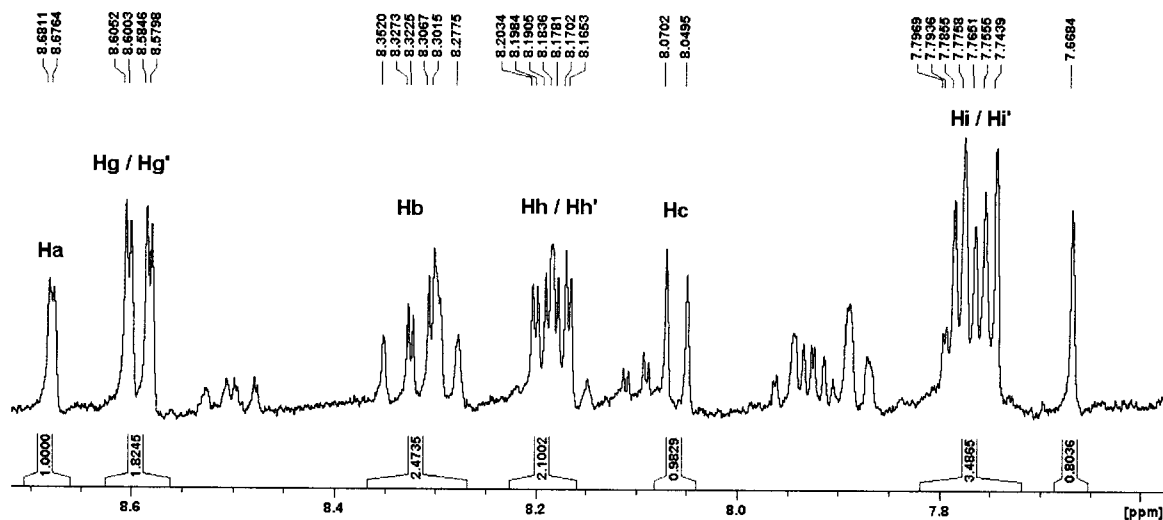


Figure 50. ^1H NMR of UV irradiated solid **31** (56.5 hours) showing both starting material and photoproduct.

The signals identified as the photoproduct aromatic C-H protons exist as two sets of signals. For example, inspection of the NMR spectrum reveals protons Hg and Hg' as the two distinct doublets at 8.19 and 8.17 ppm ($J = 1.9$ Hz). Though Hg and Hg' are chemically identical (Figures 47 and 48), each are positioned in magnetically different environments and thus furnish two separate signals in the spectrum. The origin of these different molecular surroundings for the photoproduct of **31** can be assigned to the pendant amino acids. While the central molecular architecture of the dimerized isocoumarins approximate inversion symmetry, this framework is desymmetrized by the chemically and stereochemically identical alanine groups attached to the sulfone. This spectral investigation of the solid-state reactivity of homochiral **31** not only provides evidence of the formation of a cyclobutane photoproduct constructed from isocoumarin frameworks, but also emphasizes and supports the design feature of this study to exploit reactant chirality towards enantiocontrolled reaction outcomes.

3.3 Conclusions

The content of this thesis explored two distinct projects that focused on designing organic crystals capable of undergoing chemical reactions. The first part of this research program examined heterodimerization (*i.e.* supramolecular and photochemical) from two distinctly different chemical components. When sulfonamide **23** was cocrystallized with bipyridines **24**, **25**, or **26**, the resulting crystals were a combination of the two components. In each case, crystallographic assessment of these samples (**23.24**, **23.25** and **23.26**) showed crystal components organized into tetrameric motifs by use of strong CO₂H...N interactions. The crystal structures of these systems exhibit disorder of the sulfonamidecinnamic groups and in the case **23.24** and **23.26** additional disorder of the bipyridine molecules. Dimerization was expected from UV illumination of solid samples because of the engineered tetrameric motif and alignment of the reactive C=C groups present in **23** and **26**. The lack of formation of cyclobutane photoproducts was rationalized by unfavorable alignment of adjacent olefin groups of **23** and **26**. Fumaramide **28** was also synthesized and its crystal structure determined. Cocrystal growth studies towards achieving single-crystals of the **23.28** system were unsuccessful and likely the result of mismatched component solubilities and reliable hydrogen-bond donor-accepter connections. Overall, the cocrystalline studies of **23** and components **24-26** and **28** highlight the i) structural success of forming tetrameric motifs and ii) challenge with aligning reaction centers constructed from chemically distinct components. Additional work in this area is needed to merge the critical features of supramolecular control and chemical reactivity.

The second study involved [2+2] photodimerization reactions of sulfonamide isocoumarin compounds and confirmed their ability to form cyclobutane photoproducts. This effort synthesized fish hook shape molecules by use of racemic **30** and homochiral **31** isocoumarins using a five-step synthetic sequence. UV irradiation of racemic sulfonamide isocoumarin resulted in quantitative conversion to a cyclobutane photoproduct via a single-crystal-to-single-crystal (SCSC) process. Transformations that proceed by SCSC reactions are rare and thus emphasize the importance of this contribution to the material sciences. While single crystals of homochiral isocoumarin **31** were not obtained, exposing powdered samples to UV radiation and subsequent NMR analysis provided support for cyclobutane product formation in 65% conversion.

Eight new crystal structures were presented over these two studies and their crystal structure analysis, crystal packing analysis, and hydrogen bond patterns revealed the structural tendencies of these systems. Overall, the preparation and UV illumination of these materials offered key insight to understand the structural boundaries of solid-state photodimerization reactions.

3.4 References

1. Wheeler, K. A.; Wiseman, J. D.; Grove, R. C. *Cryst. Eng. Comm.* **2011**, *13*, 3134-3137.
2. Grove, R. C.; Malehorn, S. H.; Breen, M. E.; Wheeler, K. A. *Chem. Commun.* **2010**, *46*, 7322-7324.
3. Cohen, M.; Schmidt, G. M. J. *J. Chem. Soc.* **1964**, 1996-2000.
4. Seitz, M.; Pluth, M. D.; Raymond, K. M. *Inorg. Chem.* **2007**, *46*, 351-353.
5. Enkelmann, M. K.; Brunklaus, G. *Cryst. Growth Des.* **2009**, *9*, 2354.

APPENDIX

Table 1a. Crystal data and structure refinement for cocrystal of **23** and 4,4'-dipyridyl (**24**).

Crystal data

$2(\text{C}_{12}\text{H}_{12.60}\text{NO}_6\text{S}) \cdot 0.4(\text{C}_{11}\text{H}_8\text{N}_2) \cdot \text{C}_{10}\text{H}_8\text{N}_2 \cdot 0.6\text{C}_5\text{H}_4\text{N}$	$V = 2086.47 (7) \text{ \AA}^3$
$M_r = 907.77$	$Z = 4$
Triclinic, $P\bar{1}$	$F(000) = 950$
Hall symbol: -P 1	$D_x = 1.446 \text{ Mg m}^{-3}$
$a = 11.1397 (2) \text{ \AA}$	Cu $K\alpha$ radiation, $\lambda = 1.54178 \text{ \AA}$
$b = 11.4550 (2) \text{ \AA}$	$\mu = 1.78 \text{ mm}^{-1}$
$c = 16.7925 (4) \text{ \AA}$	$T = 173 \text{ K}$
$\alpha = 93.855 (1)^\circ$	Transparent needle, colorless
$\beta = 102.058 (1)^\circ$	
$\gamma = 92.788 (1)^\circ$	

Data collection

Bruker APEXII CCD diffractometer	7361 independent reflections
Radiation source: fine-focus sealed tube	4899 reflections with $I > 2\sigma(I)$
Graphite	$R_{\text{int}} = 0.098$
phi and ω scans	$\theta_{\text{max}} = 67.8^\circ$, $\theta_{\text{min}} = 2.7^\circ$
Absorption correction: multi-scan <i>SADABS</i> (Bruker, 2010)	$h = -13 \rightarrow 13$
$T_{\text{min}} = 0.586$, $T_{\text{max}} = 0.702$	$k = -13 \rightarrow 13$
43383 measured reflections	$l = -20 \rightarrow 20$

Refinement

Refinement on F^2	Primary atom site location: structure-invariant direct methods
Least-squares matrix: full	Secondary atom site location: difference Fourier map
$R[F^2 > 2\sigma(F^2)] = 0.062$	Hydrogen site location: inferred from neighbouring sites
$wR(F^2) = 0.168$	H atoms treated by a mixture of independent and constrained refinement
$S = 1.05$	$w = 1/[\sigma^2(F_o^2) + (0.0734P)^2 + 1.8771P]$
7361 reflections	where $P = (F_o^2 + 2F_c^2)/3$
754 parameters	$(\Delta/\sigma)_{\text{max}} = 0.062$
180 restraints	$\Delta_{\text{max}} = 0.74 \text{ e \AA}^{-3}$
	$\Delta_{\text{min}} = -0.36 \text{ e \AA}^{-3}$

Table 1b. Fractional atomic coordinates and isotropic or equivalent isotropic displacement parameters (\AA^2) for cocrystal of **23** and 4,4'-dipyridyl (**24**).

	<i>X</i>	<i>y</i>	<i>Z</i>	$U_{\text{iso}}^*/U_{\text{eq}}$	Occ. (<1)
S1A	0.00023 (8)	-1.31793 (8)	-0.30020 (5)	0.0317 (2)	
O1A	0.4103 (3)	-0.6694 (3)	0.00345 (19)	0.0565 (8)	
O2A	0.2387 (3)	-0.6988 (2)	0.04994 (17)	0.0503 (7)	
H2A	0.2642	-0.6368	0.0795	0.060*	
O3A	0.0018 (3)	-1.0173 (2)	-0.36887 (17)	0.0543 (8)	
H3A	0.0043	-0.9505	-0.3444	0.065*	0.60
O4A	-0.1869 (3)	-1.0251 (3)	-0.3451 (2)	0.0635 (9)	
O5A	0.0997 (2)	-1.3931 (2)	-0.29867 (15)	0.0368 (6)	
O6A	-0.1153 (2)	-1.3633 (2)	-0.28817 (16)	0.0402 (6)	
N1A	-0.0224 (3)	-1.2656 (3)	-0.38925 (18)	0.0344 (7)	
H3	0.042 (4)	-1.240 (3)	-0.400 (2)	0.041*	
C1A	0.3183 (4)	-0.7252 (4)	0.0045 (2)	0.0428 (10)	
C2A	0.2773 (4)	-0.8364 (3)	-0.0500 (2)	0.0438 (10)	
H1	0.3349	-0.8661	-0.0795	0.053*	
C3A	0.1706 (4)	-0.8967 (3)	-0.0614 (2)	0.0384 (9)	
H5	0.1135	-0.8691	-0.0307	0.046*	
C4A	0.1311 (4)	-1.0034 (3)	-0.1172 (2)	0.0339 (8)	
C5A	0.2099 (4)	-1.0557 (3)	-0.1621 (2)	0.0359 (9)	
H5A	0.2922	-1.0240	-0.1548	0.043*	
C6A	0.1705 (3)	-1.1523 (3)	-0.2168 (2)	0.0352 (8)	
H6A	0.2245	-1.1860	-0.2475	0.042*	
C7A	0.0508 (3)	-1.1994 (3)	-0.2261 (2)	0.0299 (8)	
C8A	-0.0282 (3)	-1.1507 (3)	-0.1814 (2)	0.0340 (8)	
H8A	-0.1097	-1.1840	-0.1875	0.041*	
C9A	0.0124 (4)	-1.0530 (3)	-0.1276 (2)	0.0383 (9)	
H9A	-0.0421	-1.0194	-0.0972	0.046*	
C10A	-0.1019 (5)	-1.0698 (4)	-0.3724 (2)	0.0543 (13)	
C11A	-0.1239 (4)	-1.1921 (3)	-0.4143 (2)	0.0400 (9)	
H11A	-0.1989	-1.2296	-0.4003	0.048*	
C12A	-0.1486 (5)	-1.1852 (4)	-0.5057 (2)	0.0547 (12)	
H12A	-0.0764	-1.1477	-0.5207	0.082*	
H12B	-0.2199	-1.1389	-0.5227	0.082*	
H12C	-0.1654	-1.2644	-0.5329	0.082*	
N2A	0.1647 (5)	-0.2953 (5)	-0.0223 (4)	0.0307 (14)	0.60
N3A	0.0109 (7)	-0.8209 (5)	-0.2773 (4)	0.0425 (19)	0.60
C13A	0.2507 (7)	-0.3500 (8)	-0.0485 (5)	0.0236 (16)	0.60
H13A	0.3331	-0.3176	-0.0338	0.028*	0.60
C14A	0.2240 (7)	-0.4562 (7)	-0.0983 (5)	0.034 (2)	0.60
H14A	0.2875	-0.4949	-0.1171	0.041*	0.60
C15A	0.1058 (8)	-0.5021 (9)	-0.1186 (7)	0.007 (3)*	0.40
C16A	0.0180 (9)	-0.4435 (7)	-0.0876 (6)	0.0245 (19)	0.60
H16A	-0.0647	-0.4752	-0.0991	0.029*	0.60
C17A	0.0492 (7)	-0.3407 (7)	-0.0407 (5)	0.043 (2)	0.60
H17A	-0.0126	-0.3007	-0.0207	0.051*	0.60
C18A	0.1045 (7)	-0.7463 (5)	-0.2814 (4)	0.0356 (14)	0.60
H18A	0.1504	-0.7651	-0.3217	0.043*	0.60
C19A	0.1407 (7)	-0.6433 (7)	-0.2318 (4)	0.0284 (16)	0.60
H19A	0.2083	-0.5941	-0.2387	0.034*	0.60
C20A	0.0747 (10)	-0.6135 (8)	-0.1710 (6)	0.027 (2)	0.60
C21A	-0.0251 (11)	-0.6892 (11)	-0.1700 (8)	0.035 (3)	0.60

H21A	-0.0761	-0.6704	-0.1327	0.042*	0.60
C22A	-0.0543 (7)	-0.7908 (6)	-0.2207 (5)	0.0367 (18)	0.60
H22A	-0.1223	-0.8411	-0.2157	0.044*	0.60
S1B	0.6349 (6)	0.5187 (3)	0.3945 (2)	0.0352 (11)	0.50
O1B	0.3964 (3)	-0.1155 (3)	0.0202 (2)	0.0634 (9)	
O2B	0.2421 (3)	-0.1008 (3)	0.08481 (19)	0.0604 (9)	
H2B	0.2159	-0.1626	0.0552	0.072*	0.60
O3B	0.7793 (3)	0.2096 (3)	0.41293 (19)	0.0632 (10)	
O4B	0.6413 (3)	0.2084 (3)	0.4859 (2)	0.0784 (11)	
H4B	0.6095	0.1512	0.4531	0.094*	
O5B	0.6839 (7)	0.5936 (7)	0.3346 (5)	0.0341 (17)	0.50
O6B	0.5635 (6)	0.5621 (6)	0.4438 (4)	0.0379 (16)	0.50
N1B	0.7593 (6)	0.4663 (6)	0.4426 (4)	0.0282 (13)	0.50
H7	0.800 (7)	0.447 (7)	0.414 (5)	0.034*	0.50
N2B	0.5750 (5)	0.0088 (4)	0.3924 (3)	0.0450 (11)	0.80
N3B	0.3310 (4)	-0.5060 (3)	0.1458 (3)	0.0270 (9)	0.80
C1B	0.3477 (5)	-0.0646 (4)	0.0709 (3)	0.0634 (15)	
C2B	0.4099 (4)	0.0436 (4)	0.1170 (2)	0.0456 (10)	
H2	0.4779	0.0786	0.0993	0.055*	
C3B	0.3774 (4)	0.0942 (4)	0.1805 (2)	0.0419 (9)	
H3B	0.3082	0.0588	0.1966	0.050*	
C4B	0.4375 (3)	0.2012 (3)	0.2298 (2)	0.0345 (8)	
C5B	0.5332 (4)	0.2676 (3)	0.2096 (2)	0.0401 (9)	
H5B	0.5608	0.2454	0.1612	0.048*	
C6B	0.5889 (4)	0.3652 (3)	0.2587 (2)	0.0413 (9)	
H6B	0.6555	0.4086	0.2450	0.050*	
C7B	0.5468 (3)	0.3992 (3)	0.3280 (2)	0.0345 (8)	
C8B	0.4499 (4)	0.3371 (3)	0.3482 (2)	0.0455 (10)	
H8B	0.4200	0.3615	0.3952	0.055*	
C9B	0.3968 (4)	0.2386 (3)	0.2989 (2)	0.0453 (10)	
H9B	0.3304	0.1954	0.3130	0.054*	
C10B	0.7257 (4)	0.2594 (3)	0.4592 (2)	0.0402 (9)	
C11B	0.7441 (9)	0.3808 (7)	0.5011 (5)	0.0315 (19)	0.50
H11B	0.6749	0.3991	0.5284	0.038*	0.50
C13B	0.6402 (5)	-0.0364 (5)	0.3423 (4)	0.0436 (13)	0.80
H13B	0.7182	0.0009	0.3419	0.052*	0.80
C16B	0.4165 (5)	-0.1370 (5)	0.3413 (3)	0.0491 (14)	0.80
H16B	0.3361	-0.1693	0.3408	0.059*	0.80
C17B	0.4639 (5)	-0.0395 (5)	0.3912 (4)	0.0535 (15)	0.80
H17B	0.4160	-0.0052	0.4261	0.064*	0.80
C18B	0.4144 (5)	-0.4364 (5)	0.1212 (3)	0.0276 (10)	0.80
H18B	0.4378	-0.4583	0.0713	0.033*	0.80
C19B	0.4677 (7)	-0.3338 (6)	0.1656 (4)	0.0276 (14)	0.80
H19B	0.5270	-0.2873	0.1464	0.033*	0.80
C20B	0.4333 (9)	-0.2981 (7)	0.2401 (5)	0.032 (2)	0.80
C21B	0.3484 (7)	-0.3708 (6)	0.2633 (5)	0.0372 (17)	0.80
H21B	0.3218	-0.3506	0.3123	0.045*	0.80
C22B	0.3003 (4)	-0.4729 (3)	0.2172 (2)	0.0375 (14)	0.80
H22B	0.2431	-0.5220	0.2365	0.045*	0.80
S1C	0.6090 (4)	0.5214 (3)	0.3923 (2)	0.053 (2)	0.50
O5C	0.5101 (4)	0.5868 (3)	0.4233 (2)	0.045 (2)	0.50
O6C	0.6932 (4)	0.5837 (3)	0.3629 (2)	0.037 (2)	0.50
N1C	0.6813 (6)	0.4691 (6)	0.4814 (4)	0.0377 (16)	0.50
H6	0.628 (8)	0.440 (7)	0.510 (5)	0.045*	0.50
C11C	0.7799 (5)	0.3934 (5)	0.4726 (4)	0.038 (2)	0.50
H11C	0.8247	0.4163	0.4297	0.046*	0.50

N2C	-0.0806 (5)	-0.8177 (5)	-0.2681 (4)	0.039 (2)	0.40
N3C	0.2485 (5)	-0.3108 (5)	-0.0388 (4)	0.057 (5)	0.40
C13C	0.0214 (5)	-0.7697 (5)	-0.2856 (4)	0.035 (3)	0.40
H13C	0.0529	-0.8078	-0.3281	0.042*	0.40
C14C	0.0851 (10)	-0.6663 (10)	-0.2451 (7)	0.037 (3)	0.40
H14C	0.1533	-0.6319	-0.2628	0.044*	0.40
C15C	0.0462 (13)	-0.6172 (14)	-0.1801 (9)	0.025 (5)	0.40
C16C	-0.0538 (17)	-0.6726 (16)	-0.1557 (13)	0.029 (4)	0.40
H16C	-0.0796	-0.6435	-0.1081	0.035*	0.40
C17C	-0.1130 (11)	-0.7689 (9)	-0.2017 (7)	0.046 (3)	0.40
H17C	-0.1823	-0.8040	-0.1856	0.055*	0.40
C18C	0.3041 (10)	-0.3958 (8)	-0.0748 (6)	0.041 (2)	0.40
H18C	0.3906	-0.3850	-0.0694	0.050*	0.40
C19C	0.2467 (9)	-0.4965 (9)	-0.1185 (8)	0.031 (3)	0.40
H19C	0.2923	-0.5525	-0.1417	0.037*	0.40
C20C	0.1152 (9)	-0.5145 (10)	-0.1280 (8)	0.020 (4)*	0.40
C21C	0.0598 (13)	-0.4278 (11)	-0.0948 (9)	0.034 (4)	0.40
H21C	-0.0272	-0.4381	-0.1038	0.040*	0.40
C22C	0.1098 (4)	-0.3295 (3)	-0.0510 (3)	0.057 (5)	0.40
H22C	0.0618	-0.2748	-0.0288	0.069*	0.40
C15B	0.4878 (4)	-0.1887 (3)	0.2911 (3)	0.0342 (15)	0.80
C14B	0.5989 (4)	-0.1386 (3)	0.2886 (3)	0.0392 (12)	0.80
H14B	0.6466	-0.1703	0.2527	0.047*	0.80
N2D	0.372 (3)	-0.491 (2)	0.1275 (14)	0.061 (9)*	0.20
N3D	0.6499 (15)	0.0116 (14)	0.3651 (10)	0.029 (5)*	0.20
C13D	0.452 (3)	-0.416 (2)	0.1087 (15)	0.061 (11)*	0.20
H13D	0.4896	-0.4347	0.0640	0.073*	0.20
C14D	0.482 (4)	-0.309 (2)	0.1545 (16)	0.045 (11)*	0.20
H14D	0.5226	-0.2462	0.1352	0.054*	0.20
C15D	0.449 (3)	-0.299 (2)	0.2283 (16)	0.008 (6)*	0.20
C16D	0.370 (3)	-0.383 (2)	0.2499 (16)	0.034 (9)*	0.20
H16D	0.3469	-0.3752	0.3012	0.041*	0.20
C17D	0.3260 (19)	-0.4778 (17)	0.1938 (14)	0.028 (6)*	0.20
H17D	0.2641	-0.5321	0.2029	0.034*	0.20
C18D	0.6966 (14)	-0.0606 (11)	0.3155 (9)	0.017 (3)*	0.20
H18D	0.7760	-0.0389	0.3068	0.020*	0.20
C19D	0.6389 (16)	-0.1646 (15)	0.2756 (12)	0.030 (5)*	0.20
H19D	0.6818	-0.2168	0.2469	0.036*	0.20
C20D	0.5097 (18)	-0.192 (2)	0.2786 (16)	0.036 (8)*	0.20
C21D	0.4655 (17)	-0.1130 (15)	0.3274 (11)	0.033 (5)*	0.20
H21D	0.3831	-0.1276	0.3330	0.040*	0.20
C22D	0.5286 (16)	-0.0140 (15)	0.3694 (11)	0.026 (5)*	0.20
H22D	0.4892	0.0369	0.4013	0.031*	0.20
C2	0.8688 (4)	0.3937 (4)	0.5625 (3)	0.0664 (15)	
H2C	0.8811	0.4731	0.5897	0.100*	0.50
H2D	0.9351	0.3798	0.5334	0.100*	0.50
H2E	0.8694	0.3364	0.6033	0.100*	0.50
H2F	0.9093	0.3198	0.5613	0.100*	0.50
H2G	0.8553	0.4131	0.6175	0.100*	0.50
H2H	0.9210	0.4564	0.5476	0.100*	0.50

Table 1c. Atomic displacement parameters (\AA^2) for Cocrystal of **23** and 4,4'-dipyridyl
(24).

	U^{11}	U^{22}	U^{33}	U^{12}	U^{13}	U^{23}
S1A	0.0350 (5)	0.0270 (5)	0.0311 (4)	-0.0063 (4)	0.0058 (4)	-0.0013 (4)
O1A	0.060 (2)	0.0427 (17)	0.0625 (19)	-0.0095 (15)	0.0111 (16)	-0.0120 (15)
O2A	0.061 (2)	0.0339 (15)	0.0508 (17)	-0.0061 (14)	0.0045 (15)	-0.0016 (13)
O3A	0.078 (2)	0.0282 (15)	0.0483 (17)	-0.0073 (15)	-0.0004 (15)	-0.0058 (13)
O4A	0.078 (2)	0.0502 (19)	0.059 (2)	0.0188 (18)	0.0075 (18)	-0.0051 (16)
O5A	0.0413 (15)	0.0285 (13)	0.0394 (14)	-0.0014 (11)	0.0075 (12)	-0.0002 (11)
O6A	0.0387 (15)	0.0380 (15)	0.0432 (15)	-0.0108 (12)	0.0117 (12)	-0.0024 (12)
N1A	0.0381 (19)	0.0301 (16)	0.0318 (16)	-0.0080 (14)	0.0042 (14)	-0.0022 (13)
C1A	0.051 (3)	0.045 (2)	0.035 (2)	0.018 (2)	0.0120 (19)	0.0084 (18)
C2A	0.051 (3)	0.036 (2)	0.040 (2)	-0.0005 (19)	0.0020 (19)	-0.0019 (18)
C3A	0.052 (3)	0.035 (2)	0.0300 (19)	0.0151 (19)	0.0090 (17)	0.0064 (16)
C4A	0.042 (2)	0.034 (2)	0.0258 (17)	0.0070 (17)	0.0050 (15)	-0.0001 (15)
C5A	0.035 (2)	0.033 (2)	0.0353 (19)	-0.0029 (16)	0.0005 (16)	-0.0028 (16)
C6A	0.036 (2)	0.031 (2)	0.038 (2)	0.0006 (16)	0.0106 (16)	-0.0059 (16)
C7A	0.033 (2)	0.0280 (18)	0.0272 (17)	-0.0034 (15)	0.0047 (15)	0.0010 (15)
C8A	0.033 (2)	0.039 (2)	0.0297 (18)	-0.0006 (17)	0.0069 (15)	0.0029 (16)
C9A	0.043 (2)	0.043 (2)	0.0310 (19)	0.0123 (18)	0.0112 (17)	0.0009 (17)
C10A	0.090 (4)	0.033 (2)	0.032 (2)	0.008 (3)	-0.007 (2)	-0.0004 (18)
C11A	0.045 (2)	0.033 (2)	0.037 (2)	0.0001 (18)	-0.0019 (17)	0.0020 (17)
C12A	0.072 (3)	0.043 (2)	0.038 (2)	0.001 (2)	-0.009 (2)	-0.0022 (19)
N2A	0.014 (3)	0.041 (4)	0.040 (4)	0.012 (3)	0.010 (3)	0.012 (3)
N3A	0.058 (5)	0.025 (4)	0.036 (3)	-0.007 (4)	-0.005 (3)	-0.004 (3)
C13A	0.022 (4)	0.025 (5)	0.024 (3)	-0.002 (3)	0.009 (3)	-0.009 (3)
C14A	0.037 (5)	0.035 (5)	0.038 (4)	0.023 (4)	0.021 (3)	0.006 (4)
C16A	0.028 (5)	0.025 (4)	0.022 (4)	-0.006 (3)	0.013 (3)	0.004 (3)
C17A	0.053 (5)	0.036 (4)	0.044 (4)	-0.003 (4)	0.022 (4)	0.004 (3)
C18A	0.053 (5)	0.024 (3)	0.030 (3)	0.006 (3)	0.012 (3)	-0.005 (3)
C19A	0.029 (4)	0.027 (4)	0.031 (4)	0.001 (4)	0.013 (4)	-0.002 (3)
C20A	0.028 (5)	0.024 (4)	0.023 (4)	0.004 (3)	-0.006 (4)	0.001 (3)
C21A	0.038 (6)	0.042 (6)	0.029 (6)	0.004 (5)	0.014 (4)	0.002 (4)
C22A	0.039 (5)	0.027 (4)	0.037 (4)	-0.008 (3)	-0.006 (4)	0.004 (3)
S1B	0.0411 (16)	0.0164 (18)	0.035 (2)	-0.0045 (11)	-0.0154 (12)	-0.0105 (13)
O1B	0.071 (2)	0.0409 (18)	0.069 (2)	0.0094 (16)	-0.0004 (18)	-0.0154 (16)
O2B	0.061 (2)	0.0412 (17)	0.066 (2)	0.0063 (16)	-0.0102 (16)	-0.0205 (15)
O3B	0.070 (2)	0.0570 (19)	0.063 (2)	-0.0329 (17)	0.0344 (18)	-0.0305 (16)
O4B	0.047 (2)	0.102 (3)	0.080 (2)	-0.025 (2)	0.0187 (18)	-0.031 (2)
O5B	0.038 (4)	0.037 (4)	0.028 (4)	-0.001 (3)	0.009 (3)	0.000 (3)
O6B	0.042 (4)	0.046 (4)	0.026 (3)	-0.002 (3)	0.017 (3)	-0.022 (3)
N1B	0.031 (4)	0.022 (3)	0.031 (3)	0.001 (3)	0.004 (3)	0.004 (3)
N2B	0.044 (3)	0.041 (3)	0.044 (3)	-0.005 (2)	0.003 (3)	-0.009 (2)
N3B	0.021 (2)	0.030 (2)	0.032 (2)	-0.0002 (17)	0.0090 (18)	-0.0006 (18)
C1B	0.064 (3)	0.030 (2)	0.074 (3)	0.003 (2)	-0.034 (3)	-0.005 (2)
C2B	0.046 (3)	0.041 (2)	0.043 (2)	0.0066 (19)	-0.0054 (19)	-0.0016 (19)
C3B	0.036 (2)	0.043 (2)	0.043 (2)	0.0070 (18)	-0.0017 (17)	0.0034 (19)
C4B	0.0273 (19)	0.035 (2)	0.037 (2)	0.0029 (16)	-0.0022 (15)	-0.0021 (16)
C5B	0.040 (2)	0.045 (2)	0.0326 (19)	0.0043 (18)	0.0063 (17)	-0.0100 (17)
C6B	0.033 (2)	0.045 (2)	0.045 (2)	-0.0033 (18)	0.0118 (18)	-0.0037 (19)
C7B	0.034 (2)	0.036 (2)	0.0293 (18)	-0.0017 (16)	-0.0002 (15)	-0.0029 (16)
C8B	0.056 (3)	0.040 (2)	0.043 (2)	-0.006 (2)	0.020 (2)	-0.0094 (18)
C9B	0.044 (2)	0.042 (2)	0.050 (2)	-0.0109 (19)	0.0143 (19)	-0.0066 (19)

C10B	0.043 (2)	0.035 (2)	0.036 (2)	-0.0069 (18)	-0.0059 (18)	0.0021 (17)
C11B	0.038 (5)	0.021 (4)	0.034 (5)	0.002 (4)	0.004 (4)	0.006 (3)
C13B	0.037 (3)	0.044 (4)	0.049 (3)	-0.006 (3)	0.008 (3)	0.011 (3)
C16B	0.042 (3)	0.057 (4)	0.045 (3)	-0.009 (3)	0.013 (3)	-0.021 (3)
C17B	0.042 (3)	0.057 (3)	0.061 (3)	-0.008 (3)	0.019 (3)	-0.022 (3)
C18B	0.025 (3)	0.034 (3)	0.026 (2)	0.001 (2)	0.010 (2)	0.001 (2)
C19B	0.031 (3)	0.026 (3)	0.028 (3)	0.000 (2)	0.009 (2)	0.006 (2)
C20B	0.031 (4)	0.035 (3)	0.031 (4)	0.008 (2)	0.007 (3)	0.000 (2)
C21B	0.033 (3)	0.042 (3)	0.040 (3)	0.000 (3)	0.019 (3)	-0.006 (2)
C22B	0.032 (3)	0.038 (3)	0.049 (3)	-0.004 (2)	0.024 (3)	0.008 (2)
S1C	0.049 (3)	0.052 (3)	0.045 (3)	-0.0168 (17)	-0.0195 (17)	0.0106 (19)
O5C	0.036 (4)	0.052 (4)	0.046 (4)	-0.001 (3)	0.010 (3)	-0.012 (3)
O6C	0.050 (4)	0.030 (4)	0.030 (5)	-0.011 (3)	0.015 (4)	-0.005 (3)
N1C	0.035 (4)	0.047 (4)	0.029 (3)	-0.010 (3)	0.011 (3)	-0.013 (3)
C11C	0.036 (6)	0.039 (6)	0.036 (6)	-0.015 (4)	0.008 (4)	-0.013 (5)
N2C	0.035 (6)	0.033 (5)	0.050 (6)	0.000 (4)	0.013 (5)	0.001 (4)
N3C	0.092 (11)	0.018 (7)	0.039 (7)	0.002 (6)	-0.029 (7)	-0.008 (5)
C13C	0.015 (5)	0.031 (8)	0.058 (8)	-0.007 (6)	0.014 (5)	-0.018 (6)
C14C	0.027 (7)	0.041 (7)	0.044 (7)	-0.013 (6)	0.011 (6)	0.011 (6)
C15C	0.025 (5)	0.025 (5)	0.025 (5)	0.0018 (11)	0.0050 (15)	0.0018 (11)
C16C	0.035 (9)	0.028 (7)	0.027 (7)	-0.008 (6)	0.021 (5)	-0.007 (4)
C17C	0.052 (8)	0.038 (6)	0.058 (7)	0.008 (6)	0.030 (6)	0.014 (5)
C18C	0.049 (7)	0.032 (6)	0.034 (5)	-0.013 (6)	-0.008 (5)	-0.004 (5)
C19C	0.021 (6)	0.027 (6)	0.047 (7)	0.004 (5)	0.012 (5)	0.002 (5)
C21C	0.040 (10)	0.042 (7)	0.024 (5)	-0.007 (6)	0.017 (6)	0.011 (5)
C22C	0.099 (17)	0.035 (8)	0.028 (7)	-0.005 (10)	-0.008 (9)	0.007 (5)
C15B	0.048 (4)	0.023 (3)	0.029 (3)	0.002 (2)	0.003 (3)	0.001 (2)
C14B	0.039 (3)	0.035 (3)	0.040 (3)	-0.004 (3)	0.003 (3)	0.002 (2)
C2	0.061 (3)	0.057 (3)	0.061 (3)	0.008 (2)	-0.024 (2)	-0.028 (2)

Table 1d. Geometric parameters (Å, °) for Cocrystal of **23** and 4,4'-dipyridyl (**24**).

S1A—O6A	1.423 (3)	C8B—C9B	1.383 (5)
S1A—O5A	1.433 (3)	C8B—H8B	0.9500
S1A—N1A	1.624 (3)	C9B—H9B	0.9500
S1A—C7A	1.765 (3)	C10B—C11B	1.501 (9)
O1A—C1A	1.185 (5)	C10B—C11C	1.606 (6)
O2A—C1A	1.319 (5)	C11B—C2	1.541 (10)
O2A—H2A	0.8400	C11B—H11B	1.0000
O3A—C10A	1.265 (6)	C11B—H6	1.52 (8)
O3A—H3A	0.8400	C13B—C14B	1.424 (7)
O4A—C10A	1.252 (6)	C13B—H13B	0.9500
N1A—C11A	1.451 (5)	C16B—C17B	1.363 (7)
N1A—H3	0.82 (4)	C16B—C15B	1.396 (7)
C1A—C2A	1.510 (6)	C16B—H16B	0.9500
C2A—C3A	1.318 (6)	C17B—H17B	0.9500
C2A—H1	0.9500	C18B—C19B	1.385 (7)
C3A—C4A	1.479 (5)	C18B—H18B	0.9500
C3A—H5	0.9500	C19B—C20B	1.422 (8)
C4A—C9A	1.385 (5)	C19B—H19B	0.9500
C4A—C5A	1.403 (5)	C20B—C21B	1.364 (8)
C5A—C6A	1.381 (5)	C20B—C15B	1.496 (6)
C5A—H5A	0.9500	C21B—C22B	1.377 (7)
C6A—C7A	1.388 (5)	C21B—H21B	0.9500
C6A—H6A	0.9500	C22B—H22B	0.9500

C7A—C8A	1.386 (5)	S1C—O6C	1.3453
C8A—C9A	1.384 (5)	S1C—O5C	1.5208
C8A—H8A	0.9500	S1C—N1C	1.705 (8)
C9A—H9A	0.9500	N1C—C11C	1.457 (9)
C10A—C11A	1.510 (5)	N1C—H6	0.90 (8)
C11A—C12A	1.509 (5)	C11C—C2	1.622 (8)
C11A—H11A	1.0000	C11C—H7	1.25 (8)
C12A—H12A	0.9800	C11C—H11C	1.0000
C12A—H12B	0.9800	N2C—C13C	1.3336
C12A—H12C	0.9800	N2C—C17C	1.337 (10)
N2A—C13A	1.304 (9)	N3C—C18C	1.354 (11)
N2A—C17A	1.330 (9)	N3C—C22C	1.518 (7)
N3A—C18A	1.331 (8)	C13C—C14C	1.406 (10)
N3A—C22A	1.348 (10)	C13C—H13C	0.9500
C13A—C14A	1.411 (10)	C14C—C15C	1.354 (14)
C13A—H13A	0.9500	C14C—H14C	0.9500
C14A—C15A	1.359 (11)	C15C—C16C	1.403 (15)
C14A—H14A	0.9500	C15C—C20C	1.495 (11)
C15A—C16A	1.381 (12)	C16C—C17C	1.360 (15)
C15A—C20A	1.484 (10)	C16C—H16C	0.9500
C16A—C17A	1.359 (11)	C17C—H17C	0.9500
C16A—H16A	0.9500	C18C—C19C	1.377 (11)
C17A—H17A	0.9500	C18C—H18C	0.9500
C18A—C19A	1.389 (8)	C19C—C20C	1.442 (12)
C18A—H18A	0.9500	C19C—H19C	0.9500
C19A—C20A	1.411 (10)	C20C—C21C	1.344 (14)
C19A—H19A	0.9500	C21C—C22C	1.333 (12)
C20A—C21A	1.380 (12)	C21C—H21C	0.9500
C21A—C22A	1.378 (11)	C22C—H22C	0.9500
C21A—H21A	0.9500	C15B—C14B	1.3481
C22A—H22A	0.9500	C14B—H14B	0.9496
S1B—O6B	1.351 (7)	N2D—C13D	1.310 (15)
S1B—O5B	1.532 (8)	N2D—C17D	1.321 (15)
S1B—N1B	1.615 (9)	N3D—C18D	1.334 (14)
S1B—C7B	1.814 (5)	N3D—C22D	1.386 (15)
O1B—C1B	1.232 (6)	C13D—C14D	1.386 (16)
O2B—C1B	1.300 (6)	C13D—H13D	0.9500
O2B—H2B	0.8400	C14D—C15D	1.359 (16)
O3B—C10B	1.205 (5)	C14D—H14D	0.9500
O4B—C10B	1.259 (5)	C15D—C16D	1.387 (17)
O4B—H4B	0.8400	C15D—C20D	1.488 (13)
N1B—C11B	1.461 (9)	C16D—C17D	1.390 (17)
N1B—H7	0.76 (8)	C16D—H16D	0.9500
N2B—C13B	1.319 (7)	C17D—H17D	0.9500
N2B—C17B	1.326 (6)	C18D—C19D	1.385 (14)
N3B—C18B	1.342 (7)	C18D—H14B	1.5845
N3B—C22B	1.351 (6)	C18D—H18D	0.9500
C1B—C2B	1.476 (6)	C19D—C20D	1.470 (16)
C2B—C3B	1.305 (6)	C19D—H14B	0.4124
C2B—H2	0.9500	C19D—H19D	0.9500
C3B—C4B	1.480 (5)	C20D—C21D	1.360 (16)
C3B—H3B	0.9500	C21D—C22D	1.373 (15)
C4B—C9B	1.381 (5)	C21D—H21D	0.9500
C4B—C5B	1.392 (5)	C22D—H22D	0.9500
C5B—C6B	1.381 (5)	C2—H2C	0.9800
C5B—H5B	0.9500	C2—H2D	0.9800

C6B—C7B	1.382 (5)	C2—H2E	0.9800
C6B—H6B	0.9500	C2—H2F	0.9800
C7B—C8B	1.377 (5)	C2—H2G	0.9800
C7B—S1C	1.731 (5)	C2—H2H	0.9800
O6A—S1A—O5A	120.22 (16)	C14B—C13B—H13B	118.6
O6A—S1A—N1A	107.92 (16)	C17B—C16B—C15B	119.1 (5)
O5A—S1A—N1A	105.36 (16)	C17B—C16B—H16B	120.5
O6A—S1A—C7A	107.25 (16)	C15B—C16B—H16B	120.5
O5A—S1A—C7A	108.05 (16)	N2B—C17B—C16B	121.9 (5)
N1A—S1A—C7A	107.46 (16)	N2B—C17B—H17B	119.0
C1A—O2A—H2A	109.5	C16B—C17B—H17B	119.0
C10A—O3A—H3A	109.5	N3B—C18B—C19B	122.7 (5)
C11A—N1A—S1A	120.3 (3)	N3B—C18B—H18B	118.6
C11A—N1A—H3	113 (3)	C19B—C18B—H18B	118.6
S1A—N1A—H3	112 (3)	C18B—C19B—C20B	119.9 (6)
O1A—C1A—O2A	125.8 (4)	C18B—C19B—H19B	120.1
O1A—C1A—C2A	122.3 (4)	C20B—C19B—H19B	120.1
O2A—C1A—C2A	111.8 (4)	C21B—C20B—C19B	116.0 (6)
C3A—C2A—C1A	127.2 (4)	C21B—C20B—C15B	121.5 (6)
C3A—C2A—H1	116.4	C19B—C20B—C15B	122.5 (6)
C1A—C2A—H1	116.4	C20B—C21B—C22B	121.5 (6)
C2A—C3A—C4A	126.2 (4)	C20B—C21B—H21B	119.3
C2A—C3A—H5	116.9	C22B—C21B—H21B	119.3
C4A—C3A—H5	116.9	N3B—C22B—C21B	122.7 (5)
C9A—C4A—C5A	118.1 (3)	N3B—C22B—H22B	118.6
C9A—C4A—C3A	120.0 (3)	C21B—C22B—H22B	118.6
C5A—C4A—C3A	121.9 (3)	O6C—S1C—O5C	118.2
C6A—C5A—C4A	121.5 (4)	O6C—S1C—N1C	108.1 (3)
C6A—C5A—H5A	119.3	O5C—S1C—N1C	99.2 (3)
C4A—C5A—H5A	119.3	O6C—S1C—C7B	112.26 (18)
C5A—C6A—C7A	119.0 (3)	O5C—S1C—C7B	111.55 (19)
C5A—C6A—H6A	120.5	N1C—S1C—C7B	105.8 (3)
C7A—C6A—H6A	120.5	C11C—N1C—S1C	114.0 (5)
C8A—C7A—C6A	120.7 (3)	C11C—N1C—H6	114 (5)
C8A—C7A—S1A	121.2 (3)	S1C—N1C—H6	113 (5)
C6A—C7A—S1A	118.1 (3)	N1C—C11C—C10B	109.0 (5)
C7A—C8A—C9A	119.5 (3)	N1C—C11C—C2	106.6 (5)
C7A—C8A—H8A	120.2	C10B—C11C—C2	100.5 (4)
C9A—C8A—H8A	120.2	N1C—C11C—H7	91 (4)
C8A—C9A—C4A	121.2 (3)	C10B—C11C—H7	121 (4)
C8A—C9A—H9A	119.4	C2—C11C—H7	127 (4)
C4A—C9A—H9A	119.4	N1C—C11C—H11C	113.3
O4A—C10A—O3A	123.7 (4)	C10B—C11C—H11C	113.3
O4A—C10A—C11A	118.9 (5)	C2—C11C—H11C	113.3
O3A—C10A—C11A	117.3 (4)	H7—C11C—H11C	22.9
N1A—C11A—C12A	109.8 (3)	C13C—N2C—C17C	115.6 (5)
N1A—C11A—C10A	113.1 (3)	C18C—N3C—C22C	115.3 (6)
C12A—C11A—C10A	109.4 (3)	N2C—C13C—C14C	124.2 (5)
N1A—C11A—H11A	108.1	N2C—C13C—H13C	117.9
C12A—C11A—H11A	108.1	C14C—C13C—H13C	117.9
C10A—C11A—H11A	108.1	C15C—C14C—C13C	118.0 (9)
C11A—C12A—H12A	109.5	C15C—C14C—H14C	121.0
C11A—C12A—H12B	109.5	C13C—C14C—H14C	121.0
H12A—C12A—H12B	109.5	C14C—C15C—C16C	118.7 (11)
C11A—C12A—H12C	109.5	C14C—C15C—C20C	122.0 (11)

H12A—C12A—H12C	109.5	C16C—C15C—C20C	118.9 (12)
H12B—C12A—H12C	109.5	C17C—C16C—C15C	118.5 (11)
C13A—N2A—C17A	120.1 (7)	C17C—C16C—H16C	120.7
C18A—N3A—C22A	116.0 (6)	C15C—C16C—H16C	120.7
N2A—C13A—C14A	121.5 (6)	N2C—C17C—C16C	124.6 (10)
N2A—C13A—H13A	119.2	N2C—C17C—H17C	117.7
C14A—C13A—H13A	119.2	C16C—C17C—H17C	117.7
C15A—C14A—C13A	118.7 (7)	N3C—C18C—C19C	126.0 (10)
C15A—C14A—H14A	120.6	N3C—C18C—H18C	117.0
C13A—C14A—H14A	120.6	C19C—C18C—H18C	117.0
C14A—C15A—C16A	118.0 (8)	C18C—C19C—C20C	118.0 (10)
C14A—C15A—C20A	120.1 (10)	C18C—C19C—H19C	121.0
C16A—C15A—C20A	121.9 (8)	C20C—C19C—H19C	121.0
C17A—C16A—C15A	120.5 (8)	C21C—C20C—C19C	115.8 (10)
C17A—C16A—H16A	119.8	C21C—C20C—C15C	123.2 (11)
C15A—C16A—H16A	119.7	C19C—C20C—C15C	120.7 (10)
N2A—C17A—C16A	121.1 (8)	C22C—C21C—C20C	129.1 (11)
N2A—C17A—H17A	119.5	C22C—C21C—H21C	115.4
C16A—C17A—H17A	119.5	C20C—C21C—H21C	115.5
N3A—C18A—C19A	125.6 (6)	C21C—C22C—N3C	115.6 (7)
N3A—C18A—H18A	117.2	C21C—C22C—H22C	122.2
C19A—C18A—H18A	117.2	N3C—C22C—H22C	122.2
C18A—C19A—C20A	118.4 (7)	C14B—C15B—C16B	120.2 (3)
C18A—C19A—H19A	120.8	C14B—C15B—C20B	122.9 (4)
C20A—C19A—H19A	120.8	C16B—C15B—C20B	116.9 (5)
C21A—C20A—C19A	115.1 (7)	C15B—C14B—C13B	116.6 (3)
C21A—C20A—C15A	123.8 (9)	C15B—C14B—H14B	121.3
C19A—C20A—C15A	120.8 (9)	C13B—C14B—H14B	122.1
C22A—C21A—C20A	122.9 (8)	C13D—N2D—C17D	123.9 (18)
C22A—C21A—H21A	118.5	C18D—N3D—C22D	116.4 (13)
C20A—C21A—H21A	118.5	N2D—C13D—C14D	119.5 (19)
N3A—C22A—C21A	121.8 (7)	N2D—C13D—H13D	120.3
N3A—C22A—H22A	119.1	C14D—C13D—H13D	120.2
C21A—C22A—H22A	119.1	C15D—C14D—C13D	117.3 (17)
O6B—S1B—O5B	122.0 (4)	C15D—C14D—H14D	121.3
O6B—S1B—N1B	114.1 (5)	C13D—C14D—H14D	121.4
O5B—S1B—N1B	101.7 (5)	C14D—C15D—C16D	121.1 (15)
O6B—S1B—C7B	108.0 (4)	C14D—C15D—C20D	111.7 (16)
O5B—S1B—C7B	102.8 (4)	C16D—C15D—C20D	127.2 (17)
N1B—S1B—C7B	107.0 (3)	C15D—C16D—C17D	117.6 (16)
C1B—O2B—H2B	109.5	C15D—C16D—H16D	121.2
C10B—O4B—H4B	109.5	C17D—C16D—H16D	121.2
C11B—N1B—S1B	116.2 (6)	N2D—C17D—C16D	118.7 (16)
C11B—N1B—H7	113 (6)	N2D—C17D—H17D	120.6
S1B—N1B—H7	112 (6)	C16D—C17D—H17D	120.7
C13B—N2B—C17B	119.2 (5)	N3D—C18D—C19D	125.4 (13)
C18B—N3B—C22B	117.2 (4)	N3D—C18D—H14B	136.3
O1B—C1B—O2B	122.8 (4)	C19D—C18D—H14B	14.0
O1B—C1B—C2B	119.0 (5)	N3D—C18D—H18D	117.3
O2B—C1B—C2B	118.2 (5)	C19D—C18D—H18D	117.3
C3B—C2B—C1B	124.1 (5)	H14B—C18D—H18D	105.7
C3B—C2B—H2	118.0	C18D—C19D—C20D	118.3 (14)
C1B—C2B—H2	118.0	C18D—C19D—H14B	111.7
C2B—C3B—C4B	126.4 (4)	C20D—C19D—H14B	114.3
C2B—C3B—H3B	116.8	C18D—C19D—H19D	120.8
C4B—C3B—H3B	116.8	C20D—C19D—H19D	120.8

C9B—C4B—C5B	117.8 (3)	H14B—C19D—H19D	40.4
C9B—C4B—C3B	119.1 (3)	C21D—C20D—C19D	113.2 (13)
C5B—C4B—C3B	123.1 (3)	C21D—C20D—C15D	130.9 (17)
C6B—C5B—C4B	121.1 (3)	C19D—C20D—C15D	115.9 (15)
C6B—C5B—H5B	119.4	C20D—C21D—C22D	126.2 (15)
C4B—C5B—H5B	119.4	C20D—C21D—H21D	116.9
C7B—C6B—C5B	119.5 (4)	C22D—C21D—H21D	116.9
C7B—C6B—H6B	120.3	C21D—C22D—N3D	120.0 (14)
C5B—C6B—H6B	120.3	C21D—C22D—H22D	120.0
C8B—C7B—C6B	120.6 (3)	N3D—C22D—H22D	120.0
C8B—C7B—S1C	116.6 (3)	C11B—C2—C11C	25.4 (3)
C6B—C7B—S1C	122.8 (3)	C11B—C2—H2C	109.5
C8B—C7B—S1B	122.5 (3)	C11C—C2—H2C	110.4
C6B—C7B—S1B	116.5 (3)	C11B—C2—H2D	109.5
S1C—C7B—S1B	8.9 (3)	C11C—C2—H2D	85.9
C7B—C8B—C9B	119.0 (4)	H2C—C2—H2D	109.5
C7B—C8B—H8B	120.5	C11B—C2—H2E	109.5
C9B—C8B—H8B	120.5	C11C—C2—H2E	128.7
C4B—C9B—C8B	122.0 (4)	H2C—C2—H2E	109.5
C4B—C9B—H9B	119.0	H2D—C2—H2E	109.5
C8B—C9B—H9B	119.0	C11B—C2—H2F	109.5
O3B—C10B—O4B	122.1 (4)	C11C—C2—H2F	104.7
O3B—C10B—C11B	131.9 (5)	H2C—C2—H2F	141.1
O4B—C10B—C11B	105.9 (5)	H2D—C2—H2F	56.3
O3B—C10B—C11C	106.8 (4)	H2E—C2—H2F	56.3
O4B—C10B—C11C	131.0 (4)	C11B—C2—H2G	109.5
C11B—C10B—C11C	25.8 (3)	C11C—C2—H2G	132.3
N1B—C11B—C10B	109.9 (6)	H2C—C2—H2G	56.3
N1B—C11B—C2	103.1 (6)	H2D—C2—H2G	141.1
C10B—C11B—C2	109.4 (6)	H2E—C2—H2G	56.3
N1B—C11B—H11B	111.4	H2F—C2—H2G	109.5
C10B—C11B—H11B	111.4	C11B—C2—H2H	109.5
C2—C11B—H11B	111.4	C11C—C2—H2H	88.6
N1B—C11B—H6	87 (3)	H2C—C2—H2H	56.3
C10B—C11B—H6	116 (3)	H2D—C2—H2H	56.3
C2—C11B—H6	127 (3)	H2E—C2—H2H	141.1
H11B—C11B—H6	25.5	H2F—C2—H2H	109.5
N2B—C13B—C14B	122.8 (5)	H2G—C2—H2H	109.5
N2B—C13B—H13B	118.6		
O6A—S1A—N1A—C11A	45.7 (3)	C11C—C10B—C11B—C2	-81.8 (11)
O5A—S1A—N1A—C11A	175.2 (3)	C17B—N2B—C13B—C14B	-2.7 (8)
C7A—S1A—N1A—C11A	-69.7 (3)	C13B—N2B—C17B—C16B	2.1 (9)
O1A—C1A—C2A—C3A	-170.8 (4)	C15B—C16B—C17B—N2B	1.1 (9)
O2A—C1A—C2A—C3A	7.6 (6)	C22B—N3B—C18B—C19B	-0.5 (7)
C1A—C2A—C3A—C4A	177.9 (4)	N3B—C18B—C19B—C20B	-0.7 (11)
C2A—C3A—C4A—C9A	-175.1 (4)	C18B—C19B—C20B—C21B	0.6 (13)
C2A—C3A—C4A—C5A	3.5 (6)	C18B—C19B—C20B—C15B	179.7 (7)
C9A—C4A—C5A—C6A	1.5 (6)	C19B—C20B—C21B—C22B	0.6 (13)
C3A—C4A—C5A—C6A	-177.1 (3)	C15B—C20B—C21B—C22B	-178.5 (7)
C4A—C5A—C6A—C7A	-1.1 (6)	C18B—N3B—C22B—C21B	1.7 (7)
C5A—C6A—C7A—C8A	-0.1 (5)	C20B—C21B—C22B—N3B	-1.8 (11)
C5A—C6A—C7A—S1A	176.7 (3)	C8B—C7B—S1C—O6C	-172.9 (3)
O6A—S1A—C7A—C8A	-13.4 (3)	C6B—C7B—S1C—O6C	5.8 (4)
O5A—S1A—C7A—C8A	-144.3 (3)	S1B—C7B—S1C—O6C	53.0 (16)
N1A—S1A—C7A—C8A	102.4 (3)	C8B—C7B—S1C—O5C	-37.5 (4)

O6A—S1A—C7A—C6A	169.8 (3)	C6B—C7B—S1C—O5C	141.2 (3)
O5A—S1A—C7A—C6A	38.9 (3)	S1B—C7B—S1C—O5C	-171.7 (17)
N1A—S1A—C7A—C6A	-74.3 (3)	C8B—C7B—S1C—N1C	69.4 (5)
C6A—C7A—C8A—C9A	0.9 (5)	C6B—C7B—S1C—N1C	-111.9 (4)
S1A—C7A—C8A—C9A	-175.8 (3)	S1B—C7B—S1C—N1C	-64.8 (16)
C7A—C8A—C9A—C4A	-0.5 (6)	O6C—S1C—N1C—C11C	-59.8 (5)
C5A—C4A—C9A—C8A	-0.7 (5)	O5C—S1C—N1C—C11C	176.3 (4)
C3A—C4A—C9A—C8A	178.0 (3)	C7B—S1C—N1C—C11C	60.7 (5)
S1A—N1A—C11A—C12A	-163.0 (3)	S1C—N1C—C11C—C10B	-93.6 (5)
S1A—N1A—C11A—C10A	74.4 (4)	S1C—N1C—C11C—C2	158.7 (4)
O4A—C10A—C11A—N1A	-135.6 (4)	O3B—C10B—C11C—N1C	144.9 (5)
O3A—C10A—C11A—N1A	46.1 (5)	O4B—C10B—C11C—N1C	-32.4 (8)
O4A—C10A—C11A—C12A	101.7 (5)	C11B—C10B—C11C—N1C	-47.4 (9)
O3A—C10A—C11A—C12A	-76.6 (5)	O3B—C10B—C11C—C2	-103.3 (4)
C17A—N2A—C13A—C14A	1.6 (12)	O4B—C10B—C11C—C2	79.4 (6)
N2A—C13A—C14A—C15A	-0.3 (13)	C11B—C10B—C11C—C2	64.4 (10)
C13A—C14A—C15A—C16A	-1.7 (14)	C17C—N2C—C13C—C14C	-7.6 (9)
C13A—C14A—C15A—C20A	179.9 (9)	N2C—C13C—C14C—C15C	5.3 (17)
C14A—C15A—C16A—C17A	2.4 (16)	C13C—C14C—C15C—C16C	1 (3)
C20A—C15A—C16A—C17A	-179.1 (10)	C13C—C14C—C15C—C20C	173.7 (13)
C13A—N2A—C17A—C16A	-0.8 (13)	C14C—C15C—C16C—C17C	-4 (3)
C15A—C16A—C17A—N2A	-1.2 (15)	C20C—C15C—C16C—C17C	-177.4 (17)
C22A—N3A—C18A—C19A	1.4 (11)	C13C—N2C—C17C—C16C	3.8 (19)
N3A—C18A—C19A—C20A	0.4 (13)	C15C—C16C—C17C—N2C	2 (3)
C18A—C19A—C20A—C21A	-3.1 (15)	C22C—N3C—C18C—C19C	-1.8 (14)
C18A—C19A—C20A—C15A	-177.3 (9)	N3C—C18C—C19C—C20C	0.5 (18)
C14A—C15A—C20A—C21A	154.1 (13)	C18C—C19C—C20C—C21C	2.0 (19)
C16A—C15A—C20A—C21A	-24.3 (18)	C18C—C19C—C20C—C15C	175.2 (13)
C14A—C15A—C20A—C19A	-32.2 (16)	C14C—C15C—C20C—C21C	143.8 (17)
C16A—C15A—C20A—C19A	149.4 (11)	C16C—C15C—C20C—C21C	-44 (3)
C19A—C20A—C21A—C22A	4 (2)	C14C—C15C—C20C—C19C	-29 (2)
C15A—C20A—C21A—C22A	178.2 (12)	C16C—C15C—C20C—C19C	143.7 (18)
C18A—N3A—C22A—C21A	-0.4 (14)	C19C—C20C—C21C—C22C	-3 (2)
C20A—C21A—C22A—N3A	-3 (2)	C15C—C20C—C21C—C22C	-176.4 (15)
O6B—S1B—N1B—C11B	51.9 (7)	C20C—C21C—C22C—N3C	2 (2)
O5B—S1B—N1B—C11B	-174.9 (6)	C18C—N3C—C22C—C21C	0.7 (11)
C7B—S1B—N1B—C11B	-67.4 (6)	C17B—C16B—C15B—C14B	-3.9 (7)
O1B—C1B—C2B—C3B	-168.8 (4)	C17B—C16B—C15B—C20B	177.7 (7)
O2B—C1B—C2B—C3B	12.5 (7)	C21B—C20B—C15B—C14B	154.9 (7)
C1B—C2B—C3B—C4B	178.8 (4)	C19B—C20B—C15B—C14B	-24.1 (12)
C2B—C3B—C4B—C9B	-175.3 (4)	C21B—C20B—C15B—C16B	-26.7 (12)
C2B—C3B—C4B—C5B	5.3 (6)	C19B—C20B—C15B—C16B	154.3 (8)
C9B—C4B—C5B—C6B	2.4 (6)	C16B—C15B—C14B—C13B	3.3 (4)
C3B—C4B—C5B—C6B	-178.2 (4)	C20B—C15B—C14B—C13B	-178.4 (7)
C4B—C5B—C6B—C7B	-1.6 (6)	N2B—C13B—C14B—C15B	0.0 (6)
C5B—C6B—C7B—C8B	-0.3 (6)	C17D—N2D—C13D—C14D	-8 (6)
C5B—C6B—C7B—S1C	-179.0 (3)	N2D—C13D—C14D—C15D	16 (6)
C5B—C6B—C7B—S1B	173.8 (4)	C13D—C14D—C15D—C16D	-12 (6)
O6B—S1B—C7B—C8B	-23.8 (6)	C13D—C14D—C15D—C20D	167 (3)
O5B—S1B—C7B—C8B	-153.9 (4)	C14D—C15D—C16D—C17D	1 (6)
N1B—S1B—C7B—C8B	99.4 (5)	C20D—C15D—C16D—C17D	-179 (3)
O6B—S1B—C7B—C6B	162.3 (5)	C13D—N2D—C17D—C16D	-4 (5)
O5B—S1B—C7B—C6B	32.1 (5)	C15D—C16D—C17D—N2D	8 (5)
N1B—S1B—C7B—C6B	-74.5 (5)	C22D—N3D—C18D—C19D	-7 (3)
O6B—S1B—C7B—S1C	25.8 (15)	N3D—C18D—C19D—C20D	8 (3)
O5B—S1B—C7B—S1C	-104.4 (17)	C18D—C19D—C20D—C21D	-5 (3)

N1B—S1B—C7B—S1C	149.0 (18)	C18D—C19D—C20D—C15D	175 (2)
C6B—C7B—C8B—C9B	1.3 (6)	C14D—C15D—C20D—C21D	139 (4)
S1C—C7B—C8B—C9B	-179.9 (4)	C16D—C15D—C20D—C21D	-42 (6)
S1B—C7B—C8B—C9B	-172.4 (4)	C14D—C15D—C20D—C19D	-41 (4)
C5B—C4B—C9B—C8B	-1.4 (6)	C16D—C15D—C20D—C19D	139 (4)
C3B—C4B—C9B—C8B	179.3 (4)	C19D—C20D—C21D—C22D	2 (4)
C7B—C8B—C9B—C4B	-0.5 (7)	C15D—C20D—C21D—C22D	-178 (3)
S1B—N1B—C11B—C10B	89.8 (7)	C20D—C21D—C22D—N3D	-1 (4)
S1B—N1B—C11B—C2	-153.7 (5)	C18D—N3D—C22D—C21D	4 (3)
O3B—C10B—C11B—N1B	46.7 (9)	N1B—C11B—C2—C11C	-33.9 (7)
O4B—C10B—C11B—N1B	-137.6 (6)	C10B—C11B—C2—C11C	83.0 (10)
C11C—C10B—C11B—N1B	30.8 (7)	N1C—C11C—C2—C11B	50.8 (9)
O3B—C10B—C11B—C2	-65.9 (8)	C10B—C11C—C2—C11B	-62.8 (9)
O4B—C10B—C11B—C2	109.9 (6)		

Table 1e. Hydrogen-bond geometry (Å, °) for Cocrystal of **23** and 4,4'-dipyridyl (**24**).

<i>D</i> —H... <i>A</i>	<i>D</i> —H	H... <i>A</i>	<i>D</i> ... <i>A</i>	<i>D</i> —H... <i>A</i>
O2 <i>B</i> —H2 <i>B</i> ...N2 <i>A</i>	0.84	1.92	2.751 (7)	173
O2 <i>B</i> —H2 <i>B</i> ...N3 <i>C</i>	0.84	2.33	3.083 (6)	149
O3 <i>A</i> —H3 <i>A</i> ...N2 <i>C</i>	0.84	2.29	3.045 (6)	150
O3 <i>A</i> —H3 <i>A</i> ...N3 <i>A</i>	0.84	1.79	2.624 (7)	170
O2 <i>A</i> —H2 <i>A</i> ...N3 <i>B</i>	0.84	1.83	2.671 (5)	176
O2 <i>A</i> —H2 <i>A</i> ...N2 <i>D</i>	0.84	2.02	2.83 (2)	160
O4 <i>B</i> —H4 <i>B</i> ...N2 <i>B</i>	0.84	1.84	2.665 (6)	166
O4 <i>B</i> —H4 <i>B</i> ...N3 <i>D</i>	0.84	2.23	2.948 (15)	144
N1 <i>A</i> —H3...O3 <i>B</i> ⁱ	0.82 (4)	2.06 (4)	2.866 (4)	167 (4)
C13 <i>D</i> —H13 <i>D</i> ...O1 <i>A</i> ⁱ	0.95	2.13	2.86 (2)	133
N1 <i>B</i> —H7...O5 <i>A</i> ⁱ	0.76 (8)	2.48 (8)	3.232 (7)	169 (8)

Symmetry code: (i) -*x*+1, -*y*-1, -*z*.

Table 2a. Crystal data and structure refinement for cocrystal of **23** and of 4,4'-dipyridyl-N,N'-dioxide dihydrate (**25**).

Crystal data

$C_{12}H_{13}NO_6S \cdot C_{10}H_8N_2O_2 \cdot H_2O$	$V = 1140.50 (3) \text{ \AA}^3$
$M_r = 505.50$	$Z = 2$
Triclinic, $P\bar{1}$	$F(000) = 506$
Hall symbol: $-P\ 1$	$D_x = 1.417 \text{ Mg m}^{-3}$
$a = 7.6471 (1) \text{ \AA}$	Mo $K\alpha$ radiation, $\lambda = 0.71073 \text{ \AA}$
$b = 11.1749 (2) \text{ \AA}$	$\mu = 0.20 \text{ mm}^{-1}$
$c = 14.2557 (3) \text{ \AA}$	$T = 173 \text{ K}$
$\alpha = 72.180 (1)^\circ$	Transparent prism, colorless
$\beta = 82.938 (1)^\circ$	
$\gamma = 80.512 (1)^\circ$	

Data collection

Bruker APEXII CCD diffractometer	5161 independent reflections
Radiation source: fine-focus sealed tube	3130 reflections with $I > 2\sigma(I)$
Graphite	$R_{\text{int}} = 0.041$
phi and ω scans	$\theta_{\text{max}} = 27.9^\circ$, $\theta_{\text{min}} = 1.5^\circ$
Absorption correction: multi-scan <i>SADABS</i> (Bruker, 2010)	$h = -10 \rightarrow 9$
$T_{\text{min}} = 913$, $T_{\text{max}} = 769$	$k = -14 \rightarrow 14$
13534 measured reflections	$l = -18 \rightarrow 18$

Refinement

Refinement on F^2	Primary atom site location: structure-invariant direct methods
Least-squares matrix: full	Secondary atom site location: difference Fourier map
$R[F^2 > 2\sigma(F^2)] = 0.051$	Hydrogen site location: inferred from neighbouring sites
$wR(F^2) = 0.142$	H atoms treated by a mixture of independent and constrained refinement
$S = 1.01$	$w = 1/[\sigma^2(F_o^2) + (0.0689P)^2]$
5161 reflections	where $P = (F_o^2 + 2F_c^2)/3$
429 parameters	$(\Delta/\sigma)_{\text{max}} = 0.183$
0 restraints	$\Delta_{\text{max}} = 0.34 \text{ e \AA}^{-3}$
	$\Delta_{\text{min}} = -0.31 \text{ e \AA}^{-3}$

Table 2b. Fractional atomic coordinates and isotropic or equivalent isotropic displacement parameters (\AA^2) for cocrystal of **23** and of 4,4'-dipyridyl-N,N'-dioxide dihydrate (**25**).

	<i>x</i>	<i>y</i>	<i>z</i>	$U_{\text{iso}}^*/U_{\text{eq}}$	Occ. (<1)
S1	0.15280 (6)	0.17102 (4)	0.78820 (4)	0.04884 (13)	
O7	0.31448 (15)	0.33941 (11)	0.94582 (10)	0.0531 (4)	
O8	0.54323 (16)	0.18536 (11)	0.97141 (11)	0.0594 (4)	
H1	0.607 (3)	0.2521 (18)	0.9627 (14)	0.071*	
C7B	0.3110 (5)	0.2834 (4)	0.7241 (3)	0.0370 (12)	0.5194 (19)
N7	0.12167 (18)	0.16715 (13)	0.90305 (11)	0.0451 (4)	
H7	0.0149	0.1911	0.9275	0.054*	
O6	0.24631 (19)	0.05237 (12)	0.78283 (11)	0.0681 (4)	
C12	0.3755 (2)	0.23019 (16)	0.95912 (13)	0.0409 (4)	
O5	-0.01763 (18)	0.21374 (15)	0.75058 (11)	0.0757 (5)	
C11	0.2675 (2)	0.12478 (16)	0.96614 (13)	0.0423 (5)	
H11	0.3478	0.0552	0.9460	0.051*	
O3	0.7776 (5)	0.8049 (4)	0.4702 (3)	0.0741 (15)	0.4806 (19)
C4A	0.5474 (5)	0.4472 (4)	0.6428 (3)	0.0398 (11)	0.5194 (19)
O4	1.0149 (5)	0.6676 (4)	0.5152 (4)	0.0796 (16)	0.4806 (19)
H3	1.064 (3)	0.732 (2)	0.4966 (18)	0.096*	
C8A	0.2473 (6)	0.4067 (5)	0.6852 (4)	0.0552 (15)	0.5194 (19)
H8A	0.1231	0.4348	0.6860	0.066*	0.5194 (19)
C10	0.1974 (3)	0.07277 (19)	1.07365 (14)	0.0586 (6)	
H10A	0.1111	0.1380	1.0928	0.088*	
H10B	0.2965	0.0489	1.1162	0.088*	
H10C	0.1395	-0.0019	1.0810	0.088*	
C6B	0.4764 (8)	0.2587 (6)	0.7182 (5)	0.059 (2)	0.4806 (19)
H6B	0.5375	0.1748	0.7378	0.071*	0.4806 (19)
C2A	0.6543 (5)	0.6519 (4)	0.5485 (3)	0.0488 (10)	0.5194 (19)
H2A	0.5353	0.6906	0.5380	0.059*	0.5194 (19)
C3A	0.6829 (5)	0.5323 (4)	0.5979 (3)	0.0476 (10)	0.5194 (19)
H3A	0.8036	0.4961	0.6059	0.057*	0.5194 (19)
C5A	0.6031 (5)	0.3203 (4)	0.6861 (3)	0.0443 (12)	0.5194 (19)
H5A	0.7257	0.2870	0.6861	0.053*	0.5194 (19)
C1A	0.8032 (6)	0.7316 (5)	0.5074 (4)	0.0531 (14)	0.5194 (19)
C9A	0.3688 (6)	0.4906 (4)	0.6441 (3)	0.0490 (13)	0.5194 (19)
H9A	0.3289	0.5783	0.6167	0.059*	0.5194 (19)
O2	0.23058 (17)	0.81960 (12)	0.48431 (11)	0.0654 (4)	
O1	0.21382 (16)	1.66946 (11)	0.04131 (10)	0.0558 (4)	
N5	0.23010 (18)	0.93281 (13)	0.42064 (11)	0.0464 (4)	
N8	0.22090 (18)	1.54957 (13)	0.09815 (11)	0.0434 (4)	
C16	0.2273 (2)	1.30386 (15)	0.22121 (12)	0.0391 (4)	
C15	0.2300 (2)	1.17391 (15)	0.28986 (12)	0.0377 (4)	
C22	0.0775 (2)	0.99938 (17)	0.38487 (14)	0.0486 (5)	
H22	-0.0301	0.9632	0.4042	0.058*	
C14	0.3850 (2)	1.10120 (17)	0.32688 (14)	0.0482 (5)	
H14	0.4946	1.1346	0.3070	0.058*	
C21	0.0760 (2)	1.11892 (17)	0.32075 (14)	0.0468 (5)	
H21	-0.0335	1.1651	0.2969	0.056*	
C17	0.3786 (2)	1.36285 (17)	0.19265 (14)	0.0502 (5)	
H17	0.4888	1.3182	0.2163	0.060*	
C20	0.0726 (2)	1.37546 (17)	0.18328 (15)	0.0520 (5)	

H20	-0.0354	1.3395	0.2002	0.062*	
C13	0.3834 (2)	0.98255 (17)	0.39139 (15)	0.0521 (6)	
H13	0.4915	0.9346	0.4159	0.063*	
C18	0.3731 (2)	1.48359 (17)	0.13129 (14)	0.0508 (5)	
H18	0.4797	1.5211	0.1120	0.061*	
C19	0.0711 (2)	1.49583 (17)	0.12244 (15)	0.0525 (5)	
H19	-0.0370	1.5423	0.0969	0.063*	
C2B	0.7588 (6)	0.5850 (4)	0.5642 (3)	0.0503 (11)	0.4806 (19)
H2B	0.8303	0.5046	0.5819	0.060*	0.4806 (19)
C3B	0.5851 (5)	0.5914 (4)	0.5825 (3)	0.0437 (10)	0.4806 (19)
H3B	0.5175	0.6726	0.5597	0.052*	0.4806 (19)
O9	0.23610 (19)	1.78672 (13)	-0.16600 (11)	0.0666 (4)	
H2	0.245 (3)	1.881 (2)	-0.1794 (15)	0.080*	
H4	0.226 (3)	1.7353 (18)	-0.0917 (15)	0.080*	
C4B	0.4858 (5)	0.4856 (4)	0.6347 (3)	0.0358 (11)	0.4806 (19)
C1B	0.8421 (11)	0.6963 (6)	0.5184 (5)	0.068 (2)	0.4806 (19)
C5B	0.5677 (6)	0.3645 (5)	0.6722 (4)	0.0438 (13)	0.4806 (19)
H5B	0.6940	0.3506	0.6671	0.053*	0.4806 (19)
C6A	0.4745 (7)	0.2443 (6)	0.7290 (4)	0.0468 (16)	0.5194 (19)
H6A	0.5102	0.1582	0.7639	0.056*	0.5194 (19)
C9B	0.3039 (6)	0.5077 (5)	0.6445 (4)	0.0460 (13)	0.4806 (19)
H9B	0.2459	0.5915	0.6184	0.055*	0.4806 (19)
C8B	0.2033 (7)	0.4125 (5)	0.6907 (4)	0.0378 (13)	0.4806 (19)
H8B	0.0775	0.4324	0.6938	0.045*	0.4806 (19)
C7A	0.2784 (6)	0.2858 (5)	0.7342 (4)	0.0349 (13)	0.4806 (19)
O10	0.9637 (6)	0.6752 (4)	0.5304 (4)	0.0710 (14)	0.5194 (19)
O11	0.7651 (5)	0.8355 (4)	0.4690 (3)	0.0601 (11)	0.5194 (19)

Table 2c. Atomic displacement parameters (\AA^2) for cocrystal of **23** and of 4,4'-dipyridyl-N,N'-dioxide dihydrate (**25**).

	U^{11}	U^{22}	U^{33}	U^{12}	U^{13}	U^{23}
S1	0.0519 (3)	0.0484 (3)	0.0480 (3)	-0.0231 (2)	-0.0054 (2)	-0.0076 (2)
O7	0.0400 (6)	0.0363 (7)	0.0794 (9)	-0.0065 (5)	-0.0078 (6)	-0.0099 (6)
O8	0.0397 (7)	0.0380 (7)	0.0962 (11)	-0.0062 (6)	-0.0192 (7)	-0.0075 (7)
C7B	0.041 (2)	0.0347 (18)	0.035 (2)	-0.0239 (16)	0.0106 (16)	-0.0060 (16)
N7	0.0357 (7)	0.0501 (8)	0.0472 (9)	-0.0144 (7)	0.0020 (6)	-0.0085 (7)
O6	0.0928 (10)	0.0422 (7)	0.0691 (9)	-0.0212 (7)	0.0052 (8)	-0.0138 (7)
C12	0.0390 (9)	0.0364 (9)	0.0435 (10)	-0.0086 (7)	-0.0059 (8)	-0.0034 (8)
O5	0.0531 (8)	0.0985 (11)	0.0772 (10)	-0.0314 (8)	-0.0179 (7)	-0.0123 (9)
C11	0.0406 (9)	0.0346 (9)	0.0476 (10)	-0.0099 (7)	-0.0043 (8)	-0.0031 (8)
O3	0.052 (2)	0.099 (3)	0.079 (3)	-0.026 (2)	0.0067 (19)	-0.033 (2)
C4A	0.0313 (19)	0.042 (2)	0.042 (2)	0.0021 (17)	-0.0021 (16)	-0.0098 (17)
O4	0.068 (2)	0.046 (2)	0.111 (3)	-0.0196 (17)	0.012 (2)	-0.004 (2)
C8A	0.034 (2)	0.063 (3)	0.069 (3)	-0.003 (2)	-0.005 (2)	-0.022 (2)
C10	0.0660 (12)	0.0602 (12)	0.0440 (11)	-0.0216 (10)	0.0027 (10)	-0.0029 (9)
C6B	0.054 (3)	0.054 (3)	0.065 (4)	0.004 (3)	-0.004 (3)	-0.016 (3)
C2A	0.0398 (19)	0.055 (2)	0.048 (2)	-0.0172 (17)	0.0044 (17)	-0.0080 (18)
C3A	0.0352 (19)	0.052 (2)	0.053 (2)	-0.0060 (17)	-0.0036 (17)	-0.0121 (18)
C5A	0.0324 (19)	0.034 (2)	0.060 (3)	-0.0043 (16)	-0.0065 (17)	-0.0046 (18)
C1A	0.056 (2)	0.077 (3)	0.030 (2)	-0.046 (2)	0.0075 (19)	-0.006 (2)
C9A	0.059 (3)	0.034 (2)	0.044 (2)	-0.010 (2)	-0.004 (2)	0.0045 (17)
O2	0.0531 (8)	0.0438 (7)	0.0773 (10)	-0.0070 (6)	-0.0053 (7)	0.0147 (7)
O1	0.0517 (7)	0.0374 (7)	0.0686 (9)	-0.0138 (6)	-0.0127 (7)	0.0058 (6)

N5	0.0396 (8)	0.0377 (8)	0.0537 (9)	-0.0073 (7)	0.0006 (7)	-0.0020 (7)
N8	0.0429 (8)	0.0352 (7)	0.0494 (9)	-0.0097 (6)	-0.0067 (7)	-0.0050 (7)
C16	0.0373 (8)	0.0363 (9)	0.0447 (10)	-0.0087 (7)	-0.0002 (8)	-0.0124 (8)
C15	0.0357 (8)	0.0377 (9)	0.0392 (9)	-0.0088 (7)	0.0014 (7)	-0.0102 (7)
C22	0.0348 (9)	0.0492 (11)	0.0544 (12)	-0.0129 (8)	-0.0056 (8)	0.0004 (9)
C14	0.0345 (9)	0.0411 (10)	0.0635 (12)	-0.0100 (8)	0.0021 (8)	-0.0070 (9)
C21	0.0391 (9)	0.0438 (10)	0.0508 (11)	-0.0091 (8)	-0.0088 (8)	-0.0001 (8)
C17	0.0355 (9)	0.0484 (10)	0.0586 (12)	-0.0098 (8)	-0.0077 (9)	-0.0001 (9)
C20	0.0353 (9)	0.0394 (10)	0.0767 (14)	-0.0113 (8)	-0.0071 (9)	-0.0059 (9)
C13	0.0338 (9)	0.0460 (11)	0.0690 (13)	-0.0034 (8)	-0.0024 (9)	-0.0074 (10)
C18	0.0376 (9)	0.0447 (10)	0.0626 (12)	-0.0135 (8)	-0.0052 (9)	0.0000 (9)
C19	0.0372 (9)	0.0400 (10)	0.0764 (14)	-0.0078 (8)	-0.0125 (9)	-0.0069 (9)
C2B	0.046 (2)	0.046 (2)	0.056 (3)	-0.014 (2)	0.005 (2)	-0.009 (2)
C3B	0.046 (2)	0.043 (2)	0.037 (2)	-0.0084 (19)	-0.0020 (18)	-0.0032 (18)
O9	0.0662 (9)	0.0570 (8)	0.0741 (10)	-0.0098 (7)	-0.0086 (8)	-0.0132 (8)
C4B	0.026 (2)	0.039 (2)	0.040 (2)	-0.0068 (19)	-0.0003 (19)	-0.0078 (17)
C1B	0.104 (5)	0.049 (3)	0.055 (4)	-0.027 (3)	-0.001 (4)	-0.016 (3)
C5B	0.025 (2)	0.043 (3)	0.054 (3)	0.002 (2)	-0.0053 (18)	-0.003 (2)
C6A	0.041 (3)	0.052 (3)	0.047 (3)	-0.022 (2)	0.000 (2)	-0.006 (2)
C9B	0.046 (3)	0.038 (2)	0.050 (3)	-0.009 (2)	-0.009 (2)	-0.002 (2)
C8B	0.030 (2)	0.038 (2)	0.033 (2)	-0.0009 (17)	-0.0067 (17)	0.0060 (19)
C7A	0.0208 (19)	0.050 (3)	0.030 (2)	-0.0061 (18)	-0.0012 (16)	-0.006 (2)
O10	0.072 (3)	0.048 (2)	0.078 (3)	-0.017 (2)	0.010 (2)	0.0031 (18)
O11	0.0425 (18)	0.066 (2)	0.073 (2)	-0.0204 (15)	0.0018 (17)	-0.0178 (18)

Table 2d. Geometric parameters (Å, °) for cocrystal of **23** and of 4,4'-dipyridyl-N,N'-dioxide dihydrate (**25**).

S1—O6	1.4182 (14)	O1—N8	1.3330 (17)
S1—O5	1.4228 (14)	N5—C22	1.343 (2)
S1—N7	1.6135 (16)	N5—C13	1.345 (2)
S1—C7A	1.668 (5)	N8—C18	1.327 (2)
S1—C7B	1.845 (4)	N8—C19	1.339 (2)
O7—C12	1.1981 (19)	C16—C17	1.382 (2)
O8—C12	1.310 (2)	C16—C20	1.383 (2)
O8—H1	0.93 (2)	C16—C15	1.481 (2)
C7B—C6A	1.258 (7)	C15—C21	1.380 (2)
C7B—C8A	1.349 (6)	C15—C14	1.385 (2)
N7—C11	1.445 (2)	C22—C21	1.368 (2)
N7—H7	0.8800	C22—H22	0.9500
C12—C11	1.519 (2)	C14—C13	1.364 (2)
C11—C10	1.526 (2)	C14—H14	0.9500
C11—H11	1.0000	C21—H21	0.9500
O3—C1B	1.251 (7)	C17—C18	1.362 (2)
C4A—C9A	1.372 (5)	C17—H17	0.9500
C4A—C5A	1.380 (5)	C20—C19	1.358 (2)
C4A—C3A	1.475 (5)	C20—H20	0.9500
O4—C1B	1.305 (9)	C13—H13	0.9500
O4—H3	0.82 (2)	C18—H18	0.9500
C8A—C9A	1.380 (7)	C19—H19	0.9500
C8A—H8A	0.9500	C2B—C3B	1.317 (6)
C10—H10A	0.9800	C2B—C1B	1.428 (8)
C10—H10B	0.9800	C2B—H2B	0.9500
C10—H10C	0.9800	C3B—C4B	1.465 (6)

C6B—C5B	1.414 (8)	C3B—H3B	0.9500
C6B—C7A	1.498 (7)	O9—H2	1.03 (2)
C6B—H6B	0.9500	O9—H4	1.04 (2)
C2A—C3A	1.302 (5)	C4B—C5B	1.367 (6)
C2A—C1A	1.512 (6)	C4B—C9B	1.369 (6)
C2A—H2A	0.9500	C5B—H5B	0.9500
C3A—H3A	0.9500	C6A—H6A	0.9500
C5A—C6A	1.368 (7)	C9B—C8B	1.369 (7)
C5A—H5A	0.9500	C9B—H9B	0.9500
C1A—O11	1.127 (6)	C8B—C7A	1.414 (7)
C1A—O10	1.314 (6)	C8B—H8B	0.9500
C9A—H9A	0.9500	O10—H3	1.05 (2)
O2—N5	1.3118 (17)		
O6—S1—O5	120.08 (10)	C18—N8—C19	119.84 (15)
O6—S1—N7	108.03 (8)	O1—N8—C19	119.09 (14)
O5—S1—N7	105.11 (9)	C17—C16—C20	115.52 (15)
O6—S1—C7A	109.98 (19)	C17—C16—C15	122.20 (15)
O5—S1—C7A	106.88 (17)	C20—C16—C15	122.26 (15)
N7—S1—C7A	105.8 (2)	C21—C15—C14	116.33 (15)
O6—S1—C7B	103.21 (15)	C21—C15—C16	121.21 (14)
O5—S1—C7B	110.86 (14)	C14—C15—C16	122.45 (15)
N7—S1—C7B	109.29 (16)	N5—C22—C21	120.44 (16)
C7A—S1—C7B	6.8 (3)	N5—C22—H22	119.8
C12—O8—H1	109.2 (12)	C21—C22—H22	119.8
C6A—C7B—C8A	122.7 (5)	C13—C14—C15	121.28 (16)
C6A—C7B—S1	118.0 (4)	C13—C14—H14	119.4
C8A—C7B—S1	118.7 (3)	C15—C14—H14	119.4
C11—N7—S1	120.61 (12)	C22—C21—C15	121.44 (16)
C11—N7—H7	119.7	C22—C21—H21	119.3
S1—N7—H7	119.7	C15—C21—H21	119.3
O7—C12—O8	124.61 (17)	C18—C17—C16	121.48 (16)
O7—C12—C11	124.39 (15)	C18—C17—H17	119.3
O8—C12—C11	110.99 (15)	C16—C17—H17	119.3
N7—C11—C12	112.54 (13)	C19—C20—C16	121.68 (17)
N7—C11—C10	110.13 (14)	C19—C20—H20	119.2
C12—C11—C10	108.40 (16)	C16—C20—H20	119.2
N7—C11—H11	108.6	N5—C13—C14	120.59 (16)
C12—C11—H11	108.6	N5—C13—H13	119.7
C10—C11—H11	108.6	C14—C13—H13	119.7
C9A—C4A—C5A	119.2 (4)	N8—C18—C17	120.92 (16)
C9A—C4A—C3A	122.1 (4)	N8—C18—H18	119.5
C5A—C4A—C3A	118.6 (3)	C17—C18—H18	119.5
C1B—O4—H3	110.9 (17)	N8—C19—C20	120.54 (16)
C7B—C8A—C9A	117.7 (4)	N8—C19—H19	119.7
C7B—C8A—H8A	121.1	C20—C19—H19	119.7
C9A—C8A—H8A	121.1	C3B—C2B—C1B	121.4 (5)
C11—C10—H10A	109.5	C3B—C2B—H2B	119.3
C11—C10—H10B	109.5	C1B—C2B—H2B	119.3
H10A—C10—H10B	109.5	C2B—C3B—C4B	126.4 (4)
C11—C10—H10C	109.5	C2B—C3B—H3B	116.8
H10A—C10—H10C	109.5	C4B—C3B—H3B	116.8
H10B—C10—H10C	109.5	H2—O9—H4	114.8 (16)
C5B—C6B—C7A	116.5 (5)	C5B—C4B—C9B	118.5 (4)
C5B—C6B—H6B	121.8	C5B—C4B—C3B	122.5 (4)
C7A—C6B—H6B	121.8	C9B—C4B—C3B	119.0 (4)

C3A—C2A—C1A	122.5 (4)	O3—C1B—O4	118.4 (6)
C3A—C2A—H2A	118.7	O3—C1B—C2B	130.1 (7)
C1A—C2A—H2A	118.7	O4—C1B—C2B	110.3 (5)
C2A—C3A—C4A	126.8 (4)	C4B—C5B—C6B	124.2 (4)
C2A—C3A—H3A	116.6	C4B—C5B—H5B	117.9
C4A—C3A—H3A	116.6	C6B—C5B—H5B	117.9
C6A—C5A—C4A	117.3 (4)	C7B—C6A—C5A	122.9 (5)
C6A—C5A—H5A	121.4	C7B—C6A—H6A	118.6
C4A—C5A—H5A	121.4	C5A—C6A—H6A	118.5
O11—C1A—O10	126.2 (5)	C8B—C9B—C4B	121.9 (5)
O11—C1A—C2A	117.4 (5)	C8B—C9B—H9B	119.0
O10—C1A—C2A	115.8 (4)	C4B—C9B—H9B	119.1
C4A—C9A—C8A	119.9 (4)	C9B—C8B—C7A	122.9 (5)
C4A—C9A—H9A	120.0	C9B—C8B—H8B	118.5
C8A—C9A—H9A	120.1	C7A—C8B—H8B	118.5
O2—N5—C22	120.38 (14)	C8B—C7A—C6B	115.6 (5)
O2—N5—C13	119.73 (14)	C8B—C7A—S1	122.0 (4)
C22—N5—C13	119.89 (15)	C6B—C7A—S1	122.0 (4)
C18—N8—O1	121.08 (14)	C1A—O10—H3	113.2 (13)
O6—S1—C7B—C6A	-31.1 (5)	C16—C15—C21—C22	-179.37 (18)
O5—S1—C7B—C6A	-160.9 (4)	C20—C16—C17—C18	0.1 (3)
N7—S1—C7B—C6A	83.7 (5)	C15—C16—C17—C18	-178.41 (18)
C7A—S1—C7B—C6A	144 (3)	C17—C16—C20—C19	-0.3 (3)
O6—S1—C7B—C8A	157.0 (4)	C15—C16—C20—C19	178.21 (19)
O5—S1—C7B—C8A	27.2 (5)	O2—N5—C13—C14	-178.58 (18)
N7—S1—C7B—C8A	-88.2 (4)	C22—N5—C13—C14	1.1 (3)
C7A—S1—C7B—C8A	-28 (2)	C15—C14—C13—N5	0.2 (3)
O6—S1—N7—C11	49.26 (15)	O1—N8—C18—C17	177.29 (18)
O5—S1—N7—C11	178.60 (13)	C19—N8—C18—C17	-2.2 (3)
C7A—S1—N7—C11	-68.5 (2)	C16—C17—C18—N8	1.2 (3)
C7B—S1—N7—C11	-62.37 (19)	C18—N8—C19—C20	2.0 (3)
S1—N7—C11—C12	84.67 (17)	O1—N8—C19—C20	-177.50 (18)
S1—N7—C11—C10	-154.26 (13)	C16—C20—C19—N8	-0.8 (3)
O7—C12—C11—N7	33.8 (3)	C1B—C2B—C3B—C4B	-175.7 (5)
O8—C12—C11—N7	-147.40 (15)	C2B—C3B—C4B—C5B	0.8 (8)
O7—C12—C11—C10	-88.3 (2)	C2B—C3B—C4B—C9B	-177.6 (5)
O8—C12—C11—C10	90.55 (18)	C3B—C2B—C1B—O3	-17.7 (11)
C6A—C7B—C8A—C9A	3.9 (9)	C3B—C2B—C1B—O4	174.9 (5)
S1—C7B—C8A—C9A	175.3 (4)	C9B—C4B—C5B—C6B	2.1 (9)
C1A—C2A—C3A—C4A	178.6 (4)	C3B—C4B—C5B—C6B	-176.3 (5)
C9A—C4A—C3A—C2A	-5.9 (7)	C7A—C6B—C5B—C4B	-6.0 (9)
C5A—C4A—C3A—C2A	175.1 (4)	C8A—C7B—C6A—C5A	-7.0 (10)
C9A—C4A—C5A—C6A	-0.4 (7)	S1—C7B—C6A—C5A	-178.5 (5)
C3A—C4A—C5A—C6A	178.6 (5)	C4A—C5A—C6A—C7B	5.1 (9)
C3A—C2A—C1A—O11	-177.0 (5)	C5B—C4B—C9B—C8B	0.3 (9)
C3A—C2A—C1A—O10	-4.7 (7)	C3B—C4B—C9B—C8B	178.7 (5)
C5A—C4A—C9A—C8A	-2.3 (8)	C4B—C9B—C8B—C7A	1.8 (9)
C3A—C4A—C9A—C8A	178.7 (5)	C9B—C8B—C7A—C6B	-5.6 (9)
C7B—C8A—C9A—C4A	0.8 (8)	C9B—C8B—C7A—S1	-178.8 (5)
C17—C16—C15—C21	177.15 (18)	C5B—C6B—C7A—C8B	7.3 (8)
C20—C16—C15—C21	-1.2 (3)	C5B—C6B—C7A—S1	-179.5 (5)
C17—C16—C15—C14	-2.6 (3)	O6—S1—C7A—C8B	152.3 (5)
C20—C16—C15—C14	179.04 (19)	O5—S1—C7A—C8B	20.4 (6)
O2—N5—C22—C21	178.05 (18)	N7—S1—C7A—C8B	-91.2 (5)
C13—N5—C22—C21	-1.7 (3)	C7B—S1—C7A—C8B	147 (3)

C21—C15—C14—C13	-0.9 (3)	O6—S1—C7A—C6B	-20.4 (6)
C16—C15—C14—C13	178.84 (18)	O5—S1—C7A—C6B	-152.3 (5)
N5—C22—C21—C15	0.9 (3)	N7—S1—C7A—C6B	96.0 (5)
C14—C15—C21—C22	0.4 (3)	C7B—S1—C7A—C6B	-26 (2)

Table 2e. Hydrogen-bond geometry (Å, °) for cocrystal of **23** and of 4,4'-dipyridyl-N,N'-dioxide dihydrate (**25**).

<i>D</i> —H \cdots <i>A</i>	<i>D</i> —H	H \cdots <i>A</i>	<i>D</i> \cdots <i>A</i>	<i>D</i> —H \cdots <i>A</i>
C13—H13 \cdots O11	0.95	2.30	3.247 (4)	175
O9—H4 \cdots O1	1.04 (2)	1.81 (2)	2.839 (2)	170.6 (18)
O9—H2 \cdots O6 ⁱ	1.03 (2)	1.82 (2)	2.8439 (19)	172.6 (18)

Symmetry code: (i) *x*, *y*+2, *z*-1.

Table 3a. Crystal data and structure refinement for cocrystal of **23** and *trans*-1,2-bis(4-pyridyl)ethylene (**26**).

Crystal data

$C_{12}H_{13}NO_6S$	$V = 2226.57 (6) \text{ \AA}^3$
$M_r = 481.52$	$Z = 4$
Triclinic, $P\bar{1}$	$F(000) = 948$
Hall symbol: $-P\ 1$	$D_x = 1.350 \text{ Mg m}^{-3}$
$a = 11.5952 (2) \text{ \AA}$	Cu $K\alpha$ radiation, $\lambda = 1.54178 \text{ \AA}$
$b = 14.0108 (2) \text{ \AA}$	$\mu = 1.64 \text{ mm}^{-1}$
$c = 14.1325 (2) \text{ \AA}$	$T = 173 \text{ K}$
$\alpha = 104.009 (1)^\circ$	Transparent plate, colorless
$\beta = 91.452 (1)^\circ$	
$\gamma = 90.655 (1)^\circ$	

Data collection

Bruker APEXII CCD diffractometer	7868 independent reflections
Radiation source: fine-focus sealed tube	6499 reflections with $I > 2\sigma(I)$
Graphite	$R_{\text{int}} = 0.038$
ϕ and ω scans	$\theta_{\text{max}} = 67.9^\circ$, $\theta_{\text{min}} = 3.2^\circ$
Absorption correction: multi-scan <i>SADABS</i> (Bruker, 2009)	$h = -13 \rightarrow 13$
$T_{\text{min}} = 0.678$, $T_{\text{max}} = 0.723$	$k = -16 \rightarrow 16$
46574 measured reflections	$l = -16 \rightarrow 16$

Refinement

Refinement on F^2	Primary atom site location: structure-invariant direct methods
Least-squares matrix: full	Secondary atom site location: difference Fourier map
$R[F^2 > 2\sigma(F^2)] = 0.034$	Hydrogen site location: inferred from neighbouring sites
$wR(F^2) = 0.099$	H atoms treated by a mixture of independent and constrained refinement
$S = 1.05$	$w = 1/[\sigma^2(F_o^2) + (0.0504P)^2 + 1.0169P]$
7868 reflections	where $P = (F_o^2 + 2F_c^2)/3$
730 parameters	$(\Delta/\sigma)_{\text{max}} = 0.019$
37 restraints	$\Delta_{\text{max}} = 0.32 \text{ e \AA}^{-3}$
	$\Delta_{\text{min}} = -0.39 \text{ e \AA}^{-3}$

Table 3b. Fractional atomic coordinates and isotropic or equivalent isotropic displacement parameters (\AA^2) for cocrystal of **23** and *trans*-1,2-bis(4-pyridyl)ethylene (**26**).

	<i>x</i>	<i>y</i>	<i>z</i>	$U_{\text{iso}}^*/U_{\text{eq}}$	Occ. (<1)
S1	1.10341 (4)	1.21847 (3)	0.14085 (3)	0.02370 (12)	
O1	1.21435 (12)	1.21829 (9)	0.09862 (10)	0.0316 (3)	
S2A	0.13704 (7)	-0.34024 (5)	0.36898 (5)	0.0180 (2)	0.856 (4)
O2	1.04349 (11)	1.16034 (9)	0.38184 (10)	0.0288 (3)	
O3	0.40358 (12)	-0.35671 (10)	0.15818 (11)	0.0327 (3)	
H6	0.4291 (19)	-0.3097 (14)	0.1338 (16)	0.039*	
O4	0.86660 (11)	1.21712 (9)	0.36370 (10)	0.0280 (3)	
H1	0.8440 (18)	1.1620 (13)	0.3783 (16)	0.034*	
O5	0.92136 (12)	0.59768 (9)	0.14178 (10)	0.0331 (3)	
O6	0.23604 (11)	-0.28263 (9)	0.14458 (10)	0.0293 (3)	
O7	0.73642 (11)	0.63697 (9)	0.12726 (10)	0.0299 (3)	
H5	0.7238 (19)	0.5730 (12)	0.1191 (16)	0.036*	
O8	1.00582 (12)	1.25874 (9)	0.10107 (9)	0.0297 (3)	
O9A	0.4971 (3)	0.23088 (19)	0.3962 (2)	0.0305 (6)	0.856 (4)
H9	0.5253 (19)	0.2897 (13)	0.3960 (16)	0.037*	
O10A	0.2158 (6)	-0.3901 (6)	0.4188 (5)	0.038 (2)	0.856 (4)
N11	0.48617 (13)	-0.19789 (11)	0.11190 (11)	0.0245 (3)	
N12	1.12005 (13)	1.27664 (11)	0.25316 (11)	0.0260 (3)	
H12	1.1903	1.2925	0.2774	0.031*	
N13	0.13099 (14)	-0.39950 (11)	0.25614 (11)	0.0249 (3)	
H4	0.0726 (15)	-0.3921 (16)	0.2224 (14)	0.030*	
C13	1.11504 (16)	0.92405 (13)	0.10897 (13)	0.0260 (4)	
H13	1.1704	0.8738	0.0919	0.031*	
O14A	0.33879 (19)	0.29045 (19)	0.34128 (17)	0.0410 (6)	0.856 (4)
C14	1.14649 (16)	1.02068 (13)	0.11267 (13)	0.0256 (4)	
H14	1.2235	1.0365	0.0999	0.031*	
C15	1.06553 (16)	1.09401 (13)	0.13506 (12)	0.0231 (4)	
C16	0.95303 (16)	1.07073 (13)	0.15461 (13)	0.0246 (4)	
H16	0.8970	1.1207	0.1687	0.030*	
N17	0.57930 (14)	0.39838 (11)	0.38344 (11)	0.0264 (3)	
C17	0.92310 (16)	0.97504 (13)	0.15354 (13)	0.0245 (4)	
H2	0.8468	0.9600	0.1690	0.029*	
O18A	0.0223 (4)	-0.3272 (3)	0.4003 (3)	0.0365 (9)	0.856 (4)
C18	1.00309 (16)	0.89953 (13)	0.13002 (12)	0.0230 (4)	
C19	0.97401 (16)	0.79679 (13)	0.12816 (13)	0.0247 (4)	
H19	1.0335	0.7500	0.1124	0.030*	
N20	0.68274 (14)	0.45543 (11)	0.11682 (11)	0.0283 (4)	
C20	0.87150 (16)	0.76412 (13)	0.14675 (13)	0.0248 (4)	
H20A	0.8116	0.8099	0.1657	0.030*	
N21	0.79723 (13)	1.04434 (11)	0.37889 (11)	0.0241 (3)	
C21	0.84737 (16)	0.65812 (13)	0.13881 (13)	0.0251 (4)	
C22	0.97936 (16)	1.21889 (12)	0.35786 (13)	0.0230 (4)	
C23	1.02199 (17)	1.30403 (13)	0.31636 (14)	0.0276 (4)	
H23	0.9574	1.3242	0.2776	0.033*	
C24	1.0568 (2)	1.39090 (15)	0.39980 (16)	0.0446 (6)	
H24A	1.1231	1.3733	0.4361	0.067*	
H24B	0.9920	1.4083	0.4435	0.067*	
H24C	1.0778	1.4472	0.3736	0.067*	
C37	0.58626 (16)	-0.18677 (13)	0.07005 (13)	0.0238 (4)	

H37	0.6290	-0.2437	0.0425	0.029*	
C38	0.62989 (15)	-0.09572 (13)	0.06533 (13)	0.0231 (4)	
H38	0.7011	-0.0913	0.0348	0.028*	
C39	0.56972 (15)	-0.01044 (13)	0.10529 (12)	0.0221 (4)	
C40	0.46452 (16)	-0.02299 (13)	0.14747 (13)	0.0247 (4)	
H40	0.4194	0.0325	0.1751	0.030*	
C41	0.42672 (16)	-0.11624 (13)	0.14874 (13)	0.0258 (4)	
H41	0.3547	-0.1231	0.1772	0.031*	
C42	0.61753 (16)	0.08620 (13)	0.10197 (13)	0.0234 (4)	
H42	0.6923	0.0882	0.0765	0.028*	
C43	0.56374 (16)	0.17140 (13)	0.13205 (13)	0.0253 (4)	
H43	0.4900	0.1691	0.1593	0.030*	
C44	0.57252 (17)	0.43748 (14)	0.13326 (14)	0.0296 (4)	
H44	0.5196	0.4899	0.1410	0.035*	
C45	0.53215 (17)	0.34661 (13)	0.13953 (14)	0.0283 (4)	
H45	0.4533	0.3372	0.1524	0.034*	
C46	0.60827 (16)	0.26821 (13)	0.12680 (13)	0.0247 (4)	
C47	0.72313 (17)	0.28732 (13)	0.10889 (14)	0.0271 (4)	
H47	0.7778	0.2361	0.0994	0.033*	
C48	0.75641 (17)	0.38087 (14)	0.10507 (14)	0.0288 (4)	
H48	0.8350	0.3931	0.0936	0.035*	
C1A	0.1936 (4)	-0.05932 (17)	0.35171 (18)	0.0242 (6)	0.856 (4)
H1A	0.1513	-0.0101	0.3308	0.029*	0.856 (4)
C2A	0.1426 (3)	-0.1497 (2)	0.3472 (2)	0.0266 (8)	0.856 (4)
H2A	0.0658	-0.1629	0.3222	0.032*	0.856 (4)
C3A	0.2035 (3)	-0.2223 (2)	0.3792 (3)	0.0233 (12)*	0.856 (4)
C4A	0.3142 (4)	-0.2030 (3)	0.4163 (4)	0.0239 (10)	0.856 (4)
H4A	0.3551	-0.2515	0.4396	0.029*	0.856 (4)
C5A	0.3660 (3)	-0.1128 (2)	0.4195 (2)	0.0257 (6)	0.856 (4)
H5A	0.4430	-0.1005	0.4445	0.031*	0.856 (4)
C6A	0.3081 (3)	-0.03971 (18)	0.38721 (18)	0.0237 (6)	0.856 (4)
C7A	0.3688 (2)	0.05413 (17)	0.38977 (15)	0.0251 (6)	0.856 (4)
H7A	0.4484	0.0583	0.4080	0.030*	0.856 (4)
C8A	0.3231 (2)	0.13285 (16)	0.36925 (16)	0.0279 (6)	0.856 (4)
H8A	0.2427	0.1309	0.3539	0.033*	0.856 (4)
C9A	0.3892 (4)	0.2246 (3)	0.3685 (2)	0.0278 (6)	0.856 (4)
C10A	0.2043 (2)	-0.51597 (14)	0.11492 (16)	0.0400 (5)	
H10A	0.1723	-0.5711	0.1379	0.060*	
H10B	0.2738	-0.5370	0.0780	0.060*	
H10C	0.1470	-0.4944	0.0727	0.060*	
C11A	0.23523 (16)	-0.43091 (13)	0.20234 (14)	0.0266 (4)	
H11A	0.2919	-0.4540	0.2460	0.032*	
C12A	0.29073 (16)	-0.34766 (13)	0.16564 (13)	0.0245 (4)	
C25A	0.6913 (4)	1.0150 (4)	0.3432 (4)	0.0243 (10)	0.856 (4)
H25A	0.6435	1.0607	0.3219	0.029*	0.856 (4)
C26A	0.6485 (3)	0.9210 (2)	0.3362 (2)	0.0243 (7)	0.856 (4)
H26A	0.5734	0.9028	0.3090	0.029*	0.856 (4)
C27A	0.7158 (3)	0.8528 (2)	0.36901 (19)	0.0230 (6)	0.856 (4)
C28A	0.8267 (4)	0.8838 (2)	0.4062 (2)	0.0255 (7)	0.856 (4)
H28A	0.8762	0.8406	0.4298	0.031*	0.856 (4)
C29A	0.8623 (4)	0.9783 (3)	0.4077 (4)	0.0263 (10)	0.856 (4)
H29A	0.9386	0.9977	0.4309	0.032*	0.856 (4)
C30A	0.6663 (2)	0.75459 (17)	0.36490 (16)	0.0260 (6)	0.856 (4)
H30A	0.5870	0.7439	0.3462	0.031*	0.856 (4)
C31A	0.7228 (2)	0.67965 (17)	0.38502 (16)	0.0267 (6)	0.856 (4)
H31A	0.8026	0.6893	0.4022	0.032*	0.856 (4)

C32A	0.6941 (3)	0.4129 (3)	0.3819 (3)	0.0250 (8)	0.856 (4)
H32A	0.7436	0.3591	0.3810	0.030*	0.856 (4)
C33A	0.7421 (3)	0.5029 (2)	0.38177 (18)	0.0273 (6)	0.856 (4)
H33A	0.8235	0.5108	0.3810	0.033*	0.856 (4)
C34A	0.6707 (3)	0.58278 (19)	0.38269 (16)	0.0243 (6)	0.856 (4)
C35A	0.5522 (3)	0.56586 (19)	0.3828 (2)	0.0278 (6)	0.856 (4)
H35A	0.5002	0.6178	0.3829	0.033*	0.856 (4)
C36A	0.5109 (4)	0.4732 (3)	0.3828 (4)	0.0286 (10)	0.856 (4)
H36A	0.4298	0.4627	0.3823	0.034*	0.856 (4)
C1B	0.1472 (16)	-0.0672 (11)	0.3447 (14)	0.025 (5)*	0.144 (4)
H1B	0.0965	-0.0217	0.3262	0.030*	0.144 (4)
C2B	0.1095 (13)	-0.1601 (10)	0.3414 (13)	0.006 (4)*	0.144 (4)
H2B	0.0335	-0.1812	0.3185	0.007*	0.144 (4)
C3B	0.1835 (13)	-0.2224 (10)	0.3717 (11)	0.005 (5)*	0.144 (4)
C4B	0.295 (2)	-0.1975 (18)	0.405 (3)	0.028 (9)*	0.144 (4)
H4B	0.3435	-0.2430	0.4265	0.033*	0.144 (4)
C5B	0.3344 (15)	-0.1014 (15)	0.4066 (15)	0.024 (6)*	0.144 (4)
H5B	0.4108	-0.0806	0.4286	0.029*	0.144 (4)
C6B	0.2610 (17)	-0.0387 (10)	0.3755 (11)	0.010 (4)*	0.144 (4)
C7B	0.2943 (11)	0.0616 (8)	0.3682 (7)	0.012 (3)*	0.144 (4)
H7B	0.2354	0.0988	0.3470	0.014*	0.144 (4)
C8B	0.3997 (13)	0.1064 (11)	0.3884 (9)	0.025 (3)*	0.144 (4)
H8B	0.4603	0.0715	0.4107	0.030*	0.144 (4)
C25B	0.699 (3)	0.9967 (18)	0.344 (3)	0.035 (11)*	0.144 (4)
H25B	0.6422	1.0311	0.3164	0.042*	0.144 (4)
C26B	0.6758 (16)	0.8988 (14)	0.3444 (14)	0.021 (5)*	0.144 (4)
H26B	0.6042	0.8684	0.3190	0.025*	0.144 (4)
C27B	0.7576 (18)	0.8469 (14)	0.3824 (14)	0.021 (5)*	0.144 (4)
C28B	0.858 (2)	0.8967 (17)	0.4203 (19)	0.040 (8)*	0.144 (4)
H28B	0.9145	0.8629	0.4489	0.048*	0.144 (4)
C29B	0.881 (2)	0.9924 (16)	0.419 (2)	0.015 (6)*	0.144 (4)
H29B	0.9523	1.0232	0.4444	0.018*	0.144 (4)
C30B	0.7345 (14)	0.7439 (11)	0.3853 (9)	0.024 (3)*	0.144 (4)
H30B	0.7987	0.7100	0.4032	0.028*	0.144 (4)
C31B	0.6411 (13)	0.6945 (11)	0.3672 (9)	0.026 (3)*	0.144 (4)
H31B	0.5768	0.7277	0.3481	0.032*	0.144 (4)
C32B	0.685 (3)	0.4361 (17)	0.386 (3)	0.055 (13)*	0.144 (4)
H32B	0.7478	0.3957	0.3933	0.066*	0.144 (4)
C33B	0.7090 (15)	0.5311 (14)	0.3772 (11)	0.017 (4)*	0.144 (4)
H33B	0.7865	0.5531	0.3751	0.021*	0.144 (4)
C34B	0.6193 (18)	0.5922 (12)	0.3719 (12)	0.022 (4)*	0.144 (4)
C35B	0.5081 (16)	0.5581 (13)	0.3745 (14)	0.028 (5)*	0.144 (4)
H35B	0.4461	0.6011	0.3712	0.034*	0.144 (4)
C36B	0.4835 (19)	0.4642 (15)	0.382 (2)	0.017 (6)*	0.144 (4)
H36B	0.4061	0.4427	0.3852	0.021*	0.144 (4)
C9B	0.424 (2)	0.2055 (18)	0.3776 (19)	0.035 (7)*	0.144 (4)
O14B	0.3586 (16)	0.2524 (14)	0.3378 (13)	0.041 (5)*	0.144 (4)
O9B	0.5293 (18)	0.2252 (19)	0.4037 (17)	0.047 (7)*	0.144 (4)
S2B	0.1397 (14)	-0.3400 (11)	0.3718 (12)	0.125 (6)*	0.144 (4)
O18B	0.007 (2)	-0.3212 (15)	0.3854 (15)	0.008 (3)*	0.144 (4)
O10B	0.212 (3)	-0.392 (3)	0.424 (2)	0.013 (7)*	0.144 (4)

Table 3c. Atomic displacement parameters (\AA^2) for cocrystal of **23** and *trans*-1,2-bis(4-pyridyl)ethylene (**26**).

	U^{11}	U^{22}	U^{33}	U^{12}	U^{13}	U^{23}
S1	0.0273 (2)	0.0188 (2)	0.0255 (2)	-0.00058 (17)	0.00593 (18)	0.00579 (17)
O1	0.0341 (8)	0.0251 (7)	0.0364 (7)	-0.0011 (6)	0.0134 (6)	0.0078 (6)
S2A	0.0219 (3)	0.0155 (3)	0.0176 (3)	-0.00427 (18)	0.00265 (19)	0.00580 (18)
O2	0.0266 (7)	0.0259 (7)	0.0358 (7)	-0.0007 (6)	0.0012 (6)	0.0111 (6)
O3	0.0282 (7)	0.0245 (7)	0.0499 (9)	0.0021 (6)	0.0098 (6)	0.0169 (6)
O4	0.0264 (7)	0.0211 (6)	0.0384 (7)	-0.0009 (5)	0.0046 (6)	0.0105 (6)
O5	0.0317 (8)	0.0240 (7)	0.0444 (8)	0.0009 (6)	-0.0053 (6)	0.0106 (6)
O6	0.0276 (7)	0.0259 (7)	0.0380 (7)	0.0023 (6)	0.0050 (6)	0.0143 (6)
O7	0.0285 (7)	0.0194 (6)	0.0422 (8)	-0.0028 (5)	-0.0008 (6)	0.0088 (6)
O8	0.0371 (8)	0.0229 (6)	0.0303 (7)	0.0025 (6)	0.0022 (6)	0.0088 (5)
O9A	0.0313 (17)	0.0189 (10)	0.0442 (13)	-0.0006 (12)	-0.0006 (12)	0.0133 (8)
O10A	0.054 (3)	0.0270 (17)	0.036 (2)	-0.0063 (9)	-0.0075 (11)	0.0150 (11)
N11	0.0246 (8)	0.0221 (8)	0.0276 (8)	-0.0013 (6)	0.0008 (6)	0.0076 (6)
N12	0.0241 (8)	0.0228 (8)	0.0292 (8)	-0.0069 (6)	0.0040 (7)	0.0028 (6)
N13	0.0247 (8)	0.0245 (8)	0.0254 (8)	-0.0025 (7)	0.0010 (7)	0.0062 (6)
C13	0.0271 (10)	0.0237 (9)	0.0289 (9)	0.0052 (8)	0.0052 (8)	0.0088 (7)
O14A	0.0303 (11)	0.0309 (13)	0.0649 (14)	-0.0056 (10)	-0.0095 (9)	0.0191 (10)
C14	0.0253 (10)	0.0262 (9)	0.0274 (9)	0.0007 (8)	0.0044 (8)	0.0100 (7)
C15	0.0280 (10)	0.0209 (9)	0.0205 (8)	-0.0007 (7)	0.0017 (7)	0.0051 (7)
C16	0.0257 (10)	0.0200 (9)	0.0268 (9)	0.0014 (7)	-0.0006 (8)	0.0032 (7)
N17	0.0307 (9)	0.0224 (8)	0.0260 (8)	-0.0021 (7)	-0.0019 (7)	0.0060 (6)
C17	0.0226 (9)	0.0241 (9)	0.0254 (9)	-0.0018 (7)	-0.0007 (7)	0.0034 (7)
O18A	0.032 (2)	0.0461 (15)	0.0314 (19)	-0.0054 (12)	0.0060 (13)	0.0089 (13)
C18	0.0283 (10)	0.0216 (9)	0.0191 (8)	0.0006 (7)	-0.0008 (7)	0.0051 (7)
C19	0.0296 (10)	0.0215 (9)	0.0230 (9)	0.0038 (8)	0.0007 (7)	0.0054 (7)
N20	0.0327 (9)	0.0215 (8)	0.0312 (8)	-0.0012 (7)	-0.0012 (7)	0.0074 (6)
C20	0.0285 (10)	0.0199 (9)	0.0252 (9)	0.0015 (7)	-0.0001 (8)	0.0039 (7)
N21	0.0240 (8)	0.0240 (8)	0.0247 (8)	-0.0028 (6)	0.0033 (6)	0.0066 (6)
C21	0.0299 (10)	0.0229 (9)	0.0219 (9)	-0.0010 (8)	-0.0024 (8)	0.0047 (7)
C22	0.0268 (10)	0.0189 (8)	0.0219 (8)	-0.0001 (7)	0.0044 (7)	0.0017 (7)
C23	0.0330 (11)	0.0206 (9)	0.0292 (10)	0.0004 (8)	0.0095 (8)	0.0052 (7)
C24	0.0701 (16)	0.0253 (10)	0.0357 (11)	-0.0124 (10)	0.0171 (11)	0.0012 (9)
C37	0.0236 (9)	0.0221 (9)	0.0256 (9)	0.0023 (7)	0.0001 (7)	0.0053 (7)
C38	0.0221 (9)	0.0246 (9)	0.0230 (9)	-0.0008 (7)	0.0017 (7)	0.0062 (7)
C39	0.0241 (9)	0.0219 (9)	0.0204 (8)	-0.0011 (7)	-0.0019 (7)	0.0056 (7)
C40	0.0248 (10)	0.0228 (9)	0.0255 (9)	0.0021 (7)	0.0032 (7)	0.0039 (7)
C41	0.0245 (9)	0.0274 (9)	0.0258 (9)	-0.0005 (8)	0.0034 (7)	0.0067 (7)
C42	0.0235 (9)	0.0234 (9)	0.0236 (9)	-0.0037 (7)	0.0001 (7)	0.0063 (7)
C43	0.0269 (10)	0.0229 (9)	0.0262 (9)	-0.0017 (8)	0.0025 (8)	0.0061 (7)
C44	0.0341 (11)	0.0213 (9)	0.0331 (10)	0.0042 (8)	0.0023 (8)	0.0059 (8)
C45	0.0288 (10)	0.0244 (9)	0.0309 (10)	0.0008 (8)	0.0032 (8)	0.0047 (8)
C46	0.0310 (10)	0.0203 (9)	0.0223 (9)	-0.0003 (8)	0.0005 (8)	0.0046 (7)
C47	0.0291 (10)	0.0211 (9)	0.0311 (10)	0.0018 (8)	0.0006 (8)	0.0060 (7)
C48	0.0284 (10)	0.0261 (9)	0.0324 (10)	-0.0027 (8)	0.0003 (8)	0.0083 (8)
C1A	0.030 (2)	0.0194 (11)	0.0238 (12)	0.0040 (12)	0.0024 (14)	0.0057 (9)
C2A	0.0195 (16)	0.0317 (16)	0.0269 (14)	-0.0021 (13)	-0.0013 (13)	0.0046 (10)
C4A	0.0254 (17)	0.0226 (17)	0.0240 (19)	0.0030 (12)	0.0023 (14)	0.0062 (11)
C5A	0.0233 (15)	0.0269 (14)	0.0257 (14)	-0.0012 (12)	0.0027 (12)	0.0039 (10)
C6A	0.0231 (16)	0.0248 (13)	0.0212 (12)	-0.0009 (11)	0.0045 (11)	0.0017 (9)
C7A	0.0235 (13)	0.0256 (13)	0.0245 (11)	-0.0014 (10)	0.0012 (9)	0.0030 (9)
C8A	0.0244 (12)	0.0255 (12)	0.0326 (12)	-0.0042 (9)	-0.0002 (9)	0.0053 (9)
C9A	0.0306 (18)	0.0269 (16)	0.0254 (15)	-0.0085 (15)	0.0007 (14)	0.0058 (13)
C10A	0.0534 (14)	0.0222 (10)	0.0421 (12)	-0.0070 (9)	0.0135 (10)	0.0022 (9)
C11A	0.0291 (10)	0.0216 (9)	0.0307 (10)	0.0016 (8)	0.0059 (8)	0.0089 (7)
C12A	0.0271 (10)	0.0196 (9)	0.0259 (9)	0.0012 (8)	0.0049 (8)	0.0034 (7)

C25A	0.0240 (18)	0.0233 (16)	0.0273 (18)	0.0007 (15)	0.0026 (10)	0.0089 (15)
C26A	0.0220 (14)	0.0252 (15)	0.0266 (14)	-0.0017 (13)	0.0002 (10)	0.0082 (11)
C27A	0.0259 (16)	0.0232 (14)	0.0203 (12)	-0.0006 (13)	0.0037 (12)	0.0056 (9)
C28A	0.029 (2)	0.0237 (13)	0.0255 (14)	0.0003 (14)	-0.0005 (14)	0.0083 (11)
C29A	0.023 (2)	0.030 (2)	0.0254 (19)	-0.0046 (14)	-0.0015 (15)	0.0066 (14)
C30A	0.0254 (13)	0.0249 (13)	0.0274 (11)	-0.0021 (10)	0.0010 (10)	0.0059 (9)
C31A	0.0264 (13)	0.0243 (13)	0.0290 (11)	-0.0020 (9)	0.0025 (9)	0.0054 (9)
C32A	0.0285 (16)	0.0216 (13)	0.0244 (15)	-0.0013 (12)	-0.0014 (9)	0.0047 (12)
C33A	0.0265 (14)	0.0233 (14)	0.0322 (13)	0.0019 (12)	-0.0006 (10)	0.0071 (10)
C34A	0.0270 (16)	0.0220 (14)	0.0236 (11)	-0.0006 (12)	-0.0012 (11)	0.0049 (9)
C35A	0.0298 (19)	0.0226 (12)	0.0307 (14)	0.0013 (13)	0.0024 (14)	0.0057 (9)
C36A	0.025 (2)	0.0273 (17)	0.0328 (17)	-0.0028 (14)	0.0018 (17)	0.0064 (11)

Table 3d. Geometric parameters (Å, °) for cocrystal of **23** and *trans*-1,2-bis(4-pyridyl)ethylene (**26**).

S1—O1	1.4315 (13)	C2A—C3A	1.399 (4)
S1—O8	1.4320 (14)	C2A—H2A	0.9500
S1—N12	1.6047 (16)	C3A—C4A	1.373 (5)
S1—C15	1.7755 (18)	C4A—C5A	1.383 (3)
S2A—O18A	1.413 (5)	C4A—H4A	0.9500
S2A—O10A	1.428 (4)	C5A—C6A	1.390 (4)
S2A—N13	1.6092 (17)	C5A—H5A	0.9500
S2A—C3A	1.788 (3)	C6A—C7A	1.476 (3)
O2—C22	1.215 (2)	C7A—C8A	1.320 (4)
O3—C12A	1.320 (2)	C7A—H7A	0.9500
O3—H6	0.867 (16)	C8A—C9A	1.491 (3)
O4—C22	1.313 (2)	C8A—H8A	0.9500
O4—H1	0.885 (16)	C10A—C11A	1.526 (3)
O5—C21	1.219 (2)	C10A—H10A	0.9800
O6—C12A	1.207 (2)	C10A—H10B	0.9800
O7—C21	1.314 (2)	C10A—H10C	0.9800
O7—H5	0.885 (16)	C11A—C12A	1.529 (2)
O9A—C9A	1.298 (5)	C11A—H11A	1.0000
O9A—H9	0.883 (16)	C25A—C26A	1.382 (5)
N11—C37	1.340 (2)	C25A—H25A	0.9500
N11—C41	1.343 (2)	C26A—C27A	1.396 (4)
N12—C23	1.461 (2)	C26A—H26A	0.9500
N12—H12	0.8800	C27A—C28A	1.400 (5)
N13—C11A	1.459 (2)	C27A—C30A	1.473 (3)
N13—S2B	1.645 (16)	C28A—C29A	1.378 (5)
N13—H4	0.840 (15)	C28A—H28A	0.9500
C13—C14	1.386 (3)	C29A—H29A	0.9500
C13—C18	1.397 (3)	C30A—C31A	1.328 (4)
C13—H13	0.9500	C30A—H30A	0.9500
O14A—C9A	1.230 (5)	C31A—C34A	1.472 (3)
C14—C15	1.384 (3)	C31A—H31A	0.9500
C14—H14	0.9500	C32A—C33A	1.373 (4)
C15—C16	1.392 (3)	C32A—H32A	0.9500
C16—C17	1.377 (2)	C33A—C34A	1.397 (4)
C16—H16	0.9500	C33A—H33A	0.9500
N17—C32B	1.32 (3)	C34A—C35A	1.392 (4)
N17—C36A	1.324 (4)	C35A—C36A	1.378 (4)
N17—C32A	1.346 (4)	C35A—H35A	0.9500
N17—C36B	1.46 (2)	C36A—H36A	0.9500

C17—C18	1.399 (2)	C1B—C2B	1.357 (15)
C17—H2	0.9500	C1B—C6B	1.402 (15)
C18—C19	1.469 (2)	C1B—H1B	0.9500
C19—C20	1.324 (3)	C2B—C3B	1.364 (15)
C19—H19	0.9500	C2B—H2B	0.9500
N20—C44	1.337 (2)	C3B—C4B	1.379 (17)
N20—C48	1.339 (2)	C3B—S2B	1.72 (2)
C20—C21	1.485 (2)	C4B—C5B	1.412 (17)
C20—H20A	0.9500	C4B—H4B	0.9500
N21—C29A	1.331 (5)	C5B—C6B	1.370 (15)
N21—C25A	1.337 (5)	C5B—H5B	0.9500
N21—C25B	1.33 (3)	C6B—C7B	1.481 (17)
N21—C29B	1.41 (3)	C7B—C8B	1.36 (2)
C22—C23	1.533 (2)	C7B—H7B	0.9500
C23—C24	1.518 (3)	C8B—C9B	1.46 (3)
C23—H23	1.0000	C8B—H8B	0.9500
C24—H24A	0.9800	C25B—C26B	1.397 (17)
C24—H24B	0.9800	C25B—H25B	0.9500
C24—H24C	0.9800	C26B—C27B	1.377 (15)
C37—C38	1.384 (2)	C26B—H26B	0.9500
C37—H37	0.9500	C27B—C28B	1.379 (16)
C38—C39	1.395 (2)	C27B—C30B	1.48 (2)
C38—H38	0.9500	C28B—C29B	1.368 (18)
C39—C40	1.399 (2)	C28B—H28B	0.9500
C39—C42	1.469 (2)	C29B—H29B	0.9500
C40—C41	1.378 (3)	C30B—C31B	1.27 (2)
C40—H40	0.9500	C30B—H30B	0.9500
C41—H41	0.9500	C31B—C34B	1.47 (2)
C42—C43	1.334 (3)	C31B—H31B	0.9500
C42—H42	0.9500	C32B—C33B	1.391 (17)
C43—C46	1.465 (2)	C32B—H32B	0.9500
C43—H43	0.9500	C33B—C34B	1.366 (16)
C44—C45	1.375 (3)	C33B—H33B	0.9500
C44—H44	0.9500	C34B—C35B	1.375 (15)
C45—C46	1.397 (3)	C35B—C36B	1.371 (17)
C45—H45	0.9500	C35B—H35B	0.9500
C46—C47	1.397 (3)	C36B—H36B	0.9500
C47—C48	1.376 (3)	C9B—O14B	1.223 (16)
C47—H47	0.9500	C9B—O9B	1.273 (18)
C48—H48	0.9500	O9B—H9	0.94 (3)
C1A—C2A	1.378 (4)	S2B—O10B	1.423 (17)
C1A—C6A	1.408 (4)	S2B—O18B	1.58 (3)
C1A—H1A	0.9500		
O1—S1—O8	120.73 (8)	C5A—C6A—C7A	119.3 (3)
O1—S1—N12	106.26 (8)	C1A—C6A—C7A	122.6 (3)
O8—S1—N12	107.71 (8)	C8A—C7A—C6A	126.4 (2)
O1—S1—C15	106.97 (8)	C8A—C7A—H7A	116.8
O8—S1—C15	105.87 (8)	C6A—C7A—H7A	116.8
N12—S1—C15	108.92 (8)	C7A—C8A—C9A	124.4 (3)
O18A—S2A—O10A	119.3 (3)	C7A—C8A—H8A	117.8
O18A—S2A—N13	107.17 (18)	C9A—C8A—H8A	117.8
O10A—S2A—N13	107.5 (3)	O14A—C9A—O9A	123.2 (2)
O18A—S2A—C3A	109.0 (2)	O14A—C9A—C8A	118.4 (3)
O10A—S2A—C3A	104.4 (4)	O9A—C9A—C8A	118.4 (4)
N13—S2A—C3A	109.27 (13)	C11A—C10A—H10A	109.5

C12A—O3—H6	107.7 (15)	C11A—C10A—H10B	109.5
C22—O4—H1	109.7 (14)	H10A—C10A—H10B	109.5
C21—O7—H5	110.7 (15)	C11A—C10A—H10C	109.5
C9A—O9A—H9	109.7 (16)	H10A—C10A—H10C	109.5
C37—N11—C41	117.30 (15)	H10B—C10A—H10C	109.5
C23—N12—S1	121.90 (13)	N13—C11A—C10A	109.01 (16)
C23—N12—H12	119.1	N13—C11A—C12A	111.95 (15)
S1—N12—H12	119.1	C10A—C11A—C12A	108.79 (15)
C11A—N13—S2A	121.56 (13)	N13—C11A—H11A	109.0
C11A—N13—S2B	120.5 (6)	C10A—C11A—H11A	109.0
S2A—N13—S2B	1.2 (6)	C12A—C11A—H11A	109.0
C11A—N13—H4	116.0 (15)	O6—C12A—O3	124.67 (17)
S2A—N13—H4	117.8 (15)	O6—C12A—C11A	123.05 (17)
S2B—N13—H4	119.0 (16)	O3—C12A—C11A	112.27 (15)
C14—C13—C18	120.94 (17)	N21—C25A—C26A	122.8 (4)
C14—C13—H13	119.5	N21—C25A—H25A	118.6
C18—C13—H13	119.5	C26A—C25A—H25A	118.6
C15—C14—C13	119.90 (17)	C25A—C26A—C27A	120.0 (3)
C15—C14—H14	120.0	C25A—C26A—H26A	120.0
C13—C14—H14	120.0	C27A—C26A—H26A	120.0
C14—C15—C16	119.96 (16)	C26A—C27A—C28A	117.1 (2)
C14—C15—S1	120.93 (14)	C26A—C27A—C30A	119.0 (3)
C16—C15—S1	119.11 (14)	C28A—C27A—C30A	124.0 (3)
C17—C16—C15	119.88 (17)	C29A—C28A—C27A	118.4 (3)
C17—C16—H16	120.1	C29A—C28A—H28A	120.8
C15—C16—H16	120.1	C27A—C28A—H28A	120.8
C32B—N17—C36A	104.2 (10)	N21—C29A—C28A	124.6 (4)
C32B—N17—C32A	14.5 (10)	N21—C29A—H29A	117.7
C36A—N17—C32A	118.5 (3)	C28A—C29A—H29A	117.7
C32B—N17—C36B	117.1 (11)	C31A—C30A—C27A	125.7 (3)
C36A—N17—C36B	12.9 (8)	C31A—C30A—H30A	117.2
C32A—N17—C36B	131.4 (8)	C27A—C30A—H30A	117.2
C16—C17—C18	121.16 (17)	C30A—C31A—C34A	124.7 (3)
C16—C17—H2	119.4	C30A—C31A—H31A	117.7
C18—C17—H2	119.4	C34A—C31A—H31A	117.7
C13—C18—C17	118.12 (16)	N17—C32A—C33A	122.1 (4)
C13—C18—C19	119.33 (16)	N17—C32A—H32A	118.9
C17—C18—C19	122.54 (17)	C33A—C32A—H32A	118.9
C20—C19—C18	125.23 (17)	C32A—C33A—C34A	119.8 (3)
C20—C19—H19	117.4	C32A—C33A—H33A	120.1
C18—C19—H19	117.4	C34A—C33A—H33A	120.1
C44—N20—C48	118.08 (16)	C35A—C34A—C33A	117.2 (2)
C19—C20—C21	122.00 (17)	C35A—C34A—C31A	123.3 (3)
C19—C20—H20A	119.0	C33A—C34A—C31A	119.5 (3)
C21—C20—H20A	119.0	C36A—C35A—C34A	119.5 (3)
C29A—N21—C25A	117.1 (3)	C36A—C35A—H35A	120.2
C29A—N21—C25B	105.4 (10)	C34A—C35A—H35A	120.2
C25A—N21—C25B	11.8 (11)	N17—C36A—C35A	122.9 (4)
C29A—N21—C29B	12.4 (9)	N17—C36A—H36A	118.6
C25A—N21—C29B	129.1 (9)	C35A—C36A—H36A	118.6
C25B—N21—C29B	117.6 (12)	C2B—C1B—C6B	119.8 (14)
O5—C21—O7	123.94 (17)	C2B—C1B—H1B	120.1
O5—C21—C20	124.28 (17)	C6B—C1B—H1B	120.1
O7—C21—C20	111.78 (16)	C1B—C2B—C3B	118.4 (14)
O2—C22—O4	124.70 (16)	C1B—C2B—H2B	120.8
O2—C22—C23	123.30 (17)	C3B—C2B—H2B	120.8

O4—C22—C23	112.01 (15)	C2B—C3B—C4B	124.2 (14)
N12—C23—C24	109.15 (16)	C2B—C3B—S2B	120.5 (13)
N12—C23—C22	112.20 (14)	C4B—C3B—S2B	115.2 (13)
C24—C23—C22	109.35 (15)	C3B—C4B—C5B	117.0 (16)
N12—C23—H23	108.7	C3B—C4B—H4B	121.5
C24—C23—H23	108.7	C5B—C4B—H4B	121.5
C22—C23—H23	108.7	C6B—C5B—C4B	119.1 (15)
C23—C24—H24A	109.5	C6B—C5B—H5B	120.4
C23—C24—H24B	109.5	C4B—C5B—H5B	120.4
H24A—C24—H24B	109.5	C5B—C6B—C1B	121.3 (14)
C23—C24—H24C	109.5	C5B—C6B—C7B	124.0 (17)
H24A—C24—H24C	109.5	C1B—C6B—C7B	114.6 (13)
H24B—C24—H24C	109.5	C8B—C7B—C6B	127.4 (13)
N11—C37—C38	122.70 (16)	C8B—C7B—H7B	116.3
N11—C37—H37	118.7	C6B—C7B—H7B	116.3
C38—C37—H37	118.7	C7B—C8B—C9B	123.1 (15)
C37—C38—C39	120.27 (16)	C7B—C8B—H8B	118.4
C37—C38—H38	119.9	C9B—C8B—H8B	118.4
C39—C38—H38	119.9	N21—C25B—C26B	124 (2)
C38—C39—C40	116.57 (16)	N21—C25B—H25B	118.2
C38—C39—C42	120.09 (16)	C26B—C25B—H25B	118.2
C40—C39—C42	123.34 (16)	C27B—C26B—C25B	119.4 (18)
C41—C40—C39	119.61 (16)	C27B—C26B—H26B	120.3
C41—C40—H40	120.2	C25B—C26B—H26B	120.3
C39—C40—H40	120.2	C26B—C27B—C28B	117.0 (16)
N11—C41—C40	123.53 (17)	C26B—C27B—C30B	120.4 (18)
N11—C41—H41	118.2	C28B—C27B—C30B	122.6 (18)
C40—C41—H41	118.2	C29B—C28B—C27B	123 (2)
C43—C42—C39	124.87 (17)	C29B—C28B—H28B	118.3
C43—C42—H42	117.6	C27B—C28B—H28B	118.3
C39—C42—H42	117.6	C28B—C29B—N21	119.0 (19)
C42—C43—C46	125.81 (17)	C28B—C29B—H29B	120.5
C42—C43—H43	117.1	N21—C29B—H29B	120.5
C46—C43—H43	117.1	C31B—C30B—C27B	129.1 (17)
N20—C44—C45	123.02 (18)	C31B—C30B—H30B	115.5
N20—C44—H44	118.5	C27B—C30B—H30B	115.5
C45—C44—H44	118.5	C30B—C31B—C34B	128.3 (16)
C44—C45—C46	119.30 (18)	C30B—C31B—H31B	115.9
C44—C45—H45	120.3	C34B—C31B—H31B	115.9
C46—C45—H45	120.3	N17—C32B—C33B	124 (2)
C47—C46—C45	117.36 (17)	N17—C32B—H32B	117.9
C47—C46—C43	123.88 (17)	C33B—C32B—H32B	117.9
C45—C46—C43	118.75 (17)	C34B—C33B—C32B	118.8 (17)
C48—C47—C46	119.46 (17)	C34B—C33B—H33B	120.6
C48—C47—H47	120.3	C32B—C33B—H33B	120.6
C46—C47—H47	120.3	C33B—C34B—C35B	119.3 (14)
N20—C48—C47	122.76 (18)	C33B—C34B—C31B	120.6 (16)
N20—C48—H48	118.6	C35B—C34B—C31B	120.0 (16)
C47—C48—H48	118.6	C36B—C35B—C34B	122.2 (16)
C2A—C1A—C6A	120.2 (2)	C36B—C35B—H35B	118.9
C2A—C1A—H1A	119.9	C34B—C35B—H35B	118.9
C6A—C1A—H1A	119.9	C35B—C36B—N17	118.2 (16)
C1A—C2A—C3A	120.4 (3)	C35B—C36B—H36B	120.9
C1A—C2A—H2A	119.8	N17—C36B—H36B	120.9
C3A—C2A—H2A	119.8	O14B—C9B—O9B	128 (2)
C4A—C3A—C2A	119.8 (3)	O14B—C9B—C8B	124 (2)

C4A—C3A—S2A	120.6 (3)	O9B—C9B—C8B	107 (2)
C2A—C3A—S2A	119.5 (3)	C9B—O9B—H9	93 (2)
C3A—C4A—C5A	119.8 (4)	O10B—S2B—O18B	127.2 (19)
C3A—C4A—H4A	120.1	O10B—S2B—N13	109.5 (18)
C5A—C4A—H4A	120.1	O18B—S2B—N13	96.9 (11)
C4A—C5A—C6A	121.7 (4)	O10B—S2B—C3B	116 (2)
C4A—C5A—H5A	119.2	O18B—S2B—C3B	98.5 (12)
C6A—C5A—H5A	119.2	N13—S2B—C3B	105.2 (10)
C5A—C6A—C1A	118.1 (2)		
O1—S1—N12—C23	171.04 (13)	C29A—N21—C25A—C26A	0.4 (7)
O8—S1—N12—C23	40.36 (16)	C25B—N21—C25A—C26A	11 (10)
C15—S1—N12—C23	-74.03 (15)	C29B—N21—C25A—C26A	-3.3 (18)
O18A—S2A—N13—C11A	-176.1 (2)	N21—C25A—C26A—C27A	1.4 (7)
O10A—S2A—N13—C11A	-46.8 (4)	C25A—C26A—C27A—C28A	-1.4 (5)
C3A—S2A—N13—C11A	65.94 (19)	C25A—C26A—C27A—C30A	177.2 (3)
O18A—S2A—N13—S2B	-148 (29)	C26A—C27A—C28A—C29A	-0.3 (5)
O10A—S2A—N13—S2B	-19 (29)	C30A—C27A—C28A—C29A	-178.8 (3)
C3A—S2A—N13—S2B	94 (29)	C25A—N21—C29A—C28A	-2.2 (6)
C18—C13—C14—C15	-1.7 (3)	C25B—N21—C29A—C28A	-4 (2)
C13—C14—C15—C16	0.5 (3)	C29B—N21—C29A—C28A	164 (7)
C13—C14—C15—S1	179.73 (14)	C27A—C28A—C29A—N21	2.2 (6)
O1—S1—C15—C14	12.50 (17)	C26A—C27A—C30A—C31A	173.5 (2)
O8—S1—C15—C14	142.45 (15)	C28A—C27A—C30A—C31A	-8.0 (4)
N12—S1—C15—C14	-101.97 (16)	C27A—C30A—C31A—C34A	178.4 (2)
O1—S1—C15—C16	-168.31 (14)	C32B—N17—C32A—C33A	-8 (7)
O8—S1—C15—C16	-38.35 (16)	C36A—N17—C32A—C33A	1.3 (5)
N12—S1—C15—C16	77.23 (16)	C36B—N17—C32A—C33A	2.5 (16)
C14—C15—C16—C17	1.3 (3)	N17—C32A—C33A—C34A	-0.3 (5)
S1—C15—C16—C17	-177.91 (14)	C32A—C33A—C34A—C35A	-0.6 (4)
C15—C16—C17—C18	-2.1 (3)	C32A—C33A—C34A—C31A	178.4 (3)
C14—C13—C18—C17	0.9 (3)	C30A—C31A—C34A—C35A	-16.4 (4)
C14—C13—C18—C19	-178.19 (17)	C30A—C31A—C34A—C33A	164.6 (2)
C16—C17—C18—C13	0.9 (3)	C33A—C34A—C35A—C36A	0.5 (4)
C16—C17—C18—C19	-179.98 (17)	C31A—C34A—C35A—C36A	-178.5 (3)
C13—C18—C19—C20	179.93 (18)	C32B—N17—C36A—C35A	0.9 (19)
C17—C18—C19—C20	0.9 (3)	C32A—N17—C36A—C35A	-1.5 (6)
C18—C19—C20—C21	177.06 (16)	C36B—N17—C36A—C35A	-177 (6)
C19—C20—C21—O5	21.1 (3)	C34A—C35A—C36A—N17	0.5 (6)
C19—C20—C21—O7	-158.35 (17)	C6B—C1B—C2B—C3B	2 (3)
S1—N12—C23—C24	-156.39 (14)	C1B—C2B—C3B—C4B	0 (3)
S1—N12—C23—C22	82.24 (19)	C1B—C2B—C3B—S2B	178.5 (14)
O2—C22—C23—N12	36.7 (2)	C2B—C3B—C4B—C5B	-1 (4)
O4—C22—C23—N12	-143.01 (16)	S2B—C3B—C4B—C5B	-180 (2)
O2—C22—C23—C24	-84.5 (2)	C3B—C4B—C5B—C6B	0 (4)
O4—C22—C23—C24	95.7 (2)	C4B—C5B—C6B—C1B	1 (3)
C41—N11—C37—C38	1.1 (3)	C4B—C5B—C6B—C7B	-176 (2)
N11—C37—C38—C39	0.2 (3)	C2B—C1B—C6B—C5B	-3 (3)
C37—C38—C39—C40	-1.1 (2)	C2B—C1B—C6B—C7B	175.2 (14)
C37—C38—C39—C42	178.70 (16)	C5B—C6B—C7B—C8B	1 (2)
C38—C39—C40—C41	0.8 (3)	C1B—C6B—C7B—C8B	-176.7 (14)
C42—C39—C40—C41	-179.06 (17)	C6B—C7B—C8B—C9B	179.2 (16)
C37—N11—C41—C40	-1.5 (3)	C29A—N21—C25B—C26B	3 (4)
C39—C40—C41—N11	0.6 (3)	C25A—N21—C25B—C26B	-167 (14)
C38—C39—C42—C43	175.31 (17)	C29B—N21—C25B—C26B	0 (5)
C40—C39—C42—C43	-4.9 (3)	N21—C25B—C26B—C27B	-1 (5)

C39—C42—C43—C46	-178.09 (17)	C25B—C26B—C27B—C28B	2 (4)
C48—N20—C44—C45	0.7 (3)	C25B—C26B—C27B—C30B	179 (3)
N20—C44—C45—C46	-1.1 (3)	C26B—C27B—C28B—C29B	-2 (4)
C44—C45—C46—C47	0.5 (3)	C30B—C27B—C28B—C29B	-180 (2)
C44—C45—C46—C43	-178.99 (17)	C27B—C28B—C29B—N21	2 (4)
C42—C43—C46—C47	-14.3 (3)	C29A—N21—C29B—C28B	-13 (5)
C42—C43—C46—C45	165.13 (18)	C25A—N21—C29B—C28B	3 (4)
C45—C46—C47—C48	0.3 (3)	C25B—N21—C29B—C28B	0 (4)
C43—C46—C47—C48	179.81 (17)	C26B—C27B—C30B—C31B	-9 (3)
C44—N20—C48—C47	0.2 (3)	C28B—C27B—C30B—C31B	168 (2)
C46—C47—C48—N20	-0.7 (3)	C27B—C30B—C31B—C34B	-179.0 (15)
C6A—C1A—C2A—C3A	1.0 (4)	C36A—N17—C32B—C33B	-7 (4)
C1A—C2A—C3A—C4A	0.7 (5)	C32A—N17—C32B—C33B	165 (10)
C1A—C2A—C3A—S2A	-178.0 (2)	C36B—N17—C32B—C33B	-6 (4)
O18A—S2A—C3A—C4A	136.9 (4)	N17—C32B—C33B—C34B	4 (5)
O10A—S2A—C3A—C4A	8.4 (5)	C32B—C33B—C34B—C35B	0 (3)
N13—S2A—C3A—C4A	-106.3 (4)	C32B—C33B—C34B—C31B	177 (2)
O18A—S2A—C3A—C2A	-44.4 (3)	C30B—C31B—C34B—C33B	-15 (2)
O10A—S2A—C3A—C2A	-172.9 (4)	C30B—C31B—C34B—C35B	163.3 (17)
N13—S2A—C3A—C2A	72.4 (3)	C33B—C34B—C35B—C36B	0 (3)
C2A—C3A—C4A—C5A	-1.6 (7)	C31B—C34B—C35B—C36B	-178 (2)
S2A—C3A—C4A—C5A	177.1 (3)	C34B—C35B—C36B—N17	-2 (4)
C3A—C4A—C5A—C6A	0.8 (6)	C32B—N17—C36B—C35B	5 (3)
C4A—C5A—C6A—C1A	0.8 (5)	C36A—N17—C36B—C35B	7 (4)
C4A—C5A—C6A—C7A	-178.2 (3)	C32A—N17—C36B—C35B	2 (3)
C2A—C1A—C6A—C5A	-1.7 (4)	C7B—C8B—C9B—O14B	-10 (3)
C2A—C1A—C6A—C7A	177.3 (2)	C7B—C8B—C9B—O9B	179.1 (18)
C5A—C6A—C7A—C8A	-174.1 (2)	C11A—N13—S2B—O10B	-50.1 (19)
C1A—C6A—C7A—C8A	6.9 (4)	S2A—N13—S2B—O10B	158 (30)
C6A—C7A—C8A—C9A	-177.1 (2)	C11A—N13—S2B—O18B	176.4 (8)
C7A—C8A—C9A—O14A	174.8 (3)	S2A—N13—S2B—O18B	24 (29)
C7A—C8A—C9A—O9A	-5.0 (4)	C11A—N13—S2B—C3B	75.6 (10)
S2A—N13—C11A—C10A	158.15 (14)	S2A—N13—S2B—C3B	-77 (29)
S2B—N13—C11A—C10A	157.5 (6)	C2B—C3B—S2B—O10B	-167 (2)
S2A—N13—C11A—C12A	-81.44 (18)	C4B—C3B—S2B—O10B	12 (3)
S2B—N13—C11A—C12A	-82.1 (6)	C2B—C3B—S2B—O18B	-27.5 (18)
N13—C11A—C12A—O6	-30.2 (3)	C4B—C3B—S2B—O18B	151 (2)
C10A—C11A—C12A—O6	90.3 (2)	C2B—C3B—S2B—N13	72.1 (16)
N13—C11A—C12A—O3	151.02 (16)	C4B—C3B—S2B—N13	-109 (2)
C10A—C11A—C12A—O3	-88.5 (2)		

Table 3e. Hydrogen-bond geometry (Å, °) for cocrystal of **23** and *trans*-1,2-bis(4-pyridyl)ethylene (**26**).

<i>D</i> —H \cdots <i>A</i>	<i>D</i> —H	H \cdots <i>A</i>	<i>D</i> \cdots <i>A</i>	<i>D</i> —H \cdots <i>A</i>
O4—H1 \cdots N21	0.89 (2)	1.73 (2)	2.6018 (19)	167 (2)
O9A—H9 \cdots N17	0.88 (2)	1.69 (2)	2.571 (3)	174 (2)
O3—H6 \cdots N11	0.87 (2)	1.79 (2)	2.6427 (19)	167 (2)
O7—H5 \cdots N20	0.89 (2)	1.70 (2)	2.5800 (19)	171 (2)
N12—H12 \cdots O14A ⁱ	0.88	1.93	2.781 (3)	163
N12—H12 \cdots O14B ⁱ	0.88	2.24	3.041 (19)	151

Symmetry code: (i) *x*+1, *y*+1, *z*.

Table 4a. Crystal data and structure refinement for (E)-but-2-enediamide (**28**).

Crystal data

$C_6H_{10}N_2O_2$	$Z = 2$
$M_r = 142.16$	$F(000) = 152$
Monoclinic, $p2_1/c$	$D_x = 1.319 \text{ Mg m}^{-3}$
Hall symbol: $-P 2_1/c$	Cu $K\alpha$ radiation, $\lambda = 1.54178 \text{ \AA}$
$a = 7.7800 (6) \text{ \AA}$	$\mu = 0.84 \text{ mm}^{-1}$
$b = 4.8417 (3) \text{ \AA}$	$T = 173 \text{ K}$
$c = 9.5199 (7) \text{ \AA}$	Transparent rod, colorless
$\beta = 93.527 (4)^\circ$	$1.16 \times 0.27 \times 0.12 \text{ mm}$
$V = 357.92 (4) \text{ \AA}^3$	

Data collection

Brucker APEXII CCD	640 independent reflections
diffractometer	
Radiation source: fine-focus sealed tube	602 reflections with $I > 2\sigma(I)$
graphite	$R_{\text{int}} = 0.037$
phi and ω scans	$\theta_{\text{max}} = 67.2^\circ$, $\theta_{\text{min}} = 5.7^\circ$
Absorption correction: multi-scan	$h = -9 \rightarrow 8$
<i>SADABS</i> (Brucker, 2010)	
$T_{\text{min}} = 0.218$, $T_{\text{max}} = 0.851$	$k = -5 \rightarrow 5$
4624 measured reflections	$l = -11 \rightarrow 11$

Refinement

Refinement on F^2	Primary atom site location: structure-invariant direct methods
Least-squares matrix: full	Secondary atom site location: difference Fourier map
$R[F^2 > 2\sigma(F^2)] = 0.034$	Hydrogen site location: inferred from neighbouring sites
$wR(F^2) = 0.095$	H atoms treated by a mixture of independent and constrained refinement
$S = 1.03$	$w = 1/[\sigma^2(F_o^2) + (0.0522P)^2 + 0.1686P]$
640 reflections	where $P = (F_o^2 + 2F_c^2)/3$
50 parameters	$(\Delta/\sigma)_{\text{max}} = 0.009$
0 restraints	$\Delta_{\text{max}} = 0.17 \text{ e \AA}^{-3}$
	$\Delta_{\text{min}} = -0.18 \text{ e \AA}^{-3}$

Table 4b. Fractional atomic coordinates and isotropic or equivalent isotropic displacement parameters (\AA^2) for (E)-but-2-enediamide (**28**).

	<i>x</i>	<i>y</i>	<i>z</i>	$U_{\text{iso}}^*/U_{\text{eq}}$
O1	0.31665 (12)	0.20347 (18)	0.82844 (9)	0.0242 (3)
N1	0.25861 (14)	0.6400 (2)	0.75519 (11)	0.0201 (3)
H1	0.282 (2)	0.814 (4)	0.7699 (18)	0.024*

C1	0.33929 (15)	0.4555 (3)	0.83985 (12)	0.0178 (3)
C2	0.45882 (15)	0.5771 (3)	0.95147 (12)	0.0186 (3)
H2	0.4764	0.7713	0.9530	0.022*
C3	0.14035 (16)	0.5574 (3)	0.63823 (13)	0.0230 (4)
H3B	0.2024	0.4473	0.5713	0.034*
H3C	0.0923	0.7223	0.5909	0.034*
H3A	0.0468	0.4469	0.6738	0.034*

Table 4c. Atomic displacement parameters (\AA^2) for (E)-but-2-enediamide (**28**).

	U^{11}	U^{22}	U^{33}	U^{12}	U^{13}	U^{23}
O1	0.0311 (5)	0.0153 (5)	0.0256 (5)	-0.0028 (4)	-0.0036 (4)	-0.0020 (4)
N1	0.0233 (6)	0.0153 (6)	0.0210 (6)	-0.0014 (4)	-0.0028 (4)	-0.0014 (4)
C1	0.0194 (6)	0.0159 (7)	0.0184 (6)	-0.0006 (5)	0.0032 (5)	-0.0009 (5)
C2	0.0214 (6)	0.0143 (7)	0.0202 (6)	-0.0013 (5)	0.0018 (5)	-0.0020 (5)
C3	0.0235 (7)	0.0242 (8)	0.0206 (7)	-0.0014 (5)	-0.0040 (5)	-0.0014 (5)

Table 4d. Geometric parameters (\AA , $^\circ$) for (E)-but-2-enediamide (**28**).

O1—C1	1.2366 (16)	C2—C2 ⁱ	1.322 (2)
N1—C1	1.3340 (16)	C2—H2	0.9500
N1—C3	1.4561 (16)	C3—H3B	0.9800
N1—H1	0.874 (17)	C3—H3C	0.9800
C1—C2	1.4896 (17)	C3—H3A	0.9800
C1—N1—C3	121.99 (11)	C1—C2—H2	119.0
C1—N1—H1	117.5 (11)	N1—C3—H3B	109.5
C3—N1—H1	120.4 (11)	N1—C3—H3C	109.5
O1—C1—N1	123.26 (12)	H3B—C3—H3C	109.5
O1—C1—C2	122.14 (11)	N1—C3—H3A	109.5
N1—C1—C2	114.59 (11)	H3B—C3—H3A	109.5
C2 ⁱ —C2—C1	121.98 (14)	H3C—C3—H3A	109.5
C2 ⁱ —C2—H2	119.0		
C3—N1—C1—O1	-2.13 (19)	O1—C1—C2—C2 ⁱ	-3.2 (2)
C3—N1—C1—C2	178.48 (10)	N1—C1—C2—C2 ⁱ	176.19 (14)

Symmetry code: (i) $-x+1, -y+1, -z+2$.

Table 4e. Hydrogen-bond geometry (\AA , $^\circ$) for (E)-but-2-enediamide (**28**).

$D-H\cdots A$	$D-H$	$H\cdots A$	$D\cdots A$	$D-H\cdots A$
N1—H1 \cdots O1 ⁱⁱ	0.874 (17)	1.978 (18)	2.8452 (15)	171.5 (15)

Symmetry code: (ii) $x, y+1, z$.

Table 5a. Crystal data and structure refinement for 1-oxoisochromene-3-carboxylic acid (37-I).

Crystal data	
$C_{10}H_6O_4$	$F(000) = 784$
$M_r = 190.15$	$D_x = 1.571 \text{ Mg m}^{-3}$
Monoclinic, $P2_1/n$	Cu $K\alpha$ radiation, $\lambda = 1.54178 \text{ \AA}$
Hall symbol: -P 2yn	Cell parameters from 7427 reflections
$a = 8.2962 (4) \text{ \AA}$	$\theta = 3.9\text{--}66.1^\circ$
$b = 12.6332 (7) \text{ \AA}$	$\mu = 1.06 \text{ mm}^{-1}$
$c = 15.5101 (8) \text{ \AA}$	$T = 100 \text{ K}$
$\beta = 98.578 (3)^\circ$	Transparent plate, colorless
$V = 1607.39 (14) \text{ \AA}^3$	$0.52 \times 0.31 \times 0.06 \text{ mm}$
$Z = 8$	
Data collection	
Bruker APEXII CCD diffractometer	2864 independent reflections
Radiation source: fine-focus sealed tube	1805 reflections with $I > 2\sigma(I)$
Graphite	$R_{\text{int}} = 0.082$
Detector resolution: $8.33 \text{ pixels mm}^{-1}$	$\theta_{\text{max}} = 67.7^\circ$, $\theta_{\text{min}} = 4.5^\circ$
phi and ω scans	$h = -9 \rightarrow 9$
Absorption correction: multi-scan	$k = -15 \rightarrow 14$
SADABS (Bruker, 2009)	$l = -18 \rightarrow 18$
$T_{\text{min}} = 0.567$, $T_{\text{max}} = 0.659$	
20860 measured reflections	
Refinement	
Refinement on F^2	Primary atom site location: structure-invariant direct methods
Least-squares matrix: full	Secondary atom site location: difference Fourier map
$R[F^2 > 2\sigma(F^2)] = 0.045$	Hydrogen site location: inferred from neighbouring sites
$wR(F^2) = 0.122$	H atoms treated by a mixture of independent and constrained refinement
$S = 1.02$	$w = 1/[\sigma^2(F_o^2) + (0.0611P)^2 + 0.137P]$
2864 reflections	where $P = (F_o^2 + 2F_c^2)/3$
259 parameters	$(\Delta/\sigma)_{\text{max}} < 0.001$
0 restraints	$\Delta_{\text{max}} = 0.27 \text{ e \AA}^{-3}$
	$\Delta_{\text{min}} = -0.20 \text{ e \AA}^{-3}$

Table 5b. Fractional atomic coordinates and isotropic or equivalent isotropic displacement parameters (\AA^2) for 1-oxoisochromene-3-carboxylic acid (37-I).

	<i>x</i>	<i>y</i>	<i>z</i>	$U_{\text{iso}}^*/U_{\text{eq}}$
O1A	0.2649 (2)	0.89574 (14)	0.33168 (11)	0.0289 (5)

O2A	0.4533 (2)	0.88534 (13)	0.24213 (11)	0.0286 (4)
O3A	0.23107 (18)	0.87361 (12)	0.10357 (10)	0.0223 (4)
O4A	0.1882 (2)	0.85341 (12)	-0.03907 (11)	0.0258 (4)
C1A	0.3116 (3)	0.88946 (17)	0.25430 (16)	0.0231 (6)
C2A	0.1752 (3)	0.88802 (17)	0.18149 (15)	0.0213 (5)
C3A	0.0168 (3)	0.89755 (17)	0.18767 (16)	0.0232 (5)
H3A	-0.0168	0.9078	0.2430	0.028*
C4A	-0.1028 (3)	0.89230 (17)	0.11026 (16)	0.0224 (6)
C5A	-0.0482 (3)	0.87578 (16)	0.03053 (16)	0.0219 (5)
C6A	0.1270 (3)	0.86628 (17)	0.02566 (16)	0.0214 (5)
C7A	-0.1592 (3)	0.86683 (18)	-0.04646 (16)	0.0256 (6)
H7A	-0.1218	0.8554	-0.1007	0.031*
C8A	-0.3239 (3)	0.87490 (19)	-0.04224 (18)	0.0304 (6)
H8A	-0.4003	0.8686	-0.0941	0.036*
C9A	-0.3792 (3)	0.89203 (18)	0.03663 (17)	0.0293 (6)
H9A	-0.4928	0.8976	0.0384	0.035*
C10A	-0.2705 (3)	0.90107 (18)	0.11228 (17)	0.0261 (6)
H10A	-0.3092	0.9133	0.1661	0.031*
H1A	0.341 (3)	0.894 (2)	0.3681 (18)	0.031*
O1B	0.7189 (2)	0.87083 (13)	0.36184 (11)	0.0258 (4)
O2B	0.5292 (2)	0.88242 (12)	0.45039 (10)	0.0265 (4)
O3B	0.74806 (19)	0.86837 (13)	0.59047 (10)	0.0233 (4)
O4B	0.7874 (2)	0.85501 (13)	0.73340 (11)	0.0283 (4)
C1B	0.6709 (3)	0.87531 (17)	0.43822 (16)	0.0214 (5)
C2B	0.8069 (3)	0.87115 (17)	0.51219 (15)	0.0210 (5)
C3B	0.9658 (3)	0.87140 (17)	0.50663 (15)	0.0229 (5)
H3B	1.0010	0.8730	0.4511	0.027*
C4B	1.0837 (3)	0.86927 (17)	0.58454 (16)	0.0222 (6)
C5B	1.0268 (3)	0.86433 (17)	0.66465 (15)	0.0218 (6)
C6B	0.8504 (3)	0.86157 (18)	0.66853 (15)	0.0219 (5)
C7B	1.1356 (3)	0.86020 (18)	0.74252 (16)	0.0262 (6)
H7B	1.0962	0.8563	0.7969	0.031*
C8B	1.3010 (3)	0.86187 (19)	0.73952 (18)	0.0294 (6)
H8B	1.3759	0.8592	0.7922	0.035*
C9B	1.3588 (3)	0.86749 (18)	0.65994 (17)	0.0284 (6)
H9B	1.4729	0.8690	0.6586	0.034*
C10B	1.2518 (3)	0.87083 (18)	0.58334 (17)	0.0257 (6)
H10B	1.2923	0.8742	0.5293	0.031*
H1B	0.631 (3)	0.8716 (19)	0.3232 (18)	0.031*

Table 5c. Bond lengths [\AA°] and angles [$^\circ$] for 1-oxoisochromene-3-carboxylic acid (**37-I**)

O1A—C1A	1.317 (3)	O1B—C1B	1.306 (3)
O1A—H1A	0.78 (3)	O1B—H1B	0.87 (3)
O2A—C1A	1.219 (3)	O2B—C1B	1.221 (3)
O3A—C2A	1.369 (3)	O3B—C6B	1.374 (3)
O3A—C6A	1.379 (3)	O3B—C2B	1.375 (3)
O4A—C6A	1.201 (3)	O4B—C6B	1.204 (3)
C1A—C2A	1.474 (3)	C1B—C2B	1.486 (3)
C2A—C3A	1.338 (3)	C2B—C3B	1.334 (3)
C3A—C4A	1.440 (3)	C3B—C4B	1.437 (3)
C3A—H3A	0.9500	C3B—H3B	0.9500
C4A—C5A	1.394 (3)	C4B—C5B	1.395 (3)

C4A—C10A	1.401 (3)	C4B—C10B	1.398 (3)
C5A—C7A	1.399 (3)	C5B—C7B	1.397 (3)
C5A—C6A	1.472 (3)	C5B—C6B	1.474 (3)
C7A—C8A	1.382 (3)	C7B—C8B	1.380 (3)
C7A—H7A	0.9500	C7B—H7B	0.9500
C8A—C9A	1.386 (4)	C8B—C9B	1.391 (4)
C8A—H8A	0.9500	C8B—H8B	0.9500
C9A—C10A	1.373 (3)	C9B—C10B	1.373 (3)
C9A—H9A	0.9500	C9B—H9B	0.9500
C10A—H10A	0.9500	C10B—H10B	0.9500
C1A—O1A—H1A	110 (2)	C1B—O1B—H1B	106.6 (18)
C2A—O3A—C6A	122.16 (19)	C6B—O3B—C2B	121.70 (19)
O2A—C1A—O1A	124.4 (2)	O2B—C1B—O1B	125.0 (2)
O2A—C1A—C2A	121.9 (2)	O2B—C1B—C2B	121.4 (2)
O1A—C1A—C2A	113.7 (2)	O1B—C1B—C2B	113.6 (2)
C3A—C2A—O3A	122.7 (2)	C3B—C2B—O3B	122.8 (2)
C3A—C2A—C1A	126.4 (2)	C3B—C2B—C1B	126.5 (2)
O3A—C2A—C1A	110.8 (2)	O3B—C2B—C1B	110.7 (2)
C2A—C3A—C4A	119.9 (2)	C2B—C3B—C4B	120.1 (2)
C2A—C3A—H3A	120.1	C2B—C3B—H3B	120.0
C4A—C3A—H3A	120.1	C4B—C3B—H3B	120.0
C5A—C4A—C10A	119.1 (2)	C5B—C4B—C10B	118.9 (2)
C5A—C4A—C3A	118.2 (2)	C5B—C4B—C3B	118.1 (2)
C10A—C4A—C3A	122.7 (2)	C10B—C4B—C3B	123.0 (2)
C4A—C5A—C7A	120.7 (2)	C4B—C5B—C7B	120.7 (2)
C4A—C5A—C6A	120.8 (2)	C4B—C5B—C6B	120.5 (2)
C7A—C5A—C6A	118.6 (2)	C7B—C5B—C6B	118.8 (2)
O4A—C6A—O3A	117.0 (2)	O4B—C6B—O3B	116.9 (2)
O4A—C6A—C5A	126.7 (2)	O4B—C6B—C5B	126.4 (2)
O3A—C6A—C5A	116.3 (2)	O3B—C6B—C5B	116.7 (2)
C8A—C7A—C5A	118.9 (2)	C8B—C7B—C5B	119.2 (2)
C8A—C7A—H7A	120.6	C8B—C7B—H7B	120.4
C5A—C7A—H7A	120.6	C5B—C7B—H7B	120.4
C7A—C8A—C9A	120.9 (3)	C7B—C8B—C9B	120.5 (2)
C7A—C8A—H8A	119.6	C7B—C8B—H8B	119.8
C9A—C8A—H8A	119.6	C9B—C8B—H8B	119.8
C10A—C9A—C8A	120.4 (2)	C10B—C9B—C8B	120.3 (2)
C10A—C9A—H9A	119.8	C10B—C9B—H9B	119.8
C8A—C9A—H9A	119.8	C8B—C9B—H9B	119.8
C9A—C10A—C4A	120.1 (2)	C9B—C10B—C4B	120.4 (2)
C9A—C10A—H10A	119.9	C9B—C10B—H10B	119.8
C4A—C10A—H10A	119.9	C4B—C10B—H10B	119.8
C6A—O3A—C2A—C3A	-1.0 (3)	C6B—O3B—C2B—C3B	-2.5 (3)
C6A—O3A—C2A—C1A	178.08 (18)	C6B—O3B—C2B—C1B	178.31 (18)
O2A—C1A—C2A—C3A	-176.4 (2)	O2B—C1B—C2B—C3B	-174.6 (2)
O1A—C1A—C2A—C3A	3.5 (3)	O1B—C1B—C2B—C3B	5.3 (3)
O2A—C1A—C2A—O3A	4.6 (3)	O2B—C1B—C2B—O3B	4.5 (3)
O1A—C1A—C2A—O3A	-175.55 (19)	O1B—C1B—C2B—O3B	-175.60 (19)
O3A—C2A—C3A—C4A	0.3 (3)	O3B—C2B—C3B—C4B	-0.3 (3)
C1A—C2A—C3A—C4A	-178.7 (2)	C1B—C2B—C3B—C4B	178.7 (2)
C2A—C3A—C4A—C5A	0.9 (3)	C2B—C3B—C4B—C5B	1.5 (3)
C2A—C3A—C4A—C10A	179.6 (2)	C2B—C3B—C4B—C10B	-179.1 (2)
C10A—C4A—C5A—C7A	-0.7 (3)	C10B—C4B—C5B—C7B	-0.5 (3)
C3A—C4A—C5A—C7A	178.1 (2)	C3B—C4B—C5B—C7B	178.9 (2)

C10A—C4A—C5A—C6A	179.9 (2)	C10B—C4B—C5B—C6B	-179.44 (19)
C3A—C4A—C5A—C6A	-1.3 (3)	C3B—C4B—C5B—C6B	-0.1 (3)
C2A—O3A—C6A—O4A	-179.8 (2)	C2B—O3B—C6B—O4B	-176.9 (2)
C2A—O3A—C6A—C5A	0.5 (3)	C2B—O3B—C6B—C5B	3.8 (3)
C4A—C5A—C6A—O4A	-179.0 (2)	C4B—C5B—C6B—O4B	178.3 (2)
C7A—C5A—C6A—O4A	1.7 (3)	C7B—C5B—C6B—O4B	-0.7 (4)
C4A—C5A—C6A—O3A	0.6 (3)	C4B—C5B—C6B—O3B	-2.5 (3)
C7A—C5A—C6A—O3A	-178.77 (19)	C7B—C5B—C6B—O3B	178.5 (2)
C4A—C5A—C7A—C8A	0.2 (3)	C4B—C5B—C7B—C8B	0.5 (3)
C6A—C5A—C7A—C8A	179.5 (2)	C6B—C5B—C7B—C8B	179.5 (2)
C5A—C7A—C8A—C9A	0.3 (3)	C5B—C7B—C8B—C9B	-0.1 (4)
C7A—C8A—C9A—C10A	-0.2 (4)	C7B—C8B—C9B—C10B	-0.4 (4)
C8A—C9A—C10A—C4A	-0.4 (3)	C8B—C9B—C10B—C4B	0.4 (3)
C5A—C4A—C10A—C9A	0.9 (3)	C5B—C4B—C10B—C9B	0.0 (3)
C3A—C4A—C10A—C9A	-177.9 (2)	C3B—C4B—C10B—C9B	-179.3 (2)

Table 5d. Atomic displacement parameters (\AA^2) for 1-oxoisochromene-3-carboxylic acid (37-I).

	U^{11}	U^{22}	U^{33}	U^{12}	U^{13}	U^{23}
O1A	0.0244 (11)	0.0396 (11)	0.0215 (10)	0.0023 (8)	-0.0001 (8)	-0.0025 (8)
O2A	0.0227 (10)	0.0387 (10)	0.0231 (10)	0.0003 (7)	-0.0007 (8)	0.0012 (8)
O3A	0.0194 (9)	0.0257 (9)	0.0213 (9)	0.0007 (7)	0.0010 (7)	-0.0005 (7)
O4A	0.0266 (10)	0.0271 (9)	0.0239 (10)	0.0012 (7)	0.0041 (8)	-0.0006 (7)
C1A	0.0230 (14)	0.0185 (12)	0.0271 (15)	0.0002 (10)	0.0014 (11)	0.0000 (10)
C2A	0.0240 (14)	0.0188 (12)	0.0213 (14)	-0.0005 (9)	0.0042 (11)	0.0008 (9)
C3A	0.0273 (14)	0.0204 (12)	0.0221 (13)	0.0005 (10)	0.0047 (11)	-0.0006 (10)
C4A	0.0232 (14)	0.0167 (12)	0.0267 (14)	0.0004 (10)	0.0017 (11)	0.0020 (10)
C5A	0.0193 (13)	0.0171 (11)	0.0280 (14)	-0.0004 (9)	-0.0001 (10)	0.0020 (10)
C6A	0.0271 (14)	0.0124 (11)	0.0237 (14)	-0.0009 (9)	0.0009 (11)	0.0011 (10)
C7A	0.0290 (15)	0.0218 (12)	0.0251 (14)	0.0002 (10)	0.0011 (11)	0.0011 (10)
C8A	0.0255 (15)	0.0258 (14)	0.0375 (17)	-0.0006 (11)	-0.0030 (12)	0.0048 (12)
C9A	0.0213 (15)	0.0232 (13)	0.0416 (17)	0.0015 (10)	-0.0008 (12)	0.0048 (11)
C10A	0.0268 (15)	0.0209 (12)	0.0316 (15)	0.0017 (10)	0.0074 (12)	0.0023 (10)
O1B	0.0250 (10)	0.0316 (9)	0.0191 (9)	-0.0008 (7)	-0.0022 (7)	0.0005 (7)
O2B	0.0237 (10)	0.0315 (10)	0.0231 (9)	-0.0006 (7)	-0.0006 (7)	0.0004 (7)
O3B	0.0209 (9)	0.0276 (9)	0.0208 (9)	0.0007 (7)	0.0014 (7)	0.0010 (7)
O4B	0.0239 (10)	0.0381 (10)	0.0222 (10)	0.0001 (7)	0.0009 (8)	0.0018 (8)
C1B	0.0238 (14)	0.0163 (12)	0.0240 (13)	-0.0016 (9)	0.0036 (10)	-0.0004 (10)
C2B	0.0270 (14)	0.0166 (11)	0.0192 (13)	0.0001 (10)	0.0025 (10)	0.0002 (10)
C3B	0.0247 (14)	0.0221 (12)	0.0224 (13)	0.0007 (10)	0.0055 (11)	-0.0019 (10)
C4B	0.0229 (14)	0.0136 (11)	0.0295 (14)	-0.0004 (10)	0.0023 (11)	-0.0023 (10)
C5B	0.0204 (13)	0.0171 (11)	0.0267 (15)	0.0004 (10)	-0.0002 (11)	-0.0003 (10)
C6B	0.0257 (14)	0.0216 (12)	0.0178 (13)	-0.0017 (10)	0.0008 (11)	0.0014 (10)
C7B	0.0280 (15)	0.0251 (13)	0.0249 (14)	-0.0007 (10)	0.0020 (11)	0.0001 (10)
C8B	0.0264 (15)	0.0261 (13)	0.0319 (16)	0.0020 (10)	-0.0079 (12)	-0.0011 (11)
C9B	0.0187 (14)	0.0235 (13)	0.0413 (17)	0.0016 (10)	-0.0012 (12)	-0.0020 (11)
C10B	0.0264 (15)	0.0199 (12)	0.0316 (15)	-0.0013 (10)	0.0066 (12)	-0.0017 (10)

Table 5e. Geometric parameters (Å, °) for 1-oxoisochromene-3-carboxylic acid (**37-I**)

O1A—C1A	1.317 (3)	O1B—C1B	1.306 (3)
O1A—H1A	0.78 (3)	O1B—H1B	0.87 (3)
O2A—C1A	1.219 (3)	O2B—C1B	1.221 (3)
O3A—C2A	1.369 (3)	O3B—C6B	1.374 (3)
O3A—C6A	1.379 (3)	O3B—C2B	1.375 (3)
O4A—C6A	1.201 (3)	O4B—C6B	1.204 (3)
C1A—C2A	1.474 (3)	C1B—C2B	1.486 (3)
C2A—C3A	1.338 (3)	C2B—C3B	1.334 (3)
C3A—C4A	1.440 (3)	C3B—C4B	1.437 (3)
C3A—H3A	0.9500	C3B—H3B	0.9500
C4A—C5A	1.394 (3)	C4B—C5B	1.395 (3)
C4A—C10A	1.401 (3)	C4B—C10B	1.398 (3)
C5A—C7A	1.399 (3)	C5B—C7B	1.397 (3)
C5A—C6A	1.472 (3)	C5B—C6B	1.474 (3)
C7A—C8A	1.382 (3)	C7B—C8B	1.380 (3)
C7A—H7A	0.9500	C7B—H7B	0.9500
C8A—C9A	1.386 (4)	C8B—C9B	1.391 (4)
C8A—H8A	0.9500	C8B—H8B	0.9500
C9A—C10A	1.373 (3)	C9B—C10B	1.373 (3)
C9A—H9A	0.9500	C9B—H9B	0.9500
C10A—H10A	0.9500	C10B—H10B	0.9500
C1A—O1A—H1A	110 (2)	C1B—O1B—H1B	106.6 (18)
C2A—O3A—C6A	122.16 (19)	C6B—O3B—C2B	121.70 (19)
O2A—C1A—O1A	124.4 (2)	O2B—C1B—O1B	125.0 (2)
O2A—C1A—C2A	121.9 (2)	O2B—C1B—C2B	121.4 (2)
O1A—C1A—C2A	113.7 (2)	O1B—C1B—C2B	113.6 (2)
C3A—C2A—O3A	122.7 (2)	C3B—C2B—O3B	122.8 (2)
C3A—C2A—C1A	126.4 (2)	C3B—C2B—C1B	126.5 (2)
O3A—C2A—C1A	110.8 (2)	O3B—C2B—C1B	110.7 (2)
C2A—C3A—C4A	119.9 (2)	C2B—C3B—C4B	120.1 (2)
C2A—C3A—H3A	120.1	C2B—C3B—H3B	120.0
C4A—C3A—H3A	120.1	C4B—C3B—H3B	120.0
C5A—C4A—C10A	119.1 (2)	C5B—C4B—C10B	118.9 (2)
C5A—C4A—C3A	118.2 (2)	C5B—C4B—C3B	118.1 (2)
C10A—C4A—C3A	122.7 (2)	C10B—C4B—C3B	123.0 (2)
C4A—C5A—C7A	120.7 (2)	C4B—C5B—C7B	120.7 (2)
C4A—C5A—C6A	120.8 (2)	C4B—C5B—C6B	120.5 (2)
C7A—C5A—C6A	118.6 (2)	C7B—C5B—C6B	118.8 (2)
O4A—C6A—O3A	117.0 (2)	O4B—C6B—O3B	116.9 (2)
O4A—C6A—C5A	126.7 (2)	O4B—C6B—C5B	126.4 (2)
O3A—C6A—C5A	116.3 (2)	O3B—C6B—C5B	116.7 (2)
C8A—C7A—C5A	118.9 (2)	C8B—C7B—C5B	119.2 (2)
C8A—C7A—H7A	120.6	C8B—C7B—H7B	120.4
C5A—C7A—H7A	120.6	C5B—C7B—H7B	120.4

C7A—C8A—C9A	120.9 (3)	C7B—C8B—C9B	120.5 (2)
C7A—C8A—H8A	119.6	C7B—C8B—H8B	119.8
C9A—C8A—H8A	119.6	C9B—C8B—H8B	119.8
C10A—C9A—C8A	120.4 (2)	C10B—C9B—C8B	120.3 (2)
C10A—C9A—H9A	119.8	C10B—C9B—H9B	119.8
C8A—C9A—H9A	119.8	C8B—C9B—H9B	119.8
C9A—C10A—C4A	120.1 (2)	C9B—C10B—C4B	120.4 (2)
C9A—C10A—H10A	119.9	C9B—C10B—H10B	119.8
C4A—C10A—H10A	119.9	C4B—C10B—H10B	119.8
C6A—O3A—C2A—C3A	-1.0 (3)	C6B—O3B—C2B—C3B	-2.5 (3)
C6A—O3A—C2A—C1A	178.08 (18)	C6B—O3B—C2B—C1B	178.31 (18)
O2A—C1A—C2A—C3A	-176.4 (2)	O2B—C1B—C2B—C3B	-174.6 (2)
O1A—C1A—C2A—C3A	3.5 (3)	O1B—C1B—C2B—C3B	5.3 (3)
O2A—C1A—C2A—O3A	4.6 (3)	O2B—C1B—C2B—O3B	4.5 (3)
O1A—C1A—C2A—O3A	-175.55 (19)	O1B—C1B—C2B—O3B	-175.60 (19)
O3A—C2A—C3A—C4A	0.3 (3)	O3B—C2B—C3B—C4B	-0.3 (3)
C1A—C2A—C3A—C4A	-178.7 (2)	C1B—C2B—C3B—C4B	178.7 (2)
C2A—C3A—C4A—C5A	0.9 (3)	C2B—C3B—C4B—C5B	1.5 (3)
C2A—C3A—C4A—C10A	179.6 (2)	C2B—C3B—C4B—C10B	-179.1 (2)
C10A—C4A—C5A—C7A	-0.7 (3)	C10B—C4B—C5B—C7B	-0.5 (3)
C3A—C4A—C5A—C7A	178.1 (2)	C3B—C4B—C5B—C7B	178.9 (2)
C10A—C4A—C5A—C6A	179.9 (2)	C10B—C4B—C5B—C6B	-179.44 (19)
C3A—C4A—C5A—C6A	-1.3 (3)	C3B—C4B—C5B—C6B	-0.1 (3)
C2A—O3A—C6A—O4A	-179.8 (2)	C2B—O3B—C6B—O4B	-176.9 (2)
C2A—O3A—C6A—C5A	0.5 (3)	C2B—O3B—C6B—C5B	3.8 (3)
C4A—C5A—C6A—O4A	-179.0 (2)	C4B—C5B—C6B—O4B	178.3 (2)
C7A—C5A—C6A—O4A	1.7 (3)	C7B—C5B—C6B—O4B	-0.7 (4)
C4A—C5A—C6A—O3A	0.6 (3)	C4B—C5B—C6B—O3B	-2.5 (3)
C7A—C5A—C6A—O3A	-178.77 (19)	C7B—C5B—C6B—O3B	178.5 (2)
C4A—C5A—C7A—C8A	0.2 (3)	C4B—C5B—C7B—C8B	0.5 (3)
C6A—C5A—C7A—C8A	179.5 (2)	C6B—C5B—C7B—C8B	179.5 (2)
C5A—C7A—C8A—C9A	0.3 (3)	C5B—C7B—C8B—C9B	-0.1 (4)
C7A—C8A—C9A—C10A	-0.2 (4)	C7B—C8B—C9B—C10B	-0.4 (4)
C8A—C9A—C10A—C4A	-0.4 (3)	C8B—C9B—C10B—C4B	0.4 (3)
C5A—C4A—C10A—C9A	0.9 (3)	C5B—C4B—C10B—C9B	0.0 (3)
C3A—C4A—C10A—C9A	-177.9 (2)	C3B—C4B—C10B—C9B	-179.3 (2)

Table 5f. Hydrogen-bond geometry (Å, °) for 1-oxoisochromene-3-carboxylic acid (**37-I**)

<i>D</i> —H... <i>A</i>	<i>D</i> —H	H... <i>A</i>	<i>D</i> ... <i>A</i>	<i>D</i> —H... <i>A</i>
O1B—H1B...O2A	0.87 (3)	1.80 (3)	2.668 (2)	175 (2)
O1A—H1A...O2B	0.78 (3)	1.87 (3)	2.650 (2)	176 (3)

Table 6a. Crystal data and structure refinement for 1-oxoisochromene-3-carboxylic acid (37-II)

Crystal data

$C_{10}H_6O_4 \cdot CH_4O$	$F(000) = 928$
$M_r = 222.19$	$D_x = 1.247 \text{ Mg m}^{-3}$
Orthorhombic, $Pbca$	Cu $K\alpha$ radiation, $\lambda = 1.54178 \text{ \AA}$
Hall symbol: $-P 2ac 2ab$	Cell parameters from 8073 reflections
$a = 13.2718 (4) \text{ \AA}$	$\theta = 4.2\text{--}71.2^\circ$
$b = 7.2563 (2) \text{ \AA}$	$\mu = 0.84 \text{ mm}^{-1}$
$c = 21.0377 (6) \text{ \AA}$	$T = 296 \text{ K}$
$V = 2026.02 (10) \text{ \AA}^3$	Transparent block, colorless
$Z = 8$	$0.60 \times 0.39 \times 0.22 \text{ mm}$

Data collection

Brucker APEXII CCD diffractometer	1984 independent reflections
Radiation source: fine-focus sealed tube	1895 reflections with $I > 2\sigma(I)$
Graphite	$R_{\text{int}} = 0.028$
phi and ω scans	$\theta_{\text{max}} = 71.9^\circ$, $\theta_{\text{min}} = 4.2^\circ$
Absorption correction: multi-scan <i>SADABS</i> (Bruker, 2009)	$h = -16 \rightarrow 16$
$T_{\text{min}} = 0.633$, $T_{\text{max}} = 0.836$	$k = -8 \rightarrow 8$
27061 measured reflections	$l = -25 \rightarrow 24$

Refinement

Refinement on F^2	Primary atom site location: structure-invariant direct methods
Least-squares matrix: full	Secondary atom site location: difference Fourier map
$R[F^2 > 2\sigma(F^2)] = 0.033$	Hydrogen site location: inferred from neighbouring sites
$wR(F^2) = 0.089$	H atoms treated by a mixture of independent and constrained refinement
$S = 1.09$	$w = 1/[\sigma^2(F_o^2) + (0.0464P)^2 + 0.8383P]$
1984 reflections	where $P = (F_o^2 + 2F_c^2)/3$
152 parameters	$(\Delta/\sigma)_{\text{max}} = 0.083$
0 restraints	$\Delta_{\text{max}} = 0.27 \text{ e \AA}^{-3}$
	$\Delta_{\text{min}} = -0.25 \text{ e \AA}^{-3}$

Table 6b. Fractional atomic coordinates and isotropic or equivalent isotropic displacement parameters (\AA^2) for 1-oxoisochromene-3-carboxylic acid (**37-II**).

	<i>X</i>	<i>Y</i>	<i>Z</i>	$U_{\text{iso}}^*/U_{\text{eq}}$
O1	0.42094 (6)	0.36442 (12)	0.64790 (4)	0.0204 (2)
H1	0.3959 (11)	0.387 (2)	0.6870 (7)	0.024*
O2	0.53884 (6)	0.21435 (12)	0.70338 (4)	0.0237 (2)
O3	0.64069 (6)	0.13558 (11)	0.59782 (4)	0.0184 (2)
O4	0.78104 (6)	0.02402 (13)	0.55694 (4)	0.0268 (2)
O5	0.65705 (6)	-0.05775 (12)	0.74584 (4)	0.0212 (2)
H5	0.6213 (11)	0.014 (2)	0.7245 (7)	0.025*
C1	0.50304 (8)	0.26673 (15)	0.65307 (5)	0.0171 (2)
C2	0.54979 (8)	0.22396 (15)	0.59052 (5)	0.0162 (2)
C3	0.50944 (8)	0.26278 (16)	0.53390 (5)	0.0166 (2)
H3	0.4483	0.3251	0.5314	0.020*
C4	0.56121 (8)	0.20754 (15)	0.47676 (5)	0.0170 (2)
C5	0.65512 (8)	0.11865 (15)	0.48296 (5)	0.0176 (2)
C6	0.69903 (9)	0.08858 (16)	0.54602 (5)	0.0192 (3)
C7	0.70748 (9)	0.05929 (16)	0.42911 (6)	0.0209 (3)
H7	0.7694	0.0005	0.4333	0.025*
C8	0.66663 (9)	0.08862 (17)	0.36947 (6)	0.0230 (3)
H8	0.7010	0.0483	0.3335	0.028*
C9	0.57429 (10)	0.17822 (17)	0.36292 (5)	0.0227 (3)
H9	0.5478	0.1984	0.3226	0.027*
C10	0.52156 (9)	0.23754 (17)	0.41598 (5)	0.0199 (3)
H10	0.4600	0.2971	0.4112	0.024*
C11	0.68979 (11)	-0.2050 (2)	0.70601 (7)	0.0350 (3)
H11B	0.7178	-0.1556	0.6676	0.053*
H11A	0.6335	-0.2826	0.6958	0.053*
H11C	0.7401	-0.2760	0.7278	0.053*

Table 6c. Atomic displacement parameters (\AA^2) for 1-oxoisochromene-3-carboxylic acid (**37-II**).

	U^{11}	U^{22}	U^{33}	U^{12}	U^{13}	U^{23}
O1	0.0201 (4)	0.0248 (4)	0.0163 (4)	0.0056 (3)	0.0019 (3)	-0.0005 (3)
O2	0.0254 (4)	0.0306 (5)	0.0150 (4)	0.0083 (4)	-0.0014 (3)	-0.0005 (3)

O3	0.0164 (4)	0.0226 (4)	0.0161 (4)	0.0032 (3)	-0.0003 (3)	-0.0003 (3)
O4	0.0194 (4)	0.0356 (5)	0.0254 (5)	0.0084 (4)	-0.0006 (3)	-0.0021 (4)
O5	0.0200 (4)	0.0250 (4)	0.0185 (4)	0.0023 (3)	0.0009 (3)	0.0048 (3)
C1	0.0180 (5)	0.0160 (5)	0.0174 (5)	-0.0010 (4)	-0.0005 (4)	-0.0007 (4)
C2	0.0154 (5)	0.0154 (5)	0.0177 (5)	-0.0005 (4)	0.0005 (4)	-0.0001 (4)
C3	0.0161 (5)	0.0152 (5)	0.0184 (6)	-0.0003 (4)	0.0003 (4)	0.0005 (4)
C4	0.0189 (5)	0.0142 (5)	0.0178 (5)	-0.0031 (4)	0.0015 (4)	-0.0002 (4)
C5	0.0183 (5)	0.0163 (5)	0.0183 (6)	-0.0034 (4)	0.0017 (4)	-0.0011 (4)
C6	0.0183 (6)	0.0191 (5)	0.0203 (6)	-0.0005 (4)	0.0026 (4)	-0.0020 (4)
C7	0.0193 (6)	0.0199 (6)	0.0234 (6)	-0.0025 (4)	0.0050 (4)	-0.0023 (5)
C8	0.0271 (6)	0.0229 (6)	0.0190 (6)	-0.0050 (5)	0.0078 (5)	-0.0035 (5)
C9	0.0296 (6)	0.0223 (6)	0.0162 (5)	-0.0056 (5)	0.0002 (5)	0.0010 (5)
C10	0.0222 (6)	0.0182 (5)	0.0192 (6)	-0.0016 (4)	0.0001 (4)	0.0012 (4)
C11	0.0395 (7)	0.0409 (8)	0.0246 (6)	0.0194 (6)	0.0022 (6)	0.0011 (6)

Table 6d. Geometric parameters (Å, °) for 1-oxoisochromene-3-carboxylic acid (**37-II**).

O1—C1	1.3044 (14)	C4—C5	1.4094 (16)
O1—H1	0.901 (16)	C5—C7	1.3971 (16)
O2—C1	1.2208 (14)	C5—C6	1.4652 (16)
O3—C2	1.3748 (13)	C7—C8	1.3834 (17)
O3—C6	1.3797 (14)	C7—H7	0.9300
O4—C6	1.2071 (14)	C8—C9	1.3942 (18)
O5—C11	1.4257 (16)	C8—H8	0.9300
O5—H5	0.837 (16)	C9—C10	1.3861 (17)
C1—C2	1.4877 (15)	C9—H9	0.9300
C2—C3	1.3360 (16)	C10—H10	0.9300
C3—C4	1.4415 (15)	C11—H11B	0.9600
C3—H3	0.9300	C11—H11A	0.9600
C4—C10	1.3997 (16)	C11—H11C	0.9600
C1—O1—H1	109.3 (9)	O3—C6—C5	117.07 (10)
C2—O3—C6	121.30 (9)	C8—C7—C5	119.55 (11)
C11—O5—H5	109.0 (10)	C8—C7—H7	120.2
O2—C1—O1	124.52 (10)	C5—C7—H7	120.2
O2—C1—C2	122.65 (10)	C7—C8—C9	120.39 (11)
O1—C1—C2	112.83 (9)	C7—C8—H8	119.8
C3—C2—O3	123.35 (10)	C9—C8—H8	119.8
C3—C2—C1	125.27 (10)	C10—C9—C8	120.60 (11)

O3—C2—C1	111.38 (9)	C10—C9—H9	119.7
C2—C3—C4	119.59 (10)	C8—C9—H9	119.7
C2—C3—H3	120.2	C9—C10—C4	119.84 (11)
C4—C3—H3	120.2	C9—C10—H10	120.1
C10—C4—C5	119.22 (10)	C4—C10—H10	120.1
C10—C4—C3	122.64 (10)	O5—C11—H11B	109.5
C5—C4—C3	118.13 (10)	O5—C11—H11A	109.5
C7—C5—C4	120.39 (10)	H11B—C11—H11A	109.5
C7—C5—C6	119.37 (10)	O5—C11—H11C	109.5
C4—C5—C6	120.24 (10)	H11B—C11—H11C	109.5
O4—C6—O3	116.85 (10)	H11A—C11—H11C	109.5
O4—C6—C5	126.07 (11)		
C6—O3—C2—C3	3.17 (16)	C2—O3—C6—O4	174.56 (10)
C6—O3—C2—C1	-177.69 (9)	C2—O3—C6—C5	-6.46 (15)
O2—C1—C2—C3	173.53 (11)	C7—C5—C6—O4	4.18 (19)
O1—C1—C2—C3	-6.36 (17)	C4—C5—C6—O4	-175.47 (11)
O2—C1—C2—O3	-5.60 (16)	C7—C5—C6—O3	-174.70 (10)
O1—C1—C2—O3	174.51 (9)	C4—C5—C6—O3	5.65 (16)
O3—C2—C3—C4	1.30 (17)	C4—C5—C7—C8	0.12 (17)
C1—C2—C3—C4	-177.73 (10)	C6—C5—C7—C8	-179.53 (10)
C2—C3—C4—C10	177.56 (11)	C5—C7—C8—C9	0.58 (18)
C2—C3—C4—C5	-1.96 (16)	C7—C8—C9—C10	-0.67 (18)
C10—C4—C5—C7	-0.72 (17)	C8—C9—C10—C4	0.05 (18)
C3—C4—C5—C7	178.81 (10)	C5—C4—C10—C9	0.64 (17)
C10—C4—C5—C6	178.92 (10)	C3—C4—C10—C9	-178.88 (11)
C3—C4—C5—C6	-1.54 (16)		

Table 6e. Hydrogen-bond geometry (Å, °) for 1-oxoisochromene-3-carboxylic acid (**37-II**).

<i>D</i> —H \cdots <i>A</i>	<i>D</i> —H	H \cdots <i>A</i>	<i>D</i> \cdots <i>A</i>	<i>D</i> —H \cdots <i>A</i>
O5—H5 \cdots O2	0.837 (16)	1.871 (17)	2.6754 (12)	160.7 (15)
O1—H1 \cdots O5 ⁱ	0.901 (16)	1.629 (16)	2.5274 (11)	174.2 (14)

Table 7a. Crystal data and structure refinement for recemic 7-(3-hydroxy-2-methyl-3-oxo-propyl)sulfonyl-1-oxo-isochromene-3-carboxylic acid (**30**).

Crystal data

$C_{13}H_{11}NO_8S$	$F(000) = 704$
$M_r = 341.29$	$D_x = 1.605 \text{ Mg m}^{-3}$
Monoclinic, $P2_1/c$	Cu $K\alpha$ radiation, $\lambda = 1.54178 \text{ \AA}$
$a = 11.5746 (3) \text{ \AA}$	Cell parameters from 4548 reflections
$b = 7.7435 (2) \text{ \AA}$	$\theta = 4.0\text{--}67.4^\circ$
$c = 16.5085 (5) \text{ \AA}$	$\mu = 2.48 \text{ mm}^{-1}$
$\beta = 107.394 (2)^\circ$	$T = 173 \text{ K}$
$V = 1411.96 (7) \text{ \AA}^3$	Transparent plate, colorless
$Z = 4$	$0.39 \times 0.33 \times 0.14 \text{ mm}$

Data collection

Bruker APEXII CCD diffractometer	2448 independent reflections
Radiation source: fine-focus sealed tube	2240 reflections with $I > 2\sigma(I)$
Graphite	$R_{\text{int}} = 0.025$
Detector resolution: $8.33 \text{ pixels mm}^{-1}$	$\theta_{\text{max}} = 67.7^\circ$, $\theta_{\text{min}} = 4.1^\circ$
phi and ω scans	$h = -7 \rightarrow 13$
Absorption correction: multi-scan <i>SADABS</i> (Bruker, 2010)	$k = -8 \rightarrow 8$
$T_{\text{min}} = 0.445$, $T_{\text{max}} = 0.729$	$l = -19 \rightarrow 19$
8985 measured reflections	

Refinement

Refinement on F^2	Primary atom site location: structure-invariant direct methods
Least-squares matrix: full	Secondary atom site location: difference Fourier map
$R[F^2 > 2\sigma(F^2)] = 0.064$	Hydrogen site location: inferred from neighbouring sites
$wR(F^2) = 0.154$	H atoms treated by a mixture of independent and constrained refinement
$S = 1.17$	$w = 1/[\sigma^2(F_o^2) + (0.0378P)^2 + 2.5225P]$
2448 reflections	where $P = (F_o^2 + 2F_c^2)/3$
406 parameters	$(\Delta/\sigma)_{\text{max}} = 0.089$
134 restraints	$\Delta_{\text{max}} = 0.23 \text{ e \AA}^{-3}$
	$\Delta_{\text{min}} = -0.42 \text{ e \AA}^{-3}$

Table 7b. Fractional atomic coordinates and isotropic or equivalent isotropic displacement parameters (\AA^2) for recemic7-(3-hydroxy-2-methyl-3-oxo-propyl)sulfonyl-1-oxo-isochromene-3-carboxylic acid (**30**).

	<i>x</i>	<i>Y</i>	<i>Z</i>	$U_{\text{iso}}^*/U_{\text{eq}}$	Occ. (<1)
S1	0.03023 (7)	0.05569 (11)	0.85807 (6)	0.0596 (2)	
O1	0.7391 (4)	-0.4366 (7)	0.9978 (3)	0.0684 (14)	0.608 (2)
H1	0.8129	-0.4595	1.0190	0.082*	0.608 (2)
O2	0.7436 (5)	-0.4181 (9)	1.1382 (3)	0.080 (2)	0.608 (2)
O3	0.0388 (6)	-0.4236 (10)	0.8126 (5)	0.053 (2)	0.33
H3	0.1073	-0.4630	0.8390	0.064*	
O4	0.0269 (9)	-0.4576 (13)	0.9418 (6)	0.095 (3)	0.33
O5	-0.0025 (3)	0.1036 (6)	0.9260 (3)	0.0632 (11)	0.608 (2)
O6	0.0211 (4)	0.1704 (6)	0.7915 (3)	0.0578 (13)	0.608 (2)
O7	0.5196 (4)	-0.3043 (6)	1.0884 (3)	0.0437 (12)	0.608 (2)
O8	0.3648 (6)	-0.1983 (12)	1.1298 (4)	0.117 (3)	0.608 (2)
N1	-0.0687 (3)	-0.1016 (6)	0.8070 (3)	0.0429 (10)	0.608 (2)
C1	0.6958 (5)	-0.3894 (8)	1.0555 (4)	0.0435 (18)	0.608 (2)
C2	0.5727 (5)	-0.3041 (9)	1.0237 (4)	0.050 (2)	0.608 (2)
C3	0.5212 (5)	-0.2463 (9)	0.9470 (3)	0.0444 (17)	0.608 (2)
H4	0.5646	-0.2497	0.9065	0.053*	0.608 (2)
C4	0.3995 (5)	-0.1775 (9)	0.9226 (4)	0.054 (2)	0.608 (2)
C5	0.3441 (5)	-0.1527 (9)	0.9867 (4)	0.047 (2)	0.608 (2)
C6	0.4067 (3)	-0.2249 (6)	1.0742 (2)	0.0648 (10)	
C7	0.2261 (5)	-0.0884 (9)	0.9651 (4)	0.051 (2)	0.608 (2)
H7	0.1825	-0.0838	1.0056	0.061*	0.608 (2)
C8	0.1775 (2)	-0.0344 (4)	0.8866 (2)	0.0482 (8)	
C9	0.2238 (5)	-0.0643 (9)	0.8194 (4)	0.0527 (19)	0.608 (2)
H9	0.1784	-0.0399	0.7623	0.063*	0.608 (2)
C10	0.3380 (5)	-0.1306 (10)	0.8397 (4)	0.057 (2)	0.608 (2)
H10	0.3761	-0.1448	0.7966	0.068*	0.608 (2)
C11	-0.0140 (4)	-0.3816 (5)	0.8628 (3)	0.0799 (12)	
C12	-0.0988 (5)	-0.2412 (7)	0.8582 (3)	0.0483 (15)	0.608 (2)
H12	-0.0927	-0.1982	0.9165	0.058*	0.608 (2)
C13	-0.2351 (5)	-0.2640 (10)	0.8051 (5)	0.067 (2)	0.608 (2)
H13A	-0.2733	-0.1503	0.7921	0.100*	0.608 (2)
H13B	-0.2771	-0.3315	0.8378	0.100*	0.608 (2)
H13C	-0.2399	-0.3245	0.7520	0.100*	0.608 (2)
H2	-0.065 (5)	-0.129 (8)	0.751 (4)	0.080*	0.608 (2)
O1A	0.7700 (5)	-0.3704 (10)	1.0154 (4)	0.0566 (19)	0.392 (2)
H1A	0.8292	-0.4383	1.0300	0.068*	0.392 (2)
O2A	0.7364 (7)	-0.4289 (12)	1.1314 (6)	0.057 (3)	0.392 (2)
O3A	0.0656 (6)	-0.3958 (10)	0.8334 (5)	0.046 (2)	0.33
O4A	-0.0726 (8)	-0.5198 (11)	0.8966 (7)	0.098 (3)	0.33
O5A	0.0437 (6)	0.1908 (9)	0.9345 (5)	0.0673 (19)	0.392 (2)
O6A	0.0062 (7)	0.1197 (11)	0.7735 (6)	0.075 (3)	0.392 (2)
O7A	0.5258 (9)	-0.2669 (13)	1.0950 (6)	0.066 (3)	0.392 (2)
O8A	0.3639 (7)	-0.2454 (14)	1.1344 (5)	0.060 (2)	0.392 (2)
N1A	-0.0567 (5)	-0.0766 (9)	0.8789 (4)	0.0492 (17)	0.392 (2)
C1A	0.7094 (10)	-0.3797 (15)	1.0692 (11)	0.076 (5)	0.392 (2)
C2A	0.5819 (9)	-0.3114 (15)	1.0330 (5)	0.045 (3)	0.392 (2)
C3A	0.5276 (8)	-0.2742 (16)	0.9534 (7)	0.057 (4)	0.392 (2)
H3A	0.5644	-0.3071	0.9115	0.069*	0.392 (2)
C4A	0.4131 (7)	-0.1842 (13)	0.9279 (4)	0.035 (3)	0.392 (2)

C5A	0.3517 (7)	-0.1760 (14)	0.9896 (6)	0.041 (3)	0.392 (2)
C7A	0.2407 (8)	-0.0909 (16)	0.9717 (6)	0.046 (3)	0.392 (2)
H7A	0.2062	-0.0696	1.0162	0.055*	0.392 (2)
C9A	0.2489 (7)	-0.0353 (14)	0.8290 (6)	0.042 (3)	0.392 (2)
H9A	0.2183	0.0207	0.7757	0.050*	0.392 (2)
C10A	0.3594 (8)	-0.1139 (16)	0.8481 (6)	0.054 (3)	0.392 (2)
H10A	0.4002	-0.1206	0.8061	0.065*	0.392 (2)
C12A	-0.0919 (7)	-0.2141 (12)	0.8239 (6)	0.048 (2)	0.392 (2)
H12A	-0.0850	-0.1858	0.7664	0.058*	0.392 (2)
C13A	-0.2119 (9)	-0.3182 (17)	0.8172 (8)	0.071 (4)	0.392 (2)
H13D	-0.1953	-0.4068	0.8616	0.107*	0.392 (2)
H13E	-0.2408	-0.3735	0.7614	0.107*	0.392 (2)
H13F	-0.2740	-0.2389	0.8245	0.107*	0.392 (2)
H2A	-0.035 (9)	-0.112 (14)	0.929 (6)	0.086*	0.392 (2)
O3B	-0.0286 (11)	-0.4917 (14)	0.7942 (7)	0.126 (4)	0.33
O4B	0.0590 (6)	-0.3822 (9)	0.9263 (5)	0.0525 (18)	0.33

Table 7c. Atomic displacement parameters (\AA^2) recemic7-(3-hydroxy-2-methyl-3-oxo-propyl)sulfonyl-1-oxo-isochromene-3-carboxylic acid (**30**).

	U^{11}	U^{22}	U^{33}	U^{12}	U^{13}	U^{23}
S1	0.0399 (4)	0.0541 (5)	0.0855 (6)	0.0057 (3)	0.0198 (4)	0.0093 (4)
O1	0.046 (2)	0.089 (3)	0.066 (3)	0.007 (2)	0.0111 (19)	0.010 (2)
O2	0.072 (3)	0.109 (5)	0.042 (3)	-0.009 (3)	-0.007 (3)	-0.010 (3)
O3	0.024 (3)	0.059 (4)	0.053 (4)	-0.007 (3)	-0.024 (3)	-0.012 (3)
O4	0.114 (6)	0.087 (6)	0.099 (5)	0.035 (5)	0.054 (5)	0.026 (5)
O5	0.0393 (17)	0.071 (3)	0.083 (2)	-0.0030 (17)	0.0225 (17)	-0.035 (2)
O6	0.051 (2)	0.058 (3)	0.062 (2)	0.0084 (19)	0.0130 (19)	0.003 (2)
O7	0.0361 (18)	0.055 (2)	0.0347 (19)	0.0014 (17)	0.0024 (16)	-0.0084 (17)
O8	0.112 (4)	0.197 (8)	0.050 (3)	0.060 (4)	0.038 (3)	0.016 (4)
N1	0.0299 (17)	0.053 (3)	0.044 (2)	0.0037 (17)	0.0069 (16)	0.0045 (19)
C1	0.032 (3)	0.050 (3)	0.040 (3)	0.002 (2)	-0.003 (2)	0.008 (3)
C2	0.027 (3)	0.053 (4)	0.064 (4)	0.007 (3)	0.006 (3)	0.006 (3)
C3	0.051 (3)	0.048 (3)	0.039 (3)	0.004 (3)	0.021 (2)	0.010 (2)
C4	0.031 (3)	0.052 (4)	0.076 (5)	0.004 (3)	0.013 (3)	-0.005 (3)
C5	0.050 (3)	0.051 (4)	0.038 (3)	-0.003 (3)	0.012 (3)	0.001 (3)
C6	0.0531 (17)	0.091 (3)	0.0488 (18)	0.0037 (18)	0.0132 (15)	-0.0063 (18)
C7	0.037 (3)	0.059 (4)	0.059 (4)	-0.011 (3)	0.019 (3)	-0.016 (3)
C8	0.0345 (13)	0.0493 (17)	0.0605 (18)	-0.0014 (12)	0.0139 (13)	-0.0021 (14)
C9	0.030 (2)	0.063 (4)	0.059 (4)	-0.007 (3)	0.004 (2)	-0.001 (3)
C10	0.039 (3)	0.091 (5)	0.043 (3)	0.000 (3)	0.014 (2)	0.004 (3)
C11	0.107 (3)	0.054 (2)	0.085 (3)	0.022 (2)	0.039 (2)	-0.001 (2)
C12	0.049 (3)	0.047 (3)	0.045 (3)	-0.007 (2)	0.007 (2)	0.013 (2)
C13	0.048 (3)	0.069 (4)	0.073 (4)	-0.009 (3)	0.002 (3)	0.011 (3)
O1A	0.032 (3)	0.077 (5)	0.058 (4)	0.011 (3)	0.009 (3)	0.008 (3)
O2A	0.040 (3)	0.074 (5)	0.055 (5)	0.036 (4)	0.013 (3)	0.006 (4)
O3A	0.019 (3)	0.044 (4)	0.054 (4)	0.001 (3)	-0.022 (3)	-0.014 (3)
O4A	0.105 (5)	0.063 (5)	0.155 (7)	0.019 (4)	0.082 (5)	0.040 (5)
O5A	0.053 (3)	0.057 (4)	0.088 (4)	0.005 (3)	0.015 (3)	-0.006 (3)
O6A	0.043 (3)	0.075 (5)	0.096 (6)	0.008 (3)	0.003 (4)	-0.032 (4)
O7A	0.068 (5)	0.068 (5)	0.061 (5)	0.004 (4)	0.017 (4)	-0.014 (4)
O8A	0.040 (3)	0.094 (5)	0.044 (4)	0.010 (3)	0.012 (3)	0.015 (3)
N1A	0.039 (3)	0.057 (4)	0.049 (4)	0.002 (3)	0.010 (3)	-0.001 (3)
C1A	0.059 (7)	0.056 (7)	0.117 (11)	-0.017 (6)	0.033 (8)	-0.043 (7)
C2A	0.058 (6)	0.052 (6)	0.022 (4)	-0.014 (5)	0.007 (4)	-0.012 (4)

C3A	0.029 (4)	0.052 (6)	0.088 (9)	0.014 (4)	0.013 (5)	0.014 (6)
C4A	0.034 (4)	0.047 (6)	0.025 (4)	-0.002 (4)	0.011 (4)	0.009 (4)
C5A	0.025 (4)	0.036 (5)	0.058 (7)	0.005 (4)	0.007 (4)	-0.009 (4)
C7A	0.040 (5)	0.061 (7)	0.031 (5)	0.010 (5)	0.003 (4)	0.004 (5)
C9A	0.028 (4)	0.064 (6)	0.030 (4)	-0.006 (4)	0.003 (3)	-0.004 (4)
C10A	0.029 (4)	0.076 (7)	0.056 (6)	0.017 (4)	0.013 (4)	0.023 (5)
C12A	0.043 (4)	0.041 (4)	0.049 (5)	0.001 (3)	-0.004 (4)	0.023 (4)
C13A	0.051 (5)	0.098 (9)	0.053 (5)	-0.015 (5)	-0.003 (5)	0.019 (6)
O3B	0.121 (7)	0.087 (6)	0.129 (7)	0.029 (6)	-0.025 (6)	-0.034 (6)
O4B	0.040 (3)	0.043 (4)	0.076 (4)	0.005 (3)	0.019 (3)	0.019 (3)

Table 7d. Geometric parameters (Å, °) for recemic7-(3-hydroxy-2-methyl-3-oxo-propyl)sulfonyl-1-oxo-isochromene-3-carboxylic acid (**30**).

S1—O5	1.339 (4)	C10—H10	0.9500
S1—O6	1.393 (5)	C11—O4B	1.132 (8)
S1—O6A	1.428 (10)	C11—O3A	1.169 (9)
S1—N1A	1.545 (7)	C11—O3B	1.387 (11)
S1—O5A	1.611 (7)	C11—C12	1.452 (7)
S1—N1	1.711 (4)	C11—O4A	1.463 (9)
S1—C8	1.770 (3)	C11—C12A	1.600 (9)
O1—C1	1.255 (9)	C12—C13	1.568 (7)
O1—H1	0.8400	C12—H12	1.0000
O2—C1	1.330 (8)	C12—H2A	1.55 (10)
O3—C11	1.213 (9)	C13—H13A	0.9800
O3—H3	0.8400	C13—H13B	0.9800
O4—C11	1.379 (10)	C13—H13C	0.9800
O7—C2	1.382 (9)	O1A—C1A	1.288 (18)
O7—C6	1.400 (6)	O1A—H1A	0.8400
O8—C6	1.177 (8)	O2A—C1A	1.052 (18)
N1—C12	1.477 (7)	O7A—C2A	1.409 (15)
N1—H2	0.96 (6)	N1A—C12A	1.379 (11)
C1—C2	1.514 (7)	N1A—H2A	0.84 (10)
C2—C3	1.307 (7)	C1A—C2A	1.512 (12)
C3—C4	1.446 (7)	C2A—C3A	1.308 (11)
C3—H4	0.9500	C3A—C4A	1.444 (10)
C4—C10	1.388 (7)	C3A—H3A	0.9500
C4—C5	1.404 (8)	C4A—C10A	1.387 (10)
C5—C7	1.397 (7)	C4A—C5A	1.407 (10)
C5—C6	1.516 (7)	C5A—C7A	1.395 (11)
C6—O8A	1.246 (10)	C7A—H7A	0.9500
C6—O7A	1.357 (10)	C9A—C10A	1.365 (11)
C6—C5A	1.403 (10)	C9A—H9A	0.9500
C7—C8	1.318 (7)	C10A—H10A	0.9500
C7—H7	0.9500	C12A—C13A	1.581 (12)
C8—C9	1.388 (8)	C12A—H2	1.48 (6)
C8—C7A	1.444 (10)	C12A—H12A	1.0000
C8—C9A	1.434 (10)	C13A—H13D	0.9800
C9—C10	1.364 (7)	C13A—H13E	0.9800
C9—H9	0.9500	C13A—H13F	0.9800
O5—S1—O6	120.7 (3)	O3A—C11—O4	105.2 (6)
O5—S1—O6A	134.6 (4)	O3—C11—O4	115.6 (6)
O6—S1—O6A	20.0 (4)	O4B—C11—O3B	128.9 (7)

O5—S1—N1A	68.4 (3)	O3A—C11—O3B	61.4 (6)
O6—S1—N1A	134.3 (3)	O3—C11—O3B	40.5 (6)
O6A—S1—N1A	119.9 (4)	O4—C11—O3B	115.7 (7)
O5—S1—O5A	31.7 (3)	O4B—C11—C12	111.0 (5)
O6—S1—O5A	99.8 (3)	O3A—C11—C12	130.8 (5)
O6A—S1—O5A	119.1 (4)	O3—C11—C12	129.5 (5)
N1A—S1—O5A	100.0 (4)	O4—C11—C12	113.9 (6)
O5—S1—N1	107.2 (2)	O3B—C11—C12	120.2 (6)
O6—S1—N1	100.5 (2)	O4B—C11—O4A	87.0 (6)
O6A—S1—N1	81.9 (4)	O3A—C11—O4A	127.0 (6)
N1A—S1—N1	41.7 (3)	O3—C11—O4A	116.7 (6)
O5A—S1—N1	137.9 (3)	O4—C11—O4A	52.7 (6)
O5—S1—C8	112.2 (2)	O3B—C11—O4A	84.5 (7)
O6—S1—C8	107.5 (2)	C12—C11—O4A	100.7 (5)
O6A—S1—C8	106.7 (4)	O4B—C11—C12A	123.4 (6)
N1A—S1—C8	108.6 (3)	O3A—C11—C12A	109.2 (6)
O5A—S1—C8	100.8 (2)	O3—C11—C12A	106.3 (6)
N1—S1—C8	107.44 (17)	O4—C11—C12A	135.9 (6)
C1—O1—H1	109.5	O3B—C11—C12A	104.7 (6)
C11—O3—H3	109.4	C12—C11—C12A	23.2 (4)
C2—O7—C6	118.6 (4)	O4A—C11—C12A	118.5 (5)
C12—N1—S1	118.4 (3)	C11—C12—N1	107.9 (4)
C12—N1—H2	118 (4)	C11—C12—C13	119.7 (5)
S1—N1—H2	114 (4)	N1—C12—C13	97.6 (4)
O1—C1—O2	126.2 (5)	C11—C12—H12	110.3
O1—C1—C2	114.4 (5)	N1—C12—H12	110.3
O2—C1—C2	119.2 (6)	C13—C12—H12	110.3
C3—C2—O7	124.7 (5)	C11—C12—H2A	106 (4)
C3—C2—C1	126.5 (6)	N1—C12—H2A	80 (4)
O7—C2—C1	108.8 (5)	C13—C12—H2A	132 (4)
C2—C3—C4	121.4 (6)	H12—C12—H2A	34.6
C2—C3—H4	119.3	C1A—O1A—H1A	109.5
C4—C3—H4	119.3	C6—O7A—C2A	121.9 (8)
C10—C4—C5	119.4 (5)	C12A—N1A—S1	116.7 (6)
C10—C4—C3	122.8 (6)	C12A—N1A—H2A	110 (8)
C5—C4—C3	117.8 (5)	S1—N1A—H2A	115 (7)
C7—C5—C4	119.3 (5)	O2A—C1A—O1A	128.9 (11)
C7—C5—C6	121.7 (5)	O2A—C1A—C2A	118.9 (14)
C4—C5—C6	118.2 (5)	O1A—C1A—C2A	112.2 (12)
O8—C6—O8A	17.4 (8)	C3A—C2A—O7A	119.2 (10)
O8—C6—O7A	117.9 (6)	C3A—C2A—C1A	126.4 (11)
O8A—C6—O7A	112.5 (6)	O7A—C2A—C1A	113.9 (9)
O8—C6—O7	121.9 (4)	C2A—C3A—C4A	121.6 (10)
O8A—C6—O7	112.6 (5)	C2A—C3A—H3A	119.2
O7A—C6—O7	12.8 (5)	C4A—C3A—H3A	119.2
O8—C6—C5A	124.0 (6)	C10A—C4A—C5A	119.3 (8)
O8A—C6—C5A	131.2 (6)	C10A—C4A—C3A	125.3 (8)
O7A—C6—C5A	116.2 (6)	C5A—C4A—C3A	115.4 (8)
O7—C6—C5A	114.1 (5)	C7A—C5A—C4A	120.1 (9)
O8—C6—C5	119.2 (5)	C7A—C5A—C6	116.9 (8)
O8A—C6—C5	128.1 (5)	C4A—C5A—C6	122.1 (6)
O7A—C6—C5	119.3 (5)	C5A—C7A—C8	121.0 (9)
O7—C6—C5	118.5 (4)	C5A—C7A—H7A	119.5
C5A—C6—C5	6.5 (6)	C8—C7A—H7A	119.5
C8—C7—C5	117.5 (6)	C10A—C9A—C8	122.3 (8)
C8—C7—H7	121.3	C10A—C9A—H9A	118.8

C5—C7—H7	121.3	C8—C9A—H9A	118.8
C7—C8—C9	125.5 (4)	C9A—C10A—C4A	121.1 (9)
C7—C8—C7A	4.9 (6)	C9A—C10A—H10A	119.4
C9—C8—C7A	121.5 (5)	C4A—C10A—H10A	119.4
C7—C8—C9A	119.3 (5)	N1A—C12A—C13A	121.3 (9)
C9—C8—C9A	14.7 (5)	N1A—C12A—C11	109.9 (6)
C7A—C8—C9A	114.7 (5)	C13A—C12A—C11	89.6 (7)
C7—C8—S1	118.7 (3)	N1A—C12A—H2	95 (3)
C9—C8—S1	115.1 (3)	C13A—C12A—H2	124 (2)
C7A—C8—S1	123.1 (5)	C11—C12A—H2	117 (3)
C9A—C8—S1	121.7 (4)	N1A—C12A—H12A	111.3
C10—C9—C8	116.3 (5)	C13A—C12A—H12A	111.3
C10—C9—H9	121.8	C11—C12A—H12A	111.3
C8—C9—H9	121.8	H2—C12A—H12A	16.0
C9—C10—C4	121.0 (6)	C12A—C13A—H13D	109.5
C9—C10—H10	119.5	C12A—C13A—H13E	109.5
C4—C10—H10	119.5	H13D—C13A—H13E	109.5
O4B—C11—O3A	85.4 (6)	C12A—C13A—H13F	109.5
O4B—C11—O3	104.0 (6)	H13D—C13A—H13F	109.5
O3A—C11—O3	21.4 (4)	H13E—C13A—H13F	109.5
O4B—C11—O4	34.3 (5)		
O5—S1—N1—C12	-45.2 (4)	O3B—C11—C12—N1	-77.4 (8)
O6—S1—N1—C12	-172.2 (4)	O4A—C11—C12—N1	-167.2 (5)
O6A—S1—N1—C12	-179.5 (5)	C12A—C11—C12—N1	-24.9 (9)
N1A—S1—N1—C12	-23.1 (5)	O4B—C11—C12—C13	-147.9 (6)
O5A—S1—N1—C12	-54.4 (6)	O3A—C11—C12—C13	109.5 (7)
C8—S1—N1—C12	75.5 (4)	O3—C11—C12—C13	81.4 (8)
C6—O7—C2—C3	-5.6 (10)	O4—C11—C12—C13	-110.9 (7)
C6—O7—C2—C1	177.4 (5)	O3B—C11—C12—C13	32.7 (9)
O1—C1—C2—C3	-14.4 (10)	O4A—C11—C12—C13	-57.1 (7)
O2—C1—C2—C3	170.1 (7)	C12A—C11—C12—C13	85.2 (11)
O1—C1—C2—O7	162.6 (6)	S1—N1—C12—C11	-91.3 (4)
O2—C1—C2—O7	-12.9 (8)	S1—N1—C12—C13	144.1 (4)
O7—C2—C3—C4	-0.8 (11)	O8—C6—O7A—C2A	176.0 (10)
C1—C2—C3—C4	175.8 (6)	O8A—C6—O7A—C2A	157.6 (10)
C2—C3—C4—C10	-173.7 (7)	O7—C6—O7A—C2A	65 (2)
C2—C3—C4—C5	8.5 (10)	C5A—C6—O7A—C2A	-19.1 (13)
C10—C4—C5—C7	2.8 (9)	C5—C6—O7A—C2A	-25.5 (12)
C3—C4—C5—C7	-179.2 (6)	O5—S1—N1A—C12A	176.6 (6)
C10—C4—C5—C6	172.7 (6)	O6—S1—N1A—C12A	64.2 (7)
C3—C4—C5—C6	-9.4 (9)	O6A—S1—N1A—C12A	46.6 (8)
C2—O7—C6—O8	-168.7 (7)	O5A—S1—N1A—C12A	178.7 (6)
C2—O7—C6—O8A	174.7 (7)	N1—S1—N1A—C12A	19.4 (4)
C2—O7—C6—O7A	-93 (3)	C8—S1—N1A—C12A	-76.3 (6)
C2—O7—C6—C5A	9.2 (8)	C6—O7A—C2A—C3A	16.0 (17)
C2—O7—C6—C5	4.0 (7)	C6—O7A—C2A—C1A	-171.3 (9)
C7—C5—C6—O8	-14.1 (10)	O2A—C1A—C2A—C3A	-167.4 (14)
C4—C5—C6—O8	176.3 (7)	O1A—C1A—C2A—C3A	11.5 (17)
C7—C5—C6—O8A	4.0 (11)	O2A—C1A—C2A—O7A	20.5 (16)
C4—C5—C6—O8A	-165.6 (8)	O1A—C1A—C2A—O7A	-160.6 (10)
C7—C5—C6—O7A	-172.3 (7)	O7A—C2A—C3A—C4A	1.7 (18)
C4—C5—C6—O7A	18.1 (9)	C1A—C2A—C3A—C4A	-170.0 (11)
C7—C5—C6—O7	173.0 (6)	C2A—C3A—C4A—C10A	168.4 (12)
C4—C5—C6—O7	3.5 (8)	C2A—C3A—C4A—C5A	-14.2 (16)
C7—C5—C6—C5A	125 (5)	C10A—C4A—C5A—C7A	-3.0 (16)

C4—C5—C6—C5A	-45 (5)	C3A—C4A—C5A—C7A	179.5 (10)
C4—C5—C7—C8	-8.0 (9)	C10A—C4A—C5A—C6	-172.0 (10)
C6—C5—C7—C8	-177.4 (5)	C3A—C4A—C5A—C6	10.5 (14)
C5—C7—C8—C9	12.5 (9)	O8—C6—C5A—C7A	0.0 (14)
C5—C7—C8—C7A	-24 (8)	O8A—C6—C5A—C7A	20.1 (15)
C5—C7—C8—C9A	-3.3 (9)	O7A—C6—C5A—C7A	-163.9 (9)
C5—C7—C8—S1	-177.6 (5)	O7—C6—C5A—C7A	-177.9 (8)
O5—S1—C8—C7	17.8 (5)	C5—C6—C5A—C7A	-44 (4)
O6—S1—C8—C7	152.8 (4)	O8—C6—C5A—C4A	169.3 (9)
O6A—S1—C8—C7	173.7 (5)	O8A—C6—C5A—C4A	-170.6 (9)
N1A—S1—C8—C7	-55.8 (5)	O7A—C6—C5A—C4A	5.4 (13)
O5A—S1—C8—C7	48.7 (5)	O7—C6—C5A—C4A	-8.6 (12)
N1—S1—C8—C7	-99.7 (4)	C5—C6—C5A—C4A	126 (5)
O5—S1—C8—C9	-171.3 (4)	C4A—C5A—C7A—C8	10.1 (16)
O6—S1—C8—C9	-36.3 (4)	C6—C5A—C7A—C8	179.6 (8)
O6A—S1—C8—C9	-15.3 (5)	C7—C8—C7A—C5A	146 (9)
N1A—S1—C8—C9	115.2 (5)	C9—C8—C7A—C5A	0.7 (14)
O5A—S1—C8—C9	-140.3 (5)	C9A—C8—C7A—C5A	-14.1 (14)
N1—S1—C8—C9	71.2 (4)	S1—C8—C7A—C5A	173.9 (8)
O5—S1—C8—C7A	15.2 (7)	C7—C8—C9A—C10A	10.1 (13)
O6—S1—C8—C7A	150.2 (7)	C9—C8—C9A—C10A	-109 (3)
O6A—S1—C8—C7A	171.1 (7)	C7A—C8—C9A—C10A	12.1 (13)
N1A—S1—C8—C7A	-58.4 (7)	S1—C8—C9A—C10A	-175.8 (8)
O5A—S1—C8—C7A	46.1 (7)	C8—C9A—C10A—C4A	-5.8 (17)
N1—S1—C8—C7A	-102.3 (7)	C5A—C4A—C10A—C9A	0.8 (17)
O5—S1—C8—C9A	-156.3 (6)	C3A—C4A—C10A—C9A	178.1 (11)
O6—S1—C8—C9A	-21.3 (6)	S1—N1A—C12A—C13A	-157.7 (7)
O6A—S1—C8—C9A	-0.4 (7)	S1—N1A—C12A—C11	100.1 (7)
N1A—S1—C8—C9A	130.1 (6)	O4B—C11—C12A—N1A	-0.4 (10)
O5A—S1—C8—C9A	-125.4 (6)	O3A—C11—C12A—N1A	-97.7 (8)
N1—S1—C8—C9A	86.2 (6)	O3—C11—C12A—N1A	-120.0 (7)
C7—C8—C9—C10	-11.0 (9)	O4—C11—C12A—N1A	41.6 (11)
C7A—C8—C9—C10	-7.6 (10)	O3B—C11—C12A—N1A	-162.1 (8)
C9A—C8—C9—C10	59 (2)	C12—C11—C12A—N1A	63.0 (10)
S1—C8—C9—C10	178.8 (5)	O4A—C11—C12A—N1A	106.2 (8)
C8—C9—C10—C4	4.9 (10)	O4B—C11—C12A—C13A	-123.7 (8)
C5—C4—C10—C9	-1.4 (10)	O3A—C11—C12A—C13A	138.9 (7)
C3—C4—C10—C9	-179.3 (7)	O3—C11—C12A—C13A	116.6 (7)
O4B—C11—C12—N1	102.0 (6)	O4—C11—C12A—C13A	-81.7 (10)
O3A—C11—C12—N1	-0.6 (7)	O3B—C11—C12A—C13A	74.5 (9)
O3—C11—C12—N1	-28.7 (7)	C12—C11—C12A—C13A	-60.3 (10)
O4—C11—C12—N1	139.0 (6)	O4A—C11—C12A—C13A	-17.2 (9)

Table 8a. Crystal data and structure refinement for 7-(3-hydroxy-2-methyl-3-oxo-propyl)sulfonyl-1-oxo-isochromene-3-carboxylic acid (**31**).

Crystal data	
$C_{13}H_{10}NO_8S$	$Z = 4$
$M_r = 340.28$	$F(000) = 700$
Monoclinic, $P2_1/n$	$D_x = 1.587 \text{ Mg m}^{-3}$
$a = 11.4446 (4) \text{ \AA}$	Cu $K\alpha$ radiation, $\lambda = 1.54178 \text{ \AA}$
$b = 7.6479 (3) \text{ \AA}$	$\mu = 2.46 \text{ mm}^{-1}$
$c = 16.9341 (6) \text{ \AA}$	$T = 173 \text{ K}$
$\beta = 106.126 (2)^\circ$	$\times \times \text{ mm}$
$V = 1423.87 (9) \text{ \AA}^3$	
Data collection	
19222 measured reflections	$\theta_{\max} = 67.8^\circ$, $\theta_{\min} = 4.2^\circ$
2538 independent reflections	$h = -13 \rightarrow 13$
2127 reflections with $I > 2\sigma(I)$	$k = -7 \rightarrow 8$
$R_{\text{int}} = 0.036$	$l = -20 \rightarrow 20$
Refinement	
Refinement on F^2	29 restraints
Least-squares matrix: full	Hydrogen site location: mixed
$R[F^2 > 2\sigma(F^2)] = 0.091$	H atoms treated by a mixture of independent and constrained refinement
$wR(F^2) = 0.228$	$w = 1/[\sigma^2(F_o^2) + (0.0605P)^2 + 5.338P]$
$S = 1.13$	where $P = (F_o^2 + 2F_c^2)/3$
2538 reflections	$(\Delta/\sigma)_{\max} = 0.125$
299 parameters	$\Delta_{\max} = 0.65 \text{ e \AA}^{-3}$
	$\Delta_{\min} = -0.46 \text{ e \AA}^{-3}$

Table 8b. Fractional atomic coordinates and isotropic or equivalent isotropic displacement parameters (\AA^2) for 7-(3-hydroxy-2-methyl-3-oxo-propyl)sulfonyl-1-oxo-isochromene-3-carboxylic acid (**31**).

	<i>X</i>	<i>Y</i>	<i>Z</i>	$U_{\text{iso}}^*/U_{\text{eq}}$	Occ. (<1)
S1	0.46896 (10)	0.03456 (16)	0.13979 (9)	0.0667 (4)	
O1	-0.2403 (3)	-0.4048 (7)	-0.0203 (2)	0.1033 (16)	
O2	-0.2409 (4)	-0.3641 (6)	-0.1480 (2)	0.0918 (13)	
O3	0.4629 (4)	-0.4535 (8)	0.1730 (4)	0.097 (2)	0.621 (3)
O4	0.5774 (7)	-0.5309 (9)	0.0909 (4)	0.135 (3)	0.621 (3)
O5	0.5051 (4)	0.1023 (8)	0.0736 (3)	0.0698 (17)	0.621 (3)
O6	0.4665 (5)	0.1344 (8)	0.2094 (4)	0.0653 (19)	0.621 (3)

O7	0.1415 (15)	-0.157 (2)	-0.1344 (7)	0.161 (6)	0.379 (3)
O8	-0.0010 (3)	-0.3216 (5)	-0.10611 (18)	0.0754 (10)	
N1	0.5694 (5)	-0.1235 (8)	0.1872 (3)	0.0526 (16)	0.621 (3)
C1	-0.1875 (5)	-0.3850 (7)	-0.0744 (3)	0.0675 (14)	
C2	-0.0497 (4)	-0.4122 (6)	-0.0497 (3)	0.0567 (12)	
C3	0.0131 (4)	-0.3893 (6)	0.0436 (3)	0.0556 (12)	
H3	-0.0481	-0.3649	0.0744	0.067*	
C4	0.1143 (4)	-0.2573 (6)	0.0645 (2)	0.0492 (11)	
C5	0.1643 (4)	-0.1969 (6)	0.0042 (3)	0.0567 (12)	
C6	0.1063 (14)	-0.225 (3)	-0.0831 (10)	0.090 (7)	0.379 (3)
C7	0.2715 (4)	-0.1010 (6)	0.0258 (3)	0.0601 (12)	
H7	0.3073	-0.0608	-0.0152	0.072*	
C8	0.3251 (4)	-0.0652 (6)	0.1073 (3)	0.0535 (11)	
C9	0.2717 (4)	-0.1174 (7)	0.1674 (3)	0.0595 (12)	
H9	0.3077	-0.0869	0.2233	0.071*	
C10	0.1664 (4)	-0.2135 (7)	0.1459 (3)	0.0601 (12)	
H10	0.1294	-0.2500	0.1869	0.072*	
C11	0.5360 (2)	-0.4167 (6)	0.13979 (15)	0.104 (2)	
C12	0.6089 (6)	-0.2496 (9)	0.1365 (4)	0.058 (2)	0.621 (3)
H12	0.5996	-0.2072	0.0793	0.069*	0.621 (3)
C13	0.7442 (8)	-0.3015 (12)	0.1833 (7)	0.080 (3)	0.621 (3)
H13D	0.7958	-0.1971	0.1912	0.120*	0.621 (3)
H13E	0.7741	-0.3877	0.1507	0.120*	0.621 (3)
H13F	0.7465	-0.3518	0.2369	0.120*	0.621 (3)
H2	0.563 (5)	-0.154 (9)	0.2343 (14)	0.096*	0.621 (3)
O3A	0.4463 (5)	-0.4165 (11)	0.0820 (4)	0.068 (3)	0.379 (3)
O4A	0.5816 (9)	-0.5508 (17)	0.1750 (6)	0.422 (17)	0.379 (3)
O5A	0.4623 (8)	0.1624 (13)	0.0726 (6)	0.083 (3)	0.379 (3)
O6A	0.4965 (9)	0.1100 (15)	0.2196 (6)	0.072 (3)	0.379 (3)
O7A	0.1502 (6)	-0.2058 (10)	-0.1393 (4)	0.081 (2)	0.621 (3)
N1A	0.5615 (8)	-0.1022 (12)	0.1162 (5)	0.056 (3)	0.379 (3)
C6A	0.1094 (8)	-0.2440 (12)	-0.0850 (4)	0.061 (3)	0.621 (3)
C12A	0.6013 (8)	-0.2439 (13)	0.1748 (5)	0.062 (4)	0.379 (3)
H12A	0.5920	-0.2149	0.2303	0.075*	0.379 (3)
C13A	0.7390 (10)	-0.2459 (17)	0.1736 (11)	0.075 (5)	0.379 (3)
H13A	0.7595	-0.3618	0.1566	0.112*	0.379 (3)
H13B	0.7913	-0.2193	0.2287	0.112*	0.379 (3)
H13C	0.7514	-0.1578	0.1346	0.112*	0.379 (3)
H2A	0.574 (5)	-0.066 (9)	0.0717 (16)	0.090*	0.379 (3)

Table 8c. Atomic displacement parameters (\AA^2) for 7-(3-hydroxy-2-methyl-3-oxo-propyl)sulfonyl-1-oxo-isochromene-3-carboxylic acid (**31**).

	U^{11}	U^{22}	U^{33}	U^{12}	U^{13}	U^{23}
S1	0.0456 (5)	0.0500 (6)	0.1043 (9)	-0.0146 (5)	0.0205 (5)	-0.0228 (6)
O1	0.060 (2)	0.158 (4)	0.082 (3)	-0.023 (3)	0.0053 (19)	-0.007 (3)
O2	0.076 (2)	0.125 (3)	0.060 (2)	0.019 (2)	-0.0049 (18)	-0.003 (2)
O3	0.060 (3)	0.061 (4)	0.180 (6)	-0.018 (3)	0.049 (3)	-0.034 (4)
O4	0.233 (8)	0.070 (4)	0.138 (5)	-0.029 (5)	0.112 (5)	-0.034 (4)
O5	0.048 (3)	0.081 (4)	0.092 (3)	-0.017 (3)	0.038 (2)	-0.007 (3)
O6	0.052 (3)	0.061 (4)	0.072 (4)	-0.013 (3)	0.000 (3)	-0.016 (3)
O7	0.257 (13)	0.178 (11)	0.051 (6)	-0.161 (8)	0.046 (7)	-0.012 (7)
O8	0.092 (2)	0.081 (2)	0.0436 (15)	-0.0415 (18)	0.0031 (15)	0.0083 (16)
N1	0.045 (3)	0.055 (4)	0.052 (3)	-0.003 (3)	0.004 (2)	0.001 (3)

C1	0.065 (3)	0.056 (3)	0.066 (3)	-0.007 (2)	-0.007 (2)	0.000 (2)
C2	0.060 (2)	0.057 (3)	0.046 (2)	-0.022 (2)	0.0037 (19)	0.002 (2)
C3	0.048 (2)	0.069 (3)	0.046 (2)	-0.014 (2)	0.0066 (18)	0.000 (2)
C4	0.044 (2)	0.053 (2)	0.048 (2)	-0.0086 (19)	0.0082 (17)	-0.0026 (19)
C5	0.061 (2)	0.062 (3)	0.046 (2)	-0.019 (2)	0.0136 (18)	-0.003 (2)
C6	0.060 (8)	0.086 (12)	0.136 (14)	-0.031 (8)	0.048 (8)	-0.018 (11)
C7	0.067 (3)	0.059 (3)	0.060 (2)	-0.019 (2)	0.027 (2)	-0.005 (2)
C8	0.043 (2)	0.048 (2)	0.070 (3)	-0.0097 (18)	0.0157 (18)	-0.011 (2)
C9	0.058 (2)	0.065 (3)	0.054 (2)	-0.015 (2)	0.0121 (19)	-0.014 (2)
C10	0.058 (2)	0.075 (3)	0.051 (2)	-0.018 (2)	0.0217 (18)	-0.008 (2)
C11	0.123 (5)	0.056 (3)	0.097 (4)	-0.010 (4)	-0.031 (4)	-0.002 (3)
C12	0.067 (5)	0.046 (4)	0.051 (4)	0.004 (4)	0.001 (4)	0.001 (4)
C13	0.083 (6)	0.038 (5)	0.111 (7)	0.025 (4)	0.015 (5)	0.009 (5)
O3A	0.047 (4)	0.050 (5)	0.096 (6)	-0.002 (4)	0.002 (4)	0.003 (5)
O4A	0.49 (3)	0.123 (10)	0.43 (3)	-0.066 (15)	-0.25 (2)	0.152 (12)
O5A	0.046 (4)	0.102 (7)	0.112 (6)	-0.034 (5)	0.044 (4)	-0.050 (6)
O6A	0.041 (5)	0.075 (7)	0.085 (7)	-0.016 (5)	-0.006 (4)	0.004 (6)
O7A	0.091 (4)	0.105 (5)	0.052 (3)	-0.046 (3)	0.031 (3)	-0.015 (3)
N1A	0.053 (5)	0.054 (6)	0.058 (5)	-0.011 (5)	0.014 (4)	0.002 (5)
C6A	0.090 (6)	0.063 (5)	0.023 (3)	-0.027 (5)	0.004 (3)	0.009 (3)
C12A	0.074 (8)	0.047 (7)	0.044 (7)	-0.009 (6)	-0.020 (6)	0.008 (6)
C13A	0.070 (8)	0.021 (6)	0.113 (12)	0.015 (6)	-0.009 (8)	0.010 (7)

Table 8d. Geometric parameters (Å, °) for 7-(3-hydroxy-2-methyl-3-oxo-propyl)sulfonyl-1-oxo-isochromene-3-carboxylic acid (**31**).

S1—O5	1.398 (6)	C5—C6	1.458 (17)
S1—O6	1.411 (6)	C5—C6A	1.510 (8)
S1—O6A	1.422 (9)	C7—C8	1.374 (6)
S1—O5A	1.486 (9)	C7—H7	0.9500
S1—N1A	1.616 (9)	C8—C9	1.383 (7)
S1—N1	1.707 (6)	C9—C10	1.371 (6)
S1—C8	1.758 (4)	C9—H9	0.9500
O1—C1	1.239 (6)	C10—H10	0.9500
O2—C1	1.237 (5)	C11—O3A	1.205 (6)
O3—C11	1.164 (6)	C11—O4A	1.227 (11)
O4—C11	1.375 (7)	C11—C12	1.535 (8)
O7—C6	1.175 (14)	C11—C12A	1.553 (10)
O8—C6A	1.351 (9)	C12—C13	1.581 (10)
O8—C6	1.394 (16)	C12—H12	1.0000
O8—C2	1.413 (5)	C13—H13D	0.9800
N1—C12	1.444 (9)	C13—H13E	0.9800
N1—H2	0.854 (19)	C13—H13F	0.9800
C1—C2	1.530 (7)	O7A—C6A	1.178 (8)
C2—C3	1.554 (6)	N1A—C12A	1.455 (11)
C2—C3 ⁱ	1.571 (7)	N1A—H2A	0.853 (19)
C3—C4	1.502 (6)	C12A—C13A	1.581 (14)
C3—C2 ⁱ	1.571 (7)	C12A—H12A	1.0000
C3—H3	1.0000	C13A—H13A	0.9800
C4—C10	1.382 (6)	C13A—H13B	0.9800
C4—C5	1.382 (6)	C13A—H13C	0.9800
C5—C7	1.389 (6)		
O5—S1—O6	123.3 (4)	C7—C8—C9	121.1 (4)

O6A—S1—O5A	114.3 (6)	C7—C8—S1	121.3 (4)
O6A—S1—N1A	120.7 (5)	C9—C8—S1	117.5 (3)
O5A—S1—N1A	97.7 (5)	C10—C9—C8	119.6 (4)
O5—S1—N1	109.2 (3)	C10—C9—H9	120.2
O6—S1—N1	99.1 (3)	C8—C9—H9	120.2
O5—S1—C8	111.7 (3)	C9—C10—C4	119.9 (4)
O6—S1—C8	105.2 (3)	C9—C10—H10	120.0
O6A—S1—C8	114.5 (5)	C4—C10—H10	120.0
O5A—S1—C8	101.6 (4)	O3A—C11—O4A	123.1 (8)
N1A—S1—C8	105.2 (4)	O3—C11—O4	123.5 (6)
N1—S1—C8	106.8 (3)	O3—C11—C12	133.5 (5)
C6A—O8—C2	123.5 (4)	O4—C11—C12	103.0 (5)
C6—O8—C2	123.6 (7)	O3A—C11—C12A	121.3 (6)
C12—N1—S1	118.4 (4)	O4A—C11—C12A	115.5 (7)
C12—N1—H2	120 (5)	N1—C12—C11	105.8 (5)
S1—N1—H2	114 (5)	N1—C12—C13	107.1 (6)
O2—C1—O1	123.7 (5)	C11—C12—C13	103.9 (5)
O2—C1—C2	118.4 (5)	N1—C12—H12	113.1
O1—C1—C2	117.4 (4)	C11—C12—H12	113.1
O8—C2—C1	108.6 (4)	C13—C12—H12	113.1
O8—C2—C3	118.3 (4)	C12—C13—H13D	109.5
C1—C2—C3	114.4 (4)	C12—C13—H13E	109.5
O8—C2—C3 ⁱ	111.7 (4)	H13D—C13—H13E	109.5
C1—C2—C3 ⁱ	112.6 (4)	C12—C13—H13F	109.5
C3—C2—C3 ⁱ	90.2 (3)	H13D—C13—H13F	109.5
C4—C3—C2	115.1 (4)	H13E—C13—H13F	109.5
C4—C3—C2 ⁱ	117.4 (4)	C12A—N1A—S1	114.5 (7)
C2—C3—C2 ⁱ	89.8 (3)	C12A—N1A—H2A	138 (5)
C4—C3—H3	111.0	S1—N1A—H2A	107 (5)
C2—C3—H3	111.0	O7A—C6A—O8	116.6 (6)
C2 ⁱ —C3—H3	111.0	O7A—C6A—C5	125.2 (8)
C10—C4—C5	120.2 (4)	O8—C6A—C5	117.9 (6)
C10—C4—C3	119.2 (4)	N1A—C12A—C11	110.3 (6)
C5—C4—C3	120.1 (4)	N1A—C12A—C13A	97.0 (8)
C7—C5—C6	117.7 (7)	C11—C12A—C13A	111.2 (8)
C7—C5—C4	119.9 (4)	N1A—C12A—H12A	112.5
C6—C5—C4	122.4 (7)	C11—C12A—H12A	112.5
C7—C5—C6A	118.8 (5)	C13A—C12A—H12A	112.4
C4—C5—C6A	121.2 (5)	C12A—C13A—H13A	109.4
O7—C6—O8	118.9 (15)	C12A—C13A—H13B	109.5
O7—C6—C5	122.2 (14)	H13A—C13A—H13B	109.5
O8—C6—C5	118.6 (11)	C12A—C13A—H13C	109.5
C5—C7—C8	119.1 (4)	H13A—C13A—H13C	109.5
C5—C7—H7	120.5	H13B—C13A—H13C	109.5
C8—C7—H7	120.5		
O5—S1—N1—C12	-44.2 (6)	N1A—S1—C8—C7	-63.0 (5)
O6—S1—N1—C12	-174.2 (5)	N1—S1—C8—C7	-106.7 (4)
O6A—S1—N1—C12	-169.4 (7)	O5—S1—C8—C9	-171.8 (4)
O5A—S1—N1—C12	-50.4 (8)	O6—S1—C8—C9	-35.8 (5)
N1A—S1—N1—C12	-17.5 (6)	O6A—S1—C8—C9	-22.3 (7)
C8—S1—N1—C12	76.8 (5)	O5A—S1—C8—C9	-146.1 (5)
C6A—O8—C2—C1	145.9 (6)	N1A—S1—C8—C9	112.5 (5)
C6—O8—C2—C1	138.3 (10)	N1—S1—C8—C9	68.9 (4)
C6A—O8—C2—C3	13.3 (8)	C7—C8—C9—C10	3.1 (7)
C6—O8—C2—C3	5.7 (12)	S1—C8—C9—C10	-172.5 (4)

C6A—O8—C2—C3 ⁱ	-89.3 (7)	C8—C9—C10—C4	-0.1 (8)
C6—O8—C2—C3 ⁱ	-96.9 (11)	C5—C4—C10—C9	-3.4 (7)
O2—C1—C2—O8	30.4 (6)	C3—C4—C10—C9	168.7 (5)
O1—C1—C2—O8	-157.5 (5)	S1—N1—C12—C11	-102.0 (5)
O2—C1—C2—C3	165.0 (5)	S1—N1—C12—C13	147.7 (6)
O1—C1—C2—C3	-22.9 (7)	O3—C11—C12—N1	-0.4 (6)
O2—C1—C2—C3 ⁱ	-93.9 (6)	O3A—C11—C12—N1	93.6 (6)
O1—C1—C2—C3 ⁱ	78.2 (6)	O4A—C11—C12—N1	-110.5 (7)
O8—C2—C3—C4	5.5 (6)	O4—C11—C12—N1	-180.0 (5)
C1—C2—C3—C4	-124.5 (4)	C12A—C11—C12—N1	-31.2 (9)
C3 ⁱ —C2—C3—C4	120.5 (5)	O3—C11—C12—C13	112.3 (6)
O8—C2—C3—C2 ⁱ	-115.0 (5)	O3A—C11—C12—C13	-153.7 (7)
C1—C2—C3—C2 ⁱ	115.1 (5)	O4A—C11—C12—C13	2.2 (9)
C3 ⁱ —C2—C3—C2 ⁱ	0.001 (1)	O4—C11—C12—C13	-67.3 (6)
C2—C3—C4—C10	172.8 (4)	C12A—C11—C12—C13	81.5 (11)
C2 ⁱ —C3—C4—C10	-83.4 (6)	O5—S1—N1A—C12A	170.3 (8)
C2—C3—C4—C5	-15.1 (6)	O6—S1—N1A—C12A	51.3 (10)
C2 ⁱ —C3—C4—C5	88.8 (5)	O6A—S1—N1A—C12A	50.0 (9)
C10—C4—C5—C7	4.0 (7)	O5A—S1—N1A—C12A	174.2 (7)
C3—C4—C5—C7	-168.1 (4)	N1—S1—N1A—C12A	16.9 (5)
C10—C4—C5—C6	-173.8 (10)	C8—S1—N1A—C12A	-81.4 (7)
C3—C4—C5—C6	14.1 (11)	C6—O8—C6A—O7A	-103 (7)
C10—C4—C5—C6A	179.6 (6)	C2—O8—C6A—O7A	164.4 (7)
C3—C4—C5—C6A	7.5 (8)	C6—O8—C6A—C5	71 (7)
C6A—O8—C6—O7	87 (7)	C2—O8—C6A—C5	-21.7 (10)
C2—O8—C6—O7	178.2 (15)	C7—C5—C6A—O7A	0.0 (13)
C6A—O8—C6—C5	-99 (7)	C6—C5—C6A—O7A	81 (8)
C2—O8—C6—C5	-7.7 (19)	C4—C5—C6A—O7A	-175.7 (8)
C7—C5—C6—O7	-7 (2)	C7—C5—C6A—O8	-173.4 (6)
C4—C5—C6—O7	171.4 (16)	C6—C5—C6A—O8	-93 (8)
C6A—C5—C6—O7	-109 (8)	C4—C5—C6A—O8	11.0 (10)
C7—C5—C6—O8	179.6 (10)	S1—N1A—C12A—C11	105.1 (7)
C4—C5—C6—O8	-2.5 (19)	S1—N1A—C12A—C13A	-139.1 (8)
C6A—C5—C6—O8	77 (8)	O3—C11—C12A—N1A	-107.0 (7)
C6—C5—C7—C8	176.8 (10)	O3A—C11—C12A—N1A	-16.0 (8)
C4—C5—C7—C8	-1.1 (7)	O4A—C11—C12A—N1A	164.2 (8)
C6A—C5—C7—C8	-176.8 (6)	O4—C11—C12A—N1A	87.2 (8)
C5—C7—C8—C9	-2.4 (7)	C12—C11—C12A—N1A	49.6 (8)
C5—C7—C8—S1	173.0 (4)	O3—C11—C12A—C13A	146.5 (8)
O5—S1—C8—C7	12.6 (5)	O3A—C11—C12A—C13A	-122.5 (9)
O6—S1—C8—C7	148.6 (5)	O4A—C11—C12A—C13A	57.8 (9)
O6A—S1—C8—C7	162.1 (6)	O4—C11—C12A—C13A	-19.3 (10)
O5A—S1—C8—C7	38.3 (6)	C12—C11—C12A—C13A	-56.9 (11)

Symmetry code: (i) -x, -y-1, -z.